

**EXPERIMENTAL INVESTIGATIONS ON DUAL-FUEL MODE  
HCCI ENGINE EMISSION CONTROL BY SUPPLY OF  
VARIOUS ALCOHOL-BASED FUELS AND OPTIMIZATION OF  
PREMIXED RATIO**

*A Thesis Submitted in partial fulfillment of the requirements for  
the award of the Degree of*

**DOCTOR OF PHILOSOPHY**

**in**

**MECHANICAL ENGINEERING**

**by**

**Ganesh Rupchand Gawale  
(Roll No.: 716133)**

**Supervisor**

**Dr. G. Naga Srinivasulu  
(Associate Professor)**



**DEPARTMENT OF MECHANICAL ENGINEERING  
NATIONAL INSTITUTE OF TECHNOLOGY,  
WARANGAL (TS), INDIA 506004  
JUNE 2021**



**NATIONAL INSTITUTE OF TECHNOLOGY  
WARANGAL (T.S) INDIA 506 004**

**CERTIFICATE**

This is to certify that the dissertation work entitled **Experimental Investigations on Dual-Fuel Mode HCCI Engine Emission Control by Supply of Various Alcohol-Based Fuels and Optimization of Premixed Ratio**, which is being submitted by **Mr. Ganesh Rupchand Gawale** (Roll No. 716133), is a bonafide work submitted to the Department of Mechanical Engineering, National Institute of Technology, Warangal in partial fulfillment of the requirement for the award of the degree of **Doctor of Philosophy in Mechanical Engineering**.

To the best of our knowledge, the work incorporated in this thesis has not been submitted elsewhere for the award of any degree.

**Dr. G. Naga Srinivasulu**  
Supervisor  
Department of Mechanical Engineering  
National Institute of Technology  
Warangal-506004

**Prof. A. Kumar**  
Head,  
Department of Mechanical Engineering  
National Institute of Technology  
Warangal-506004

*Dedicated*

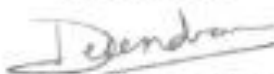
*to*

- ❖ **My beloved grandparents, parents & All my family members**
- ❖ **All my Teachers and Professors who taught and encouraged me with positive thoughts.**

## APPROVAL SHEET FOR Ph.D

The Thesis entitled "**Experimental Investigations on Dual-Fuel Mode HCCI Engine Emission Control by Supply of Various Alcohol-Based Fuels and Optimization of Premixed Ratio**" by **Mr. Ganesh Rupchand Gawale** (Roll no:716133) is approved for the Degree of Doctor Philosophy.

### Examiners



**Dr. Devendra Laxmanrao Deshmukh**

Associate Professor, Mechanical Engineering Department  
Indian Institute of Technology Indore, Indore



**Prof. Shirish Hari Sonawane**

Professor, Chemical Engineering Department  
National Institute of Technology Warangal



**Dr. G. Naga Srinivasulu**

(Supervisor)

Associate Professor, Mechanical Engineering Department, NIT Warangal



Chairman

**Prof. Adepu Kumar**

*Vc* Head, Mechanical Engineering Department, NIT Warangal

Date:20/01/2022



**NATIONAL INSTITUTE OF TECHNOLOGY  
WARANGAL (T.S) INDIA 506 004**

---

---

**DECLARATION**

This is to certify that the work presented in the thesis entitled "**EXPERIMENTAL INVESTIGATIONS ON DUAL-FUEL MODE HCCI ENGINE EMISSION CONTROL BY SUPPLY OF VARIOUS ALCOHOL-BASED FUELS AND OPTIMIZATION OF PREMIXED RATIO**" is a bonafide work done by me under the supervision of **Dr. G. Naga Srinivasulu** and was not submitted elsewhere for the award of any degree. I declare that this written submission represents my ideas in my own words and where other's ideas or words have been included, I adequately cited and referenced the original sources. I also declare that I have adhered to all principles of academic honesty and integrity and have not misrepresented or fabricated or falsified any idea/data/fact/source in my submission. I understand that any violation of the above will be a cause for disciplinary action by the Institute and can also evoke penal action from the sources which have thus not been properly cited or from whom proper permission has not been taken when needed.

Date: 07/01/2022  
Place: Warangal

**(Ganesh Rupchand Gawale)**  
Research Scholar,  
Roll No.716133

## ACKNOWLEDGEMENTS

I would like to express my sincere gratitude and it gives me an immense pleasure to acknowledge the people who were the part of this research work in plenty ways. It would not have been possible without close association with many people. I take this opportunity to extend my sincere gratitude and appreciation to all those who made this research work possible. First and foremost, I would like to express my sincere gratitude to my research supervisor Dr. G. Naga Srinivasulu for his continuous guidance, advice, inspiration, encouragement, for facilitating all the requirements and continuous support, throughout my research work. His enthusiasm, integral view on research and mission for providing high-quality work, has made a deep impression on me. I indebted to him for his persistence in moulding me as a researcher with his methodical supervision that enabled me to complete the research work in the present form. I will never forget his association and encouragement and whole hearted support during my entire tenure of research. During our course of interaction, I have learnt many things, like how to explore new possibilities and how to approach a problem by systematic thinking. I owe him with lots of gratitude for showing me this way of research.

I am grateful to Prof. N.V. Ramana Rao, Director-NIT Warangal who has been a constant source of inspiration for me. I thank Prof. A. Kumar, Head of the Department of Mechanical Engineering for providing the necessary facilities to carry out the research. I would like to express my sincere thanks to Dr. V. R. K. Raju, Dr. Devanuri Jaya Krishna, Dr. K. Narasimhulu (Biotechnology Engineering Department), learned members of my Doctoral Scrutiny Committee for being helpful and generous during the entire course of this work.

This work was not possible without inspiration of my M. Tech. Supervisors Prof. D. G. Thombare (Automobile Engg. Dept., RIT Isalmpur, Maharashtra). He inspired me during my post-graduation studies and accelerated my passion of pursuing higher studies with greater impact. He is my constant source of the inspiration throughout my life.

I am always grateful to my institute NITW, where I learn many things along with the research. I express my heart-felt gratitude to Dr. M Raja Vishwanathan, Humanities & Social Science Department and other faculty members of the institute during the stay. They are very kind enough to extend their help at various phases of this research, whenever I approached them, and I do hereby acknowledge all of them.

I am also thankful to all the supporting and technical staff of Department of Mechanical Engineering who has directly or indirectly helped during the course of my work. I am very thankful to all Thermal lab technical staff and section head.

My heartfelt thanks to fellow-scholars for their consistent help, moral support and encouragement. My special thanks to Dr. Venkateswarlu Velisala, Dr. Srinivas Reddy, Dr. K V Koteswara Rao, Murali Krishna Boni, Satish M, Ramesh M, B Rama Krishna, N Siva Prasad, Chandra Sekhar Reddy, Markendelu, Kranti, Manoj Dundi, Pritam Das, Dr. Ganesh Babu, Dr. Vinod Babu, Dr. Ravichandra, Dr. Ganesh Warkhade, and many others for always standing by my side and sharing a great relationship as compassionate friends. I will always cherish the warmth shown by them.

I am very much thankful to all my special Marathi Mandal and fellow research scholars specially, to Dr. Uday Bagle, Dr. Prashant Suryawanshi, Dr. Abhay Lingayat, Dr. Vinay Rangari, Dr. Harshal Patil, Dr. Gajanan Suryawanshi, Mr. Roshan Bodile, Mr. Upendra Maurya, Mr. Kishor Ingle, Mr. Avinash Bongaonkar, Mr. Swapnil Adsul, Mr. Vikas Hakke, Mr. Sandip Khobragale, Ms. Vividha Landge, Ms. Sneha Korpe, Ms. Shital Potdar, Ms. Diksha Pandey, Ms. Sarita Prasad, Ms. Sana. I am very much thankful to all my M. Tech friends Dhananjay Singh, Sanbhitt, and Himalaya.

In this auspicious moment, I owe my deepest regards to my family members and well-wishers for their eternal support and understanding of my goals and aspirations. My heartfelt regards go to my parents, Sri Rupchand Gawale and Smt. Vatsala Gawale and dear wife Smt. Dipali Gawale. My special regards to my all brother-in laws and sisters for their patience and understanding during the entire period of the research work. I also must thank all my hostel mates for making my stay at NIT Warangal become more memorable.

As always it is impossible to mention everybody who had an impact on this work, however, there are those whose spiritual support is even more important. I feel a deep sense of gratitude to each and every one who directly or indirectly extended their support to fulfill my research. Finally, I am thankful to library staff and administrative staff of NITW for their cooperation.



NIT Warangal

**(Ganesh Rupchand Gawale)**

January 2022

## ABSTRACT

Homogeneous charge compression ignition (HCCI) engine has fuel flexibility and the potential to reduce NO<sub>x</sub> and soot emissions. The aim of this work is to investigate the performance and exhaust emissions of dual-fuel mode HCCI (DF-HCCI) engine. The existing CI Engine is converted into a DF-HCCI engine by attaching the carburetor to the inlet manifold. Royal Enfield bullet 500 cc, Mikarb type carburetor was attached outside the engine cylinder to prepare the homogenous air-fuel mixture. Alcohol-based fuel (low reactivity fuel) was supplied through the carburetor at the time of suction stroke and diesel/biodiesel blend/butanol blends (high reactivity fuel) were injected to start the combustion at the end of the compression stroke.

To examine the influence of carburetor location on DF-HCCI engine performance, three different length (6-inch, 9-inch, and 12-inch) inlet manifold pipes were chosen. Experimentation was done for the different carburetor locations, it was revealed that a nearer location of the carburetor outside the engine was preferable to avoid the evaporation losses and friction losses.

To vary the mass flow rate (MFR) of alcohol-based fuel different diameters of fuel jets were used. In this study jet 40, jet 47.5, jet 60, jet 70, jet 80, and jet 90 were selected to change the MFR of alcohol-based fuel in the carburetor. The effect of varying the MFR of alcohol-based fuel and its optimization for premixed ratio at each load condition was investigated. It was observed that an increase in the MFR of alcohol-based fuel extends the ignition delay (ID) and it resists the start of combustion (SOC). Alcohol-based fuels have high octane number and high autoignition temperature which helps to increase ID.

In the case of E100+D DF-HCCI engine, it was observed that NO<sub>x</sub> and smoke opacity was reduced a lot with great improvement in the BTE, however, HC and CO emission increased. In this study cumulative performance of emission reduction and BTE improvement was examined by Simple Additive Weighting (SAW) optimization method. In SAW four different weightage sets were assigned to each alternative parameter. With the help of SAW optimization, optimum fuel jet and premixed ratio for each load condition were investigated. In E100+D DF-HCCI engine it was observed that jet 40 is suitable for 20% load condition, jet 70 was suitable for 40% load condition, jet 80 was suitable for 60% load conditions and jet 90 was suitable for 80% and 100% load conditions. The optimum premixed ratio for E100+D DF-HCCI engine was varied from 47.55% to 75.94% at different load conditions.

In the case of P100+D, B100+D DF-HCCI engine similar performance was observed in  $\text{NO}_x$  and smoke opacity reduction as well as BTE improvement. However, P100+D showed great improvement in the BTE and B100+D showed a great reduction in the smoke opacity. The premixed ratio range for P100+D DF-HCCI engine varied from 58.98% to 73.92% at different load conditions. For B100+D DF-HCCI engine it varied from 45.84% to 63.02% at different load conditions.

In the case of M100+D DF-HCCI engine  $\text{NO}_x$  emission, reduced lot but smoke opacity was increased and BTE was reduced. It showed poor performance at low load conditions compared to a conventional diesel engine. Further, its premixed ratio range was also very low, i.e. in between 31.40% to 43.97%. Further in the comparison of all alcohol-based DF-HCCI engine for fuel jet 60, at 20%, 40%, and 100% load conditions P100+D DF-HCCI showed the best cumulative performance and at 60% and 80% load conditions B100+D DF-HCCI engine showed the best performance.

Experiments were performed to investigate the influence of Neem biodiesel blend 20 (Bio20) instead of diesel in alcohol-based DF-HCCI engine on engine combustion and emission. It revealed that inherent oxygen in the Bio20 helps to reduce HC and CO emission for all alcohol-based DF-HCCI engines. In the case of E100+Bio20, P100+Bio20, and B100+Bio20 reduction was observed in HC and CO emission, however smoke opacity increased compared to E100+D, P100+D, and B100+D respectively. But in the case of M100+Bio20, Bio20 substitution instead of diesel gave a good reduction in HC, CO, and smoke opacity as well as improvement in the BTE. It was observed that Bio20 substitution instead of diesel for Methanol DF-HCCI engine was most favorable compared to the rest of the alcohol-based DF-HCCI engine.

Further technical feasibility of butanol blend (B10/B20/B30) instead of diesel in the propanol DF-HCCI engine was investigated. In this study, butanol was mixed with the diesel on a volume basis and injected at the end of compression stroke instead of diesel in propanol DF-HCCI engine. It was observed that the presence of oxygen and low cetane number of butanol assist to reduce the total blend cetane number and increase its LHV. Increasing LHV and reduction in cetane number of butanol blend assist to reduce the combustion temperature due to that high reduction in  $\text{NO}_x$  emission was observed. The presence of oxygen in the butanol blend helps to reduce CO and HC emission compared to P100+D DF-HCCI engine. From the optimization it

was observed that At 20% and 80% load conditions P100+B30, for 40% and 60% load conditions P100+B10, and for 100% load conditions P100+B20 DF-HCCI engine gave an optimized performance.

## Content

<b>ACKNOWLEDGEMENTS .....</b>	<b>V</b>
<b>ABSTRACT.....</b>	<b>VII</b>
<b>Content.....</b>	<b>X</b>
<b>List of Figures.....</b>	<b>XIV</b>
<b>List of Tables .....</b>	<b>XIX</b>
<b>Nomenclature .....</b>	<b>XXI</b>
<b>Chapter-1 .....</b>	<b>1</b>
<b>Introduction.....</b>	<b>1</b>
1.1 General .....	2
1.2 Vehicle emissions and their effect on human health.....	4
1.2.1 Effect of CO emission .....	4
1.2.2 Effect of HC emission .....	5
1.2.3 Effect of NO <sub>X</sub> emission .....	5
1.2.4 Effect of PM or smoke.....	5
1.3 Advance combustion strategies.....	6
1.4 Introduction of HCCI engine .....	7
1.4.1 Advantages .....	9
1.4.2 Disadvantages .....	9
1.4.3 Challenges in HCCI engine .....	9
1.4.3.1 Difficult to start in cold condition.....	10
1.4.3.2 High HC and CO emissions.....	10
1.4.3.3 Combustion phasing control .....	10
1.4.3.4 Extend the operating range .....	11
1.5 Introduction of present research on dual fuel mode HCCI engine.....	12
1.6 Thesis organization .....	12
<b>Chapter – 2 .....</b>	<b>14</b>
<b>Literature Review .....</b>	<b>14</b>
<b>2.1 General .....</b>	<b>15</b>
2.2 External homogeneous charge preparation technique.....	16
2.3 Internal homogenous charge preparation .....	20

2.3.1 Early direct injection .....	20
2.3.1.1 Premixed Lean Diesel Combustion (PREDIC).....	21
2.3.1.2 Premixed compression ignition (PCI).....	22
2.3.1.3 Multi-stage diesel combustion (MULDIC).....	23
2.3.1.4 Homogeneous charge intelligent Multiple Injection Combustion System (HiMiCS) .....	23
2.3.1.5 Uniform Bulky Combustion System (UNIBUS) .....	24
2.3.1.6 MULINBUMP compound combustion .....	25
2.3.1.7 Narrow-angle direct injection (NADI <sup>TM</sup> ).....	25
2.3.2 Multiple direct injections.....	27
2.3.3 Late direct injection .....	27
2.3.3.1 Modulated kinetics combustion (MK Combustion) .....	28
2.4 Premixed and direct injection homogenous charge preparation techniques .....	29
2.4.1 Gaseous fuel dual fuel HCCI engine .....	29
2.4.2 Gasoline diesel dual fuel HCCI engine .....	33
2.4.3 Methanol diesel dual fuel HCCI engine .....	35
2.4.4 Ethanol, propanol, and butanol dual fuel HCCI engine .....	38
2.5 Various other combustion control strategy .....	41
2.6 Summary .....	43
2.7 Observations and gaps identified from the literature .....	43
2.8 Objectives of the research work .....	44
<b>Chapter – 3 .....</b>	<b>46</b>
<b>Experimental Setup and Instrumentation.....</b>	<b>46</b>
3.1 General .....	47
3.2 Test engine .....	47
3.3 Selection of carburetor .....	50
3.4 Fuels selected for dual fuel HCCI engine .....	51
3.5 Experimental test setup and instrumentation .....	54
<b>Chapter - 4.....</b>	<b>58</b>
<b>Experimental Procedure and Optimization Method.....</b>	<b>58</b>
4.1 General .....	59

4.2 Experimental procedure .....	59
4.3 Performance parameters.....	61
4.4 Uncertainty analysis .....	63
4.5 Optimization of operating parameter .....	64
<b>Chapter - 5 .....</b>	<b>68</b>
<b>Results and Discussion.....</b>	<b>68</b>
<b>Experimentally Analyzed the Performance of DF-HCCI Engine over Conventional Diesel Engine .....</b>	<b>68</b>
5.1 General .....	69
5.2 Objective 1 .....	69
To experimentally investigate the influence of carburetor location on dual fuel mode HCCI engine performance. .....	69
5.2.1 General.....	69
5.2.2 Combustion and emission characteristics.....	69
5.3 Objective 2 .....	73
5.3.1 General.....	73
5.3.2 Ethanol-diesel DF-HCCI engine performance for different load conditions .....	73
5.3.2.1 In-cylinder pressure for different load conditions .....	73
5.3.2.2. Influence of a different MFR of Ethanol on combustion and emission characteristics.....	74
5.3.2.3 Optimize the MFR and premixed ratio at each load conditions .....	83
5.3.3 Methanol diesel DF-HCCI engine performance for different load conditions.....	84
5.3.3.1 Impact of varying MFR of methanol on combustion and emission characteristics	85
5.3.3.2 Optimization of MFR and the premixed ratio of methanol at different load conditions .....	90
5.3.4 Propanol-diesel DF-HCCI engine performance for different load conditions .....	92
5.3.4.2 Optimization of MFR and the premixed ratio of propanol at different load conditions.....	96
5.3.5 Butanol-diesel DF-HCCI engine performance for different load conditions .....	98
5.3.5.1 Influence of varying MFR of butanol on combustion and emission characteristics .....	98
5.3.5.2 Optimization of MFR and the premixed ratio of butanol at different load conditions .....	103

5.3.6 Summary.....	105
5.4 Objective 3 .....	106
5.4.1 Combustion and emission characteristics for different alcohol-based fuels in DF-HCCI engine under different load conditions .....	106
5.4.2 Optimization of alcohol-based fuel in DF-HCCI engine at different load conditions	113
5.4.3 Summery.....	115
5.5 Objective 4 .....	116
5.5.1 M100+Bio20 DF-HCCI engine performance over M100+D DF-HCCI engine .....	116
5.5.1.1 Influence of Bio20 instead of diesel on combustion and emission characteristics .....	116
5.5.2 Impact of Bio20 instead of diesel on reduction of CO emission in alcohol-based DF-HCCI engine .....	122
5.5.3 Summery.....	125
5.6 Objective 5 .....	126
5.6.1 Influence of Butanol blend (B10/B20/B30) on diesel ignited propanol DF-HCCI engine combustion and emissions .....	126
5.6.2 Optimization to find out best high reactivity fuel (D/B10/B20/B30) for propanol DF-HCCI engine .....	131
5.6.3 Summery.....	132
<b>Chapter - 6.....</b>	<b>133</b>
<b>Conclusions and Future Scope.....</b>	<b>133</b>
6.1 Conclusion.....	134
6.2 Future scope .....	140
<b>Publication on this Research.....</b>	<b>157</b>

## List of Figures

<b>Figure no.</b>	<b>Figure tittle</b>	<b>Page No</b>
Figure 1.1	India's petroleum oil production and consumption, 2000-2019	3
Figure 1.2	Influence of vehicle emission on human health	4
Figure 1.3	Comparison of SI, CI, and HCCI engine	7
Figure 1.4	HCCI engine challenges and remedies	11
Figure 2.1	HCCI engine classification based on homogenous charge preparation	15
Figure 2.2	Execution of early external homogenous charge preparation strategies	20
Figure 2.3	Early direct injection strategy	21
Figure 2.4	PREDIC strategy with water injection	22
Figure 2.5	MULDIC injection pattern	23
Figure 2.6	HiMiCS injection pattern	24
Figure 2.7	UNIBUS single and double injection strategy	24
Figure 2.8	Multi pulse injection and bump combustion chamber	25
Figure 2.9	(a) Diesel engine spray angle (b) Narrow spray angle in HCCI engine	26
Figure 2.10	MK combustion strategy	28
Figure 3.1	Flow chart of present research work	49
Figure 3.2	Mechanical emulsifier blending machine	52
Figure 3.3	Schematic representation of alcohol-based dual fuel HCCI engine	55
Figure 3.4	(a) Actual experimental setup of dual fuel HCCI engine (b) Carburetor location	56
Figure 3.5	Photographic view of the emission analyzers	57
Figure 4.1	(a) carburetor location outside the engine cylinder (b) Various length of inlet manifold pipe	61

Figure 4.2	(a) Fuel jet location in the carburetor (b) Different number fuel jets	61
Figure 5.1	(a) In-cylinder pressure Vs. CA, (b) PRR Vs. CA, (c) ID Vs. engine load, (d) CD Vs. engine load, (e) MFR Vs. engine load, (f) BTE Vs. engine load	70
Figure 5.2	(a) Smoke opacity Vs. engine load, (b) NO <sub>x</sub> Vs. engine load, (c) HC Vs. engine load, (d) HC Vs. different load	72
Figure 5.3	Comparing diesel and dual-fuel mode HCCI engine in-cylinder pressure Vs. crank angle under different load conditions, for jet 60	73
Figure 5.4	The variation of in-cylinder pressure for different fuel jets of DF-HCCI combustion at different engine loads (a) 100% (b) 80% (c) 60% (d) 40% (e) 20%	75
Figure 5.5	Variation of (a) heat release rate and (b) pressure rise rate, for different fuel jets under 100% load conditions	76
Figure 5.6	(a) Ignition delay (ID) Vs. Engine load, (b) Combustion duration (CD) Vs. Engine load, (c) Cooling potential Vs. Engine load, (d) Exhaust gas temp Vs. Engine load	77
Figure 5.7	Variation of (a) NO <sub>x</sub> Vs. Engine load, (b) Smoke opacity Vs. Engine load, (c) HC Vs. Engine load, (d) CO Vs. Engine load, (e) Brake thermal efficiency Vs. Engine load, (f) bsfc Vs. Engine load	79
Figure 5.8	Improvement of E100+D DF-HCCI engine over diesel engine at different load condition for various MFR (a) NO <sub>x</sub> emissions reduction, (b) smoke opacity reduction, (c) BTE increment	81
Figure 5.9	Premixed ratio of ethanol Vs. Engine load	82
Figure 5.10	M100+D DF-HCCI engine (a) In-cylinder pressure Vs. CA, (b) PRR Vs. CA, (c) Ignition delay (ID) Vs. Engine load, (d) Combustion duration (CD) Vs. Engine load, (e) Cooling potential Vs. Engine load, (f) Exhaust gas temp Vs. Engine load	86
Figure 5.11	Variation of (a) NO <sub>x</sub> Vs. Engine load, (b) Smoke opacity Vs. Engine load, (c) CO Vs. Engine load, (d) HC Vs. Engine load, (e) Brake thermal efficiency Vs. Engine load, (f) bsfc Vs. Engine load	87
Figure 5.12	Improvement of M100+D DF-HCCI engine over neat diesel engine at different load condition for various MFR (a) NO <sub>x</sub> emissions reduction, (b) Smoke opacity reduction, (c) BTE increment	89

Figure 5.13	Premixed ratio of methanol under various load conditions for different fuel jets	90
Figure 5.14	Variation of (a) In-cylinder pressure Vs. CA, (b) PRR Vs. CA, (c) HRR Vs. CA for different MFR of propanol in DF-HCCI engine	92
Figure 5.15	Variation of (a) ID Vs. engine load, (b) CD Vs. engine load, (c) Cooling potential Vs. engine load (d) Exhaust gas temp Vs. engine load, for different MFR of propanol in DF-HCCI engine	93
Figure 5.16	Variation of (a) NO <sub>x</sub> Vs. engine load, (b) Smoke opacity Vs. engine load, (c) CO Vs. engine load (d) HC Vs. engine load (e) Brake thermal efficiency Vs. engine load, (f) bsfc Vs. engine load, for different MFR of propanol in DF-HCCI engine	94
Figure 5.17	Improvement of performance over diesel engine (a) NO <sub>x</sub> emission reduction Vs. engine load, (b) Smoke opacity reduction Vs. engine load, (c) BTE increased Vs. engine load for different MFR of propanol in DF-HCCI engine	95
Figure 5.18	Premixed ratio of propanol under various load conditions for different fuel jets	96
Figure 5.19	Variation of (a) In-cylinder pressure Vs. CA, (b) PRR Vs. CA, (c) HRR Vs. CA for different MFR of butanol in DF-HCCI engine	99
Figure 5.20	Variation of (a) ID Vs. engine load, (b) CD Vs. engine load, (c) Cooling potential Vs. engine load (d) Exhaust gas temp Vs. Engine load, for different MFR of Butanol in DF-HCCI engine	100
Figure 5.21	Variation of (a) NOX Vs. engine load, (b) Smoke opacity Vs. engine load, (c) CO emission Vs. engine load (d) HC emission Vs. Engine load (e) Brake thermal efficiency Vs. Engine load, (f) bsfc Vs. Engine load, for different MFR of butanol in DF-HCCI engine	101
Figure 5.22	Improvement of performance over neat diesel engine (a) NO <sub>x</sub> emission reduction Vs. engine load, (b) Smoke opacity reduction Vs. engine load, (c) BTE increased Vs. engine load for different MFR of butanol in DF-HCCI engine	102
Figure 5.23	Premixed ratio of Butanol under various load conditions for different fuel jets	103
Figure 5.24	Variation of (a) In-cylinder pressure Vs. Crank angle, (b) PRR Vs. Crank angle, (c) HRR Vs. Crank angle, for different alcohol-based fuel DF-HCCI engine	107

Figure 5.25	Comparison of (a) ID Vs. Engine load, (b) CD Vs. Engine load, (c) cooling potential Vs. Engine load, (d) Exhaust gas temperature Vs, Engine load, for different alcohol-based fuel in DF-HCCI engine	108
Figure 5.26	Variation of (a) NO <sub>x</sub> emission Vs. Engine load, (b) Smoke opacity Vs. Engine load, (c) CO emission Vs. Engine load, (d) HC emission Vs. Engine load, (e) BTE Vs. Engine load, (f) bsfc Vs. Engine load, for different alcohol-based fuel under various load conditions	110
Figure 5.27	Improvement of alcohol-based DF-HCCI engine performance over neat diesel engine (a) NO <sub>x</sub> emission reduction Vs. engine load, (b) Smoke opacity reduction Vs. Engine load, (c) BTE improvement Vs. Engine load	112
Figure 5.28	Premixed ratio of all four alcohol-based fuel under various load conditions for DF-HCCI engine	113
Figure 5.29	Variation of (a) In-cylinder pressure Vs. Crank angle, (b) PRR Vs. Crank angle, (c) HRR Vs. Crank angle, (d) Exhaust gas temp. Vs. engine load, for methanol DF-HCCI engine	117
Figure 5.30	Impact of Bio20 in place of diesel on ID and CD of methanol DF-HCCI engine	118
Figure 5.31	Impact of Bio20 instead of diesel on CO (% vol.) and HC (ppm) emissions of methanol DF-HCCI engine	119
Figure 5.32	Impact of Bio20 instead of diesel on Smoke opacity and NO <sub>x</sub> emissions of methanol DF-HCCI engine	120
Figure 5.33	Impact of Bio20 instead of diesel on (a) BTE Vs. Engine load, (b) bsfc Vs. Engine load in methanol DF-HCCI engine	121
Figure 5.34	Performance improvement of M100+Bio20 over M100+D DF-HCCI engine	121
Figure 5.35	Increment and decrement of (a) CO emission, (b) HC emission, (C) NO <sub>x</sub> emission, (d) smoke opacity, (e) BTE, of Bio20 ignited alcohol-based DF-HCCI engine over diesel ignited alcohol-based DF-HCCI engine	123
Figure 5.36	Influence of butanol blend (B10/B20/B30) injection on (a) in-cylinder pressure, (b) PRR, (c) HRR, over diesel ignited propanol DF-HCCI engine under 100% load conditions	127
Figure 5.37	ID and CD for different butanol blends in propanol DF-HCCI engine	128

Figure 5.38	Comparison of different propanol DF-HCCI engine (a) CO emissions (b) HC emissions (c) NO <sub>x</sub> emissions (d) Smoke opacity, (e) BTE, (f) bsfc, under various load conditions	129
-------------	--	-----

## List of Tables

<b>Table no.</b>	<b>Table tittle</b>	<b>Page No</b>
Table 1.1	Euro emission norms for passenger car	3
Table 1.2	Comparison between conventional SI engine and HCCI engine	8
Table 1.3	Comparison between conventional diesel engine and HCCI engine	8
Table 3.1	Engine details	50
Table 3.2	Carburetor details	51
Table 3.3	Fuel properties and characteristics	53
Table 3.4	Density and lower calorific value of different blends	54
Table 3.5	Accuracy, range and resolution of Indus gas analyzer	56
Table 3.6	Accuracy, range and resolution of Smoke Meter	56
Table 4.1	Uncertainty of parameters	64
Table 4.2	Decision table in MADM methods	65
Table 5.1	Ranking of different fuel jets for various weightage sets under each load conditions	83
Table 5.2	Optimum jet number, MFR, and the premixed ratio of Ethanol	84
Table 5.3	Ranking of different fuel jets for various weightage sets under each load conditions	91
Table 5.4	Optimum fuel jet number, MFR and the premixed ratio of Methanol	91
Table 5.5	Ranking of different fuel jet for various weightage sets under each load conditions	97
Table 5.6	Optimum fuel jets, MFR and the premixed ratio of Propanol	98
Table 5.7	Ranking of different fuel jets for various weightage sets under each load conditions	104
Table 5.8	Optimum fuel jet, MFR and the premixed ratio of Propanol	105
Table 5.9	Ranking of different fuel jet for various weightage sets under each	114

	load conditions	
Table 5.10	Overall average performance improvement for Bio20 injection over diesel ignited alcohol-based DF-HCCI engine (+ve value means reduction, -ve value means increment)	125
Table 5.11	Ranking of CI engine and different butanol blend ignited propanol DF-HCCI engine	131

## Nomenclature

<b>Abbreviation</b>	
AHP	Analytic Hierarchy Process
ARC	Activated Radical Combustion
ATAC	Active-Thermo Atmosphere Combustion
aTDC	After Top Dead Center
B10	10% butanol and 90% diesel blend by volume
B100	100% Butanol
B100+Bio20	Biodiesel ignited butanol DF-HCCI engine
B100+D	Diesel ignited butanol DF-HCCI engine
B20	20% butanol and 80% diesel blend by volume
B30	30% butanol and 70% diesel blend by volume
Bio20	20% biodiesel and 80% diesel blend by volume
BMEP	Brake Mean Effective Pressure
BP	Brake power
Bsfc	Brake Specific Fuel Consumption
bTDC	Before Top Dead Center
BTE	Brake Thermal Efficiency
CA	Crank Angle
CD	Combustion Duration
CNG	Compressed Natural Gas
CO	Carbon monoxide
CV	Calorific Value
DF-HCCI	Dual fuel – homogeneous charge compression ignition
DMCC	Diesel Methanol Compound Combustion
DMDF	Diesel/Methanol Dual Fuel
E100	100% Ethanol
E100+Bio20	Biodiesel ignited ethanol DF-HCCI engine
E100+D	Diesel ignited ethanol DF-HCCI engine

ECU	Engine Control Unit
EGR	Exaust Gas Recirculation
FC	Fuel Consumption
GA	Genetic Algorithm
GCI	Gasoline Compression Ignition
HC	Hydrocarbon
HCII	Homogenous Charge Induced Ignition
Himics	Homogeneous Charge Intelligent Multiple Injection Combustion System
ICT	Inlet Charge Temperature
IMEP	Indicated Mean Effective Pressure
Jet 40	Fuel jet with 0.4 mm diameter
Jet 47.5	Fuel jet with 0.475 mm diameter
Jet 60	Fuel jet with 0.6 mm diameter
Jet 70	Fuel jet with 0.7 mm diameter
Jet 80	Fuel jet with 0.8 mm diameter
Jet 90	Fuel jet with 0.9 mm diameter
LHV	Latent Heat of Vaporization
LPG	Liquified Petroleum Gas
LTC	Low Temperature Technology
M100	100% Methanol
M100+Bio20	Biodiesel ignited methanol DF-HCCI engine
M100+D	Diesel ignited methanol DF-HCCI engine
MADM	Multiple Attribute Decision Making
MFB10	10% mass fraction burn
MFB90	90% mass fraction burn
MFR	Mass Flow Rate
MODM	Multiple Objective Decision Making
MULDIC	Multi Stage Diesel Combustion
NADI <sup>TM</sup>	Narrow-Angle Direct Injection
NO <sub>x</sub>	Nitrogen oxide

OTC	Open Throttle Carburetor
P100	100% propanol
P100+B10	B10 ignited propanol DF-HCCI engine
P100+B20	B20 ignited propanol DF-HCCI engine
P100+B30	B30 ignited propanol DF-HCCI engine
P100+Bio20	Biodiesel ignited propanol DF-HCCI engine
P100+D	Diesel ignited propanol DF-HCCI engine
PCCI	Premixed Charge Compression Ignition
PCI	Premixed Compression Ignition
PFLP	Peak fuel line pressure
PID	Proportional Integral Derivative
PODE	Poly oxymethylene Dimethyl Ethers
PPCCI	Predominantly Premixed Charge Compression Ignition
PPRR	peak PRR
PR	Premixed Ratio
PREDIC	Premixed Lean Diesel Combustion
RCCI	Reactivity Controlled Compression Ignition
SAW	Simple Additive Weighting
SOC	Start of Combustion
SOF	Soluable Organic Fraction
SOI	Start of Injection
TOPSIS	Technique for Order Preference by Similarity to Ideal Solution
TS	Toyota-Soken
UNIBUS	Uniform Bulky Combustion System
VCR	Variable Compression Ratio
WPM	Weighted Product Method
WSM	Weighted Sum Method
<b>Symbol</b>	
A	Engine cylindrical area
AFR <sub>stoich</sub>	stoichiometric air-fuel ratio

$C_d$	Coefficient of Discharge
$C_p$ air	Specific heat of air
$CV_a$	Calorific value of alcohol-based fuel
$CV_D$	Calorific value of direct injection fuel
$FC_a$	Fuel consumption of alcohol based fuel
$FC_D$	Fuel consumption of direct injection fuel
$H_{fg}$ fuel	Latent heat of vaporization of fuel
$L$	Stroke length
$m_a$	MFR of alcohol-based fuel
$m_D$	MFR of direct injection fuel
$n$	Engine rpm
$\sigma$	Standard deviation
$\sigma_m$	Standard deviation mean
$\rho$	Density of fluid
$\varphi$	Equivalnce ratio of a fuel

## **Chapter-1**

### **Introduction**

---

## 1.1 General

Globally, the need of energy sources increasing drastically with the exponential growth in the population and eases in living standards. The source of energy for industrial purposes, domestic purposes, and transportation purposes are only fossil fuels. All over the world, internal combustion (IC) engine is using for transportation purpose or any power generation purpose for industrial or domestic.

Internal combustion (IC) engine is the main source of power generation in the automotive sector, industrial sector, agriculture sector, and daily domestic purpose. IC engine is working on two different cycles i.e. on Otto cycle and Diesel cycle. Otto cycle was used in the spark ignition (SI) engine while the diesel cycle was used in the compression ignition (CI) engine. Both engines have different benefits as per applications. SI engine is mainly used in portable power generation, in the home application such as lawnmowers, chain saws, outboard motorboat engine, and in a motorcycle. In this application low cost, lightweight, small bulk characteristics are more important than the fuel economy, engine vibration, and engine durability, etc. Although CI engine is more applicable for large and stationary power generation purposes. Such as in cars, trucks, marine engines, and for geneset application, etc. CI engine has more compression ratio (CR) range than SI engine, which helps to give more fuel economy than SI engine [1].

To produce effective power SI engine required gasoline fuel while the CI engine required diesel fuel. Day by day crude oil sources are diminishing, prices are reaching milestones. India was the most consumer of crude oil and petroleum products after the China and United state in 2019. Day by day consumption of crude oil in India is increasing than the production. The gap between production and consumption is widening (shown in **Figure 1.1**). In 2019 crude oil production reaches one million barrels per day and the requirement is extended up to 4.9 million barrel per day. In petroleum products, diesel demand is more in India. For transportation, industry, and agriculture purposes, almost 39% diesel consumption was done in 2019 among a total petroleum product. While gasoline consumption around 14% of India's total oil consumption [2]. Consumption of fossil fuel in the IC engine produces global greenhouse gas (GHG) emissions which cause an adverse effect on human health and the environment. IC engine is the biggest contributor of air pollution. SI emission emits hydrocarbon (HC), carbon

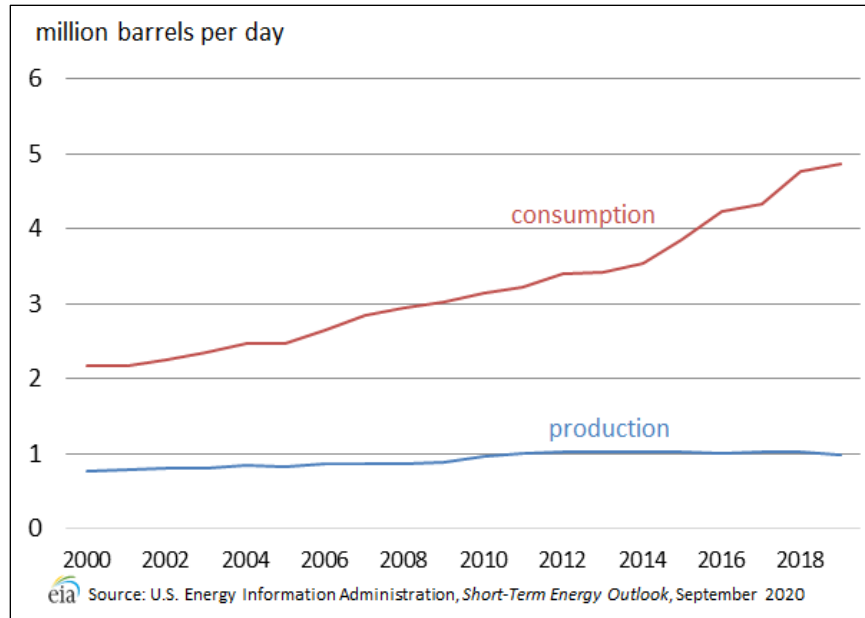


**Figure 1.1** India's petroleum oil production and consumption, 2000-2019 [2]

**Table 1.1** Euro emission norms for passenger car [3]

Phases	Date	HC	CO	NO <sub>x</sub>	PM	HC+NO <sub>x</sub>
<b>Gasoline (SI engine)</b> g/km						
Euro 1	1992	-	2.72	-	-	0.97
Euro 2	1996	-	2.2	-	-	0.5
Euro 3	2000	0.2	2.3	0.15	-	-
Euro 4	2005	0.1	1.0	0.08	-	-
Euro 5	2009	0.1	1.0	0.06	0.005	-
Euro 6	2014	0.1	1.0	0.06	0.005	-
<b>Diesel (CI engine)</b>						
Euro 1	1992	-	2.72	-	0.14	0.97
Euro 2	1996	-	1.0	-	0.08	0.7
Euro 3	2000	-	0.64	0.50	0.05	0.56
Euro 4	2005	-	0.50	0.25	0.025	0.30
Euro 5	2009	-	0.50	0.18	0.005	0.23
Euro 6	2014	-	0.50	0.08	0.005	0.17

monoxide (CO), and Nitrogen oxide (NO<sub>x</sub>) major emissions, while CI engine emits NO<sub>x</sub> and smoke or PM major emissions. These all emission shows an adverse effect on human health and environment. Hence the emission norms are getting more stringent for automobile vehicles,

**Table 1.1** shows the Euro norms for a passenger car.

## 1.2 Vehicle emissions and their effect on human health

Vehicle emissions are the main source of air pollution. Air pollution affects human health and the environment. Vehicles are emitting carbon monoxide (CO), hydrocarbon (HC), Nitrogen oxide (NO<sub>x</sub>), Particulate matter (PM) hazardous emissions in the surrounding air. **Figure 1.2** shows the impact of vehicle emissions on human health.

### 1.2.1 Effect of CO emission

Carbon monoxide (CO) emission occurs in IC engine due to incomplete combustion or lack of oxygen. CO emission is colorless, tasteless, and odorless gas which is very less dense than air. Excess consumption of CO causes carboxyhemoglobin. When the hemoglobin combines with the CO emission it constrains the ability of hemoglobin to supply oxygen from the lungs to the total body this is called carboxyhemoglobin. Excess inhalation of CO produces more carboxyhemoglobin, if the 50% hemoglobin converted into carboxyhemoglobin may result in fatality, coma. Inhalation of CO damage the heart and brain, miscarriage may happen in female, it may damage the growth of the fetus, heart failure, etc [4,5].

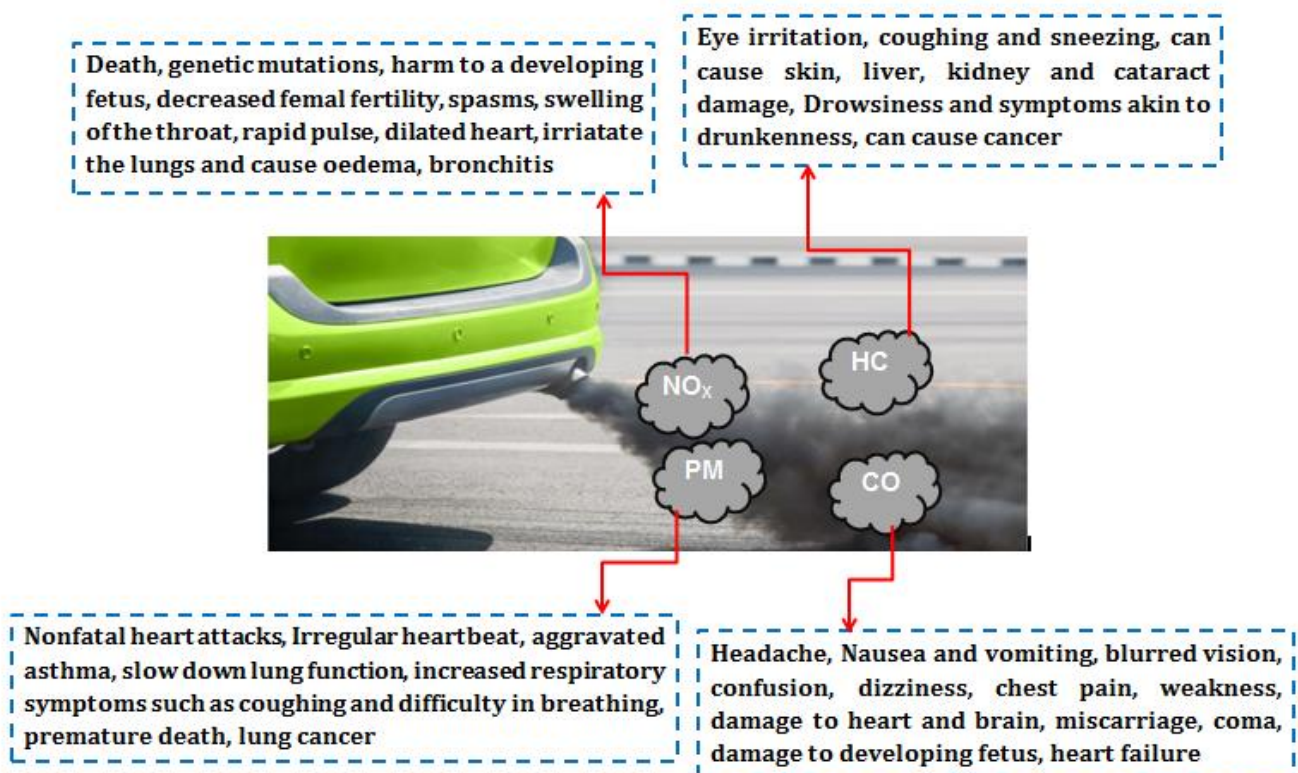


**Figure 1.2** Influence of vehicle emission on human health

### **1.2.2 Effect of HC emission**

Due to misfire, or incomplete combustion HC emission is occurred in the IC engine. Also, high fuel-rich regions and incomplete combustion help to generate HC emission. HC emission level of harmfulness relies on the chemical composition of hydrocarbon. Benzene, pentane, methane, acetaldehyde, acrolein, etc are the various hydrocarbons, which are very hazardous to a human being. Inhalation of HC emission can damage the liver, skin, kidney. It may show symptoms like coughing, sneezing, or eye irritation [4].

### **1.2.3 Effect of NO<sub>x</sub> emission**

High combustion temperature and lean air-fuel mixture are the favorable conditions to produce NO<sub>x</sub> emission in the IC engine. NO<sub>x</sub> emission is a very hazardous emission for a human being. Inhalation of low level of nitrogen oxide can irritate eyes, nose, throat, probably causing to coughing, breath shortness, tiredness. Inhalation of high nitrogen oxide can cause rapid burning, swelling of throat and upper respiratory system, the reduced oxygen level in tissues, generate fluid in the lungs may cause death [4]. High concentration of NO<sub>x</sub> may cause genetic mutations, it may harm the growing fetus, may decrease female fertility etc. If NO<sub>x</sub> combines with hemoglobin generates methemoglobin which produces an obstacle to the transformation of oxygen from the lungs to the body tissues. Also, NO<sub>x</sub> reacts with water and oxygen may fall into acid rain.

### **1.2.4 Effect of PM or smoke**

Particulate matter (PM) is produced in the rich air-fuel region in the combustion chamber, it may be produced due to incomplete combustion of the rich fuel region. PM is produced by the combination of carbon molecules with other chemical molecules such as hydrocarbon, sulfates, nitrates, and metals. PM includes smoke, soot, dirt, dust, and liquid droplets. Few particles are visible by naked eyes and some need microscope to see. PM is classified based on a particle size such as ultrafine particle, fine particle, and coarse particle. Inhalation of PM particles causes nonfatal heart attacks, irregular heartbeat, aggravated asthma, slow down lung function, premature death in people with heart or lung disease. PM particle is the most dangerous emission to human beings, inhalation of PM causes difficulty in breathing and long exposure causes cancer.

CO, HC, NO<sub>X</sub>, and PM are the most dangerous vehicle emissions for a human being. To reduce these kinds of emission and to reduce the gap of production and consumption of crude oil need to find advance combustion methods which have high fuel economy capacity and low emission. Indirectly efficient use of energy sources is energy saving. High thermal efficiency combustion mode is required to find. Also, the combustion mode is required who can replace conventional fuel (gasoline or diesel) use in IC engine. To reduce engine emission and to achieve stringent norms advance combustion strategy is required. To overcome these IC engine problems few strategies were used in the IC engine.

### **1.3 Advance combustion strategies**

Engine efficiency can be improved by the use of new technologies such as direct injection gasoline engine, variable geometry turbocharger (VGTs) [6–8], variable valve control (VVA), and variable compression ratio (VCR) systems [9,10]. In the direct injection gasoline engine, gasoline fuel was injected into the cylinder before the start of ignition to improve the fuel economy and reduce the NO<sub>X</sub> emission [11]. While in the VVA inlet valve closing and opening time varied to reduce the effective CR. Inlet valve close early or late, reduce the effective CR it leads to reduce the PRR and maximum in-cylinder pressure, due to which reduction in NO<sub>X</sub> emission. Further, in VCR engine different CR was handle by changing the clearance volume to control the combustion phasing and combustion temperature [9,12,13]. However, these strategies are more complicated as well as costly to incorporate in the conventional engine. Further to reduce the engine emission split injection, biodiesel blends, butanol blends [14], alcohol blends, catalytic converter, particulate filter, etc. was used [15,16]. By the use of oxygenic fuel in the blend it reduces HC, and CO emissions but it increased most hazardous NO<sub>X</sub> and soot emissions. Further, the blend fraction is limited to 20% or 30% in conventional (diesel or gasoline) fuels [17,18]. By using after-treatment methods energy losses may be possible due to extra backpressure [4,19].

In advanced combustion technology, homogeneous charge compression ignition (HCCI) engine is the most effective strategy. HCCI engine is a low-temperature combustion (LTC) strategy that helps to reduce NO<sub>X</sub> and soot emission. HCCI engine can achieve more stringent norms as well as it can adopt any fuel other than conventional fuels [20].

## 1.4 Introduction of HCCI engine

Homogeneous charge compression ignition (HCCI) is the low-temperature combustion (LTC) technology. In HCCI engine lean homogeneous charge prepared outside the combustion chamber (CC) supplied to the engine and due to compression, it reaches its autoignition temperature. Multiple sparks produce at an instant in the combustion chamber promote spontaneous combustion at low temperatures. HCCI engine operates on a combination of SI and CI engine mode [19]. In the SI engine, a homogeneous charge is prepared outside the engine cylinder, and combustion starts with the help of a spark plug. Whereas in CI engine air compressed in the engine cylinder and near to the compression stroke fuel get injected through the injector to start the combustion. However, in the case of HCCI engine, homogeneous charge preparation and compression ignition both operations performed in a single mode [21,22]. **Figure 1.3** shows the comparison of SI, CI, and HCCI engine. The homogeneous nature of air-fuel mixture in the HCCI engine reduces fuel-rich region in the combustion chamber assist to reduce PM emission or smoke opacity. However lean air-fuel mixture and spontaneous combustion reduce combustion temperature assist to reduce NO<sub>x</sub> emission. Whereas CI engine operates on heterogeneous nature of air-fuel mixture initiate to produce high PM and NO<sub>x</sub> emission and SI engine has a high flame propagation which results in high combustion temperature leads to high NO<sub>x</sub> emission [23].

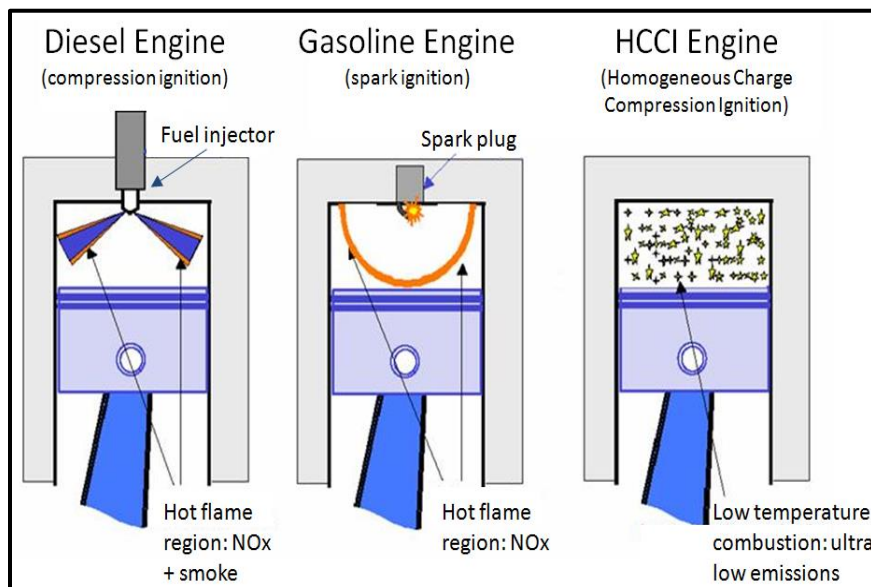


**Figure 1.3** Comparison of SI, CI, and HCCI engine [24]

In the SI engine, there are throttle losses and low CR promotes low brake thermal efficiency (BTE), while in CI engine high-temperature combustion increases heat transfer losses promotes low BTE. However, in the case of HCCI engine, no throttle losses or heat losses initiate to increase its BTE compared to SI or CI engine. HCCI engine can operate at high CR assist to improve its BTE. The most unique and attractive characteristic of HCCI engine is that it can accommodate any fuel for combustion. SI engine or CI engine can operate at particular fuel such as for SI engine gasoline is required and for CI engine diesel is needed. Conversely, HCCI engine can operate at various fuels such as gasoline, diesel, biodiesel, alcohol-based fuels, natural gases, biogases, etc.

**Table 1.2** Comparison between conventional SI engine and HCCI engine [25]

Features of comparison	SI engine	HCCI engine
Compression ratio	Low	High
Efficiency	Less	More
Combustion duration	More	Less
Combustion flame	Flame propagation	Multipoint autoignition
Injection type	Manifold injection	Both manifold and direct injection
Throttle losses	More	No
NO <sub>x</sub> emission	Comparatively more	Less
Major emission	CO, HC, and NO <sub>x</sub>	CO and HC emission

**Table 1.3** Comparison between conventional diesel engine and HCCI engine [25]

Features of comparison	CI engine	HCCI engine
Combustion temperature	1900-2100 K	800-1100 K
Efficiency	High	Equally high
Combustion duration	More	Less
Combustion flame	Diffusive flame	Multipoint autoignition
Injection time	Direct injection	Both manifold and direct injection
Cost	Comparatively high	Less
PM and NO <sub>x</sub> emission	More	Less
Major emission	NO <sub>x</sub> and PM	HC and CO emission

**Table 1.2** shows the comparison between the SI and HCCI engine and **Table 1.3** shows the comparison between the CI and HCCI engine.

#### 1.4.1 Advantages

- High CR, no throttle losses, and other losses lead to improving thermal efficiency in HCCI engine.
- Lean homogenous air-fuel mixture outside the combustion chamber assist to reduce PM or smoke opacity and NO<sub>X</sub> emission.
- HCCI engine having high fuel flexibility hence it can easily replace diesel or gasoline by alternative fuel.
- HCCI engine cost is less than the SI engine because there is no need of a spark plug or throttle valve.

#### 1.4.2 Disadvantages

- Difficult to start at cold condition.
- CO and HC emissions are high.
- Autoignition is difficult to control, hence pressure rise rate (PRR) and heat release rate (HRR) is high and engine is unable to run at high load condition.

#### 1.4.3 Challenges in HCCI engine

HCCI engine is working on LTC strategy, in this lean homogeneous charge was supplied to the engine cylinder, it leads to reduce engine combustion chamber temperature. If the atmospheric temperature is very low then the initial air temperature contributed to the combustion chamber temperature and getting difficult to start the ignition. Further due to LTC combustion HCCI engine produce high HC and CO emission. In the HCCI engine, spontaneous combustion occurs when fuel reaches its autoignition temperature, there is no combustion controller like SI engine has spark plug, and the diesel engine has an injector. At high load conditions, there is difficult to control engine combustion [26][27]. HCCI engine has various challenges as shown in the **Figure 1.4.**

#### ***1.4.3.1 Difficult to start in cold condition***

HCCI engine has a hurdle to start at geographical cold places. HCCI engine combustion was completed at low temperature due to a lean homogeneous mixture. Compressed charge emits more heat to the cold engine cylinder at cold atmospheric conditions. So HCCI engine is not able to start the ignition of fuel in such cold conditions [28]. To overcome this challenge glow plug can be used in the combustion chamber to warm up the engine for short period at the time of engine start. Also, this problem can be overcome by starting the engine on conventional SI or CI mode for a short warm-up duration and then shift to HCCI mode.

#### ***1.4.3.2 High HC and CO emissions***

In the HCCI engine, NO<sub>x</sub> and PM emission were highly reduced but HC and CO emission got increased more. HC and CO emission mainly produce due to the absence of oxygen means too rich air-fuel mixture or too lean air-fuel mixture. Some portion of air-fuel mixture accumulate in the cylinder piston crevices and escaped from the combustion at the time of compression. Due to low-temperature burn gas flame unable to consume this re-entered unburned air-fuel mixture at the time of expansion stroke promotes more HC and CO emission [29]. Further due to very low-temperature combustion HC and CO are unable to complete oxidation into H<sub>2</sub>O and CO<sub>2</sub> respectively. LTC promotes cylinder impingement and leads to produce more HC and CO emissions. This impact on combustion efficiency of the engine, low combustion efficiency leads to deteriorating HCCI engine performance at low load conditions than high load conditions. Whereas the use of a catalytic converter can reduce these HC and CO emissions, but catalytic converter assists to increase backpressure and impact on engine efficiency [5].

#### ***1.4.3.3 Combustion phasing control***

One of the supreme challenge of HCCI engine is to control combustion. In HCCI engine there is no combustion control, whenever fuel reaches its autoignition temperature by compression spontaneous ignition may arise. However, in SI engine combustion control on spark timing and CI engine combustion control on fuel injection timing. Premixed homogeneous air-fuel mixture autoignition depends upon multiple parameters such as fuel chemical properties, engine specification, and uncontrolled parameters. Combustion control of HCCI engine depends on the autoignition temperature of the fuel, octane number of fuel, latent heat of vaporization (LHV), compression ratio (CR), residual rate, exhaust gas recirculation (EGR) concentration, wall

temperatures, inlet temperature, and pressure of fuel, homogeneity of mixture, cooling temperature etc. Therefore HCCI combustion control at various load and speed conditions is a challenging task. Combustion control directly influences engine power output and engine efficiency. If too early combustion occurs before top dead center (bTDC) gives less power and low thermal efficiency, whereas combustion retarded after top dead center (aTDC), increases misfiring chances. Hence to control the combustion is an interesting task in HCCI engine. It can also control by VCR and VVT.

#### 1.4.3.4 Extend the operating range

HCCI engine is not able to operate at mid-load or full load conditions. It is more suitable for low-load conditions. Controlling the combustion for full load and high speed is the main challenge in HCCI engine. HCCI engine works on self-ignited spontaneous combustion. If the load increase on the engine, fuel demand increases, more fuel liberate more heat energy in the spontaneous combustion. Whenever more fuel burns at instant, combustion pressure and heat release increases abruptly. Its HRR and PRR are more than its normal operating range. It may lead to engine knocking and vibration. Seviour vibration and engine knocking may lead to physical damage of engine accessories such as piston, connecting rod, engine cylinder, engine outer parts, etc. To extend the operating range for wide load conditions and high speed, combustion duration should increase. Extend the operating range of two different reactivity fuels, different fuel blends, EGR implementation, etc may be useful [4].

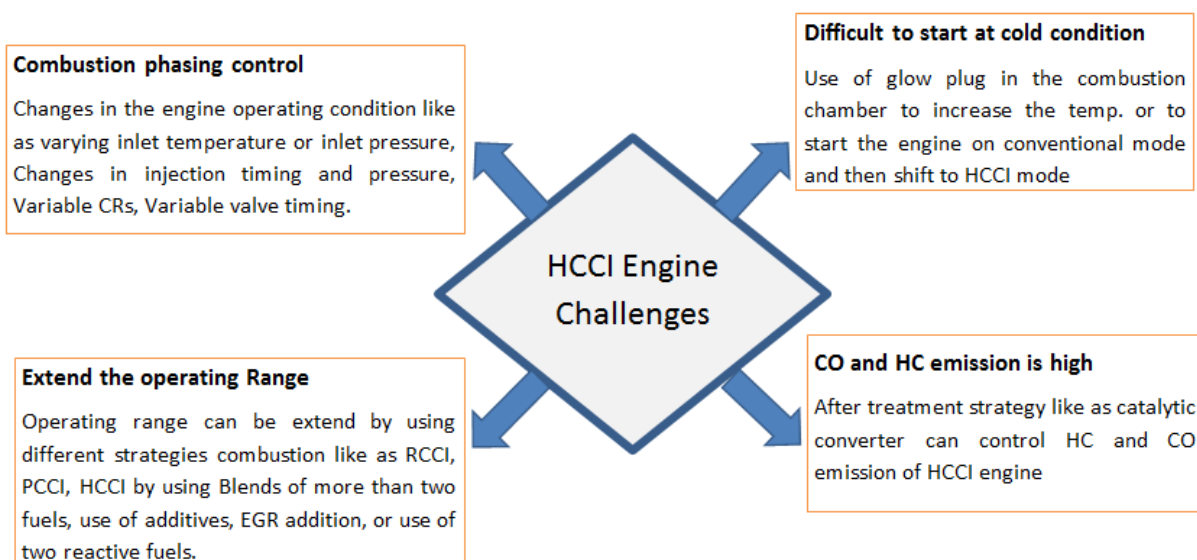


**Figure 1.4** HCCI engine challenges and remedies

These are the main challenges of HCCI engine. Control the combustion and extend the operating range is the major hurdle of HCCI engine. To extend the operating range and elongate the combustion various strategies are used in HCCI engine.

Dual fuel HCCI engine strategy will overcome the existing problem by supply of various alcohol-based fuels in different proportion at the time of suction stroke. Further to ignite the alcohol-based fuel homogeneous mixture diesel need to supply at the end of compression stroke. This leads to control the sudden pressure rise rate and therefore engine run at all load conditions with lower NO<sub>x</sub> and smoke opacity without a penalty of fuel consumption.

## **1.6 Introduction of present research on dual fuel mode HCCI engine**

In the present research study, a single-cylinder CI engine is converted into dual fuel mode HCCI engine by attaching a carburetor to the outside of the engine manifold. Alcohol-based high volatile fuel supplied through the carburetor at the time of suction stroke and diesel or biodiesel fuel was injected into the engine cylinder. To vary the mass flow rate of alcohol-based fuel different diameter fuel jet was used in the carburetor. In this research, the alcohol-based fuels were compared and the best alcohol-based fuel was found for dual fuel HCCI engine with lowest NO<sub>x</sub> and smoke opacity emissions without penalty of fuel economy. Optimum mass flow rate and optimum premixed ratio for each alcohol-based fuel under individual load conditions were examined with the help of simple additive weighting (SAW) method. Further, instead of diesel fuel supply, the biodiesel blend 20% or butanol blend from 10% to 30% was supplied to investigate the dual fuel mode HCCI engine performance and reduction of HC and CO emissions.

## **1.7 Thesis organization**

In the current study, six chapters are involved. Chapter-1 describes the outline of IC engine benefits, applications, and drawbacks. Further, conventional fuel consumption and production scenario. Impact of IC engine emissions on human health and environment. In this chapter, various advanced combustion methods are discussed to overcome the IC engine challenges. This chapter includes the basic working principle of HCCI engine, its advantages, and challenges.

Detail literature review of HCCI engine is included in chapter-2. In this chapter history of HCCI engine and its current research is discussed. Research finding and research objective for the current study based on literature gap is included.

In the next chapter-3, research methodology, selection of engine, selection of carburetor, and alcohol-based fuel for the current research are explained. Detailed experimental setup for dual fuel HCCI engine is described. Specifications of all engine apparatus and measuring instruments are included.

Chapter-4 includes the detailed experimental procedure of dual fuel HCCI engine. All required combustion parameters and performance parameters definitions are explained with formulae. Detailed optimization procedures and methods with different weightage are explained in this chapter.

In chapter-5 all experimental results are discussed. The influence of carburetor location on engine performance and emission was explained in the first objective of chapter-5. Influence of different mass flow rates on engine emissions and performance is explained with the optimum premixed ratio for each load condition in objective-2 of chapter-5. Different alcohol-based fuel performance was compared in objective three of chapter-5. Chapter-5 represents the experimental results of the dual fuel HCCI engine for different load conditions.

Finally, the overall conclusion of this current research is drawn and some future recommendations are included in chapter-6.

## **Chapter – 2**

### **Literature Review**

---

## 2.1 General

Widening the operating range and controlling the combustion are the major challenges of HCCI engine. To extend the operating range and elongate the combustion duration various strategies are used in HCCI engine. HCCI engine is classified based on homogenous charge preparation. Availability of proper homogenous charge at a suitable time in the combustion is the heart of HCCI engine. A proper homogeneous mixture improves the combustion process and gives high fuel economy and low engine emissions. HCCI engine is classified based on homogenous charge preparation. High viscous or low volatile fuels are making obstacles to form a homogenous mixture. So by understanding different fuel nature homogenous charge preparation for HCCI engine is necessary. External homogenous charge preparation was done outside the engine cylinder at the time of suction stroke by using port injection, manifold injection, fumigation, or open throttle carburetion, etc. Whereas internal homogenous charge preparation was done in the engine cylinder by varying injection timing, early injection, late injection, and multiple injections.

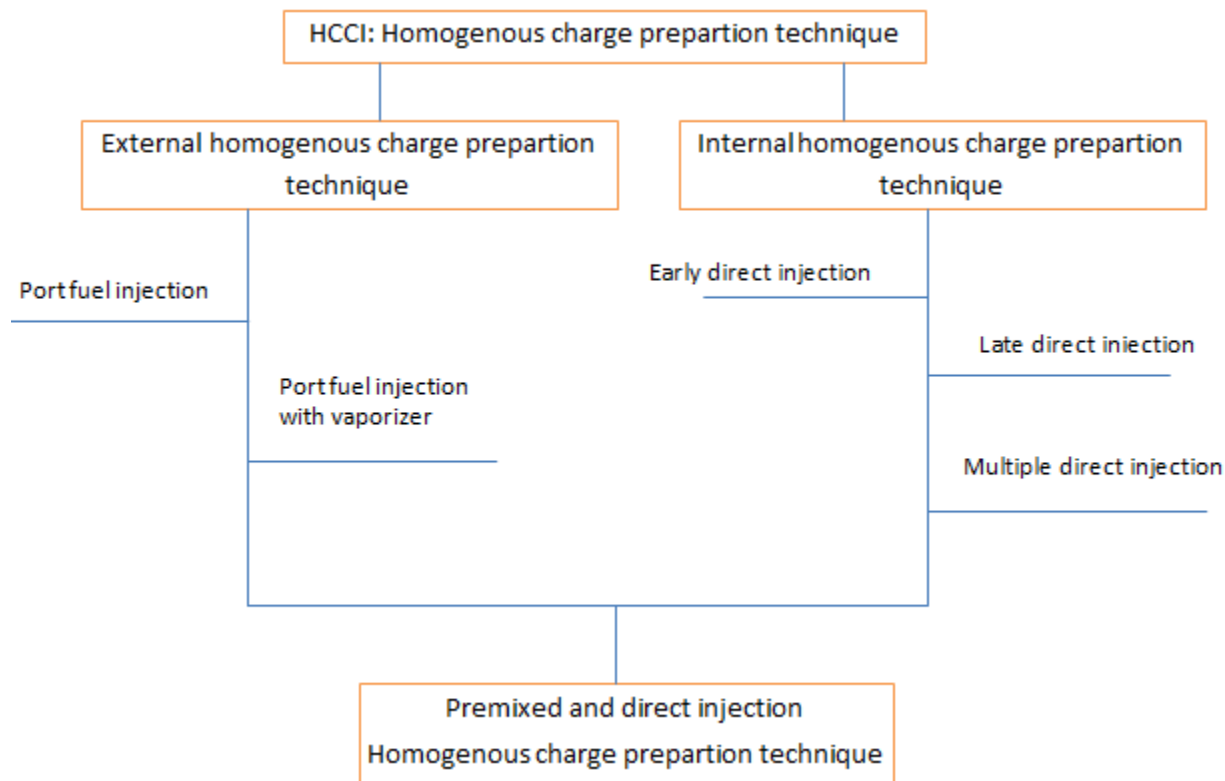


**Figure 2.1** HCCI engine classification based on homogenous charge preparation

## 2.2 External homogeneous charge preparation technique

The homogeneous charge prepared outside the engine cylinder is the supreme efficient technique for gaseous, or more volatile nature fuels such as gasoline and alcohol-based fuels. This technique is more effective because more time is available for the preparation of homogenous charge before ignition. In this strategy, fuel is mixed with the fresh air at the time of suction stroke. To inject the fuel, port injection, manifold injection or open throttle carburetion is a suitable method.

First HCCI engine mode combustion was implemented in the SI engine in 1979. Onishi et al. [30] performed HCCI combustion process on two-stroke engines. There was spontaneous combustion done at a time and there is no flame propagation. They called it “active-thermo atmosphere combustion” (ATAC). In the ATAC start and end of combustion were not specified. Moderate performance was observed for low load conditions only. Further, stable operation and absence of misfiring occurred in the wide range of part throttle operations.

The same combustion was demonstrated at the Toyota Motor Co. Ltd. and named as “TS (Toyota-Soken) combustion” Noguchi et al. [31]. This self-ignited combustion is called “RUN-ON” combustion. They carried out experiments with a horizontal opposed-piston two-stroke SI engine. It was observed that at no-load conditions HC emissions and fuel consumption were improved.

Later Thring [32] exhibits that HCCI can operate at high EGR and high inlet air temperature. Further, he concluded that four-stroke engine can operate on HCCI mode for low load and low speed, which gives low and high fuel economy compared to a conventional CI engine.

With the help of Honda R&D Co., Ltd Ishibashi Y. et al. [33] worked on self-ignited two-stroke gasoline engine and name it activated radical combustion (ARC). The ARC improved fuel economy and reduced HC emissions by 57% and 60% respectively.

Aoyama et al. [34] manufactured premixed charge compression ignition (PCCI) engine by the use of gasoline port injection. Air fuel range of 33-44 was given for stable PCCI engine performance. For extending the stable combustion range inlet air heating and supercharging were useful. PCCI engine operated stably at 80 air-fuel ratio with  $170^0$  C inlet air temperature. PCCI

engine achieved low NO<sub>x</sub> emissions but low fuel economy because of little stable range of combustion.

For the initial research above researcher used a two-stroke or four-stroke gasoline engine for HCCI combustion and a homogenous charge was prepared outside the engine cylinder. Further to control the ignition timing various researchers used exhaust gas recirculation (EGR), varying inlet temperature and pressure, varying swirl ratio, varying CR, VVT, etc strategies in the external mixture formation HCCI engine [35,36]. An engine control unit (ECU) was used to control the HCCI engine combustion by varying EGR substitution ratio, VVT [37]. EGR contains various gases that assist to absorb temperature leads to increase ignition delay (ID). To change the fuel quantity and EGR adjustment in HCCI engine for extension of load limit variable valve timing (VVT) method is appropriate. In VVT early closing of exhaust valve and late opening of inlet valve can trap exhaust gases in the engine cylinder, which may help to delay the start of combustion (SOC) of homogenous fuel [38] [39].

Lei Shi et al. [38] implemented external and internal EGR to extend the combustion duration of HCCI engine with the help of VVT. It was revealed that cooled external EGR can delay combustion leads to avoid knocking at high load conditions. An increase in EGR percentage in HCCI combustion reduced NO<sub>x</sub> emission compared to a diesel engine. Also if the EGR percentage increased in the HCCI engine won't affect smoke opacity however if EGR increased in a conventional diesel engine it effect on smoke opacity due to lack of homogeneity (high fuel-rich region). Due to lack of oxygen and incomplete combustion in HCCI engine CO emission was increased.

Nakano et al. [40] used EGR with varying inlet temperatures to control HCCI ignition. In this study, three different fuel blends (65% iso-octane plus 25% toluene plus 10% n-heptane) were used for the preparation of a homogenous charge. Substitution of EGR increased ignition delay (ID) and increasing inlet temperature promoted the combustion. It was observed that cooled EGR can control the HCCI combustion.

The preparation of low volatile or viscous fuel (diesel or biodiesel) homogeneous charge outside the engine cylinder is difficult. With high viscous fuel, HCCI engine is not able to achieve low emission and high fuel economy. Diesel vaporizer is the tool to vaporize the low volatile fuel in the vaporization chamber. In the diesel vaporizer, the copper vaporizing chamber is covered with

a band heater and that controlled by ECU. In the vaporization warm-up time and cut-off time need to control for that purpose proportional integral derivative (PID) controller is required. Low volatile fuel and air send to vaporization unit for the preparation of homogeneous mixture outside of engine cylinder [41].

To achieve a homogeneous charge of air and fuel Ganesh et al. [42] inducted diesel in a vaporizer before the engine cylinder. In the vaporizer, diesel is heated at 90° C to acquire the diesel fuel in vapor form. Also to control the early ignition of vaporized diesel, cooled EGR strategy was implemented. It is concluded that diesel vapor induction with 10% EGR reduced more NO<sub>x</sub> and smoke opacity compared to diesel vapor induction without EGR. Further, it was observed that this strategy was applicable up to 75% load condition, at high load condition combustion is not under control so shifted on conventional diesel mode. Also, it gave low fuel economy because of vaporization losses and unburned fuel consumption.

A similar kind of experimentation was done by Ganesh et al. [43] for high EGR percentage (10%, 20%, 30%) with vapor form of diesel in HCCI engine. It was observed that the lowest NO<sub>x</sub> and smoke emission was attained for diesel vapor induction with 30% EGR in HCCI engine with 12% more fuel consumption penalty compared to baseline diesel engine.

Maurya, and Agarwal [44] introduced port injection technique for the external homogenous charge preparation in HCCI engine. Ethanol fuel was injected into the intake manifold with the hot fresh air. Intake air temperature increased with the help of preheater in the intake manifold and varied from 120, 140, and 160° C at different air-fuel ratios. The whole system was controlled by ECU and engine experiments performed for different intake air temperatures with varying air-fuel ratios at a constant speed. It was observed that richer mixture ignited properly for low intake air temperature, conversely richer mixture tends to knock or very high-pressure rise rate may occur with increasing intake temperature. However higher intake air temperature gives good HCCI engine combustion performance for a leaner mixture.

Gajendra et al. [45] used biodiesel blend 20 and 40 instead of diesel for external homogenous charge preparation and examined the effect of biodiesel blend over diesel vaporization. In this study, port injected fuel vaporization was done in the vaporizer, and to control the combustion various EGR substitution (0%, 15%, and 30%) was used. Biodiesel blend HCCI engine showed more stable results compared to diesel HCCI engine. However, a reduction in fuel economy and

power output was observed with a minor increase in CO, HC, and smoke emissions. Because biodiesel blend has low calorific value and less evaporation rate which impact on fuel economy and smoke emission. But a significant reduction in NO<sub>x</sub> emission was observed for biodiesel HCCI engine.

Cinar et al. [46] used VVT mechanism to trap the hot exhaust gases in the gasoline HCCI engine. Inlet air temperature also changed between 20<sup>0</sup>C to 120<sup>0</sup>C to vaporize the fuel and a four-valve mechanism was used to extend the operating range of HCCI engine. Low valve lift can trap the hot exhaust gases and help to extend the combustion duration for a rich mixture. It assists to avoid misfiring or knocking at higher load conditions.

Harisankar and Murugan [47] performed a similar kind of experiment for ethanol HCCI engine. In this study, inlet air temperature varied from 130<sup>0</sup>C to 170<sup>0</sup>C, and ethanol fuel was injected in the inlet manifold. It was concluded that 170<sup>0</sup>C inlet air temperature improved brake thermal efficiency and combustion efficiency compared to the rest of the inlet air temperature. Further NO<sub>x</sub> and smoke reduced a lot but HC and CO emissions got increased.

The same kind of work was carried out by Girish, and Suryawanshi [48] in HCCI engine, they called this combustion as PCCI. They used vaporized diesel with EGR and without EGR. With EGR NO<sub>x</sub> and smoke were reduced but HC and CO showed increment with low fuel economy in without EGR PCCI engine compared to CI engine. Further with 30% EGR PCCI engine reduced more NO<sub>x</sub> emission but high HC and CO emission was observed.

Computational study was carried out by Karthikeya et al. [49] to investigate the effect of induction swirl, boost pressure, equivalence ratio, compression ratio, and EGR concentration on HCCI engine performance parameters. In this study diesel homogenous charge was prepared outside the combustion chamber. They reported that when swirl ratio of 4 with 30% EGR then 21% reduction in peak pressures compared to a swirl ratio of 1 with 0% EGR. It was found that for reducing peak pressure lower compression ratios, higher EGR concentrations, lower equivalence ratios, lower boost pressures, and higher swirl ratios were favorable conditions for HCCI engine combustion.

In this external homogeneous mixture formation, various strategies were used by various researchers to achieve the HCCI engine smooth combustion. **Figure 2.2** indicates the various names of external mixture formation strategies of HCCI engine.

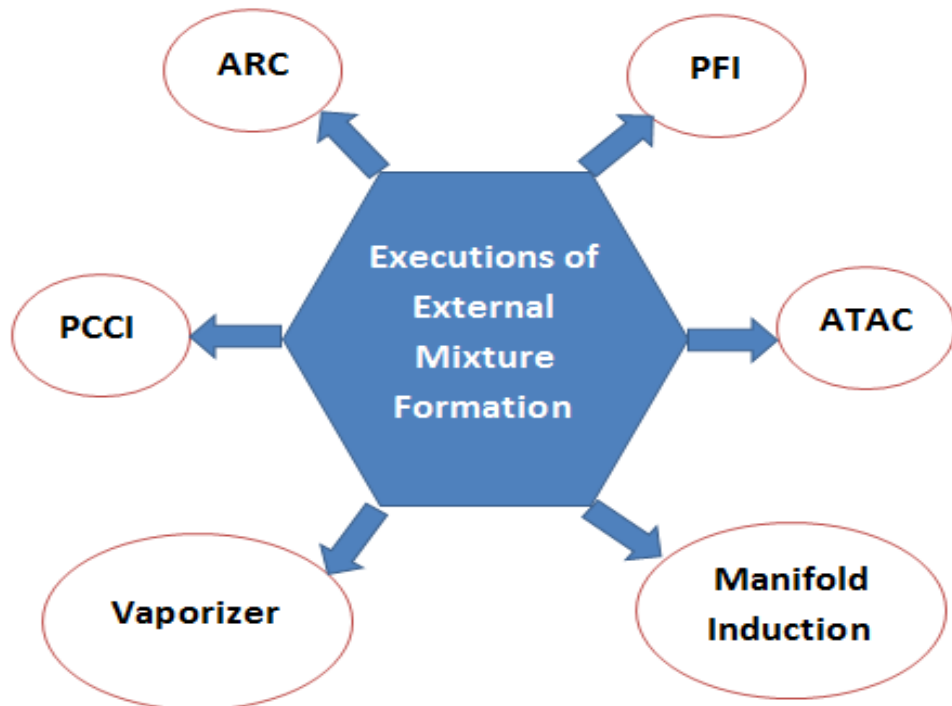


**Figure 2.2** Execution of early external homogenous charge preparation strategies

## 2.3 Internal homogenous charge preparation

In this strategy, a homogenous charge is prepared in the engine cylinder by varying the injection timing. In the conventional diesel engine fuel is injected near the TDC, but in this technique, early fuel injection, late fuel injection, or multiple fuel injection was done to control the HCCI engine combustion. In the early fuel injection, injection is done in the compression stroke before TDC however in the late injection, injection is done in the power stroke after the TDC. While multiple injection fuel was injected more than two times in the compression as well as in the power stroke means before TDC and after TDC.

### 2.3.1 Early direct injection

Early direct injection method is mostly used in the diesel engine to prepare the homogenous charge before combustion. Early injection tolerates more ID which makes proper air-fuel mixture leads to autoignition. In the early injection, fuel is colliding on the cylinder wall and some fuel particles get stick to it. When high fuel demand increases more fuel gets to accumulate on the cylinder wall. Because in this method injection is done when the cylinder not near to the TDC or mid of the compression stroke so fuel get an adequate cylindrical area to accumulate on the wall.

Due to the accumulation of fuel particle on the cylinder liner excess incomplete combustion happen which leads to increase PM or soot and HC emission more. This problem can be overcome by using a sophisticated high injection pressure system with narrow-angle direct injection (NADI). Another challenge of early direct injection HCCI combustion can be overcome by advanced injection strategy. All advanced injection and combustion strategies for early direct injection are shown in **Figure 2.3**.

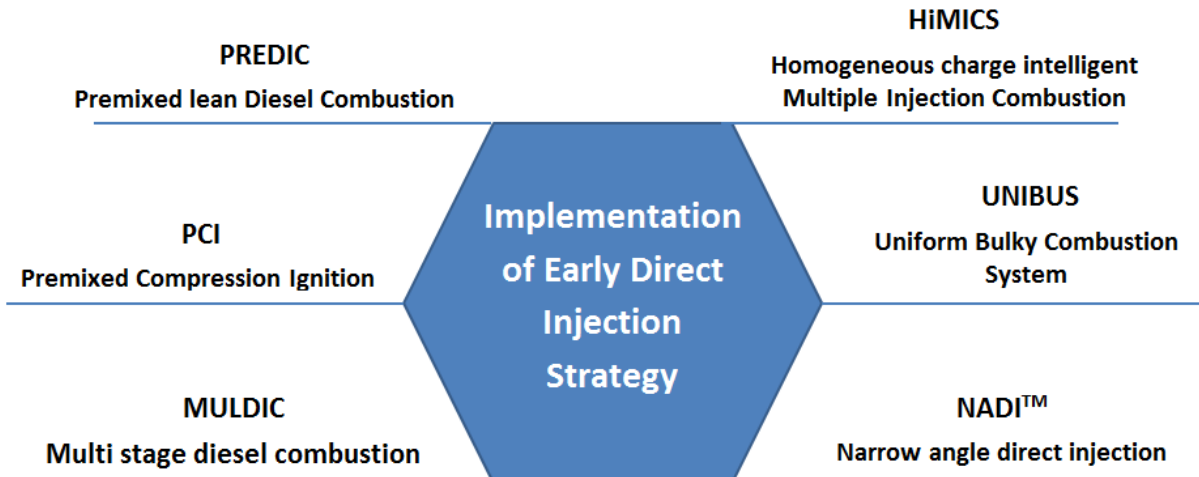


**Figure 2.3** Early direct injection strategy

#### **2.3.1.1 Premixed Lean Diesel Combustion (PREDIC)**

Premixed lean diesel combustion (PREDIC) is the advanced injection method was used by Takeda et al. [50] to avoid fuel collision on the cylinder wall. In this study, early in-cylinder fuel injection was done to achieve a homogenous air-fuel mixture. Three different fuel injector was used, one at center and rest at two sides of the cylinder. At the same injection timing side injector injecting fuel at the center of cylinder. At that instant collision of two fuel sprays may occur at the center of cylinder and injection of fuel spray on cylinder wall was avoided. Due to this proper homogenous mixture is prepared at the center of the cylinder. In this study NO<sub>x</sub> emission was greatly reduced however HC and CO got increased. Influence of swirl was not shown great influence on NO<sub>x</sub> emission. This early injection HCCI engine may perform for partial load condition which was handled by lean mixture, for high load condition difficult to control the combustion.

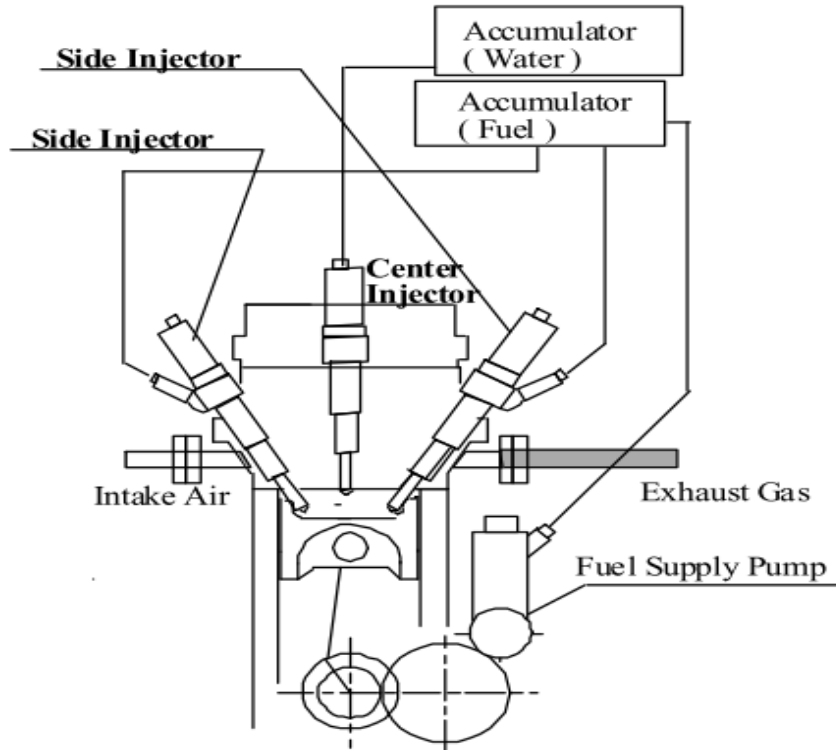


**Figure 2.4** PREDIC strategy with water injection [51]

A similar PREDIC strategy was used by Nishijima et al. [51] to reduce  $\text{NO}_x$  and HC emission simultaneously with considerable improvement in fuel economy. In this study, the third injector injected water to extend the combustion duration and to control the HC emission. **Figure 2.4** shows the experimental setup. First injection was done  $-30$  or  $-40^\circ$  aTDC and then water injection was done at  $-180$  or  $-270^\circ$  aTDC. Also, the water injection quantity was equal to the fuel injection quantity for the control of HC and CO emission. Finally, it was concluded that the split injection at  $-40^\circ$  aTDC and water injection at  $-180^\circ$  aTDC can simultaneously reduce  $\text{NO}_x$  and HC emission with fuel consumption improvement in PREDIC mode.

### 2.3.1.2 Premixed compression ignition (PCI)

PCI combustion strategy was used to reduce fuel consumption, expanding the load range, and reduce HC emission. Iwabuchi et al. [52] used premixed compression ignition (PCI). In this study, fuel was injected early in the compression stroke and fuel gets ignited at its self-ignition temperature. To avoid the fuel collision on engine cylinder nozzle with an angle of  $80^\circ$  was used, which is throwing downward spray compared to conventional engine spray. Further engine

operating range with PCI combustion was limited; it was useful for low load conditions only. PCI combustion was found to be more clean (reduction in  $\text{NO}_x$  and smoke emission) and efficient compared to a conventional diesel engine, however, HC emission produced more.

### 2.3.1.3 Multi-stage diesel combustion (MULDIC)

Multi-stage diesel combustion (MULDIC) is developed to overcome the PREDIC strategy challenge like a low operating range. In this combustion mode, three injectors used like as PREDIC strategy, and combustion did in two stages. In the first stage, early injection was done to prepare the premixed lean mixture and spontaneous combustion occurred. Successively second stage injection done in the hot gases. Detailed injection timing and injection pressure is shown in **figure 2.5**. Hashizume et al. [53] used multi-stage diesel combustion (MULDIC) mode in diesel engine. This concept was used to reduce  $\text{NO}_x$  emission under higher load conditions. In MULDIC, first stage injection was fixed at 150deg bTDC, which corresponds to lean combustion produce low  $\text{NO}_x$ . And the second stage combustion related to diffusion combustion which was varied from 2deg bTDC to 30deg aTDC. It was concluded that in the second stage combustion  $\text{NO}_x$  produced more but fuel-rich combustion near to TDC reduced  $\text{NO}_x$  as well as smoke, however, fuel consumption was more compared to baseline diesel engine.

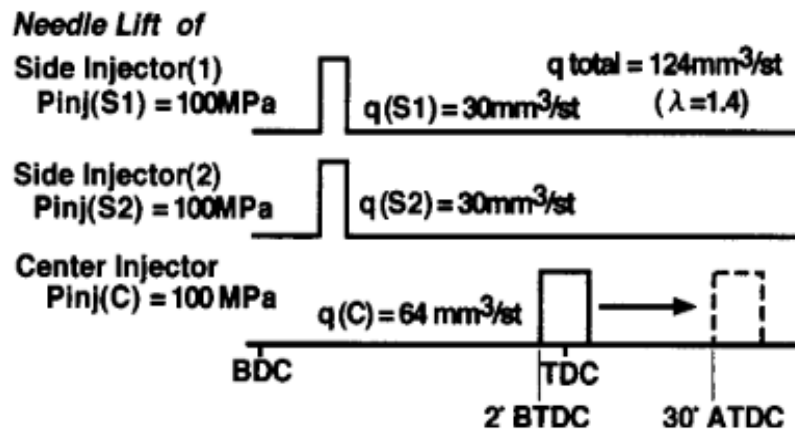


**Figure 2.5** MULDIC injection pattern [53]

### 2.3.1.4 Homogeneous charge intelligent Multiple Injection Combustion System (HiMiCS)

HiMiCS strategy was used to reduce simultaneously  $\text{NO}_x$  and smoke opacity. Yokota [54] incorporated HiMICS (Homogeneous charge intelligent Multiple Injection Combustion System) combustions which is the combination of premixed compression ignition combustion and

multiple injections. In HiMiCS concept, the pre-mixture was formed at the time of suction stroke to the mid of compression stroke. In this strategy pilot injection (P), main injection (M), Early injection (E), and late injection (A) like this multiple injections were used. Set of injections with quantity was shown in **Figure 2.6**. Narrow spray angle was used in order to permit multiple injections. It was concluded that  $\text{NO}_x$  and smoke were reduced at retarded injection timing, however, HC and CO emissions increased with less fuel economy.

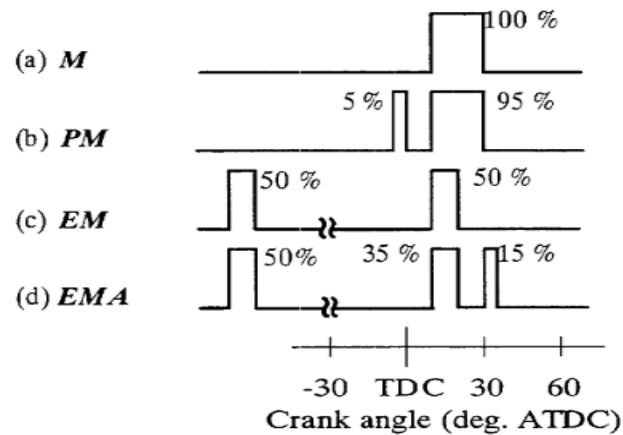


**Figure 2.6** HiMiCS injection pattern [54]

### 2.3.1.5 Uniform Bulky Combustion System (UNIBUS)

Hasegawa et al. [55] carried out experimentation on UNIBUS (Uniform Bulky Combustion System) mode. This technique was used to control combustion. In this strategy, two stages of combustion done, first done too early to form a premixed homogenous charge. Inlet temperature and pressure also control in such a way that high-pressure reaction should not start before the second injection.

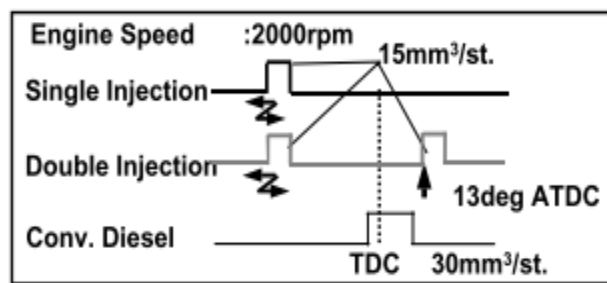


**Figure 2.7** UNIBUS single and double injection strategy [55]

The injection strategy is shown in **Figure 2.7**. In experiments, the first injection timing was varied from  $-54$  degrees aTDC to  $-4$  degrees aTDC and second injection timing is fixed that  $13$  degree aTDC. Low  $\text{NO}_x$  and smoke were observed in both injection stages.  $\text{NO}_x$  was reduced below  $70$  ppm and smoke near to zero was recognized in the Japanese test mode.

### 2.3.1.6 MULINBUMP compound combustion

Su et al. [56] used compound combustion technology by using multi-pulse fuel injection and BUPP combustion chamber. The premixed combustion was achieved by multi-pulse injection. This pulse injection timing, ideal time in between two pulses, duration for each pulse injection, number of pulses in one working cycle all are controlled. The aim behind this pulse control is to restrict the fuel spray penetration on the cylinder liner and to prepare a proper air-fuel mixture. Further, this premixed combustion proceeds in the BUMP combustion chamber to enrich the mixing rate with the help of BUMP ring which leads to lean diffusive combustion. Multi-fuel injection and BUMP combustion chamber are shown in **Figure 2.8**. Especially soot emission reduced a lot in the BUMP chamber, overall great reduction in  $\text{NO}_x$  and soot emissions was noticed for less load limit.

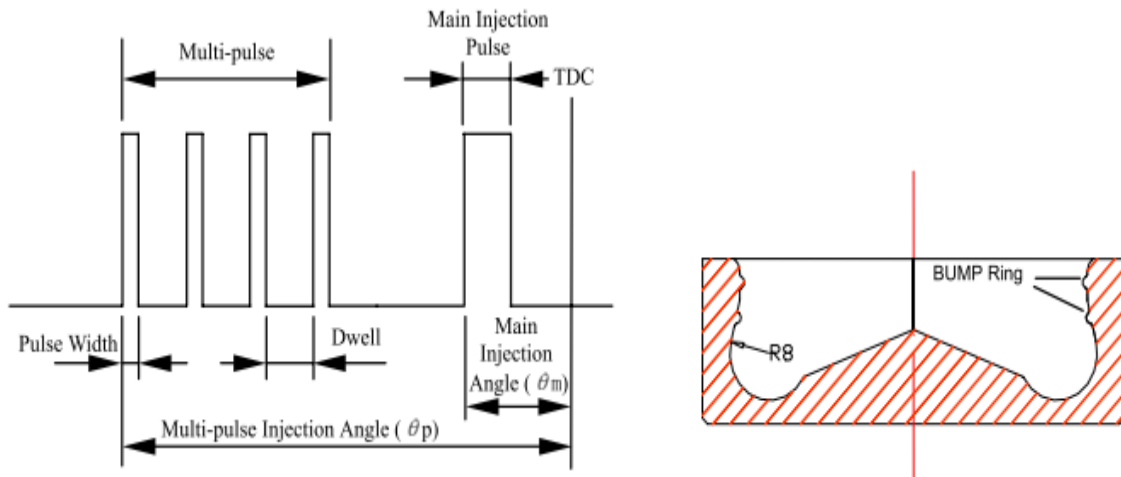


**Figure 2.8** Multi pulse injection and bump combustion chamber [56]

### 2.3.1.7 Narrow-angle direct injection (NADI<sup>TM</sup>)

In the very early direct injection more cylinder surface exposed to the fuel spray, fuel use to accumulate on the cylinder liner due to wide fuel spray angle in the conventional diesel engine. Narrow-angle direct injection (NADI) has the benefits to escape the fuel deposition on the

cylinder liner. Fuel spray should be at the center of the engine cylinder to avoid unnecessary HC and soot emission. Walter and Gatellier [57] used NADI<sup>TM</sup> strategy to extend the engine load range, and zero NO<sub>x</sub> and particulate matter emission. Less than 100-degree fuel spray angle was used to avoid fuel impingement.

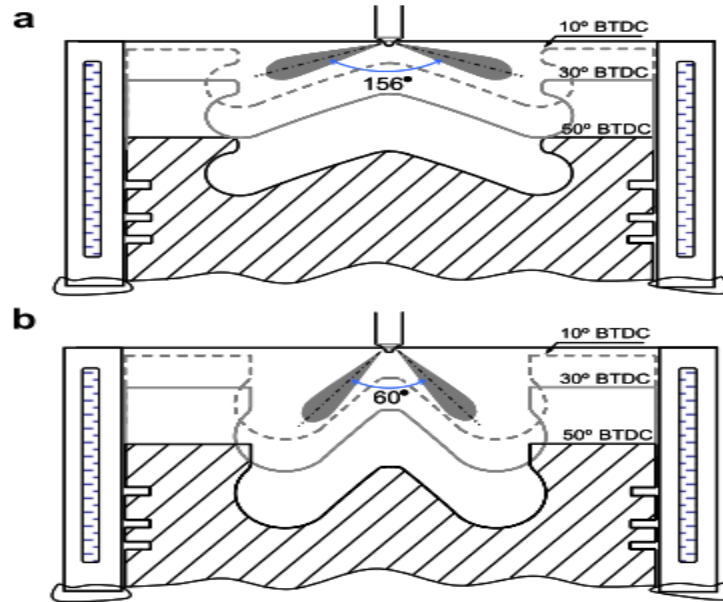


**Figure 2.9** (a) Diesel engine spray angle, (b) Narrow spray angle in HCCI engine [58]

Kim and Lee [58] used dual-injection technique with a narrow spray angle to suppress the NO<sub>x</sub> and smoke. In this study injection angle of the diesel engine was narrowed from 156-degree to 60-degree to avoid the fuel impingement on engine cylinder as shown in **Figure 2.9**. Also to avoid the advance ignition of premixed charge prepared by early direct injection CR reduced from 17.8:1 to 15:1. **Figure 2.9(a)** shows the conventional engine spray angle and **Figure 2.9(b)** shows the narrow injection spray angle. In this study, three different kinds of injection were used as conventional diesel injection, early injection, dual injection. It was revealed that dual injection strategy with narrow-angle spray reduced the NO<sub>x</sub> emission due to early HCCI combustion start by early injection and CO emission reduced by second late injection which leads to improving the fuel economy.

Reveille et al. [59] executed a CFD study to reduce the near zero NO<sub>x</sub> and Particulate matter by using NADI<sup>TM</sup> strategy in the dual mode engine. Dual fuel HCCI combustion mode applies for part-load condition and shifted to conventional diesel mode for high load condition. It was

observed that at part load condition almost zero NO<sub>x</sub> and PM emission achieved with good thermal efficiency.

### **2.3.2 Multiple direct injections**

Fang et al. [60] incorporated multiple injection techniques in a high-speed direct injection (HSDI) diesel engine to investigate the impact of injection angle and injection pressure. Two different spray angle was used that is 150-degree and 70-degree with two different injection pressure is 100 bar and 600 bar. The multi injection was done in two stages, the first injection was done at -40° aTDC means early injection, and the second stage injection done at 8° aTDC means late injection. In the first stage of injection with high pressure in the case of 150-degree angle, premixed combustion was observed with non-luminous flame while in the case of 70-degree two types of flame observed non-luminous and luminous. In the second stage of injection, ignition occurs near the spray tip of bowl wall in the case of 150-degree while in the case of 70-degree ignition occurs central region of bowl. 150-degree angle fuel spray performed like PCCI combustion with little soot emission, however in the case of 70-degree spray angle more soot was observed. Conversely, a 70-degree spray angle gives the lowest NO<sub>x</sub> emission for both injection pressure.

Dual-injection technique was used by Das et al. [61] to run the diesel engine on HCCI mode in order to reduce NO<sub>x</sub> and smoke emissions. In this experiment, pilot injection was made at the time of suction stroke and main injection at the end of compression near the top dead center (TDC). Experimentation was performed for constant speed and 0-67% engine load conditions. In this study premixed ratio was used from 0% to 80% and the effect of 15% and 30% EGR rate studied for 80% premixed ratio. It was found that increasing the mass of pilot fuel advances the start of combustion (SOC), PRR, and HRR. Further using 80% premixed ratio and 30% EGR reduced NO<sub>x</sub> by 76% and smoke opacity by 40%. From the study it was concluded that if premixed ratio rises from 0-80%, 17.8% peak pressure increases with 1.5 deg advancement; for the same peak pressure, reduced by 4.5% and 12.7% for 15% and 30% EGR respectively.

### **2.3.3 Late direct injection**

Late direct injection was developed to overcome the early direct injection problem like as extending the combustion range and simultaneous reduction of NO<sub>x</sub> and soot emission without

suppression in the fuel economy. Modulate kinetics combustion (MKC) developed by Nissan Motor Co., Ltd. [62,63]

### 2.3.3.1 Modulated kinetics combustion (MK Combustion)

Reduction of simultaneously  $\text{NO}_x$  and smoke with high fuel economy Kimura et al. [62] developed modulated kinematics combustion concept in the direct injection diesel engine. For the reduction of  $\text{NO}_x$  emission less concentration of oxygen is required to reduce the combustion temperature means EGR induction is a suitable option but it increases smoke. To reduce the smoke opacity more ID is required to get more time to preparation of fuel mixture. Hence injection timing retarded to extend the ID. Further to control the HC and soluable organic fraction (SOF) higher swirl with a toroidal combustion chamber was used. This avoided the cooling losses and improves the fuel economy. These all MK combustion schemes are explained in **Figure 2.10**. It was concluded that MK combustion can achieve high load conditions at a chemically corrected air-fuel ratio with less smoke. It was observed that  $\text{NO}_x$  emission was reduced by 88% and smoke was reduced up to 96% with suppression in fuel consumption.

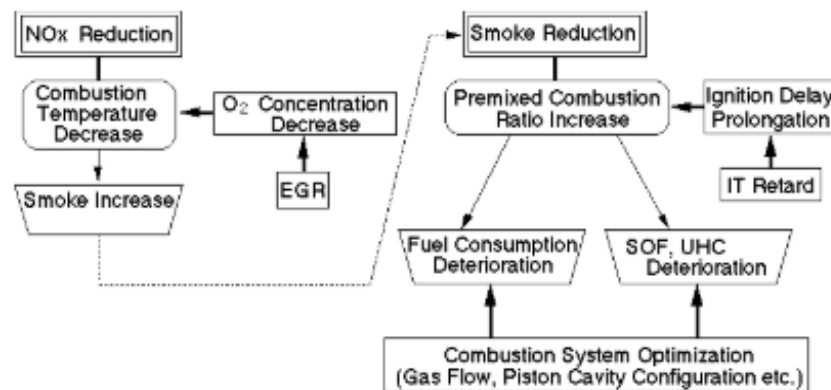


**Figure 2.10** MK combustion strategy [62]

In further research low CR, cooled EGR and high injection pressure were executed in the multi-cylinder engine to achieve premixed combustion at a wide load range. Also to avoid the HC emission combustion chamber design optimized and concluded that a large cavity is the best design for reduction of HC emission [63].

## 2.4 Premixed and direct injection homogenous charge preparation techniques

Premixed and direct injection homogenous charge preparation technique is the combination of external and internal direct injection charge preparation techniques. This technique can overcome the HCCI engine challenges like extending the operating range and control on combustion phasing with great improvement in fuel economy [5,64]. In the premixed charge preparation, a major quantity of fuel is injected in the suction stroke to prepare a suitable air-fuel mixture. To ignite the homogenous charge small amount of fuel is injected at the end of compression stroke directly into the cylinder. This technique is known as reactivity controlled compression ignition (RCCI) or dual-fuel HCCI (DF-HCCI) engine. In this technique, two different reactivity fuels choose for premixed combustion and direct injection. Low reactivity fuel means high autoignition temperature or high octane number fuel is used for premixed charge preparation because it has high knocking resistance ability. So fuel won't burn automatically in between the compression stroke. Whereas high reactivity fuels means high cetane number fuel or low octane number fuel used for in-cylinder direct injection to start the combustion. High reactivity fuel promotes combustion and burns quickly if injected in the high temperature and pressure mixture. Due to two different autoignition temperatures and octane number combustion duration may elongate which leads to sustain the wide range of engine load. Also due to direct injection of high reactivity fuel combustion may be in control which leads to reduce high-pressure rise rate (PRR) and heat release rate (HRR). Also to control the combustion by using two different reactivity fuels some researchers did changes in the fuel mixture or changes in the engine operating parameters. Various fuel was used to operate dual fuel HCCI (DF-HCCI) engine operation. Few used gaseous fuel in the manifold injection and high reactivity fuel for direct injection. Few used alcohol-based fuel for port injection and diesel or biodiesel for direct injection.

### 2.4.1 Gaseous fuel dual fuel HCCI engine

Gaseous fuels such as compressed natural gas (CNG), biogas, liquified petroleum gas (LPG), hydrogen, etc, have gaseous nature which can mix with the inlet fresh air to form a homogenous mixture.

Liquified petroleum gas (LPG) is a gaseous product of petroleum refining consist of propane, butane, and other light hydrocarbons. The transportation and storage of LPG are easier than the

remaining gaseous fuel. It can convert into a liquid at atmospheric pressure. The LPG has a high calorific value (CV) and high octane number. It will be a good fuel for DF-HCCI engine. LPG is a low reactivity fuel that can be used at the time of suction in the inlet port in a DF-HCCI engine [65].

Kumaraswamy, et al. [66] used LPG and diesel DF-HCCI mode engine. To control the combustion EGR incorporated with the LPG in the inlet manifold and to start the combustion pilot diesel injection done near the TDC. Experimentation was done at 20% to 100% load condition with EGR and without EGR for DF-HCCI engine. It was concluded that LPG with EGR reduces more NO<sub>x</sub> and smoke emission for all load conditions compared to without EGR. Conversely, thermal efficiency improved for the LPG without EGR dual-fuel engine compared to with EGR. However, use of EGR with LPG increased more HC and CO emission compared to conventional and without EGR, LPG HCCI engine.

Similar kind of research was done by Tira et al. [67] on LPG and diesel DF-HCCI engine with EGR at the time of inlet air. In this experimental study influence of different direct injection fuel such as rapeseed methyl ester and gas-to-liquid diesel fuels on engine combustion was investigated. Experimentation was done for three different levels of LPG i. e. 0.2%, 0.5%, and 1% of the total volume of inlet air. Engine operated for 3 bar and 5 bar IMEP engine load and EGR varied from 0% to 20%. The result showed that different direct injection fuel has no effect on HC and CO emission but there is considerable reduction was observed in NO<sub>x</sub> and soot emission. Gas to liquid diesel reduced highest NO<sub>x</sub> and soot emission compared to rapeseed methyl ester and diesel. Further EGR contribution was helpful to run the engine at a wide load range.

Brijesh et al. [68] investigated the LPG-diesel RCCI engine performance for 75% load condition. LPG was varied from 0% to 40% with an inlet fresh air at the time of suction, while diesel injected into the cylinder. Increasing the percentage of LPG reduced NO<sub>x</sub>, PM, and CO emission however HC was increased and thermal efficiency deteriorated. Further, they concluded that LPG-diesel RCCI recorded the lowest emission such as NO<sub>x</sub>, PM, CO with a tolerable range of HC and thermal efficiency for 10% LPG substitution.

Also instead of LPG, hydrogen is a good gaseous fuel for IC engines. Hydrogen is a clean emission fuel that does not produce CO<sub>2</sub>, CO, HC, or soot emissions. This promotes a high fuel

economy with clean combustion [69–71]. The various researchers used hydrogen in the SI engine or CI engine. Ibrahim and Ramesh [72] used hydrogen in diesel ignited DF-HCCI engine to investigate the influence of hydrogen to diesel energy ratio and EGR on HCCI engine combustion performance. An experiment was performed on 2 bar, 3 bar and 4 bar brake mean effective pressure (BMEP) with EGR and without EGR. Hydrogen is supplied with fresh air and diesel injected into the cylinder. It is observed that the hydrogen diesel DF-HCCI engine improved thermal efficiency without EGR for 2 bar load and with EGR for 3 bar and 4 bar load. NO<sub>x</sub> emission reduced with increasing the energy ratio of hydrogen but due to axial diesel injection CO, HC and soot were increased. Hydrogen diesel DF-HCCI engine shows a reduction in HC and CO emission compared to diesel HCCI engine.

Similarly, biogas is also the best alternative gaseous fuel for IC engine. Biogas is a renewable fuel that can be produced by anaerobic digestion of organic matter like cooking waste, agricultural waste, animal dung, and urban waste. In the biogas, methane contribution is a maximum which is around 60% and the remaining carbon dioxide. To run the engine-based generator biogas is the best option in a rural area. In the previous research, biogas was used in the SI engine and CI engine. Due to high octane number and high self-ignition temperature biogas is the best low reactivity fuel for dual fuel HCCI engine [73].

Mohamed Ibrahim et al. [74] carried out an experimental study to investigate the predominantly premixed charge compression ignition (PPCCI) mode engine performance. This engine worked like a DF-HCCI engine. They used biogas along with the air and diesel injected through the common rail system into the cylinder. Engine operated for 2 bar to 4 bar BMEP load with varying inlet charge temperature (ICT) from 40<sup>0</sup> C to 100<sup>0</sup> C and varying direct injection timing from 50<sup>0</sup> to 100<sup>0</sup> bTDC. The result showed that 55-70<sup>0</sup> bTDC was an effective injection range for diesel injection, 80% biogas from total energy, and 50-90<sup>0</sup> C were the best intake charge temperature for the best performance of the engine. However, in PPCCI mode HC and NO<sub>x</sub> level was less compared to dual fuel mode.

Further natural gas is also a good alternative that has high octane number and high autoignition temperature which can sustain a high CR HCCI engine. Natural gas is a mixture of several hydrocarbon molecules such as methane, ethane, propane, butane with an inert diluent such as nitrogen and carbon dioxide. In natural gas, methane is the main constituent compared to the rest

of the molecules. The contribution of molecules in natural gas depends upon geographical resources, time decay, treatment applied during production, etc. Further natural gas is clean emission fuel compared to conventional fuels [75]. Due to its superior properties, it is the best fuel to use as low reactivity fuel in the DF-HCCI engine. Nieman et al. [76] executed a numerical study by using a genetic algorithm (GA) on natural gas diesel RCCI engine. In this study, natural gas was injected into the inlet port and diesel was injected two times in the engine cylinder. The influence of methane amount, diesel injection timing and quantity, and the EGR substitution investigated on engine performance. Engine operated at low load, mid load, and high load conditions. Engine load varied from 4 bar to 23 bar indicated mean effective pressure (IMEP) and 800 to 1800 rpm. NO<sub>x</sub> and soot emission reduced greatly up to 13.5 bar IMEP load without the use of EGR with maintaining high efficiency.

Kakaee et al. [77] extended the previous research on natural gas diesel RCCI engine. In this study numerical study was done for 9 bar IMEP load with two different kinds of natural gas based on their internal composition (Methane number and Wobbe number). The performance was investigated base on fuel composition, different inlet temperatures, and different engine speeds. It was observed that increasing initial temperature increased NO<sub>x</sub> emission due to advanced combustion. Further higher wobbe number fuel increased NO<sub>x</sub> emission and lowers HC and CO emissions. At low engine speed with a lower Wobbe number produced more unburned combustion like HC and CO emission. They conclude that for higher efficiency and low emission higher Wobbe number is suitable for high engine speed conditions.

Numerical simulation study was done by Yousefi and Birouk [78] to investigate the effect of natural gas energy ratio and injection timing of diesel on DF-HCCI engine performance under low load conditions. In this study, natural gas was injected into the inlet port while pilot diesel was injected in the premixed combustion chamber for better mixing. Experimentation was done for 25% load condition with varying natural gas energy ratios from 0% to 60%. It was revealed that 50% natural gas energy fraction gives maximum thermal efficiency at 12<sup>0</sup> and 20<sup>0</sup> bTDC diesel injection timing. Increasing natural gas contribution reduced NO<sub>x</sub> emission and 60% natural gas energy fraction gives the lowest NO<sub>x</sub> emission. Further use of pre-combustion chamber reduced unburned methane emission by 46% compared to without premixed combustion chamber HCCI engine.

## 2.4.2 Gasoline diesel dual fuel HCCI engine

Yang et al. [79] implemented DF-HCCI engine strategy for the extension of HCCI engine load range. They used gasoline fuel in the inlet port and to ignite the premixed charge stratified direct injection of gasoline or methanol was done. Gasoline stratification leads to advance combustion and an increase more HRR and NO<sub>x</sub> emissions at higher load conditions. It assists to reduce fuel economy and CO emission. While methanol stratification prolongs the combustion because of delays the ignition timing which leads to reduce PRR and 50% load attain range was extended. Further NO<sub>x</sub> and CO emission got reduced however HC got increased due to methanol stratification compared to gasoline stratification.

Instead of throttle Xiao et al. [80] used EGR to control the combustion in gasoline diesel dual fuel HCCI engine. Gasoline was supplied in the inlet port and diesel injected in the cylinder. Influence of various gasoline energy ratios and different diesel injection times on engine combustion and performance was investigated for 4.3 bar to 8 bar IMEP engine load. Increasing the gasoline proportion delay the combustion which leads to reduce in-cylinder pressure and HRR. Further, late direct injection timing of diesel increased PM emission and reduced thermal efficiency. NO<sub>x</sub> emission reduced for increasing gasoline proportion and 77% gasoline ratio gave highest thermal efficiency.

Tong et al. [81] conducted an experimental study to examine the influence of polyoxymethylene dimethyl ethers (PODE) in place of diesel in gasoline diesel DF-HCCI engine. Gasoline was supplied through the inlet port at 133<sup>0</sup>bTDC and diesel or PODE directly injected into the engine cylinder. Further intake pressure of air varied from 0.18 MPa to 0.22 MPa for various gasoline premixed ratios (i.e. from 55% to 85%). It was concluded that gasoline with PODE gave a better performance in terms of thermal efficiency improvement and reduction in smoke compared to gasoline/diesel HCCI engine. Further gasoline/PODE engine can operate up to 1.76 MPa IMEP engine load with single direct injection while gasoline/diesel can operate up to 1.39 MPa IMEP with double direct injection. In both cases maintained low smoke and considerable thermal efficiency. However, in gasoline/PODE NO<sub>x</sub>, CO, HC was increased compared to gasoline/diesel engine.

Kavuri et al. [82] compared RCCI and gasoline compression ignition (GCI) combustion strategies at high load conditions (20 bar IMEP at 1300 rpm). It was observed that RCCI has

better combustion control compared to the GCI, due to the smaller ID of diesel than gasoline. However, GCI strategy gave less soot emission compared to RCCI. In another aspect, both strategies have high efficiency and fewer NO<sub>x</sub> emissions. It was observed that RCCI has high PRR compared to GCI but it was in an acceptable range for wide load conditions. GCI strategy was found to be more sensitive to adopt small changes in the inlet charge conditions compared to RCCI.

Tong et al. [83] incorporated DF-HCCI combustion and called it homogenous charge induced ignition (HCII). In this study, two different reactivity fuels such as gasoline through port injection and diesel as a direct injection were used. For various premixed gasoline ratios, engine performance was examined for 25% to 100% load. In this strategy, incomplete combustion was observed for 10% to 30% gasoline ratio, while high HRR occurred for above 90% gasoline ratio. But 70% to 80% gasoline ratio noticed as the best range for smooth combustion and lowest emissions. In this study, NO<sub>x</sub> and soot emission were reduced and fuel consumption also improved for DF-HCCI engine, conversely, HC and CO increased.

To extend the RCCI engine range Benajes et al. [84] increased piston bowl volume to reduce the CR from 17.5:1 to 15.3:1, in medium-duty gasoline diesel RCCI engine. Gasoline was injected into inlet port and diesel was injected into cylinder. In this strategy, three modes of combustion were used, up to 8 bar IMEP fully premixed RCCI combustion, then up to 15 bar IMEP highly premixed RCCI combustion mode and to achieve high load diffusive dual-fuel mode combustion was used. Fully premixed RCCI attained lowest NO<sub>x</sub> and soot emission at low load, while to reduce the knocking tendency diesel injection retarded in highly premixed RCCI strategy it helps to reduce NO<sub>x</sub> emission but little high soot emission attained compared to fully premixed RCCI strategy. To attain the combustion at 75% to full load diffusive dual-fuel combustion technique was suitable compared to the rest of the strategy. This technique shows little more NO<sub>x</sub> and soot compared to the rest of the strategy but higher thermal efficiency and emission than the conventional diesel engine.

Vipavanich et al. [85] performed the experimentation on a gasoline diesel DF-HCCI engine at 50% load condition. Gasoline was supplied through the manifold and diesel which is the combination of 95% pure diesel and 5% biodiesel by volume injected in the cylinder. The gasoline mass flow rate (MFR) varied from 0 to 0.06 g/s without EGR substitution. It was

concluded that with increasing the MFR of gasoline HRR, PRR was increased and combustion duration (CD) got shorten over a conventional diesel engine. Fuel consumption was reduced it leads to improving thermal efficiency.

Xu et al. [86] carried out an experiment on gasoline/diesel dual-fuel engine for optimization of gasoline fraction, diesel injection pulse, diesel injection timing, EGR rate under 70 Nm-1800 rpm load and 50 Nm-1400 rpm load. With increasing gasoline ratio NO<sub>x</sub> emission and soot emission reduced, 66% gasoline ratio showed highest fuel economy with a reduction in NO<sub>x</sub> and soot emissions. At load 50 Nm for 1400 rpm fuel consumption was more compared to diesel engine by single diesel injection strategy. It was observed that under higher load conditions double diesel injection was more suitable for the lowest NO<sub>x</sub> and soot emission with the highest fuel economy. Further addition of hot EGR improved fuel economy with low NO<sub>x</sub> and soot emission under 1400 rpm and 50 Nm load.

Wang et al. [87] conducted an experiment to determine the influence of several parameters (intake pressure, EGR rate, gasoline proportion, diesel injection timing, etc) on RCCI engine. Here gasoline was supplied at the time of suction and diesel was injected after compression of a homogeneous mixture. It was observed that gasoline/diesel RCCI engine was suitable for moderate to high load conditions with very low NO<sub>x</sub>, soot emissions, and improved thermal efficiency; however, for low load conditions, single-shot fuel injection was better. Further, high EGR rate, increasing gasoline fraction, and early injection timing was favorable for RCCI combustion at high load condition; conversely, very high EGR rate or more advanced fuel injection caused uncontrolled combustion.

Further experiments and numerical analyses were done by A. Lalwani et al. [88]; they used gasoline for port injection and diesel for direct injection. They concluded that HCCI mode possibly would not persist after 40% of engine load, hence after 40% engine load, the engine shifted on diesel mode. In HCCI mode, NO<sub>x</sub>, CO<sub>2</sub>, and thermal efficiency improved by 80%, 30%, and 15% correspondingly. However, HC and CO emissions severely increased at part load conditions compared to a conventional diesel engine.

#### **2.4.3 Methanol diesel dual fuel HCCI engine**

Various researchers executed methanol fuel in the inlet port of DF-HCCI engine. Methanol (CH<sub>3</sub>OH) is a low reactivity fuel compared to gasoline, which has a very high octane number and

very less cetane number. Methanol is the alternative fuel it can be produced from various biomass, natural gas, coal or it can be recovered from carbon dioxide (CO<sub>2</sub>) [89]. Methanol has a high latent heat of vaporization (LHV) and self-ignition temperature which leads to elongate the ID. More ID helps to produce proper premixed combustion in HCCI engine. Methanol has a superior combustion characteristic compared to gasoline fuel [90]. Alcohol-based fuels are always given superior combustion characteristics compared to gasoline fuel [91].

Yao et al. [92] employed methanol in the inlet port and diesel in the combustion chamber. They called it diesel methanol compound combustion (CMCC). The experiment was performed for 10% to 100% load conditions with two different engine speeds (i.e. 2200 rpm, 3200 rpm). In the DMCC combustion mode, longer ID was observed, due to high LHV of methanol. Further NO<sub>x</sub> emission was reduced a lot however CO, HC emissions were increased. Due to more soluble organic fraction PM emission also increased compared to diesel engine.

Geng et al. [93] performed the experiment on diesel/ methanol dual fuel (DMDF) combustion to investigate the PM emission for different load conditions. Experiments were conducted for low load, medium load, and high load conditions for varying energy ratio of methanol. Methanol energy ratio with diesel varied from 10% to 30%. It was observed that at low and medium load dry soot emission was suppressed, conversely at high load, it was increased. With increasing the contribution of methanol in the engine inlet air temperature got reduced, which leads to reduce particle matter up to mid load condition but at high load condition, it was increased.

Liu et al. [94] used the same combustion technology (i.e. DMDF) to invest the influence of injection pressure on methanol diesel dual-fuel engine performance. Experiments were carried out for different injection pressure of diesel (i.e. 70, 85, 100, 115, and 130 MPa) and constant methanol energy ratio (i.e. 45%) under 30% and 80% engine load. It was concluded that NO<sub>x</sub> and smoke emission was reduced although HC and CO were increased in the DMDF mode compared to a diesel engine. The increase in the injection pressure of diesel suppressed smoke, CO, and HC emission but NO<sub>x</sub> emission increased with a penalty of more fuel consumption.

Similarly, Li et al. [95] investigated the diesel injection parameter effect on DMDF engine performance. They performed the experiment under 25%, 60%, and 100% load conditions, for varied direct injection pressure (70 MPa to 115 MPa), varied direct injection timing (3° CA bTDC to 15° CA bTDC), and varied direct injection quantity (45 mg/cycle to 52 mg/cycle) of

diesel fuel. It was concluded that rapid combustion was increased for higher diesel injection pressure while suppressed for high injection quantity and early injection of diesel. NO<sub>x</sub> and smoke emission got reduced compared to diesel engine mode however increment was observed in HC and CO emissions. For higher diesel injection pressure and early injection timing, smoke reduced more however NO<sub>x</sub> emission increased for the same case.

Tutak, and Szwaja [96] executed CFD analysis on methanol diesel dual-fuel engine to understand the engine emission performance. The study was performed for 20% and 50% methanol energy ratio and five different diesel direct injection timing (i.e. 3.5, 6, 8.5, 11, 13.5, 16, 18.5<sup>0</sup> CA bTDC). It was observed that the combustion process was shorter than diesel engine due to premixed combustion of methanol. With retarding the direct injection timing cylinder pressure was reduced with high ID. It suppressed soot emission and improved thermal efficiency but NO<sub>x</sub> emission got increased due to rapid and short combustion.

Pan et al. [97] investigated the influence of intake air temperature on methanol diesel DF-HCCI engine combustion and emissions. An experimental study was performed for 75% load condition. Methanol fraction varied from 0-40% and intake temperature varied from 20-80<sup>0</sup> C. It was perceived that NO<sub>x</sub> emission reduced with increasing methanol fraction, while increased with increasing inlet temperature. HC and CO emission got suppressed at higher inlet air temperature however HC and CO increased with increasing methanol fraction. Also, PM emission was reduced for higher methanol fraction, however, it increased at a higher temperature without penalty of fuel consumption.

Diesel ignited methane DF-HCCI engine was studied by Guerry et al. [98] to examine the impact of diesel injection timing on engine emissions and combustion performance. An experiment was performed under two load conditions (4.1 bar IMEP and 12.1 bar IMEP) for constant speed. The results show that at any start of injection (SOI) of diesel smoke emissions were very low (<0.05 FSN) for both load conditions. It was observed that to prevent maximum PRR and knocking tendency, SOI timing should be 310<sup>0</sup> CA to 340<sup>0</sup> CA for 12.1 bar load. Further, beyond 280<sup>0</sup> advance, SOI crank angle (CA) engine operation was unstable under both load conditions.

Experiments with methanol and diesel DF-HCCI engine was carried out by Jia, and Denbratt [99] to examine the effect of methanol in three different locations. Here methanol fuel was injected at three different timings; port injection was injected at -350<sup>0</sup> aTDC, direct injection

(DI\_E) at  $-358^0$  aTDC, and direct injection at the compression stroke at (DI\_L)  $-100^0$  aTDC. Diesel was injected two times near to the TDC at  $-48$  and  $-15^0$ CA ATDC. An experiment was performed for constant speed 1500 rpm under 5 bar IMEP with  $60^0$  C inlet air temperature. The results show that the DI\_L combustion strategy gave poorer performance than port injection and DI\_E injection. The authors came to the conclusion that the DI\_E strategy showed very low NO<sub>x</sub> and soot emission compared to the remaining two strategies.

Dou et al. [100] performed experiments to examine the impact of methanol contribution, EGR, intake temperature, injection timing on soot emission in diesel/methanol dual-fuel engine. Methanol was supplied into the intake manifold and diesel was injected into the combustion chamber. The experiment was conducted at constant speed (1660 rpm) and at 50% of engine load. The results indicate that increase in methanol percentage and retardation of diesel injection timing were responsible for the drop-off soot and PM emissions, compared to early injection of diesel.

#### **2.4.4 Ethanol, propanol, and butanol dual fuel HCCI engine**

HCCI engine has fuel flexibility ability it can run on ethanol, propanol, or butanol. Methanol fuel has very little heat carrying capacity; the consumption of methanol is more compared to ethanol, propanol, or butanol. Ethanol also has high octane number that helps to resist the knocking of the engine, high LHV of ethanol permitting dense air, and lean combustion. While propanol and butanol have more CV compared to ethanol, methanol.

Maurya, and Agarwal [101] employed ethanol fuel in the inlet port and diesel injected near to the TDC in the diesel engine to convert it into DF-HCCI engine. Engine operated under constant speed for varying inlet air temperature (i.e.  $120\text{--}150^0$  C) and different relative air-fuel ratios (i.e. 2-5). In this study, stable HCCI engine operation was obtained for 2-5 relative air-fuel ratio. Further highest indicated thermal efficiency was achieved for 2.5 relative air-fuel ratios at  $120^0$  C inlet air temperature. During DF-HCCI mode engine was able to withdraw a maximum 4.3 bar IMEP. Very low NO<sub>x</sub> emission was observed but high HC and CO emission was noted compared to a diesel engine.

Sarjovaara et al. [102] converted a turbocharged stationary engine into diesel ignited ethanol DF-HCCI engine. For the conversion modification was done in lowering the CR, importing port injection system, and turbocharger. Experiments were performed for 75% and 100% load

conditions at 1500 rpm constant speed. They concluded that up to 90% ethanol energy ratio can be contributed for high load conditions.

Kim et al. [103] implemented DF-HCCI engine strategy on SI engine. They used ethanol at various injection timing ( $540^0$  bTDC,  $305^0$  bTDC,  $270^0$  bTDC) at the time of suction and gasoline directly injected in the cylinder ( $305^0$  bTDC). They used 2 different CR ( 9.5 and 13.3) for full load conditions. It was observed that if the ethanol injection timing at the inlet valve open helps to reduced engine knocking. It was concluded that HC and  $\text{NO}_x$  emission got increased in ethanol gasoline DF-HCCI engine while CO and PM got reduced at 13.3 CR. However, at 9.5 CR very minimal changes were observed in the ethanol-gasoline DF-HCCI engine.

Qian et al. [104] performed the experiment on dual fuel SI engine by using ethanol for port injection and gasoline surrogate for direct injection. In this study port injection fuel was fixed and the direct injection fuel octane number changed. It was observed that indicate thermal efficiency of directly injected fuel (research octane number 75) with 35% ethanol similar to direct-injected gasoline (octane number 95) spark-ignition engines. Further increasing ethanol fraction with direct injection of gasoline fuel with 95 research octane number reduces  $\text{NO}_x$ , HC, ethane, olefins gradually.

Chu et al. [105] implemented gaseous propanol to form a premixed homogeneous charge and to ignite the charge pilot diesel injection was done in the cylinder. Experiment performed under high load condition at 14.5 bar IMEP with 1500 rpm speed. Maximum PRR was observed below 7 bar/deg CA at higher load conditions with high indicated thermal efficiency and lowest emissions. It was observed that 36.1% EGR can control rapid premixed combustion and reduction of  $\text{NO}_x$  emission. In propanol diesel DF-HCCI engine 81%  $\text{NO}_x$  and 65% soot emission were reduced compared to a diesel engine.

Polk [106] employed a diesel ignited propanol DF-HCCI engine strategy in the heavy-duty six-cylinder diesel engine. An experiment was performed for varying propanol energy substitution under four different load conditions (i.e. 5, 10, 15, and 20 bar at constant 1500 rpm). 86% maximum energy substitution of propanol was permissible under 5 bar BMEP load, while for 10 bar, 15 bar, and 20 bar BMEP it was 60%, 33%, and 25% respectively. With increasing the propanol substitution  $\text{NO}_x$  emission decreased while smoke emission reduced for 5 bar and 10

bar BMEP for further load conditions, smoke was invariant. However, with increasing propanol HC and CO emission increased for all load conditions.

Krishnan et al. [107] implemented a diesel-ignited propane dual fuel LTC combustion strategy to investigate the effect of fuel injection pressure, timing, and inlet boosting pressure on engine performance and emission. Diesel injection timing varied from  $280\text{--}355^0$  CA, diesel injection pressure varied from 200–1300 bar, and inlet pressure varied from 1.1–1.8 bar. An experiment was performed under constant load 5.1 bar BMEP for constant speed 1500 rpm with 80% propanol energy substitution. It was revealed that as increasing injection pressure peak cylinder pressure suppressed and the more homogeneous charge was observed. It helps to reduce  $\text{NO}_x$  emission but HC and CO were increased however fuel conversion efficiency was invariant. 500 bar injection pressure observed optimum pressure for lowest emission. Increasing inlet pressure reduced ID and increases in-cylinder pressure it leads to an advance HRR profile. Additionally, it helps to increase fuel conversion efficiency. Further  $320^0$  CA showed the lowest  $\text{NO}_x$  and smoke emission while HC and CO were more for the late injection timing with higher conversion efficiency.

Hodges et al. [108] investigated the influence of propanol energy ratio on engine emission and performance of diesel ignited propanol DF-HCCI engine. An experiment was performed for constant 3.3 bar BMEP at 1500 rpm load. In this experiment, injection timing was fixed at  $310^0$  aTDC with 500 bar injection pressure without the use of EGR. It was demonstrated that HC and CO emission was lower for a low premixed ratio, while  $\text{NO}_x$  was increased but PM was invariant. Combustion efficiency was suppressed as increasing propanol energy ratio, 71% propanol energy ratio observed optimum for combustion efficiency.

Chen et al. [109] incorporated butanol fuel in the inlet manifold of diesel engine. They examine the effect of diesel ignited butanol DF-HCCI engine performance over direct injection mode of butanol-diesel blend engine. An experiment was performed at 1.0 MPa IMEP at 1900 rpm with EGR substitution. It was demonstrated that increasing the contribution of butanol ratio increases peak cylinder pressure, HRR, and short CD under low EGR rate. However, at high EGR rate peak cylinder pressure, HRR decreased and CD elongated with increasing butanol energy ratio. With increasing, butanol substitution soot and  $\text{NO}_x$  were reduced while HC and CO

were increased, and fuel economy deteriorates. Further with the increasing EGR rate NO<sub>x</sub> was reduced but soot, HC, and CO were increased.

Yadav, and Ramesh [110] implemented a butanol diesel DF-HCCI engine strategy to investigate the influence of multiple injections of direct injection fuel (i.e. diesel) on engine performance and emissions. Experiments were conducted for 75% and 100% load conditions under constant speed (1800 rpm). Butanol fuel supplied through the port injection and diesel injection was done at various times in the engine cylinder. Diesel injection was done in three different ways such as Pilot plus Main Injection (PMI), Main plus Post Injection (MPI), and Main Plus Two Post Injections (MPTPI). It was concluded that MPI injection with port injection of butanol gives the lowest smoke and NO<sub>x</sub> emission with the highest BTE compared to the rest of the two diesel injection strategies. However, HC and CO emissions increased a lot. While PMI diesel injection strategy was reduced NO<sub>x</sub> emission with a penalty of high fuel consumption and increased smoke emission.

Similarly, Ganesh et al. [111] used butanol diesel RCCI strategy to investigate the optimum operating conditions. In this study, butanol was injected into the inlet port and diesel was injected into the cylinder. An experimental investigation was performed for 0-100% load condition, with varying diesel injection timing, injection pressure, intake air temp., and butanol mass. It was concluded that at 71% butanol mass fraction reduced 99% NO<sub>x</sub> and 91% smoke emission with 4% improvement in thermal efficiency under 2.7 bar BMEP load. However, for the same load condition and same butanol mass fraction HC and CO were increased by 98% and 60% respectively. Further HC and CO emissions were reduced with increasing diesel injection pressure.

## 2.5 Various other combustion control strategy

The various researchers implemented different fuel blends to reduce heat release rate and pressure rise rate in HCCI engine under an external mixture preparation strategy. Fuel blending is the most popular method to control HCCI combustion.

L. Xingcai et al. [112] implemented ethanol and n-heptane fuel blends in the HCCI engine to control the combustion. An experiment was performed for 0% to 50% ethanol and n-heptane blends in the port injection for 1.5 bar to 2.5 bar load for constant speed (1800 rpm). It was observed that due to the high octane number of ethanol ID was increased and low-temperature

combustion (LTC) occur. The increasing contribution of ethanol in the n-heptane delays the start of combustion which leads to prolonge the CD. It reduces HRR and combustion temperature compared to pure n-heptane HCCI combustion mode. It was observed that HC emission increased for 30% to 50% blends compared to pure n-heptane and 10-20% blends, however, CO emission was high for all load conditions.

S. Swami Nathan et al. [113] used two different fuels in the inlet manifold of a diesel engine. They used biogas in the inlet manifold and to control the combustion diesel was injected at the same time in inlet manifold with varying inlet air temperature. Initially, the engine was started at  $85^0$  C inlet air temperature when diesel was injected in the inlet manifold, then the substitution of biogas increased slowly with reducing the diesel quantity. Engine operation was performed for 50% engine load with three different inlet air temperatures i.e.  $80^0$ ,  $100^0$ , and  $135^0$  C as per the air plus diesel plus biogas proportion. It was observed that the best proportion ratio of biogas and diesel is 50% means 50% biogas and 50% diesel. It reduced  $\text{NO}_x$  and smoke for all inlet temperatures however HC emission was reduced for high inlet temperature and fuel economy also deteriorated.

Similar kind of HCCI engine numerical study was done by H. Guo, and W. Neill [69] on n-heptane HCCI engine with the addition of hydrogen. In this study, hydrogen was injected in the inlet port after the injection of n-heptane. It was revealed due to the chemical effect of hydrogen leads to retard combustion phasing of n-heptane HCCI engine. Hydrogen addition reduces the combustion duration at a constant CR. Further with an increase in the proportion of hydrogen improves the thermal efficiency at higher CR and reduces the HC emission, however, it increases HC emission per unit burned n-heptane mass.

Turkcan et al. [114] interrogated the influence of ethanol and methanol blends on combustion and emissions of gasoline direct injection HCCI engine. In this study, gasoline, E10, E20, M10, and M20 blend fuels were used; the first injection timing was fixed at  $120^0$  aTDC and second injection timing was varying from  $30^0$  to  $15^0$  CA bTDC. During the experiment, 80% of the total amount of fuel was injected at  $120^0$  aTDC and the rest of the fuel was injected on second injection timing. It was concluded that the retard of second injection timing delayed the SOC, reduced cylinder pressure, and HRR. Further, second injection timing did not affect HC and CO emissions compared to  $\text{NO}_x$  and soot emissions. Gasoline-alcohol blends suppress the  $\text{NO}_x$ , HC

and CO emission and increase the indicated efficiency for optimum second injection timing at low equivalence ratio.

S. Polat [115] converted SI engine into HCCI engine by increasing the CR and changing inlet air temperature. In this study, port injection strategy was used to investigate the impact of diethyl ether- ethanol fuel blends on HCCI engine emission and performance. E30/D70 (30% ethanol–70% diethyl ether by volume), similarly E40/D60 and E50/D50 fuels were used at various inlet air temperatures (i.e. 333, 353, 373, and 393 K). It was observed that combustion duration was increased and ID was decreased with increasing inlet air temperature. With increasing the ethanol proportion in the diethyl ether blend engine was not able to perform at a leaner mixture because of high autoignition temperature and octane number of ethanol. E40/D60 shows higher indicated thermal efficiency at 353 K inlet air temperature and lowest NO<sub>X</sub> emission compared to E30/D70 fuel blend. However, HC and CO were increased with an increasing amount of ethanol in the blends.

## 2.6 Summary

From the literature, it was concluded that HCCI combustion mode is the advanced combustion strategy over conventional SI and CI engine. HCCI combustion gives the lowest NO<sub>X</sub> and smoke with great improvement in the fuel economy. Uncontrolled spontaneous combustion and limited operating range is the main drawback of HCCI engine. To overcome the HCCI engine challenges various methods were used, RCCI or dual fuel HCCI (DF-HCCI) engine combustion methods were more appropriate was observed. It was concluded that DF-HCCI engine can use alternative fuels in the HCCI combustion with lower emission and higher efficiency under a wide operating range. Hence present work is mainly focused on DF-HCCI engine mode combustion. In DF-HCCI engine, alcohol fuel shows superior performance as a low reactivity fuel compared to gaseous fuel at high load conditions [116]. Also, butanol blends and biodiesel blend will be a good replacement for the diesel in DF-HCCI engine for the reduction of extra NO<sub>X</sub>, HC, and CO emissions [117–119].

## 2.7 Observations and gaps identified from the literature

From the literature, the following observations are noted in brief as follows.

- Dual fuel HCCI or RCCI engine is the most suitable method to control the HCCI

combustion and to extend the operating range.

- Alcohol-based fuels are the most suitable low reactivity fuel for DF-HCCI engine due to their high anti-knocking property and high autoignition temperature.
- Alcohol-based fuel can easily mix with the air due to its volatile nature as well as high latent heat of vaporization
- Carburetor is a suitable attachment to mix the air-fuel mixture outside the combustion chamber.
- Biodiesel blend can reduce the HC and CO emission, due to the presence of inherent oxygen.
- Butanol blend will be a good fuel replacement in the HCCI engine instead of diesel.

**The following gaps were identified for the research review.**

- From the literature review, it is observed that little work is found on comparing different alcoholic fuels as low reactivity fuel and diesel or biodiesel as high reactivity fuel.
- Very few authors attempted the experiment on different loads applied on HCCI mode engine.
- Very limited author defined optimum alcohol-based fuel substitution ratio or the premixed ratio for each load condition in DF-HCCI engine for different alcohol-based fuels.
- Use of a carburetor for the preparation of homogenous charge and the influence of its location on the engine inlet manifold is a new concept.
- Limited literature is found on the impact of biodiesel blend (Bio20) and butanol blend (B10/B20/B30) in dual fuel mode HCCI engine on HC and CO emissions.

## **2.8 Objectives of the research work**

Main objective of the research is to design dual fuel mode HCCI engine and investigate its performance under different load conditions by using various alcohol-based fuels. The present study contributes toward the future dual fuel mode HCCI engine to decide which alcohol-based fuel to be used at what proportion in the dual fuel HCCI engine along with diesel under different

load conditions for better combustion and lowest emission. The following are the objectives of the present work.

- 1) To experimentally investigate the influence of carburetor location on dual fuel mode HCCI engine performance.
- 2) To optimize mass flow rate and premixed ratio under each load, for methanol, ethanol, propanol, butanol alcohol-based fuels by using different fuel jets in the carburetor.
- 3) Experimentally recognize the suitable fuel among the fuels: Methanol, Ethanol, Propanol, and Butanol with port fuel injection technique which yields HCCI like performance.
- 4) To investigate the influence of biodiesel blend (Bio20) in place of diesel in dual fuel HCCI engine on combustion performance and emissions.
- 5) To investigate the technical feasibility of various butanol blends (B10/B20/B30) in the propanol dual fuel mode HCCI engine.

## **Chapter – 3**

### **Experimental Setup and Instrumentation**

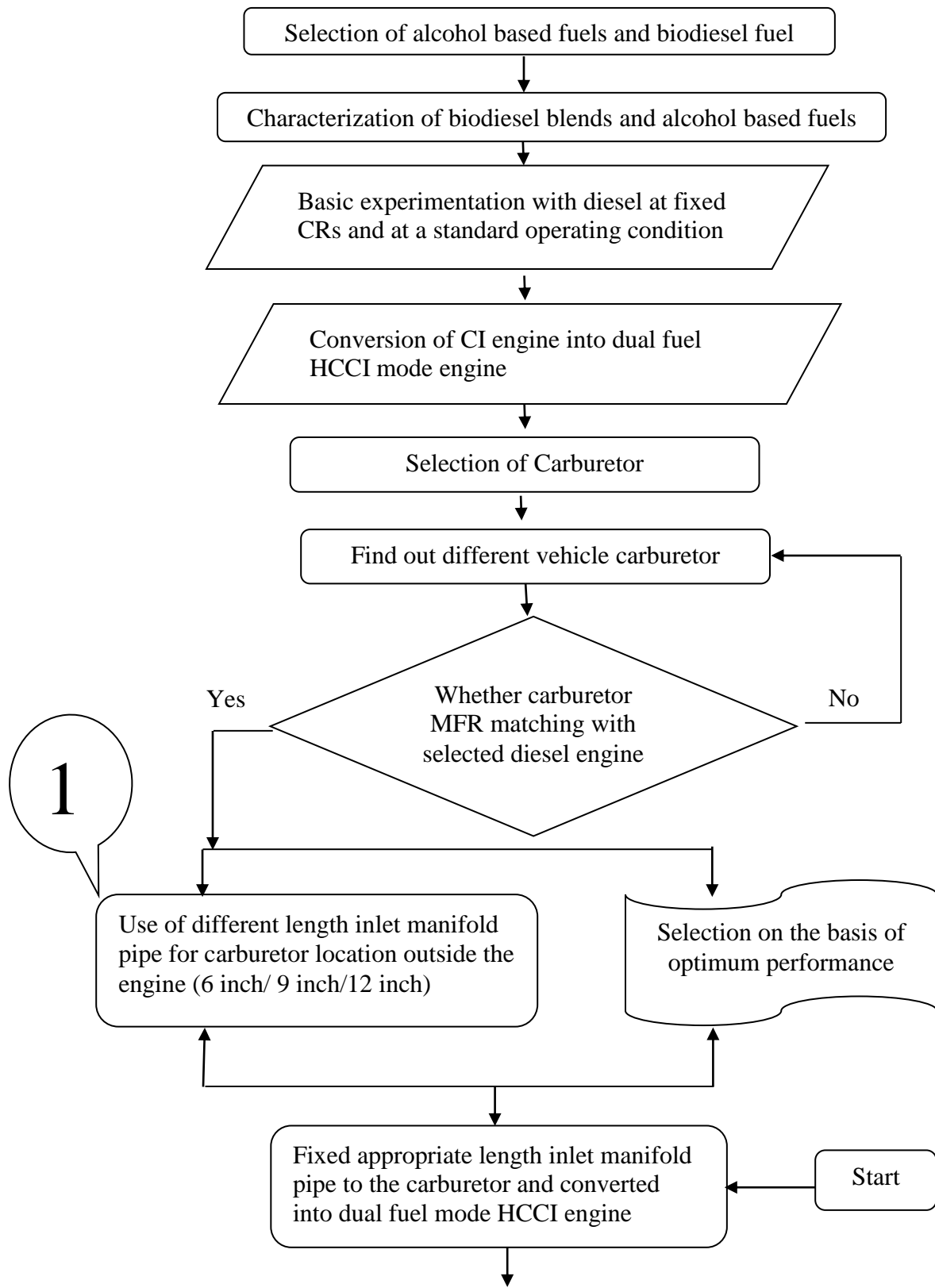
---

### 3.1 General

Before carrying out research, a basic idea of the instrumentations and materials is vital. In this chapter, a detail of test engine, instruments, and developed experimental setup were explained. To develop the required experimental setup selection of engine, selection of fuels, selection of premixed fuel injection system, selection of tools were elaborately discussed in this chapter. Whole experimental setup along with loading device, and emission measuring instruments were discussed. **Figure 3.1** shows the flow chart of present research work.

### 3.2 Test engine

To investigate the performance of dual-fuel HCCI (DF-HCCI) engine, a single-cylinder, 4-stroke, water-cooled, direct injection, naturally aspirated, constant speed, compression ignition (CI) engine was selected. In the present research, the existing CI engine is converted into DF-HCCI engine by attaching the carburetor to the inlet manifold for the supply of homogenous charge. Carburetor selection is made based on the required charge mass flow rate (MFR) for the engine. The engine parameters selected are : compression ratio 17.5, injection timing  $23^0$  bTDC, injection pressure 210 bar, and engine speed 1500 rpm. Three-hole nozzle injector was used to inject the fuel. Detailed specification of the engine is shown in **Table 3.1**.



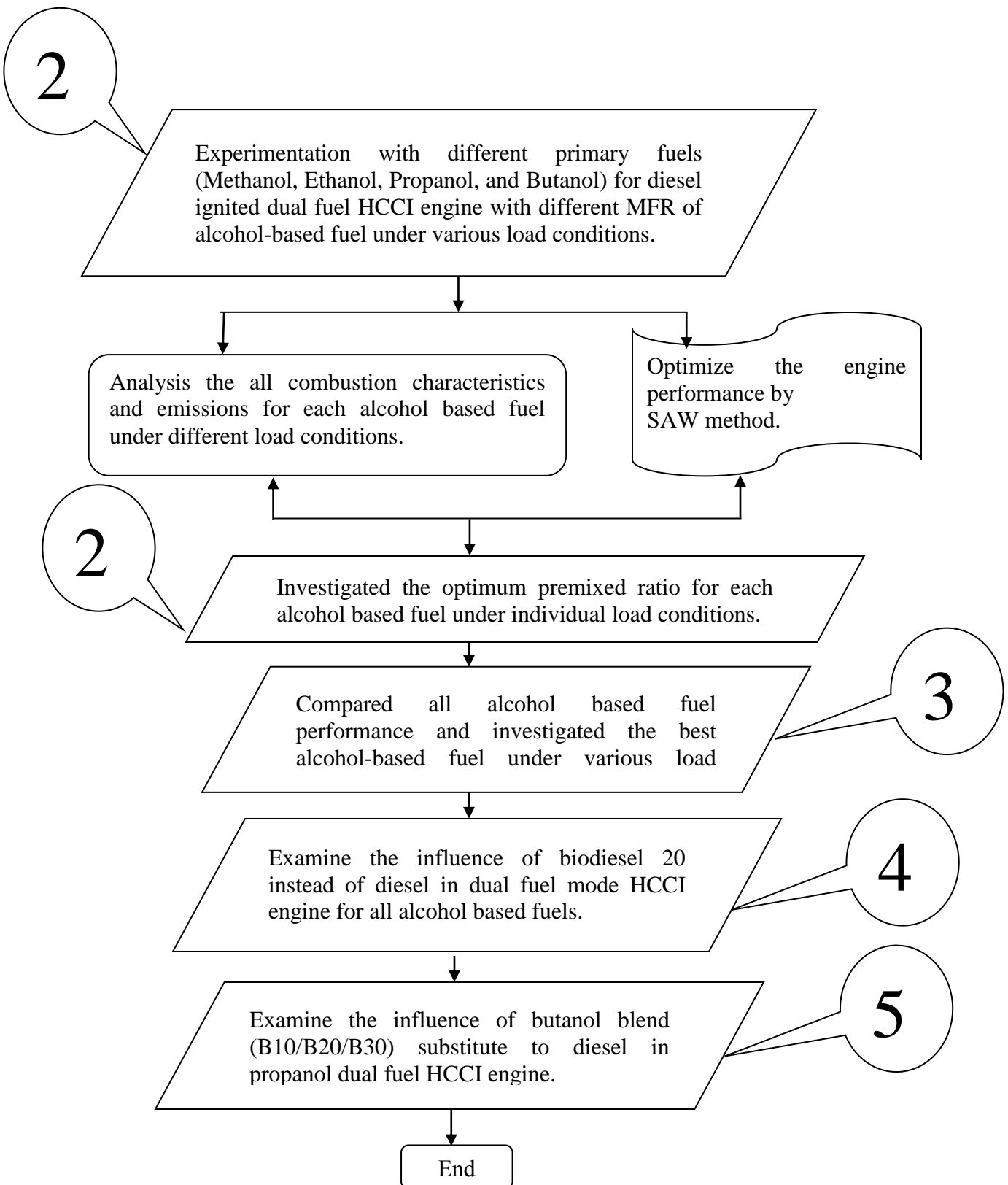


**Figure 3.1** Flow chart of present research work

**Table 3.1:** Engine details

Engine Type	AV1, Kirloskar oil diesel engine
Cylinder/ Stroke	1/ 4- Stroke Engine
Bore (mm)	87.5
Stroke length (mm)	110
Compression ratio	17.5:1
Rated speed (rpm)	1500
Rated output kW(HP)	3.5 (5)
Volume (cc)	661.45
Connecting rod length (mm)	234
Direct injection pressure (bar)	210
No of holes per nozzle	3
Fuel injection Timing	23° BTDC

### 3.3 Selection of carburetor

A carburetor was attached to the engine manifold for the supply of low reactivity fuels in the combustion chamber to achieve a premixed homogeneous charge. In the present study 5 HP CI engine was selected. To choose the suitable carburetor for DF-HCCI engine, the MFR capacity of carburetor should be equal to or more than the capacity of a conventional CI engine. Engine air intake capacity depends on the volume of the engine, density of the fluid, speed of the engine, and coefficient of discharge. Equation 3.1 gives the MFR of air in the engine cylinder.

Mass flow rate (MFR) of air in the cylinder [1]

$$\begin{aligned}
 m_a &= C_d * A * L * \rho * n & (3.1) \\
 &= 0.85 \times 0.661 \times 10^{-3} \times 1.2 \times 750 / 60 \\
 &= 8.42 \text{ g/s}
 \end{aligned}$$

Where,  $C_d$  indicates the coefficient of discharge,  $A$  indicates the engine cylindrical area in  $\text{m}^2$ ,  $L$  indicates the stroke length in meter,  $\rho$  indicates the fluid density  $\text{kg/m}^3$ , and  $n$  indicates the engine rpm.

From the above equation, it is observed that MFR capacity of air for the selected CI engine is 8.42 g/s. Hence the carburetor should have more than this MFR capacity or at least 8.42 g/s to run the DF-HCCI engine.

To meet the above MFR capacity, Royal Enfield 500 cc dual spark engine carburetor was selected because it satisfies the requirement of DF-HCCI engine operation. The make of the carburetor is Mikcarb VM-28. This is a simple float type carburetor with zinc and aluminum main jet and needle jets. **Table 3.2** shows the details of carburetor.

**Table 3.2** Carburetor details

Manufacture	Mikcarb (500cc)
type	VM-28
Material	Zinc
Model	1850000000
Main jet	110
Main jet material	Zinc and aluminum
Cubic capacity	500 CC
Engine output	22BHP/5400 RPM

### **3.4 Fuels selected for dual fuel HCCI engine**

From the literature, it was found that in the DF-HCCI engine two different reactivity fuels are suitable which having different octane numbers and cetane numbers. Fuel supplied at the time of suction stroke must have low reactivity means low cetane number and to ignite the homogeneous charge the injected fuel must have high reactivity means high cetane number. In this study, Methanol, Ethanol, Propanol, and Butanol fuels have been selected as these fuels have low reactivity in nature to form the premixed charge. To start the combustion, Diesel or Neem biodiesel 20 (Bio20) or butanol blend (B10/B20/B30) have been selected as these fuels have a high reactivity in nature. Alcohol-based fuels are volatile and easy to mix with the inlet air outside the combustion chamber, with high autoignition temperature due to which the charge resists the early start of combustion. Also, alcohol-based fuels have high octane number and low cetane number which resist engine knocking. Further, alcohol-based fuels have high latent heat of vaporization (LHV) it helps to reduce the engine combustion chamber temperature, assist to

improve combustion performance. High LHV absorbs the heat from the inlet air which assists to complete low-temperature combustion (LTC). The detailed properties and characteristics of all alcohol-based fuels and conventional fuels are shown in **Table 3.3**.

In this study diesel as a high reactivity fuel was used to ignite the premixed homogenous charge in DF-HCCI engine. Also, the experiments were conducted by supplying 20% blend Neem biodiesel (Bio20) instead of clean diesel. Blending was done based on volume, 20% biodiesel was mixed with 80% diesel. Further butanol blends with diesel were used as high reactivity fuel, butanol blends were done on basis of volume. B10 indicate 10% butanol plus 90% diesel, B20 indicates 20% butanol plus 80% diesel and B30 indicate 30% butanol plus 70% diesel. Bio20, B10, B20, and B30 these four blends prepared in a mechanical emulsifier, which is available in NIT Warangal thermal engineering lab as shown in **Figure 3.2**. The density and calorific value of blends were measured by hydrometer and bomb calorimeter respectively; the measured values are shown in **Table 3.4**.



**Figure 3.2** Mechanical emulsifier blending machine

**Table 3.3** Fuel properties and characteristics [120–124][110]

Parameters	Units	Methanol	Ethanol	Propanol	Butanol	Gasoline	Diesel
Chemical Formula	-	CH <sub>3</sub> OH	C <sub>2</sub> H <sub>5</sub> OH	C <sub>3</sub> H <sub>7</sub> OH	C <sub>4</sub> H <sub>9</sub> OH	C <sub>4</sub> to C <sub>12</sub>	C <sub>8</sub> to C <sub>25</sub>
Molecular Weight	g/mol	32.04	46.06	60.09	74.12	100 - 105	190 - 211.7
Specific Gravity	-	0.789	0.785	0.803	0.807	0.744	0.830
Boiling Point	°C	64.7	78.4	97.1	117.5	25 - 215	170 - 340
LHV	kJ/kg	1168	920	757	708	380-500	270
Lower CV	MJ/kg	21.4	28.9	31.1	34.2	43.8	43.5
Stoichiometric air/fuel ratio	-	6.47	9.0	10.33	11.2	14.7	14.5
Flash Point	°C	11-12	17	11.7	35-37	-42	>70
Auto-Ignition Temp.	°C	463	434	350	345	300	210
Research Octane Number	-	108.7	108	117	103	95	-
Motor Octane Number	-	88.6	92	99	91	85	-
Cetane Number	-	5	6	12	17	-	40 – 55
Viscosity at 40° C	mm/s <sup>2</sup>	0.58	1.13	1.74	2.22	0.56	2.72
Carbon	% Wt	37.48	52.14	59.96	64.82	86	86.13
Oxygen	% Wt	49.93	34.73	26.62	21.59	0	0
Hydrogen	% Wt	12.48	13.02	13.31	13.49	14	13.87
Flammability limit	% vol	6.7-36	3.3-19	2.2-13.7	1.49-11.25	1.3-7.6	0.6-7.5

**Table 3.4** Density and lower calorific value of different blends

Type of Blend	Density (kg/m <sup>3</sup> )	Lower Calorific Value (kJ/kg)
Bio100	881	38720
Bio20	839	43220
B100	807	34200
B10	827	42541
B20	825	41525
B30	823	40500
Diesel	830	43500

### 3.5 Experimental test setup and instrumentation

The experiments were performed on dual fuel HCCI (DF-HCCI) engine. The schematic and actual experimental setup of a DF-HCCI engine is shown in **Figure 3.3 and Figure 3.4** respectively. Figure 3.4(a) shows the actual experimental setup and Figure 3.4(b) shows the carburetor location outside the engine cylinder. Conventional CI engine is converted into DF-HCCI engine by attaching the carburetor to the inlet manifold outside the engine cylinder.

Eddy current (Model AG10) water-cooled dynamometer was used to apply load on the engine. The selected dynamometer load was controlled by S-type strain gauge which has 0-50 kg range and 185 mm arm length. Exhaust gases, inlet, and outlet cooling water temperatures were measured by RTD PT100 and thermocouple sensors. Cooling water temperature for engine was kept in the range of 55<sup>0</sup>C - 60<sup>0</sup>C and accordingly MFR of engine cooling water was varied with the help of Rotameter. To measure in-cylinder pressure and fuel line pressure, two different piezoelectric transducers (Model-S111A22) were used. One was installed in the fuel line and another was installed in the combustion chamber. By using in-cylinder pressure data with crank angle (CA), HRR, PRR, cumulative heat release rate, indicated mean effective pressure (IMEP) were calculated by engine software.

“ICEnginesoft” software was used for combustion and performance analysis of engine. Complete engine setup was computer interfaced; engine data was controlled by ECU (Make - PE USA, Model PE3) and captured on monitor screen. Digital control panels of engine included engine load control knob, fuel measuring burette, engine load indicator, and orifice meter for air-fuel

ratio measurement. Kubler crank angle sensor (Model- 8.KIS40.1361.0360) was used to measure engine speed, fuel injection timing, and enabled a generation of cam and crankshaft time pulse relation. Mass of air flow measured by airflow transmitter (Make- Wika Germany, Pressure transmitter, Range 0-250 mm WC) which is fixed at air box outside the engine. Fuel flow transmitter (Make-Yokogawa Japan, DP transmitter, Range 0-500 mm WC) fixed in the burette to measure the fuel flow. Finally, air-fuel ratio was recorded on the screen of Enginesoft. 50 consecutive combustion cycles were considered for each test of engine to analyze engine performance.

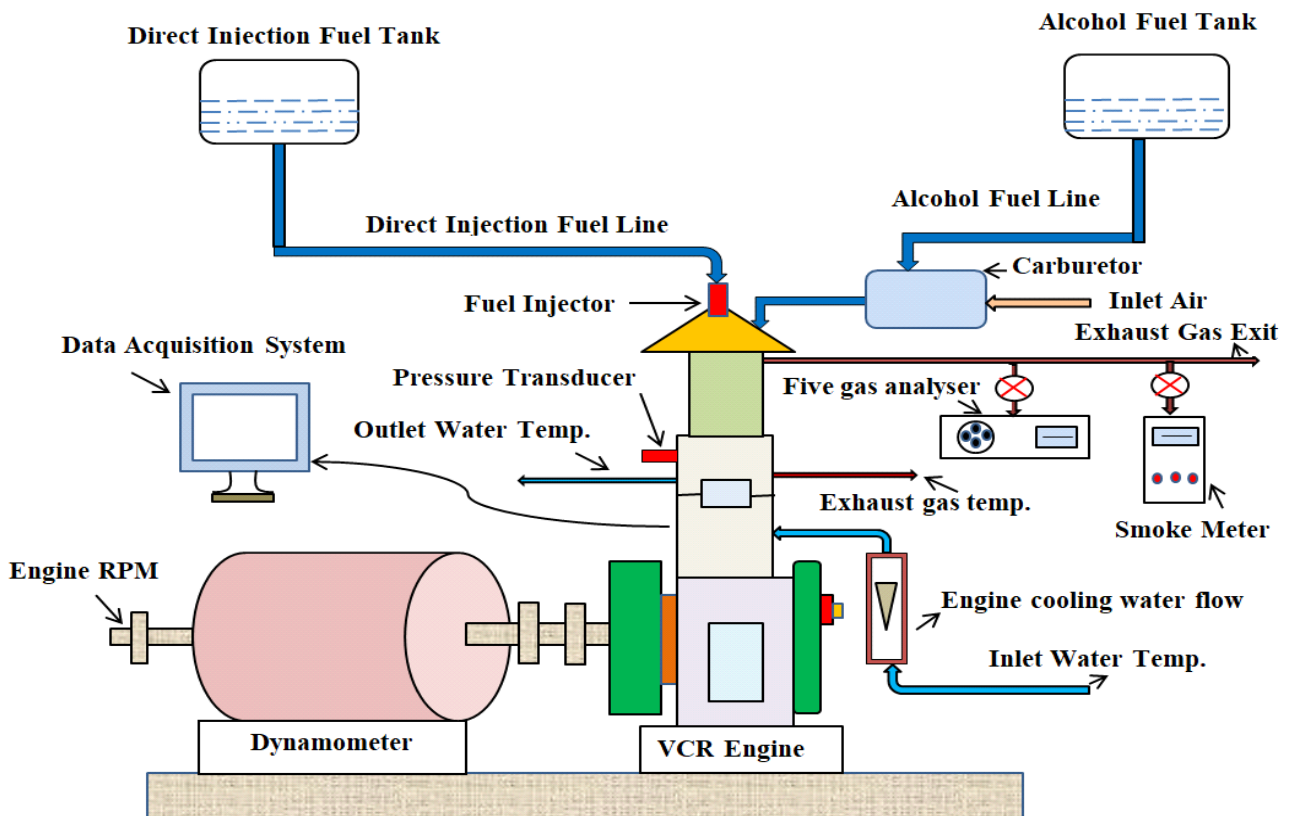


**Figure 3.3** Schematic representation of alcohol-based dual fuel HCCI engine

Exhaust gases were measured by INDUS five gas analyzer (PEA 205N, Make- INDUS), which is attached outside the exhaust gas pipe. INDUS 5-gas analyzer was recorded CO in % vol., HC in ppm, CO<sub>2</sub> in % vol., O<sub>2</sub> in % vol., and NO<sub>x</sub> in ppm. Smoke opacity was recorded by NETEL smoke meter (model no.NPM-SM-111B). The Accuracy, range and resolution of INDUS five gas analyzer and NETEL smoke meter is shown in **Table 3.5** and **Table 3.6**. A photographic

view of gas analyzer and smoke meter is shown in **Figure 3.5**.

**Table 3.5** Accuracy, range and resolution of Indus gas analyzer

Exhaust gases	HC	CO	NO <sub>x</sub>
Resolution of gases	$\leq 2.0:1$ ppm vol.	0.01% Vol.	1 ppm vol.
Accuracy of gases	< 2000 ppm vol.: $\pm 4$ ppm vol.	$\pm 0.02$ % Vol.	$\pm 5$ ppm vol.
Range of gases	0 - 30000 ppm	0 – 15% vol.	0 - 5000 ppm

**Table 3.6** Accuracy, range and resolution of Smoke Meter

Parameters	Accuracy	Range	Resolution
K	$\pm 0.1 \text{ m}^{-1}$	0- $\infty$	0.01
HSU	-	0-99.9	0.1%

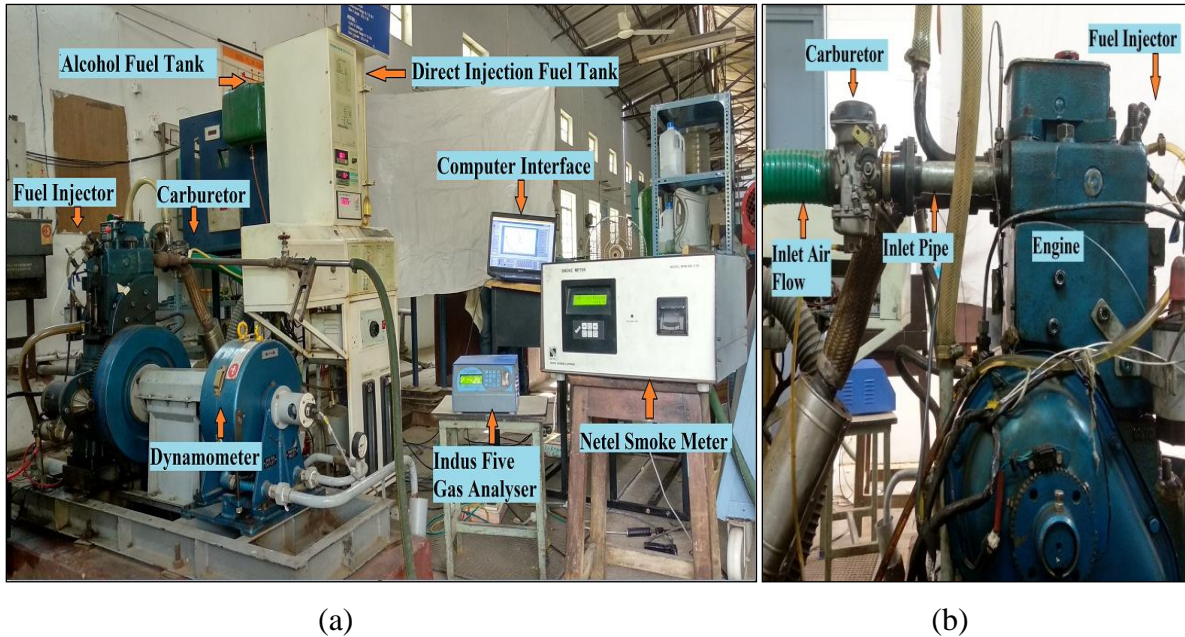


**Figure 3.4** (a) Actual experimental setup of dual fuel HCCI engine (b) Carburetor location



**Figure 3.5** Photographic view of the emission analyzers

## **Chapter - 4**

### **Experimental Procedure and Optimization Method**

---

## 4.1 General

In this chapter, total experimental procedure is explained. Further combustion characteristics such as Ignition delay (ID), Combustion duration (CD), brake specific fuel consumption (bsfc), brake thermal efficiency (BTE), premixed ratio, cooling potential, performance improvement were defined. Also, brake power (BP), net heat release rate (HRR) was defined. Uncertainty analysis is included for the measuring parameters. Further, various optimization techniques were discussed among these simple additive weighting (SAW) technique was applied.

## 4.2 Experimental procedure

In this study diesel or biodiesel blend 20 (Bio20) or butanol blend (B10/B20/B30) ignited alcohol-based DF-HCCI engine combustion performance and emissions were investigated by varying MFR of alcohol-based fuel under different load conditions.

Initially, standard operating conditions are fixed like 17.5 CR, diesel injection timing 23 bTDC, and injection pressure 210 bar for constant speed i.e. 1500 rpm. Basic experiment conducted on conventional CI mode engine by diesel fuel supply for 20% load to 100% load in the interval of 20% load.

Then engine CI engine is converted into DF-HCCI engine by attaching the Bullet 500 cc carburetor to the inlet manifold of the engine to investigate the DF-HCCI engine performance.

In the present study, alcohol-based fuel was supplied through the carburetor at the time of suction stroke as a low reactivity fuel, and diesel or Bio20 or butanol blend (B10/B20/B30) was supplied through the injector at the end of compression stroke as a high reactivity fuel.

All experimental tests were performed under different load conditions (20% to 100% load) in the interval of 20% load. DF-HCCI engine performance was compared with a conventional diesel engine.

Through the open throttle carburetor, a constant amount of fuel was supplied and the engine load is controlled by varying the diesel fuel supply.

During an experiment test on a particular load, initially, the load was set in load indicator of engine panel with the help of load control knob and then to achieve constant 1500 rpm speed direct injection diesel fuel was manually controlled.

Carburetor fuel consumption was measured manually with the help of stopwatch for 10 ml fuel consumption.

To fix the carburetor location outside the engine cylinder three different lengths of inlet manifold pipe were selected. In this study, 6-inch, 9-inch, and 12-inch lengths of inlet manifold pipe were used to fix the carburetor location as shown in **Figure 4.1**. In this case, ethanol fuel is supplied through the carburetor and diesel injected near to the TDC. From the DF-HCCI engine performance, best length of inlet manifold pipe was chosen for rest of the experiments.

In the next set of experiments, various alcohol-based fuels (methanol, ethanol, propanol, and butanol) were used in the DF-HCCI engine. To vary the MFR of alcohol-based fuel in the carburetor, different fuel jets were used. In this study jet 40, jet 47.5, jet 60, jet 70, jet 80, and jet 90 were chosen. **Figure 4.2** shows the different fuel jets and their location in the carburetor.

Initially, an experiment was performed for ethanol-diesel DF-HCCI engine with varying MFR of ethanol. The optimum MFR of ethanol and the optimum premixed ratio were found for each load condition by using simple additive weighting (SAW) optimization method for the lowest emission and highest fuel economy.

Similarly, for methanol, propanol, and butanol optimum MFR and optimum premixed ratio were found for each load condition by using SAW optimization method.

All alcohol-based fuels were compared based on the performance of engine and the best alcohol-based fuel can be found.

Further influence of biodiesel blend 20 (Bio20) instead of diesel on HC and CO emission of alcohol-based DF-HCCI engine was investigated.

After that technical feasibility of butanol blend (B10/B20/B30) in place of diesel in propanol, DF-HCCI engine was investigated.



Figure 4.1 (a) Carburetor location outside the engine cylinder (b) Various length of inlet manifold pipe

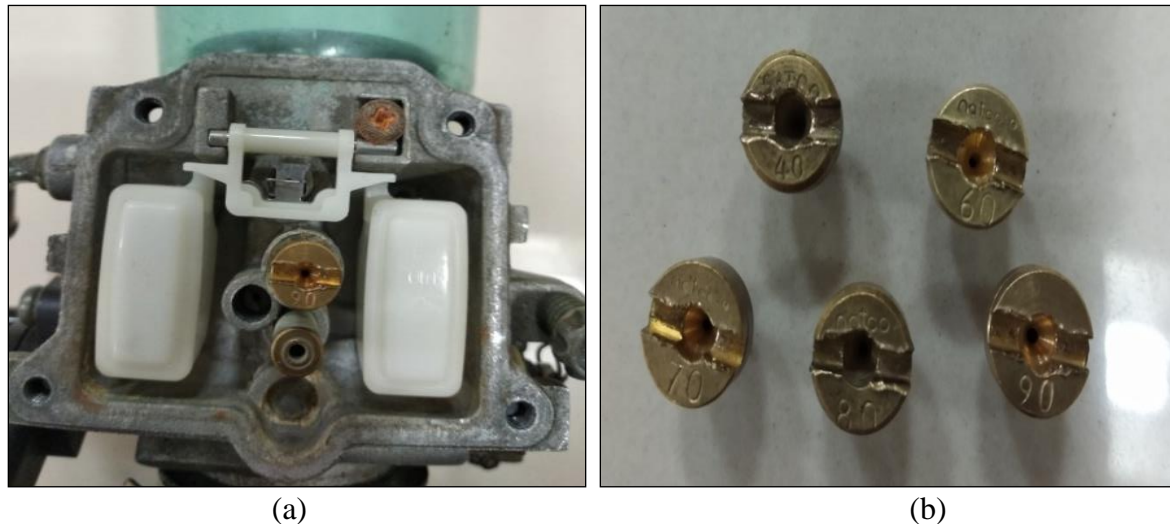


Figure 4.2 (a) Fuel jet location in the carburetor (b) Different number fuel jets

### 4.3 Performance parameters

In this study, combustion and performance analysis was done with the help of ignition delay (ID), combustion duration (CD), premixed ratio (PR), brake thermal efficiency (BTE), brake specific fuel consumption (bsfc), performance improvement, and cooling potential parameters which are defined below.

$$\text{Ignition Delay (ID)} (\text{°CA}) = \text{CA}_{\text{PPRR}} - \text{CA}_{\text{PFLP}} \quad (4.1)$$

Eq. 4.1 defines ignition delay (ID) as CA interval of peak pressure rise rate (PPRR) and peak fuel line pressure (PFLP) [125].

$$\text{Combustion Duration (CD)} (\text{°CA}) = \text{CA}_{\text{MFB 90}} - \text{CA}_{\text{MFB 10}} \quad (4.2)$$

Eq. 4.2 defines CD as the CA interval between 90% fuel mixture combustion to 10% fuel mixture combustion [126,127].

$$\text{Premixed ratio (PR) (\%)} = \frac{(m_a CV_a)}{[(m_D CV_D) + (m_a CV_a)]} \times 100 \quad (4.3)$$

Eq. 4.3 defines premixed ratio, as the ratio of heat energy utilized by alcohol-based fuel to the heat energy utilized by both fuels (alcohol-based fuel and direct injection fuel) [128][104].

$$\text{Brake thermal efficiency (BTE)(\%)} = \frac{BP}{[(m_a CV_a) + (m_D CV_D)]} \times 3600 \times 100 \quad (4.4)$$

In Eq. 4.3 and Eq. 4.4 'm' define the MFR of fuel and CV indicates calorific value; suffix 'a' indicates alcohol-based fuel and the suffix 'D' indicates direct injection fuel. Eq. 4.4 defines brake thermal efficiency (BTE) as the ratio of brake power (BP) to heat energy supplied by both fuels (alcohol-based fuel and direct injection fuel) [80][1].

$$\text{Brake specific fuel consumption (bsfc) (kg/kW.h)} = \frac{(FC_a) + (FC_D)}{BP} \quad (4.5)$$

Eq. 4.5 defines brake-specific fuel consumption (bsfc) as the ratio of fuel consumption (FC) to the brake power (BP) generated at that load. In Eq. 4.5 FC indicated that fuel consumption in kg/hr, suffix 'a' indicates alcohol-based fuel, and the suffix 'D' indicates direct injection fuel.

$$\text{Improvement (\%)} = \frac{(\text{Parameter}_{CI}) - (\text{Parameter}_{HCCI})}{\text{Parameter}_{CI}} * 100 \quad (4.6)$$

Eq. 4.6 defines the improvement of engine parameter, "Parameter<sub>CI</sub>" indicates the value of any parameter of conventional CI engine and "Parameter<sub>HCCI</sub>" indicates the value of any parameter of HCCI engine. The difference of both divided by conventional CI engine parameter value indicates improvement of performance.

$$\text{Cooling Potential (K)} = \frac{\varphi * H_{fg \text{ fuel}}}{AFR_{\text{Stoich}} * C_p \text{ air}} \quad (4.7)$$

Eq. 4.7 defines the cooling potential of alcohol-based fuels. It is the ratio of the product of equivalence ratio and latent heat of vaporization (LHV) to the product of stoichiometric air-fuel ratio and specific heat of air. Here  $\varphi$  indicate an equivalence ratio of a particular fuel,  $H_{fg \text{ fuel}}$  is the LHV,  $AFR_{\text{stoich}}$  is the stoichiometric air-fuel ratio and  $C_p \text{ air}$  is the specific heat of air [129].

Complete engine setup was computer interfaced; engine data was controlled by ECU and

captured on monitor screen. By using in-cylinder pressure data with crank angle (CA), HRR, was calculated by engine software.

The net heat release rate (HHR) was calculated from the in-cylinder pressures attained during experiments by applying the first law of thermodynamics with suitable assumptions as per the formulation in Equation 4.9.

$$\frac{dQ_{hr}}{d\theta} = \frac{\gamma}{\gamma-1} P \frac{dV}{d\theta} + \frac{1}{\gamma-1} V \frac{dP}{d\theta} + \frac{dQ_{ht}}{d\theta} \quad (4.8)$$

$$\frac{dQ_{hr}}{d\theta} - \frac{dQ_{ht}}{d\theta} = \frac{dQ_n}{d\theta} = \frac{\gamma}{\gamma-1} P \frac{dV}{d\theta} + \frac{1}{\gamma-1} V \frac{dP}{d\theta} \quad (4.9)$$

Where  $\frac{dQ_{hr}}{d\theta}$  indicates the rate of combustion heat release with crank angle and  $\gamma = \frac{c_p}{c_v}$  is the

ratio of specific heats, P, V are the instantaneous pressure and volume of the cylinder measured by the sensors during experimentation,  $\frac{dQ_{ht}}{d\theta}$  is the rate heat transfer loss from the cylinder wall

by convection,  $\frac{dQ_n}{d\theta}$  is the net heat release rate,  $\frac{dV}{d\theta}$  is the change of cylinder volume with crank

angle and  $\frac{dP}{d\theta}$  is the rate of change of cylinder pressure with crank angle.

Brake power is the engine output power measure by engine crank angle speed sensor and load sensor (strain gauge).

$$\text{Brake power (BP)} = \frac{2\pi N T}{60000} \quad (kW) \quad (4.10)$$

Where N indicates the engine speed in rpm, T is the torque applied on the engine in Nm.

#### 4.4 Uncertainty analysis

Uncertainty analysis was performed to check the accuracy of the measured parameters. During the experiment, individual reading was varying with each other due to manual error, uncontrolled environmental parameters, poor sensor calibration, etc. Thus it was necessary to take the mean of all readings for calculations. If individual reading is denoted by  $y_i$ , and there are  $n$  readings, then arithmetic mean ( $y_m$ ) is estimated by:

$$y_m = \frac{1}{n} \sum_{i=0}^n y_i \quad (4.11)$$

The deviation for individual reading is defined by  $d_i = y_i - y_m$

The standard deviation ( $\sigma$ ) is:

$$\sigma = \sqrt{\frac{1}{n} \sum_{i=0}^n (y_i - y_m)^2} \quad (4.12)$$

The standard deviation of the mean ( $\sigma_m$ ) is defined as,

$$\sigma_m = \frac{\sigma}{\sqrt{n}} \quad (4.13)$$

The uncertainty (or) error of recorded data is  $\pm \sigma_m$  is shown in **Table 4.1**.

Overall uncertainty of experimentation is calculated by the square root of the sum of the squares of each measurent uncertainty [130–132].

Overall uncertainty = square root of  $((0.0135)^2 + (2.56)^2 + (4.84)^2 + (1.29)^2 + (1.42)^2 + (0.1)^2) = 5.78\%$

**Table 4.1:** Uncertainty of parameters

Measurement	Uncertainty
CO (% vol)	$\pm 0.0135$
HC (ppm)	$\pm 2.56$
NO <sub>X</sub> (ppm)	$\pm 4.84$
Smoke Opacity (HSU)	$\pm 1.29$
Engine Speed (rpm)	$\pm 1.42$
Torque (Nm)	$\pm 0.10$

## 4.5 Optimization of operating parameter

The objective of the present study is to optimize the premixed ratio and MFR of alcohol-based fuel (methanol, ethanol, propanol, and butanol) at each load condition by considering the lowest emissions, and highest fuel economy.

In the optimization for decision making multiple objective decision making (MODM) and multiple attribute decision making (MADM) these methods are important. MODM methods is useful for infinite or large number of alternatives choices while MADM method is useful for a limited number of alternatives. MADM approach is to find out the best alternative among the

limited number of alternatives. MADM method proves that how to attribute information is perfect for particular alternatives at a suitable weight. The MADM decision matrix is depend upon four terms i.e. alternatives, attributes, weight or relative importance of each attribute, and measures of performance of alternatives with respect to the attributes. The decision table is shown in **Table 4.2**. The decision table shows alternatives,  $A_i$  (for  $i = 1, 2, \dots, N$ ), attributes,  $B_j$  (for  $j = 1, 2, \dots, M$ ), weights of attributes,  $W_j$  (for  $j=1, 2, \dots, M$ ) and the measures of performance of alternatives,  $m_{ij}$  (for  $i= 1, 2, \dots, N; j=1, 2, \dots, M$ ).

A decision maker aims to find out the best alternative or to rank the complete set of alternatives. Attributes may not be in the same units so before adding in the decision table all should be normalized in the same units, so that all attributes may be considered in the decision problem. To solve MADM problem five different methods are commonly used i.e. Simple Additive Weighting (SAW) Method, weighted product method (WPM), four modes of the Analytic Hierarchy Process (AHP) Method, Revised AHP, and technique for order preference by similarity to ideal solution (TOPSIS).

**Table 4.2:** Decision table in MADM methods

Alternatives	Attributes					
	$B_1$ ( $W_1$ )	$B_2$ ( $W_2$ )	$B_3$ ( $W_3$ )	- (-)	- (-)	$B_M$ ( $W_M$ )
$A_1$	$m_{11}$	$m_{12}$	$m_{13}$	-	-	$m_{1M}$
$A_2$	$m_{21}$	$m_{22}$	$m_{23}$	-	-	$m_{2M}$
$A_3$	$m_{31}$	$m_{32}$	$m_{33}$	-	-	$m_{3M}$
-	-	-	-	-	-	-
-	-	-	-	-	-	-
$A_N$	$m_{N1}$	$m_{N2}$	$m_{N3}$	-	-	$m_{NM}$

In the present study, simple additive weighting (SAW) optimization method was used to examine the best MFR of fuel or fuel jet number (jet 40, jet 60, jet 70, jet 80, and jet 90) for any individual load conditions. Additionally, the same method was used to find out the best blend of high reactivity fuel instead of diesel in an alcohol-based DF-HCCI engine.

SAW method is also known as weighted sum method (WSM). This is the most simple and widest used MADM method. In this, every single attribute is assigned with some weight and the sum of weights should be 1. Each alternative is evaluated with regard to every attribute. Initially SAW is particularly used for the same unit attributes. However, if all the units of attributes normalized then SAW may be best for any number of attributes. The overall performance score of an alternative is the sum of all products of the normalized attribute value and the weight assigned to that attribute given by Equation 4.14.

$$Y_i = \sum_{j=1}^M W_j (m_{ij})_{normal} \quad (4.14)$$

where  $(m_{ij})_{normal}$  represents the normalized value of  $m_{ij}$ , and  $Y_i$  is the overall or composite score of the alternative  $A_i$ . The alternative with the highest value of  $Y_i$  is considered as the best alternative.

Normalization was done on the basis of beneficial attributes and non-beneficial attributes. Beneficial means that higher value is better and non-beneficial means lower value is better among the alternatives considered.

In this study, non-beneficial attribute (Smoke opacity,  $NO_x$ , HC, and CO) normalization was done by  $(m_{ij})_K / (m_{ij})_L$ , where  $(m_{ij})_K$  is value of attribute for K-th alternative, which is the lowest value among all alternatives considered, while  $(m_{ij})_L$  is value of measured attribute for the L-th alternative.

Beneficial attribute (BTE) normalization was done by  $(m_{ij})_L / (m_{ij})_K$ , where  $(m_{ij})_L$  is the value of measured of the attribute for L-th alternative, and  $(m_{ij})_K$  is the value of attribute for the K-th alternative, which is the highest value among all alternatives considered.

In MADM optimization technique weightage and importance of output parameters totally depend on the required design of engine [133,134]. In the present study, optimization was done based on the lowest exhaust emissions and highest BTE. The aim is to reduce  $NO_x$  and smoke opacity without loss in fuel economy by the use of alcohol-based DF-HCCI engine combustion mode. For optimization of MFR of alcohol-based fuel or fuel jet no or premixed ratio at individual load conditions, four different sets of weightages were considered. Also to optimize the butanol blend in the alcohol-based DF-HCCI engine same weightages were used. Four different sets of weightage are shown in equation 4.15-4.18.

$$Y_1 = 0.333 \text{ BTE} + 0.333 \text{ Smoke opacity} + 0.333 \text{ NO}_X + 0.0 \text{ HC} + 0.0 \text{ CO} \quad (4.15)$$

In Eq. 4.15 equal weightage was assigned to BTE, smoke opacity, and NO<sub>X</sub> emission attributes i.e. 33.33% each, but HC and CO emissions attribute assigned 0% weightage. The main aim of this study was to control NO<sub>X</sub> and smoke opacity because HC and CO can be easily controlled by after-treatment methods [135].

$$Y_2 = 0.4 \text{ BTE} + 0.25 \text{ Smoke opacity} + 0.25 \text{ NO}_X + 0.05 \text{ HC} + 0.05 \text{ CO} \quad (4.16)$$

In Eq. 4.16, 40% weightage was assigned to BTE, 25% each was assigned to smoke opacity and NO<sub>X</sub> emission, and very low means 5% each was assigned to HC and CO emissions.

$$Y_3 = 0.3 \text{ BTE} + 0.25 \text{ Smoke opacity} + 0.25 \text{ NO}_X + 0.1 \text{ HC} + 0.1 \text{ CO} \quad (4.17)$$

In Eq. 4.17, 30% weightage was assigned to BTE, 25% each was assigned to smoke opacity and NO<sub>X</sub> emission and a little more means 10% each was assigned to HC and CO emissions.

$$Y_4 = 0.5 \text{ BTE} + 0.25 \text{ Smoke opacity} + 0.25 \text{ NO}_X + 0.0 \text{ HC} + 0.0 \text{ CO} \quad (4.18)$$

In Eq. 4.18, HC and CO emission attributes weightage was 0% and the highest weightage was assigned to BTE i.e 50% and 25% each were assigned to smoke opacity and NO<sub>X</sub> emission attribute.

To investigate the optimum alternative parameter all attributes normalized values submitted in each equation for example in eq. 4.15 by considering 33.3% weightage to each attribute i.e. BTE, NO<sub>X</sub> emission, and smoke opacity, finally the score noted for each alternative. A similar procedure was done for each alternative. The highest score among all alternatives indicates the best alternative for particular weightage selection sets.

Similarly, the best alternative was found for 3 more sets of weightage equation i.e. equation 4.16, 4.17, and 4.18.

## **Chapter - 5**

### **Results and Discussion**

**Experimentally Analyzed the Performance of DF-HCCI Engine over  
Conventional Diesel Engine**

---

## 5.1 General

In this section, experimentally the alcohol-based DF-HCCI engine performance was analyzed and compared with the conventional diesel engine. The influence of carburetor location on the DF-HCCI engine performance was examined. Combustion characteristics such as in-cylinder pressure, heat release rate (HRR), pressure rise rate (PRR), Mass fraction burn, ignition delay (ID), combustion duration (CD), were discussed for various alcohol-based DF-HCCI engine. Performance characteristics such as brake thermal efficiency (BTE), brake specific fuel consumption (bsfc), oxide of nitrogen ( $\text{NO}_x$ ) emission, Hydrocarbon (HC), carbon monoxide (CO), Smoke opacity, were analyzed. Different alcohol-based fuel premixed ratio was fixed for individual load condition by considering SAW optimization. Further, the influence of butanol blends and biodiesel blend instead of diesel on alcohol-based DF-HCCI engine was investigated for different load conditions.

## 5.2 Objective 1

**To experimentally investigate the influence of carburetor location on dual fuel mode HCCI engine performance.**

### 5.2.1 General

Experimentation was done for ethanol-diesel (E100+D) DF-HCCI engine at a constant MFR of ethanol. Ethanol fuel was supplied through the carburetor and to ignite the premixed ethanol charge at the end of compression stroke diesel was injected. Fuel jet 60 was used in the carburetor for all load conditions and the varying load was controlled by diesel injection. Three different lengths of inlet manifold pipe such as 6-inch, 9-inch, and 12-inch were used to fix the carburetor location outside the engine. Influence of these three different carburetor locations on DF-HCCI engine performance and emissions were investigated under various load conditions.

### 5.2.2 Combustion and emission characteristics

**Figure 5.1(a)** shows the in-cylinder pressure with crank angle (CA). With increasing the length of inlet manifold pipe little increment was observed in-cylinder pressure. If the carburetor location away from the engine cylinder little more in-cylinder pressure was noted.

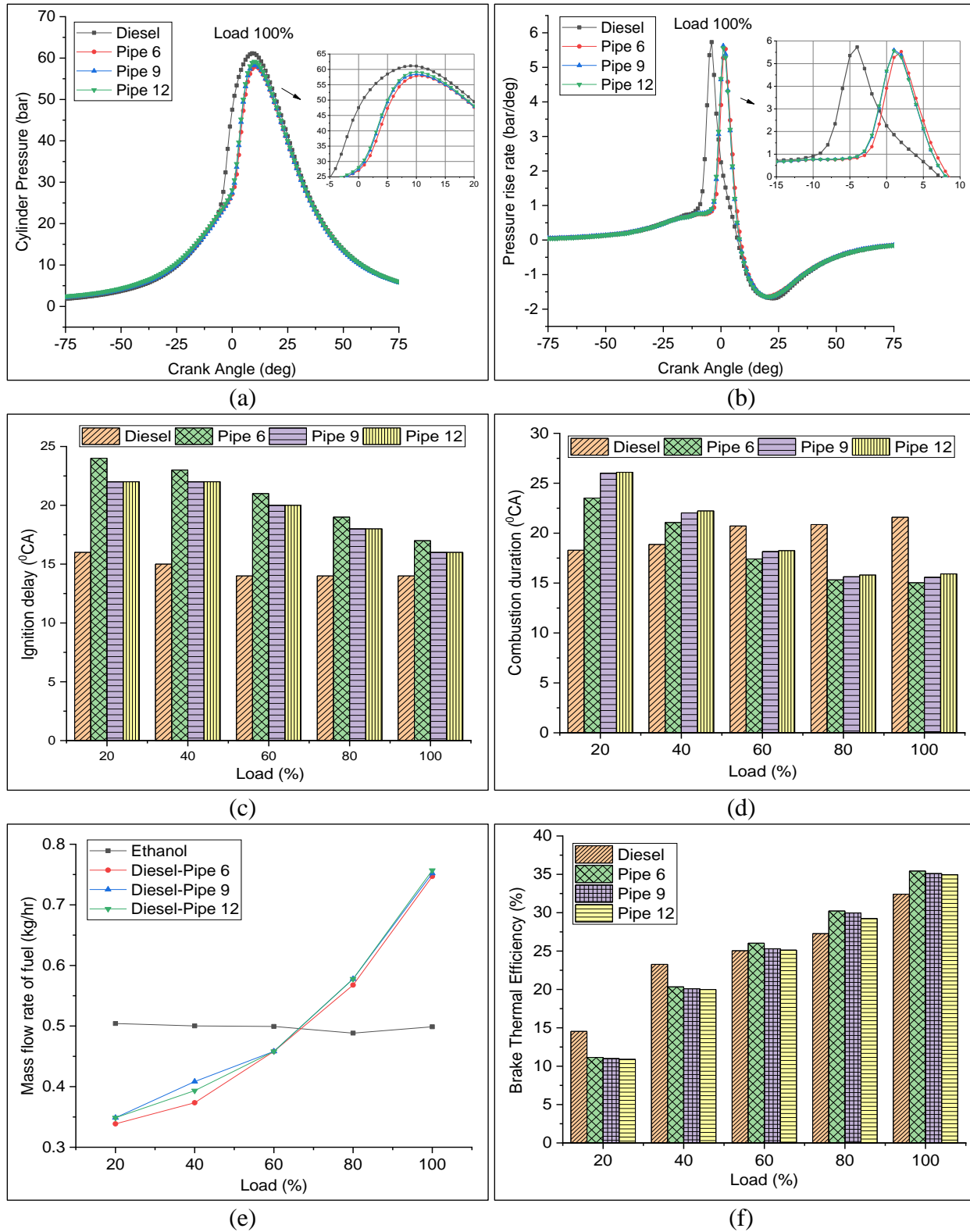


**Figure 5.1** (a) In-cylinder pressure Vs. CA, (b) PRR Vs. CA, (c) ID Vs. engine load, (d) CD Vs. engine load, (e) MFR Vs. engine load, (f) BTE Vs. engine load

If the carburetor location is 12-inch away from the engine cylinder the in-cylinder pressure is

observed as 59.16 bar while at 9-inch and 6-inch location in-cylinder pressure is 58.45 bar and 57.89 bar respectively.

**Figure 5.1(b)** shows PRR with CA for various locations of carburetor outside the engine. PRR was observed below  $6 \text{ bar} / {}^0\text{CA}$  for all inlet manifold pipe lengths. It shows that the engine is working without knocking at any carburetor location outside the engine [88,105].

**Figures 5.1(c) and 5.1(d)** show ignition delay (ID) and combustion duration (CD) for different engine loads. An increase in length of inlet manifold pipe reduced ID and increased CD. Since the carburetor location away from the engine cylinder, alcohol-based fuel (ethanol) get more time to prepare air and fuel mixture outside the engine, which leads to reduce the ID. **Figure 5.1(e)** shows the mass flow rate (MFR) of ethanol and diesel for different carburetor locations under various load conditions. With increasing the length of the inlet manifold pipe diesel consumption was increased. If the alcohol-based fuel (i.e. ethanol) transportation gap in between engine cylinder and injection point is more fuel may evaporate or friction losses may be added [136]. If the carburetor location was set 12-inch away from the engine cylinder ethanol may evaporate, some friction losses may happen, fuel may atomize so to fulfill the required amount of power and to achieve the constant rpm more diesel fuel was consumed. More diesel consumption leads to extend the diffusion combustion phase, which assists to elongate the CD. Hence with increasing the length of the inlet manifold pipe CD got increased.

More diesel consumption for 9-inch and 12-inch inlet manifold pipe helps to a little increment in the in-cylinder pressure. This diesel consumption also impacts brake thermal efficiency (BTE) as shown in **figure 5.1(f)**. If the carburetor location is near (6-inch pipe) to the engine cylinder a little improvement in BTE compared to the rest of the locations (9-inch, 12-inch).

In the case of emission characteristics, there were not any considerable changes in the  $\text{NO}_x$  emission, smoke opacity, HC emission, and CO emission against carburetor location outside the engine as shown in **figure 5.2(a), 5.2(b), 5.2(c), and 5.2(d)**.

In this study, varying the carburetor location was not showing considerable changes in the engine emission and in-cylinder pressure but to avoid the evaporation losses, friction losses, fuel atomization, fuel molecule sticking to the manifold [137,138], a nearer location of the carburetor was better. Nearer carburetor location will impact the fuel economy of the DF-HCCI engine. Hence to fix the carburetor location in DF-HCCI engine 6-inch length inlet manifold pipe was

selected for further studies.

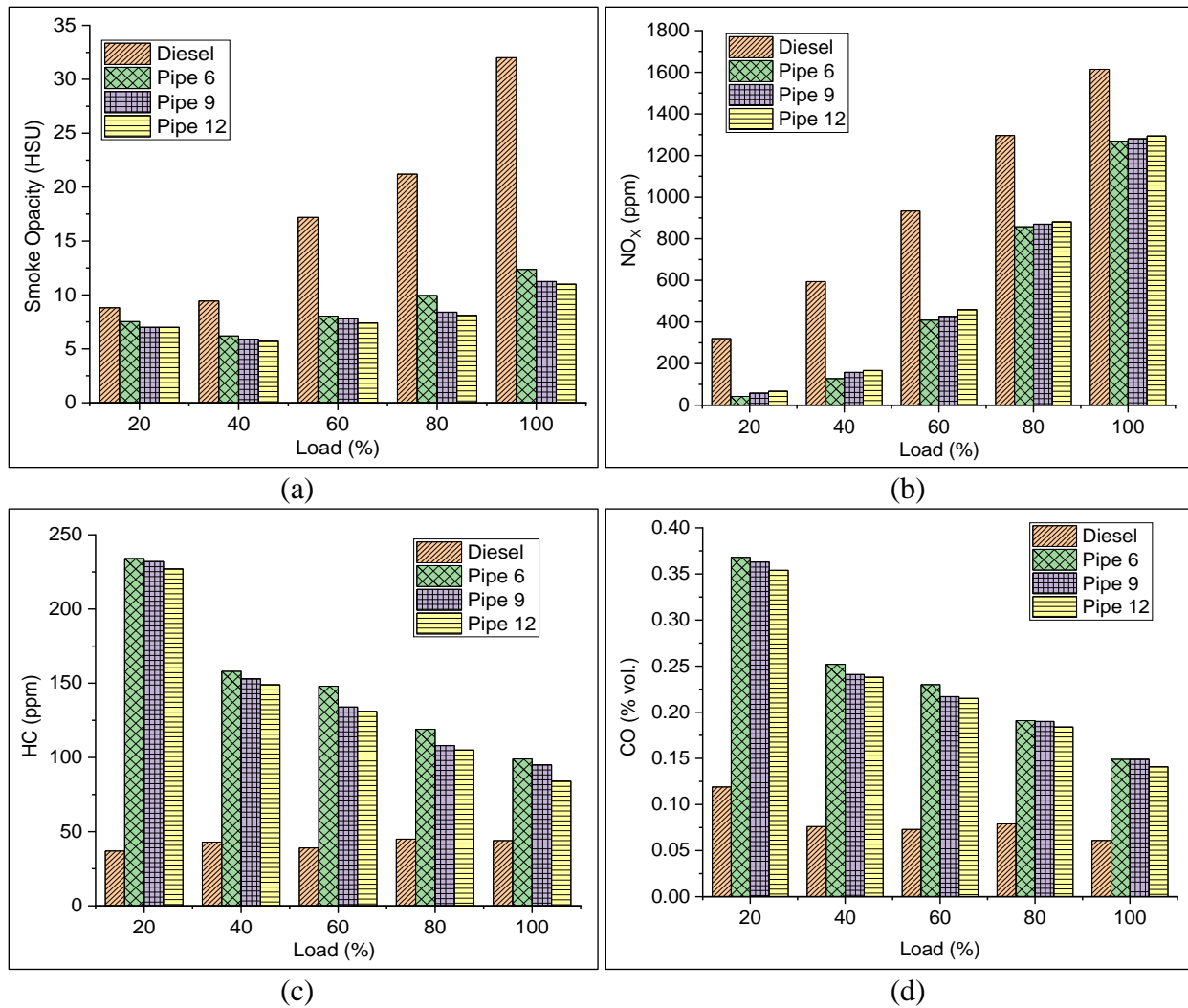


**Figure 5.2** (a) Smoke opacity Vs. engine load, (b) NO<sub>x</sub> Vs. engine load, (c) HC Vs. engine load, (d) HC Vs. different load

## 5.3 Objective 2

To optimize mass flow rate and premixed ratio under each load, for methanol, ethanol, propanol, butanol alcohol-based fuels by using different fuel jets in the carburetor.

### 5.3.1 General

Under this experimentation, four different alcohol-based fuels were chosen methanol, ethanol, propanol, and butanol. All alcohol-based fuel was supplied at the time of suction stroke through the carburetor and to ignite this homogenous charge diesel was injected at the end of compression stroke. To vary the mass flow rate (MFR) of alcohol-based fuel different fuel jet was used in the carburetor. Optimum premixed ratio and MFR were investigated for each alcohol-based fuel under individual load conditions. SAW optimization method was used to find out the optimum MFR and premixed ratio for four different weightage sets.

### 5.3.2 Ethanol-diesel DF-HCCI engine performance for different load conditions

In this experiment ethanol fuel was supplied at the time of suction stroke through the carburetor and diesel was injected at the end of a compression stroke. To vary the MFR of ethanol five different fuel jets such as jet 40, Jet 60, jet 70, jet 80, and jet 90 were used.

#### 5.3.2.1 In-cylinder pressure for different load conditions

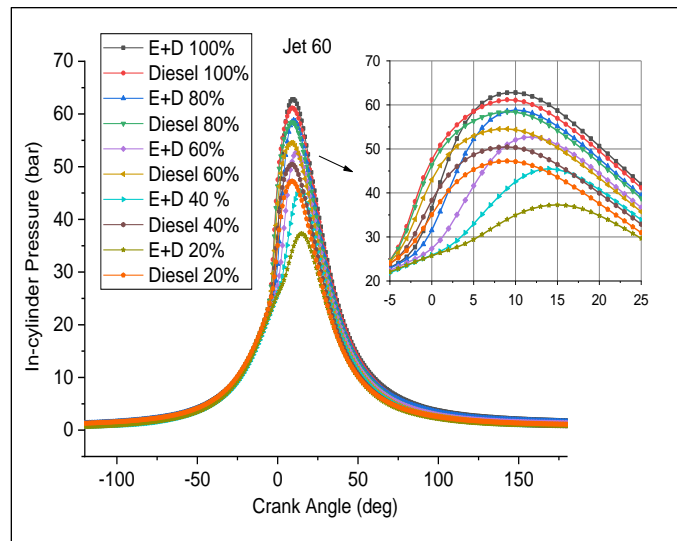


**Figure 5.3.** Comparing diesel and dual-fuel mode HCCI engine in-cylinder pressure Vs. crank angle under different load conditions, for jet 60

**Figure 5.3** presents in-cylinder pressure with respect to CA for 20% to 100% rated power of engine using fuel jet 60. It was observed that for both neat diesel and DF-HCCI engines, in-

cylinder pressure was increasing with increasing load on the engine. Increasing load on engine demanding more fuel, and burning more fuel releases more energy which results to increase in-cylinder pressure [139]. In the DF-HCCI mode, start of combustion (SOC) is delayed compared to neat diesel engine. The results indicated that Ethanol-Diesel (E100+D) DF-HCCI engine in-cylinder pressure curves are shifting forward compare to neat diesel engine. It indicates that ethanol contribution resists SOC and it helps to low temperature combustion (LTC).

### **5.3.2.2. Influence of a different MFR of Ethanol on combustion and emission characteristics**

**Figure 5.4** indicates in-cylinder pressures of the engine for different MFR of ethanol by the use of different fuel jets in the carburetor. **Figure 5.4(a)** shows in-cylinder pressure for 100% rated load on the engine. In-cylinder pressure curve is shifted towards TDC. It means that with increasing MFR of ethanol, combustion got delayed in the DF-HCCI engine compared to neat diesel engine. It increases ID (shown in **Figure 5.6(a)**) and ignition timing is retarded due to high auto-ignition temperature and high octane number of ethanol. Increasing MFR of ethanol retards the combustion phase (ethanol is low reactivity fuel so it retards the combustion) and more part of combustion is completed in the expansion stroke so that it leads to lower in-cylinder pressure. This helps to run the engine at LTC mode which reduces NO<sub>x</sub> emissions. Similar results have been noticed in the case of gasoline/methanol port injected fuel with diesel as a direct injection fuel [140,141]. It is noticed that in-cylinder pressure for jet 70, jet 80, and jet 90 is lower than diesel engine. However, jet 40 and jet 60 in-cylinder pressures are found equal to a neat diesel engine. The maximum in-cylinder pressure values for jet 40, jet 60, jet 70, jet 80, and jet 90 are 62.05 bar, 62.79 bar, 61.98 bar, 58.42 bar, and 55.07 bar respectively, but, neat diesel engine in-cylinder pressure is 61.16 bar. Similarly, peak pressure CA for jet 40, jet 60, and jet 70 are 10<sup>0</sup> aTDC, for jet 80 is 13<sup>0</sup> aTDC, for jet 90 is 15<sup>0</sup> aTDC, whereas for diesel is 9<sup>0</sup> aTDC.

**Figure 5.4(b)** shows the in-cylinder pressure for 80% engine load. Jet 40, jet 60, jet 70, jet 80, and jet 90 were used for 80% engine load. Similar nature of in-cylinder pressure was found for 80% engine load, peak in-cylinder pressures for jet 40, jet 60, jet 70, jet 80, and jet 90 are 58.25 bar, 58.82 bar, 55.42 bar, 47.85 bar, and 42.3 bar respectively; however, diesel peak in-cylinder pressure is 58.45 bar. Peak pressure crank angle for jet 40, jet 60, are 10<sup>0</sup> aTDC, for jet 70 it is 12<sup>0</sup> aTDC, for jet 80 it is 17<sup>0</sup> aTDC and for jet 90 is it 20<sup>0</sup> aTDC, whereas for diesel engine it was 9<sup>0</sup> aTDC.

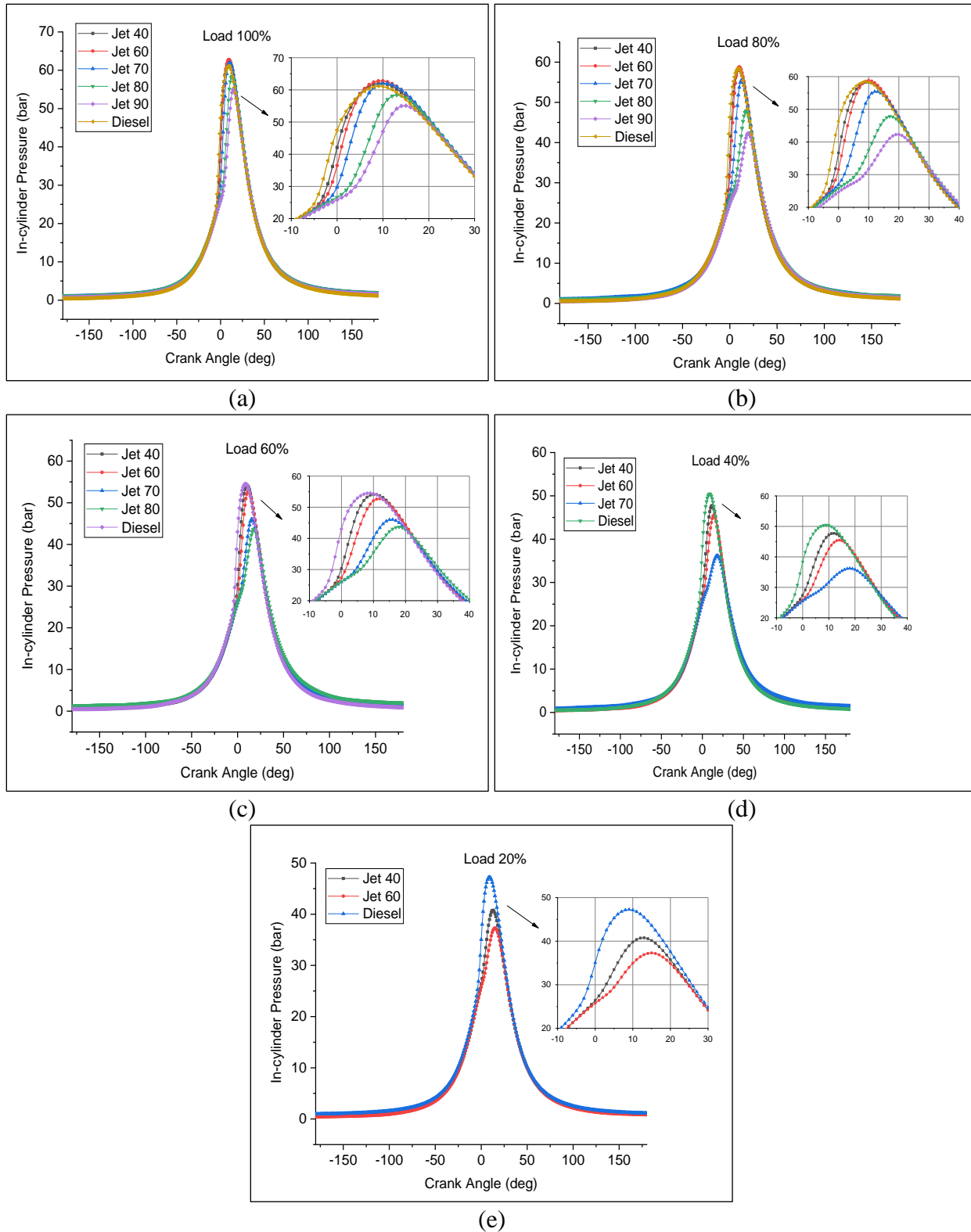


**Figure 5.4** The variation of in-cylinder pressure for different fuel jets of DF-HCCI combustion at different engine loads (a) 100% (b) 80% (c) 60% (d) 40% (e) 20%

**Figure 5.4(c)** shows the in-cylinder pressure for 60% engine load. For 60% engine load jet 40, jet 60, jet 70, jet 80 were used. In this load condition, in-cylinder pressures are reduced and the combustion phase retarded was similar to engine load 80 and 100%. Peak in-cylinder pressure and CA for jet 40 is 54.13 bar at  $10^0$  aTDC, for jet 60 it is 52.71 bar at  $12^0$  aTDC, for jet 70 it is 46.04 bar at  $16^0$  aTDC and for jet 80 it is 43.67 bar at  $18^0$  aTDC.

**Figure 5.4(d)** shows the in-cylinder pressure with a CA for 40% engine load. For 40% engine load, jet 40, jet 60, and jet 70 were used. Peak in-cylinder pressure and CA for jet 40 is 47.12 bar at  $12^0$  aTDC, for jet 60 it is 45.49 bar at  $14^0$  aTDC and for jet 70 it is 36.21 bar at  $18^0$  aTDC, however, diesel engine in-cylinder pressure is 50.46 bar at  $9^0$  aTDC.

**Figure 5.4(e)** shows the in-cylinder pressure for 20% engine load. Peak in-cylinder pressures with a CA for jet 40, jet 60 are 40.77 bar at  $13^0$  aTDC, 37.29 bar at  $15^0$  aTDC respectively; however, for diesel, it was 47.26 bar at  $9^0$  aTDC.

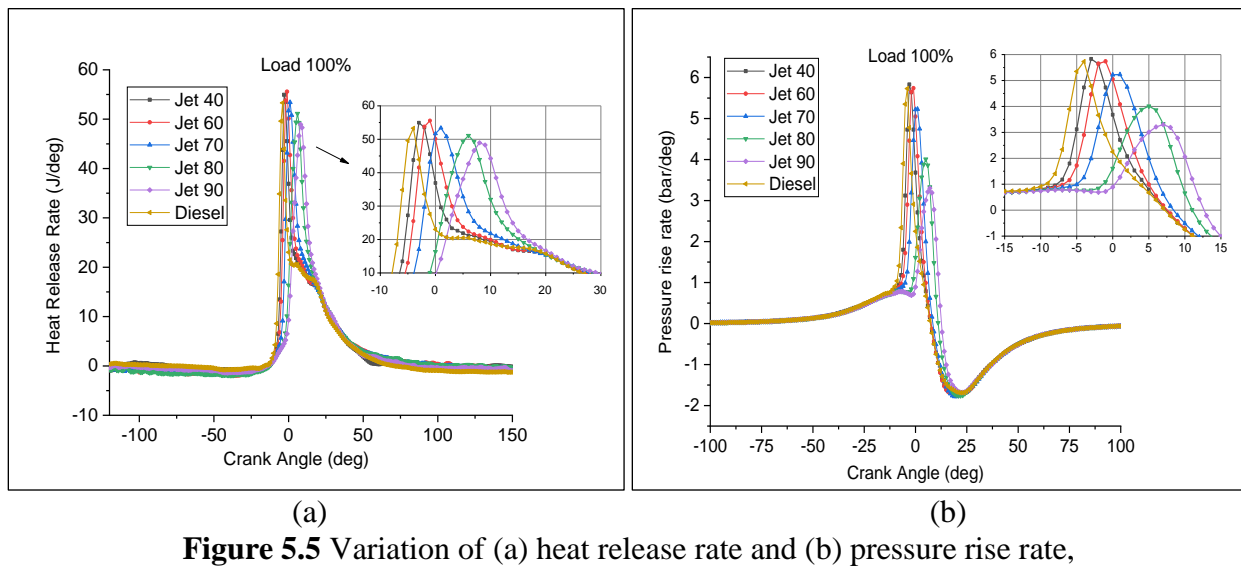


**Figure 5.5** Variation of (a) heat release rate and (b) pressure rise rate, for different fuel jets under 100% load conditions

**Figure 5.5(a)** and **figure 5.5(b)** illustrate the effect of increasing the MFR (jet number) on HRR and PRR of E100+D DF-HCCI engine combustion for 100% rated load. It is noticed that the increase of ethanol MFR, retards the peak HRR and peak PRR crank angle. This is due to delay in SOC; which results in LTC in dual fuel mode HCCI engine compared to the neat diesel engine. Therefore low HRR and PRR are observed. Further, it is noticed that E100+D DF-HCCI engine running very smoothly without knocking. In this test, PRR is less than the 6 bar/ $^0$  CA for

all loads. The majority of researchers define the knocking criteria of the engine in PRR value, which should be less than 10-20 bar/CA [88,105,142,143].

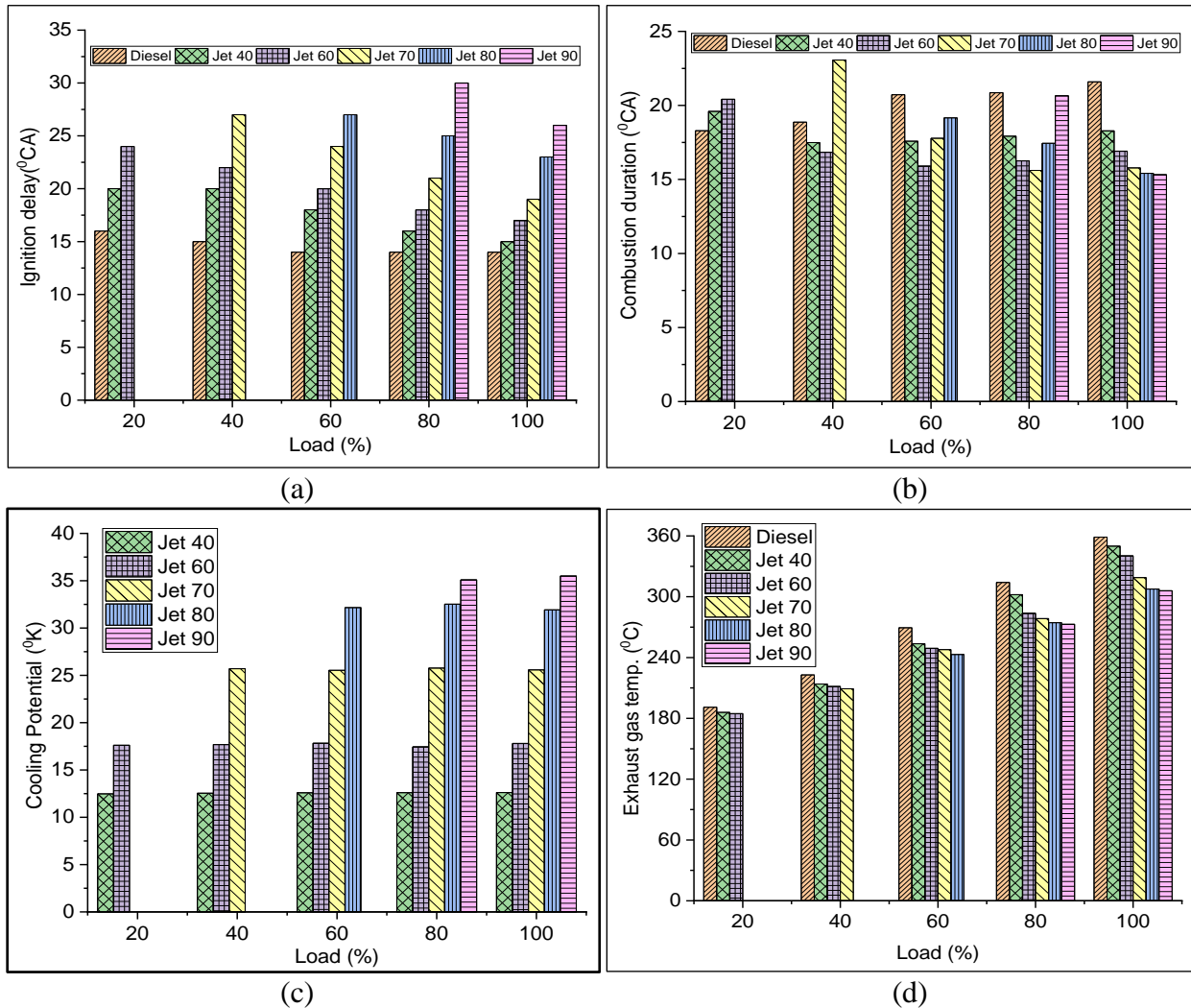


**Figure 5.6** (a) Ignition delay (ID) Vs. Engine load, (b) Combustion duration (CD) Vs. Engine load, (c) Cooling potential Vs. Engine load, (d) Exhaust gas temp Vs. Engine load

**Figure 5.6 (a)** shows the ID with an increase in jet number for different load conditions. The ID is increased with increase in ethanol MFR because ethanol has high self-ignition temperature, high octane number and higher latent heat of vaporization (LHV) compared to neat diesel; so it absorbs more energy from the compressed air and it increases the ignition timing and delays SOC. High self-ignition temperature allows the fuel to resist the start of ignition leads to an increased ID. With increasing the MFR of ethanol ID was increased because ethanol substitution increases its cooling potential (as shown in **figure 5.6(c)**). If the high LHV fuel contribution increases its ability to absorb the heat from the compressed air increases, it leads to extend the ID

[129][115] and reduce the engine combustion temperature assist to reduce the exhaust gas temperature (shown in **Figure 5.6(d)**).

**Figure 5.6(b)** presents the combustion duration (CD) for increasing MFR of ethanol under different load conditions. The results show that CD is reduced with the increase of MFR of ethanol. Homogeneous fuel has a longer ID due to the maximum amount of fuel burns in the rapid combustion phase aTDC in a low-temperature environment; very less fuel is burnt in diffusion combustion, therefore, it reduces CD. Similar results have been found for alcohol-based fuel with diesel RCCI engine [111]. However, at 60% engine load condition CD was increased for jet 70 and jet 80 because at this load condition more than the requirement premixed fuel was supplied through the carburetor, and to ignite this premixed charge minimum amount of diesel was injected. This extra diesel and extra ethanol fuel promotes diffusion combustion and leads to extend the CD. A similar kind of results appeared at 80% load condition for jet 80 and jet 90.

**Figure 5.7(a)** represents  $\text{NO}_x$  emission with varying loads of the engine. It is observed that  $\text{NO}_x$  emissions are reduced with an increase in the MFR of ethanol (increase in jet number) for all load conditions compared to a neat diesel fuel engine. DF-HCCI engine is working on the lean homogeneous mixture because of which combustion occurs at low temperature and for  $\text{NO}_x$  emissions, temperature of the combustion chamber is the main affecting factor. Further, ethanol has high LHV, and it helps to absorb the heat from combustion chamber and reduces the combustion chamber temperature. **Figure 5.4** displays the low peak in-cylinder pressure and **Figure 5.5(b)** displays low PRR with increase in jet number means that the DF-HCCI engine working on LTC mode and it helps to reduce  $\text{NO}_x$  emissions. In the present experiment, Jet 60 reduces  $\text{NO}_x$  emission from 320 ppm to 42 ppm for 20% engine load. And jet 90 reduces  $\text{NO}_x$  emission from 1614 ppm to 585 ppm for 100% load conditions. Maximum 92.5%  $\text{NO}_x$  emission was reduced for jet 90 at 80% load while jet 70 reduced 96.46% at 40% load conditions. On average 85%  $\text{NO}_x$  emission was reduced by E100+D DF-HCCI engine compared to a neat diesel engine for all load conditions. Overall performance improvement in  $\text{NO}_x$  emission for various MFR under different load conditions as shown in **figure 5.8(a)**.

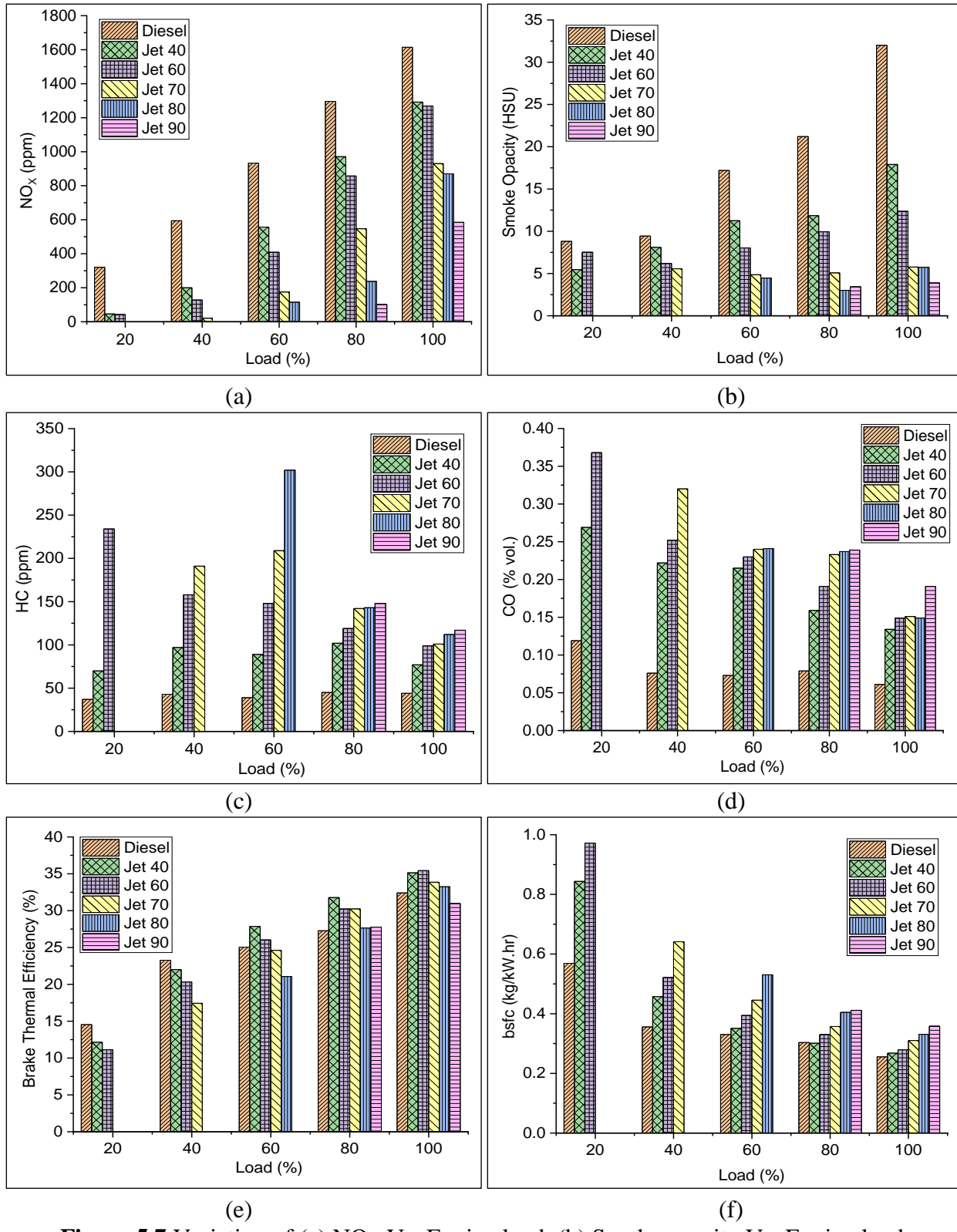


**Figure 5.7** Variation of (a) NO<sub>x</sub> Vs. Engine load, (b) Smoke opacity Vs. Engine load,  
 (c) HC Vs. Engine load, (d) CO Vs. Engine load,  
 (e) Brake thermal efficiency Vs. Engine load, (f) bsfc Vs. Engine load

**Figure 5.7(b)** shows the smoke opacity in HSU with varying loads for different MFR of ethanol (different fuel jets). The results display that the smoke opacity is reduced with an increase in jet numbers. Smoke opacity depends on the inhomogeneity of air-fuel mixture in the combustion chamber. In this study, ethanol is supplied with air at the time of suction stroke and plenty of time is available for ethanol to mix with air. High ID permits the fuel for proper homogenous charge it leads to reduces the fuel-rich region in the combustion chamber helps to reduce the smoke opacity. Further, ethanol is the most volatile fuel and it easily mixes with air and forms a homogenous mixture, most of the charge burn in the premixed phase combustion promotes a reduction in smoke opacity of E100+D DF-HCCI engine compared to neat diesel engine. The results show that smoke opacity reduced almost 87.84% for jet 90 at 100% load. It was observed that an increase in ethanol mass contribution at the time of suction reduced smoke opacity compared to a neat diesel fuel engine. For 100% load, smoke opacity reduced from 32 HSU to 3.89 HSU for E100+D DF-HCCI engine.

**Figure 5.7(c)** and **Figure 5.7(d)** displays HC and CO emission with varying loads for different jet numbers. The results show that HC and CO emissions increase with increase in jet number at any particular load compared to a neat diesel engine. HC and CO emissions occur due to LTC, incomplete combustion, and the combustion near the misfire. Jet 60 results show that HC and CO emissions are very high for low load conditions and they reduce with increase in load conditions. It indicates that for any particular load in E100+D DF-HCCI engine if the contribution of ethanol fuel is more compared to diesel fuel, combustion is done near misfire at low temperature and impingement on the wall of the cylinder, it promotes the formation of HC and CO emissions.

**Figure 5.7(e)** shows the brake thermal efficiency (BTE) with varying loads for different fuel jets. It is observed that BTE for 60%, 80%, and 100% engine load are more than the neat diesel engine. Jet 40 and jet 60 showed the highest BTE for 60%, 80%, and 100% engine load. The mass flow rate of ethanol for jet 40 and jet 60 is low and ID is also low. The peak in-cylinder pressure is nearly equal to neat diesel engine but due to a homogeneous mixture of ethanol, total fuel is properly utilized to obtain the required power hence BTE increases for 60%, 80%, and 100% engine load. While at low load conditions due to more than requirement fuel is consumed leads to reduce the BTE compared to neat diesel engine. However, NO<sub>x</sub> and smoke opacity emissions are very poor for jet 40 and jet 60. Jet 90 shows less fuel economy compared to neat

diesel engine because jet 90 ID is highest and peak pressure is also reduced due to late combustion so that more fuel is utilized to achieve the required power of the engine.

**Figure 5.7(f)** shows the comparison of bsfc under different load conditions. The results show that bsfc for DF-HCCI engine is high as compared to diesel engine because the calorific value (CV) of ethanol fuel is 27 MJ/kg and diesel is 43.5 MJ/kg. The contribution of ethanol fuel is more compared to diesel to attain the requisite power. Hence to attain the same power in DF-HCCI engine more ethanol fuel consumption is required compared to diesel engine.

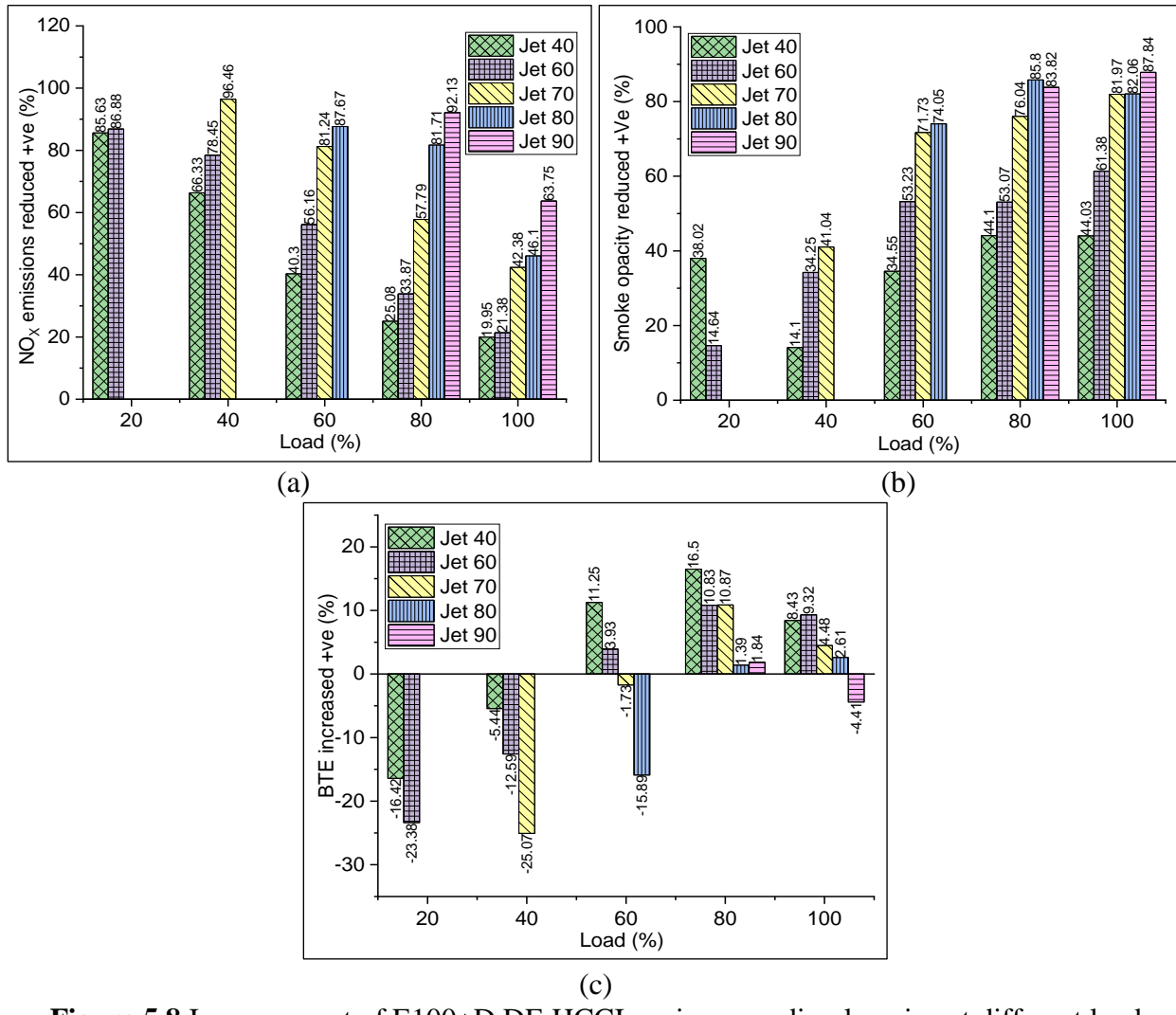


**Figure 5.8** Improvement of E100+D DF-HCCI engine over diesel engine at different load condition for various MFR (a) NO<sub>x</sub> emissions reduction, (b) smoke opacity reduction, (c) BTE increment

**Figure 5.8** shows the improvement (reduction of emission and increment of BTE) of E100+D DF-HCCI engine over diesel engine. Positive value on Y-axis denotes the favorable improvement (i.e. reduction of NO<sub>x</sub>, reduction of smoke opacity, and increment of BTE) and the negative value on Y-axis denotes unfavorable improvement. **Figure 5.8(a)** shows the NO<sub>x</sub> emission reduction for various fuel jet numbers under different load conditions. Maximum NO<sub>x</sub> reduction was occurred at 40% engine load for jet 70, while jet 40 reduced the lowest percentage NO<sub>x</sub> emission at 100% load. **Figure 5.8(b)** shows smoke opacity reduction at different load conditions for different fuel jets. Maximum smoke opacity was reduced for jet 90 under 100% load, while the minimum smoke opacity reduction was noticed for jet 40 at 40% load. **Figure 5.8(c)** indicates BTE improvement for various fuel jet numbers under different load conditions. Jet 40 given the highest BTE for 80% engine load.

**Figure 5.9** presents the premixed ratio of ethanol for various MFR of ethanol (various fuel jet numbers) under different load conditions. The results show that with increasing the fuel jet number contribution of ethanol energy ratio increases at different load conditions. This premixed ratio of ethanol indicates the amount of heat energy contributed by ethanol among ethanol and diesel consumption. Jet 90 at 80% load condition contributed a maximum 75.94% ethanol premixed ratio. To generate the power at 80% load, 75.94% power is generated by ethanol fuel consumption and the remaining 24.06% power is generated by diesel fuel consumption. High premixed ratio is possible because the amount of ethanol fuel supplied will replace the conventional diesel fuel result in low NO<sub>x</sub> and smoke opacity without penalty of BTE.

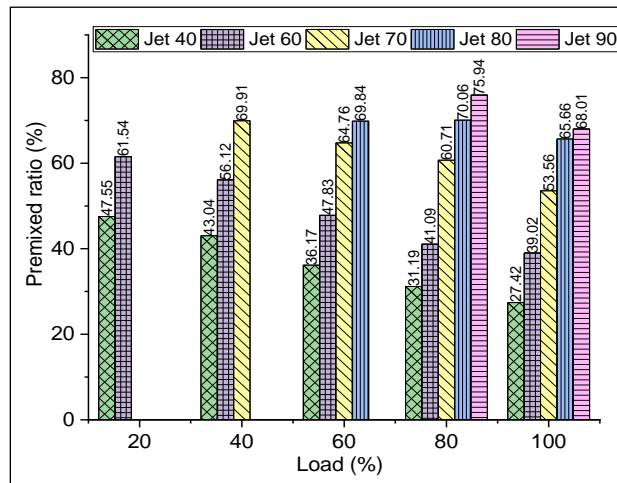


**Figure 5.9** Premixed ratio of ethanol Vs. Engine load

### 5.3.2.3 Optimize the MFR and premixed ratio at each load conditions

From this study, it was observed that jet 70 helps to reduce maximum NO<sub>X</sub> emission at 40% load condition, while jet 90 reduced maximum smoke opacity at 100% load, and jet 40 increased maximum BTE at 80% load condition. It was very difficult to judge the best fuel jet number or MFR at any individual load condition. Hence optimization was done to finalize the cumulative performance of different fuel jets at individual load conditions. SAW optimization method was used to find out the best fuel jet number or MFR at individual load conditions for lowest emission and highest BTE or fuel economy.

**Table 5.1** Ranking of different fuel jets for various weightage sets under each load conditions

Load (%)	Type of jet	Y <sub>1</sub>	Rank	Y <sub>2</sub>	Rank	Y <sub>3</sub>	Rank	Y <sub>4</sub>	Rank
20	CI	0.583	3	0.687	3	0.687	3	0.687	3
	Jet 40	0.915	1	0.861	1	0.826	1	0.896	1
	Jet 60	0.829	2	0.762	2	0.709	2	0.814	2
40	CI	0.541	4	0.656	2	0.656	2	0.656	4
	Jet 40	0.578	3	0.615	4	0.56	4	0.67	3
	Jet 60	0.644	2	0.643	3	0.584	3	0.702	2
	jet 70	0.915	1	0.822	1	0.771	1	0.874	1
60	CI	0.426	5	0.555	5	0.565	3	0.545	5
	Jet 40	0.533	4	0.589	4	0.528	5	0.65	4
	Jet 60	0.589	3	0.611	3	0.547	4	0.676	3
	jet 70	0.818	2	0.771	2	0.707	2	0.835	2
	Jet 80	0.917	1	0.824	1	0.77	1	0.878	1
80	CI	0.359	6	0.498	6	0.512	4	0.484	6
	Jet 40	0.452	5	0.536	4	0.483	5	0.589	4
	Jet 60	0.457	4	0.525	5	0.469	6	0.581	5
	jet 70	0.576	3	0.608	3	0.545	3	0.67	3
	Jet 80	0.766	2	0.738	2	0.683	2	0.792	2
	jet 90	0.916	1	0.85	1	0.795	1	0.906	1
100	CI	0.465	6	0.586	6	0.595	4	0.578	6
	Jet 40	0.553	5	0.615	5	0.567	6	0.663	5
	Jet 60	0.591	4	0.636	4	0.579	5	0.693	4
	jet 70	0.752	3	0.75	3	0.696	3	0.803	3
	Jet 80	0.762	2	0.753	2	0.699	2	0.806	2
	jet 90	0.957	1	0.884	1	0.831	1	0.937	1

In this study, four different sets of weightage were assigned to the BTE, NO<sub>X</sub>, smoke opacity, HC, and CO attributes (output parameters). Normalized values of all attributes submitted to each equation and the highest score define the best alternative. Similarly, another three different sets

of weightages were assigned to the output parameters to find out the best alternatives (fuel jet number). Each alternative score and rank for every set of weightage is shown in **Table 5.1**. The assigned weightages are shown in the equation 4.15 to 4.19.

From **Table 5.1** it is concluded that all optimum fuel jets are suitable at a particular load by maintaining the highest fuel economy (BTE) and lowest emission compared to neat diesel engine. Jet 40 is suitable for 20% load conditions for all four weightage sets of output parameters. Similarly, jet 70 is suitable for 40% load conditions, jet 80 is suitable for 60% load conditions and jet 90 is suitable for 80% and 100% load conditions.

From this optimization at each load condition best MFR of ethanol is found for the lowest emission and highest BTE showed in **Table 5.2**. From the MFR and CV of ethanol and diesel, optimum premixed ratio is found for each load condition is shown in Table 5.2.

**Table 5.2** Optimum jet number, MFR, and the premixed ratio of Ethanol

Load (%)	Optimized Fuel jet	Optimized Ethanol MFR (kg/hr)	Optimized premixed ratio (%)
20	40	0.340	47.55
40	70	0.697	69.9
60	80	0.869	69.83
80	90	0.957	75.94
100	90	0.957	68
Average			66.244

**Table 5.2** shows the optimum premixed ratio for each load in the E100+D DF-HCCI engine. The premixed ratio range is between 47.5% to 75.94%. Means on an average 66.224% diesel fuel can be replaced by ethanol with lower emissions and higher BTE compared to diesel engine.

### 5.3.3 Methanol diesel DF-HCCI engine performance for different load conditions

In this experimental study, Methanol fuel was used in the carburetor at the time of suction stroke and diesel was injected at the end of the compression stroke to start the combustion. In this set of an experiment to vary the MFR of methanol 3 different types of fuel jet were used in the carburetor i. e. jet 40, jet 47.5, and jet 60. Further, large number fuel jet was not used because of unstable engine rpm and misfiring. Methanol-diesel (M100+D) DF-HCCI engine combustion performance and emission for all different loads are discussed in this section.

### **5.3.3.1 Impact of varying MFR of methanol on combustion and emission characteristics**

**Figure 5.10(a)** shows the in-cylinder pressure curves against CA for 100% load condition. These graphs show a similar nature as ethanol for varying MFR. With increasing the MFR of methanol in-cylinder pressure curves shifted forward due to very high ID (shown in figure 5.10(c)). Methanol fuel has a high autoignition temperature and octane number compared to neat diesel fuel which assists to delay the start of ignition. With increasing the contribution of methanol in-cylinder pressure was retarded.

**Figure 5.10(b)** shows the PRR with crank angle for 100% load conditions. The result shows that PRR was not more than the 7 bar/  $^{\circ}$ CA, which is lower than the engine knocking PRR range.

**Figure 5.10(c)** shows the ID for varying fuel jet numbers at different load conditions. With increasing methanol contribution in the DF-HCCI engine, ID was increased. Methanol fuel has high octane number and autoignition temperature with high LHV which leads to an increased ID. Further methanol has high LHV due to this cooling potential of inlet charge is high which assist to increase the ID (as shown in figure 5.10(e)).

**Figure 5.10(d)** indicates the combustion duration (CD) for different fuel jets under various load conditions. The result shows that with increasing the methanol contribution at low load condition CD was increased because of the very high cooling potential of methanol. Due to very high ID and cooling potential, the combustion chamber temperature is reduced and hence to burn the fuel takes more time to catch the fire. It is also observed that at high load condition CD was reduced with increasing the fuel jet number. Because at high load condition enough temperature was developed in the combustion chamber and with increasing the MFR of methanol, high ID contribute a fast spontaneous premixed combustion hence CD was reduced.

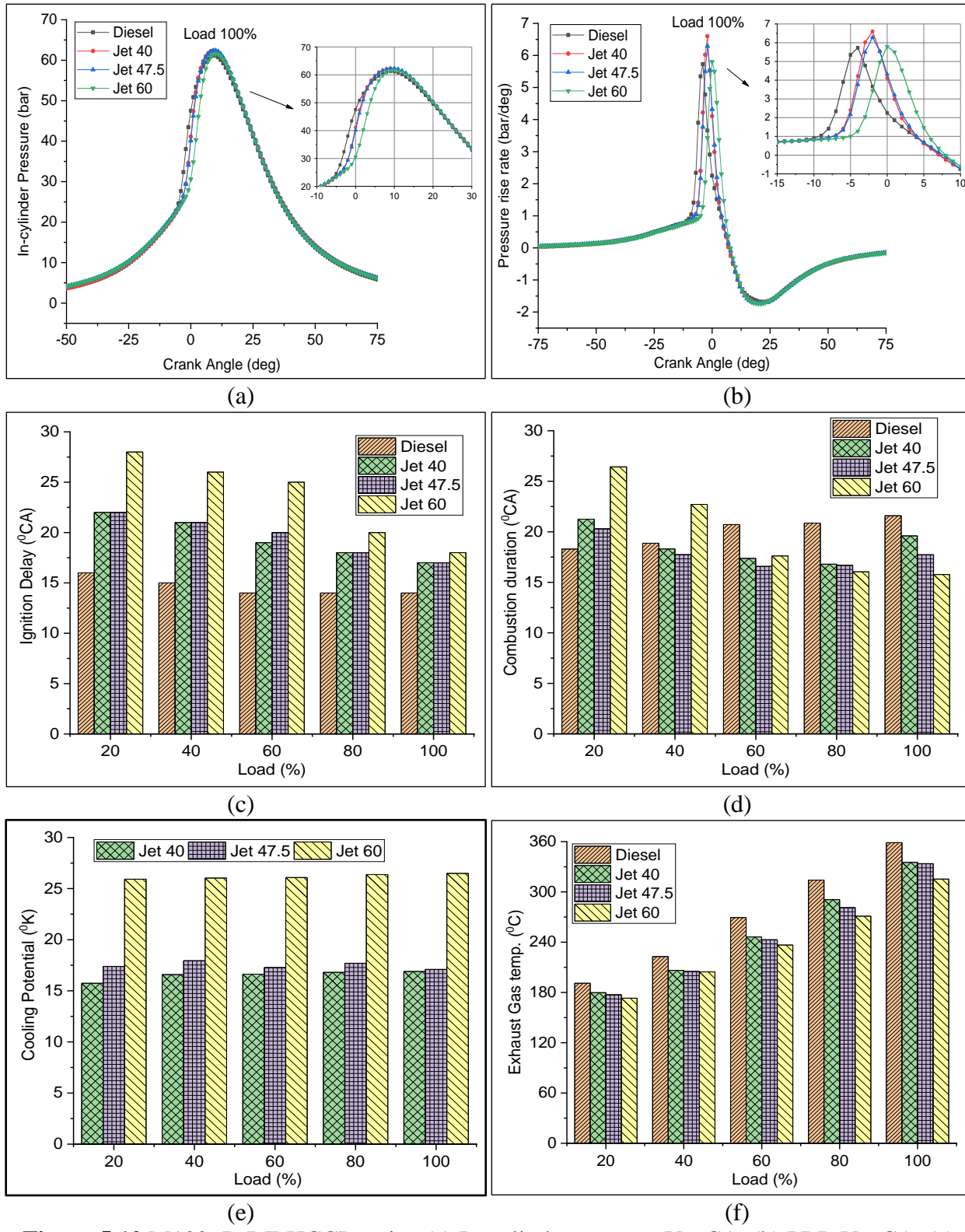


**Figure 5.10** M100+D DF-HCCI engine (a) In-cylinder pressure Vs. CA, (b) PRR Vs. CA, (c) Ignition delay (ID) Vs. Engine load, (d) Combustion duration (CD) Vs. Engine load, (e) Cooling potential Vs. Engine load, (f) Exhaust gas temp Vs. Engine load

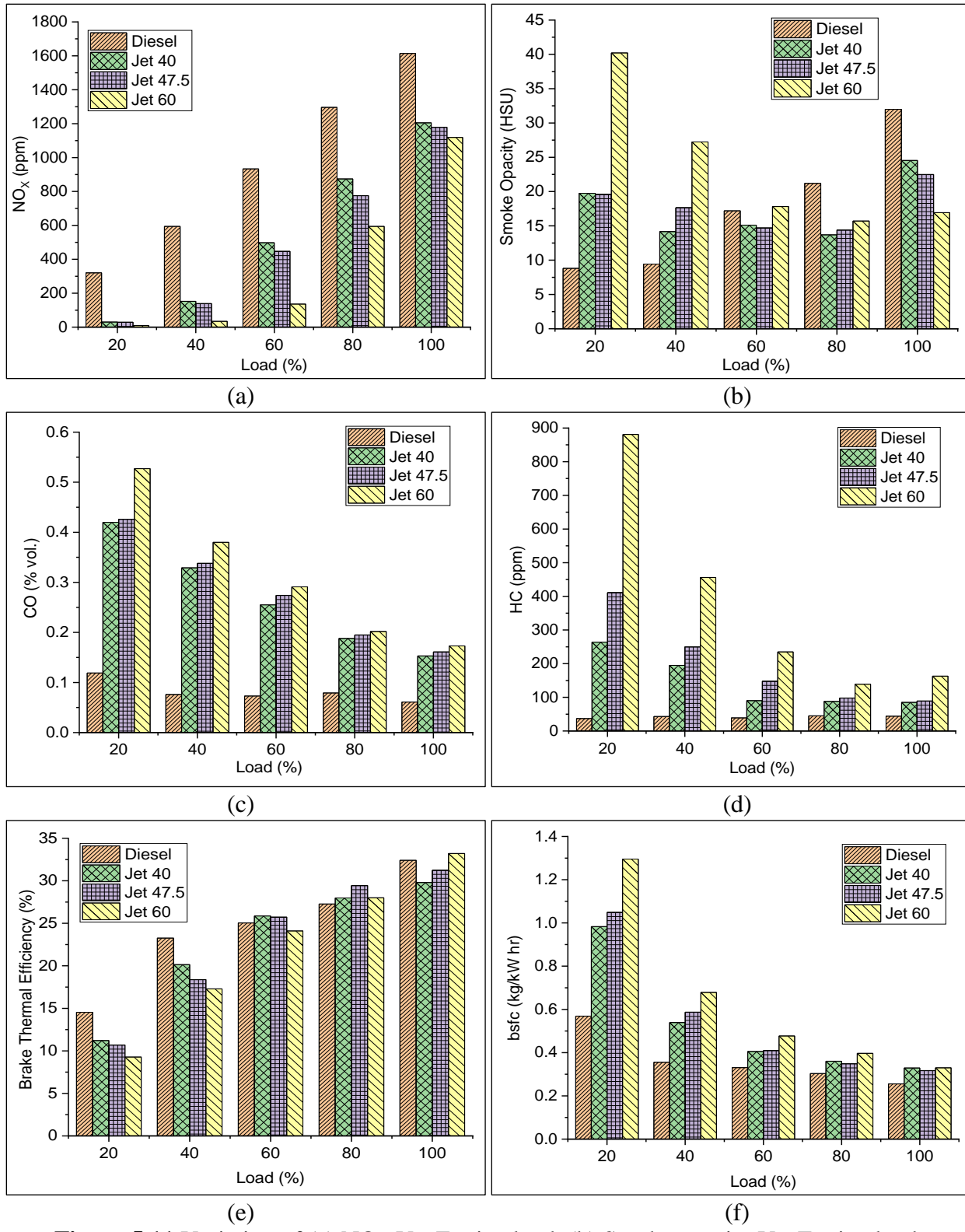


**Figure 5.11** Variation of (a) NO<sub>x</sub> Vs. Engine load, (b) Smoke opacity Vs. Engine load, (c) CO Vs. Engine load, (d) HC Vs. Engine load, (e) Brake thermal efficiency Vs. Engine load, (f) bsfc Vs. Engine load

M100+D DF-HCCI engine emitted low NO<sub>x</sub> emission due to high LHV and low in-cylinder temperature. With increasing the MFR of methanol NO<sub>x</sub> emission reduced compared to diesel engine shown in **Figure 5.11(a)**. However, M100+D DF-HCCI engine shows the adverse effect on smoke opacity shown in **Figure 5.11(b)** at low load conditions. At low load conditions, smoke opacity was increased because of low-temperature incomplete combustion, while at high load conditions it was reduced compared to diesel engine.

**Figure 5.11(c)** and **Figure 5.11(d)** shows the CO and HC emission respectively for different MFR of methanol under various load condition. With increasing the MFR of methanol CO and HC emission were increased. Methanol fuel has high LHV which reduced the combustion chamber temperature and leads to incomplete combustion. This results in more HC and CO emission compared to diesel engines.

**Figure 5.11(e)** presents the BTE of M100+D DF-HCCI engine at different load conditions. It was observed that at low load condition very poor engine performance because of LTC. Due to this more Methanol fuel need to supply to get the required power and engine rpm. However, at high load conditions, the engine performance is not much affected.

**Figure 5.11(f)** indicates bsfc for M100+D DF-HCCI engine for various load conditions. The results show high bsfc of M100+D DF-HCCI engine compared to diesel engine under all load conditions. Methanol fuel CV is 21.4 MJ/kg while diesel fuel CV is 43.5 MJ/kg, hence to full fill the requirement of power and engine rpm more methanol fuel need to supply.

**Figure 5.12** shows the performance improvement in M100+D DF-HCCI engine over diesel engine. Positive value on Y-axis denotes the favorable improvement (i.e. reduction of NO<sub>x</sub>, reduction of smoke opacity, and increment of BTE) and the negative value on Y-axis denotes unfavorable improvement. **Figure 5.12(a)** shows the reduction of NO<sub>x</sub> emission over diesel engine for various load conditions. Maximum 97.19% NO<sub>x</sub> emission was reduced at low load conditions for jet 60.

**Figure 5.12(b)** shows the reduction of smoke opacity of M100+D DF-HCCI engine over diesel engine for different load conditions. At load 60%, 80%, and 100% smoke opacity were reduced compared to diesel engine while at 20% and 40% smoke opacity was increased. Maximum 47.13% smoke opacity was reduced at 100% load condition for fuel jet number 60.

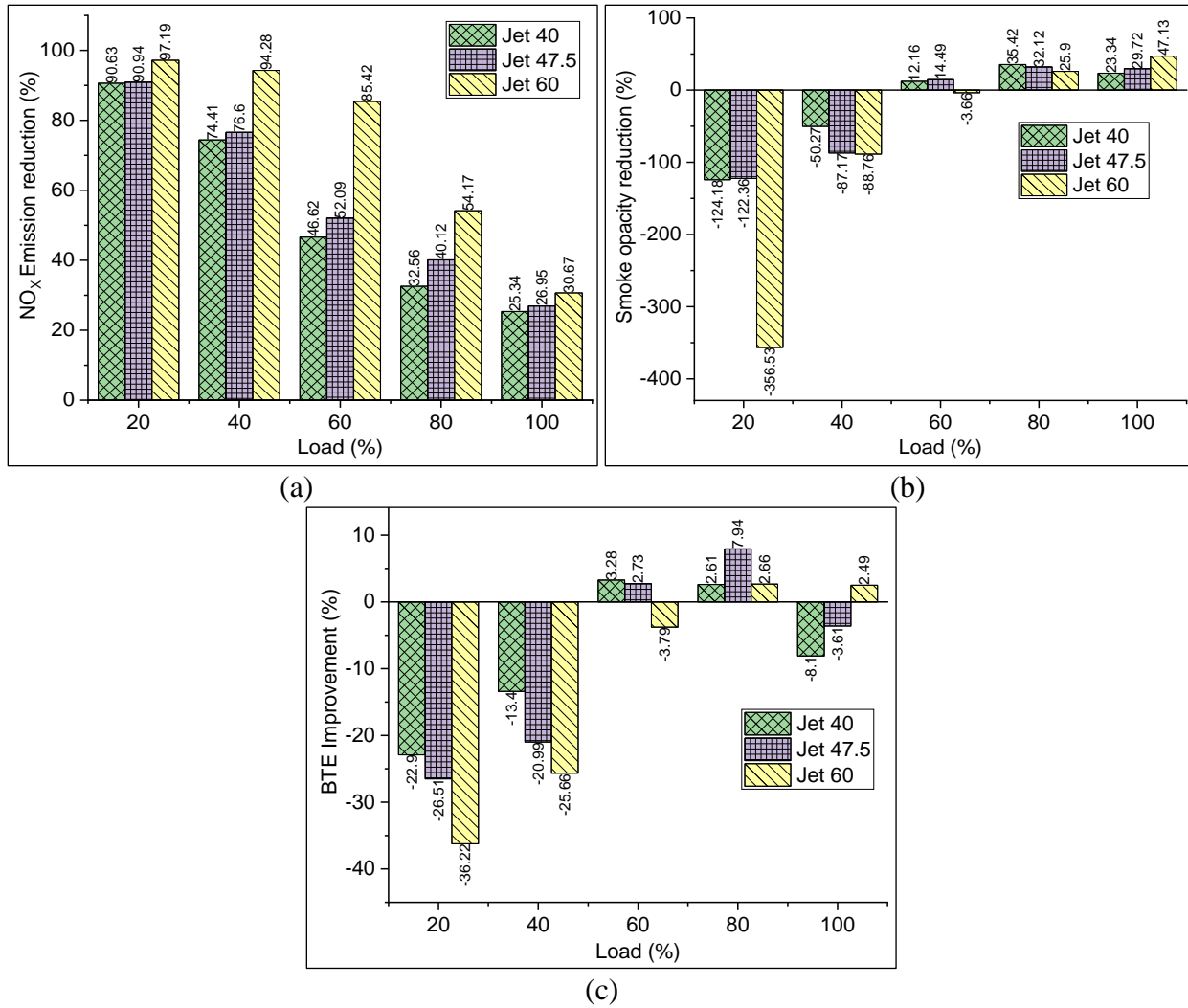


**Figure 5.12** Improvement of M100+D DF-HCCI engine over neat diesel engine at different load condition for various MFR (a) NO<sub>x</sub> emissions reduction, (b) Smoke opacity reduction, (c) BTE increment

**Figure 5.12(c)** indicates the increment of BTE in M100+D DF-HCCI engine over diesel engine. The result shows that at 20% and 40% load condition BTE was reduced lot and at 60% to 100% the BTE is almost equal to diesel engine.

**Figure 5.13** shows the premixed ratio for three different fuel jets at different load conditions. At 20% load conditions 43.97% maximum methanol premixed ratio can be used without knocking the engine.

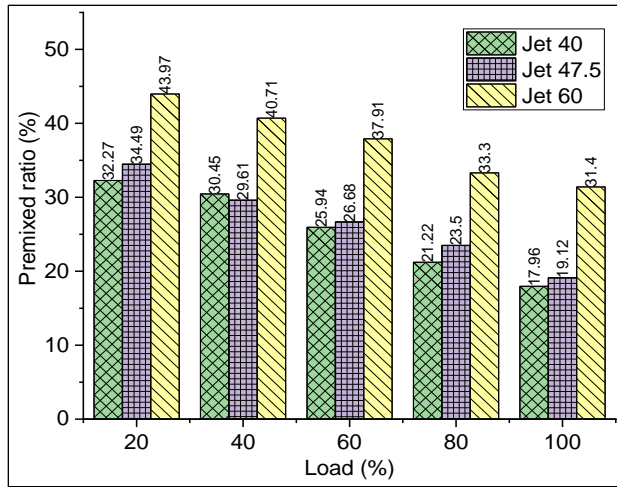


**Figure 5.13** Premixed ratio of methanol under various load conditions for different fuel jets

#### 5.3.3.2 Optimization of MFR and the premixed ratio of methanol at different load conditions

Similar sets of weightage and SAW method were applied to find out the optimum fuel jet number at different load conditions. **Table 5.3** shows the combined score and ranking of different fuel jet numbers under different load conditions.

From **Table 5.3** it is concluded that all optimum fuel jets are suitable at a particular load by maintaining the highest fuel economy (i.e. BTE) and lowest emission compared to diesel engine. Conventional diesel engine combustion mode is suitable for 20% and 40% load conditions compared to M100+D DF-HCCI engine mode. While jet 60 is suitable for 60%, 80% and 100% load conditions for all four weightage sets of output parameters.

From this optimization at each load condition best MFR of methanol is found for lowest emission and highest BTE shown in **Table 5.4**. From the MFR and CV of methanol and diesel optimum premixed ratio is found for each load condition shown in **Table 5.4**.

**Table 5.3** Ranking of different fuel jets for various weightage sets under each load conditions

Load (%)	Type of jet	Y1	Rank	Y2	Rank	Y3	Rank	Y4	Rank
20	CI	0.675	1	0.757	1	0.757	1	0.757	1
	Jet 40	0.505	3	0.516	3	0.46	4	0.572	3
	jet 47.5	0.497	4	0.502	4	0.447	3	0.557	4
	Jet 60	0.618	2	0.573	2	0.522	2	0.623	2
40	CI	0.685	2	0.764	1	0.764	1	0.764	1
	Jet 40	0.584	3	0.591	3	0.527	3	0.655	3
	jet 47.5	0.522	4	0.53	4	0.471	4	0.589	4
	Jet 60	0.695	1	0.648	2	0.589	2	0.708	2
60	CI	0.655	4	0.737	4	0.74	2	0.734	4
	Jet 40	0.748	3	0.747	3	0.683	3	0.811	3
	jet 47.5	0.765	2	0.75	2	0.677	4	0.823	2
	Jet 60	0.917	1	0.849	1	0.777	1	0.922	1
80	CI	0.676	4	0.746	4	0.753	4	0.739	4
	Jet 40	0.875	3	0.846	3	0.798	3	0.895	3
	jet 47.5	0.904	2	0.872	2	0.815	2	0.929	2
	Jet 60	0.939	1	0.884	1	0.824	1	0.943	1
100	CI	0.731	4	0.795	4	0.798	2	0.793	4
	Jet 40	0.837	3	0.809	3	0.765	4	0.853	3
	jet 47.5	0.879	2	0.845	2	0.794	3	0.895	2
	Jet 60	0.999	1	0.931	1	0.862	1	1	1

**Table 5.4** Optimum fuel jet number, MFR and the premixed ratio of Methanol

Load (%)	Optimized Fuel jet	Optimized Methanol MFR (kg/hr)	Optimized Premixed ratio (%)
20	60	0.557	43.96
40	60	0.557	40.70
60	60	0.557	37.90
80	60	0.557	33.30
100	60	0.557	31.40
Average			37.45

If we consider M100+D DF-HCCI engine for all load conditions the premixed ratio range is between 43.96% to 31.40%. Means on an average 37.45% diesel fuel can be replaced by methanol with lower emissions and higher BTE compared to diesel engine.

### 5.3.4 Propanol-diesel DF-HCCI engine performance for different load conditions

In this experiment propanol fuel was supplied through the carburetor with the fresh air at the time of suction stroke and diesel was injected at the end of a compression stroke. In this set of experiments jet 40, jet 60, jet 70, jet 80, and jet 90 were used to change the MFR of propanol at different load conditions. Propanol-diesel (P100+D) DF-HCCI engine performance was compared to the diesel engine.

#### 5.3.4.1 Influence of varying MFR of propanol on combustion and emission characteristics

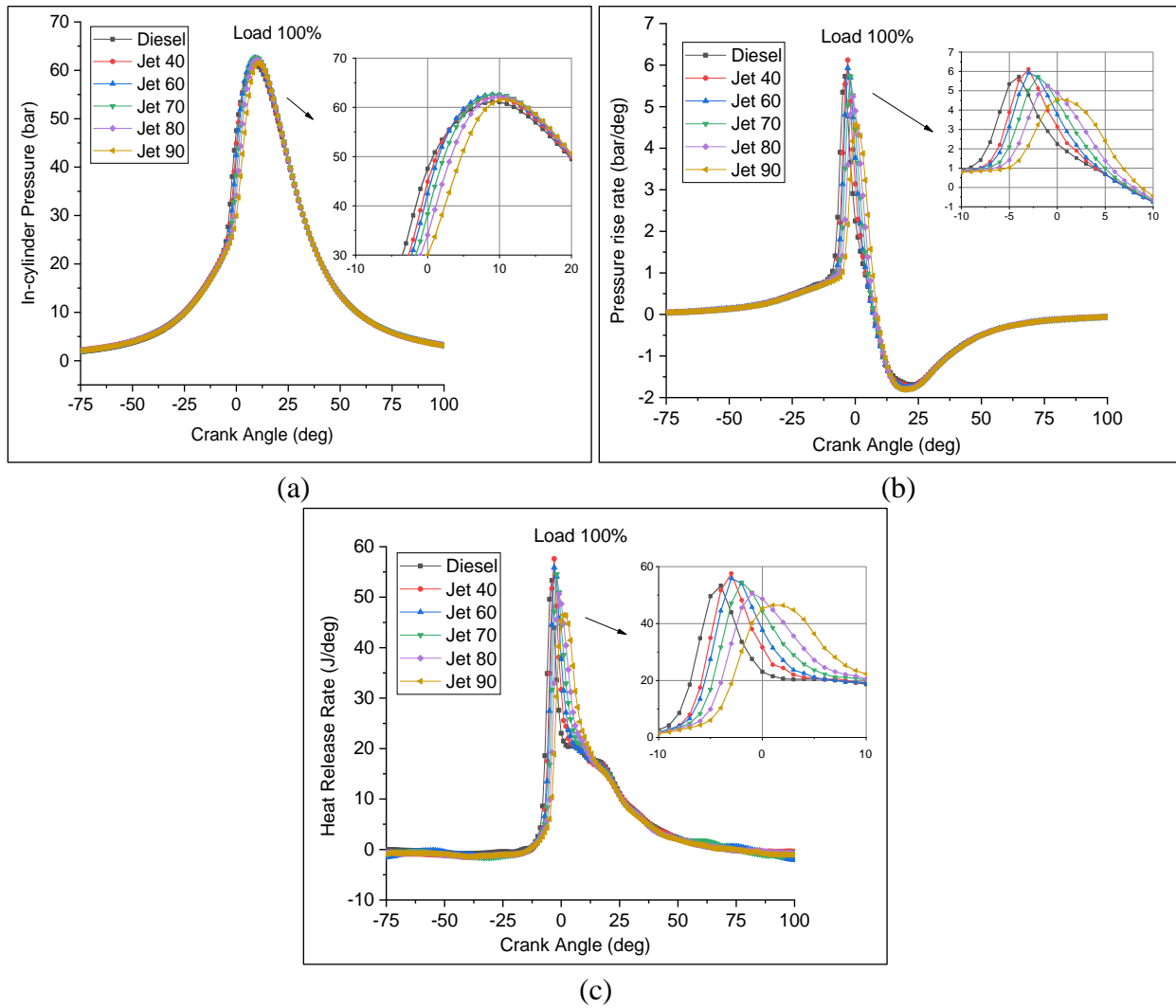


**Figure 5.14** Variation of (a) In-cylinder pressure Vs. CA, (b) PRR Vs. CA, (c) HRR Vs. CA for different MFR of propanol in DF-HCCI engine

Propanol diesel (P100+D) DF-HCCI engine showed similar performance like as the E100+D DF-HCCI engine. Nature of the curves of in-cylinder pressure, PRR, HRR for varying MFR is the same but values are different because of propanol characteristics as shown in **Figure 5.14**.

Further **Figures 5.15** shows the ID, CD, cooling potential, and exhaust gas temperature for different MFR of propanol under various load conditions. All the graphs showed similar kind of nature like as E100+D DF-HCCI engine.

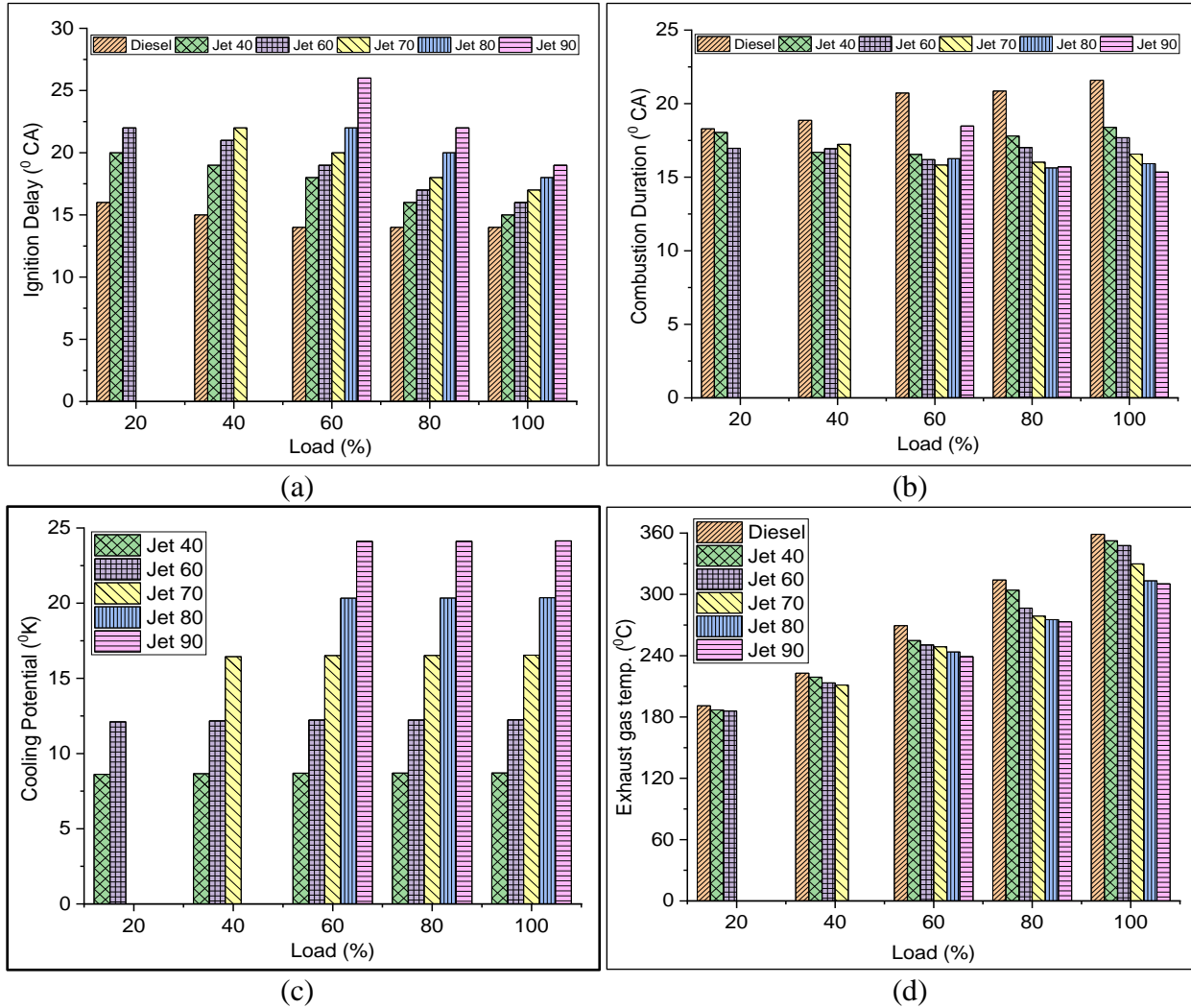


**Figure 5.15** Variation of (a) ID Vs. engine load, (b) CD Vs. engine load, (c) Cooling potential Vs. engine load (d) Exhaust gas temp. Vs. engine load, for different MFR of propanol in DF-HCCI engine

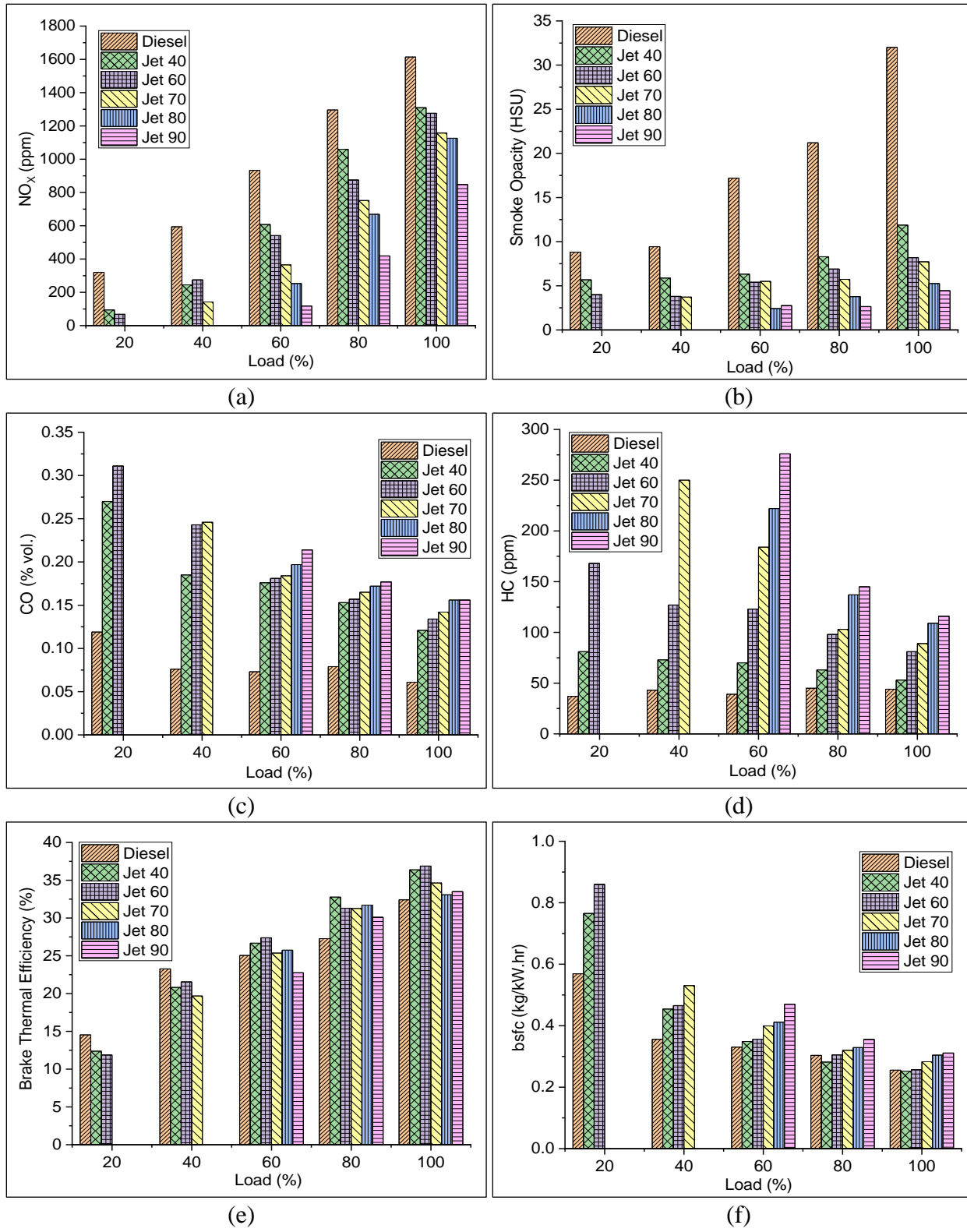


**Figure 5.16** Variation of (a) NO<sub>x</sub> Vs. engine load, (b) Smoke opacity Vs. engine load, (c) CO Vs. engine load (d) HC Vs. engine load (e) Brake thermal efficiency Vs. engine load, (f) bsfc Vs. engine load, for different MFR of propanol in DF-HCCI engine

**Figure 5.16** shows all engine emission and performance graphs for varying MFR of propanol under different load conditions. NO<sub>x</sub> emission and smoke opacity reduced a lot for increasing MFR of propanol while HC and CO emission was increased compared to diesel engine [106]. In the case of P100+D DF-HCCI engine BTE was improved nicely for high load conditions compared to diesel engine. The technical reason for the reduction of NO<sub>x</sub>, reduction of smoke opacity and improvement in BTE is same as E100+D and M100+D DF-HCCI. Since ethanol, methanol, and propanol are the same nature alcohol-based fuels.

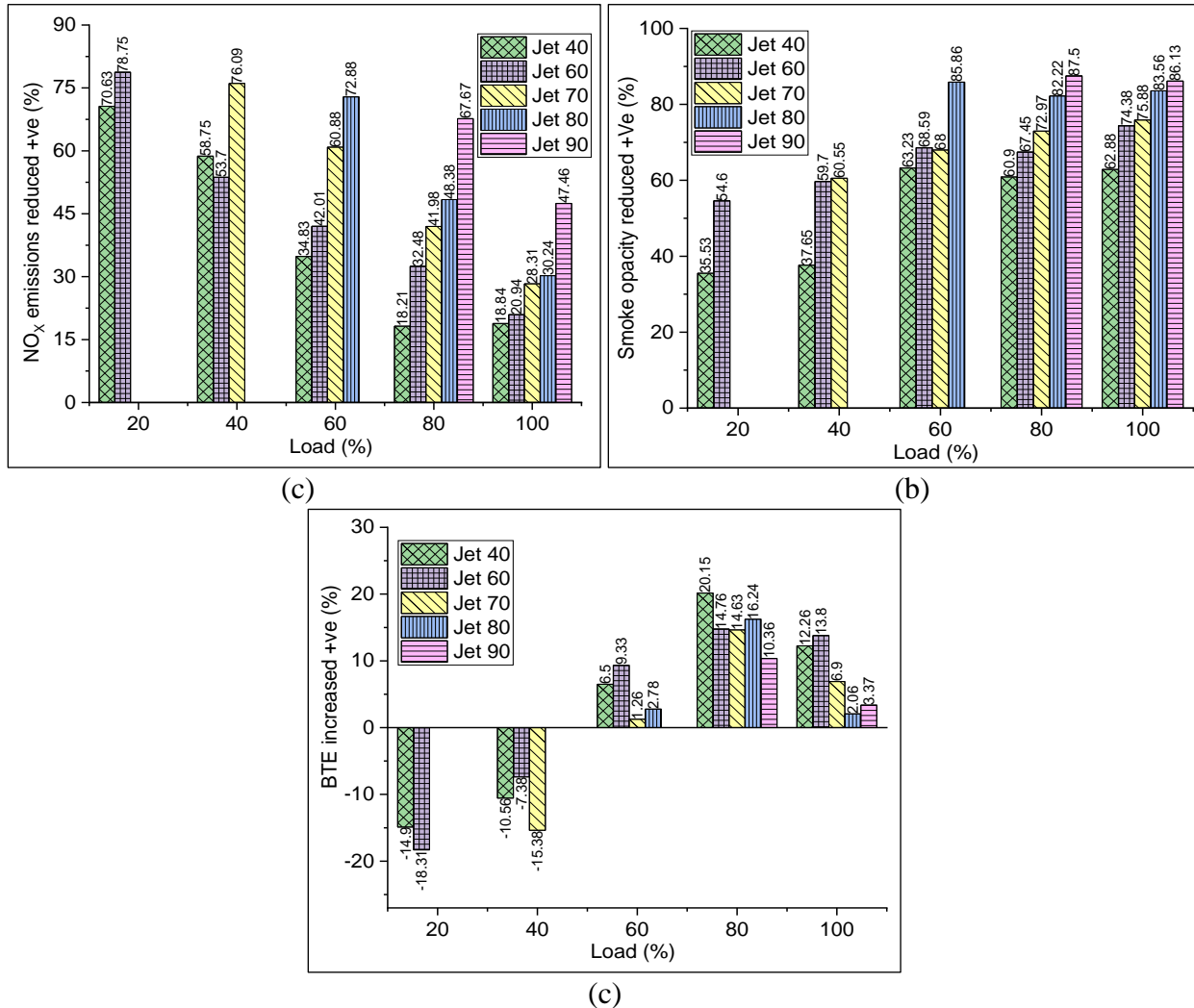


**Figure 5.17** Improvement of performance over diesel engine (a) NO<sub>x</sub> emission reduction Vs. engine load, (b) Smoke opacity reduction Vs. engine load, (c) BTE increased Vs. engine load for different MFR of propanol in DF-HCCI engine

**Figure 5.17** shows the performance improvement of P100+D DF-HCCI engine over diesel engine. The positive value on Y-axis denotes the favorable improvement (i.e. NO<sub>x</sub> emission

reduction, smoke opacity reduction, and BTE increment) and the negative value on Y-axis denotes non-favorable improvement. **Figure 5.17(a)** shows the reduction of NO<sub>x</sub> emission over diesel engine for various load conditions. Maximum 78.75% NO<sub>x</sub> emission was reduced at 20% load conditions for jet 60, while at 100% load 47.46% NO<sub>x</sub> was reduced for jet 90.

**Figure 5.17(b)** shows the reduction of smoke opacity of P100+D DF-HCCI engine over diesel engine for different load conditions. At all load conditions, smoke opacity was reduced compared to diesel engine. At 80% load maximum 87.5% smoke opacity was reduced for jet 90, while at 20% load minimum 35.63% smoke opacity was reduced for jet 40.

**Figure 5.17(c)** indicates the increment of BTE in P100+D DF-HCCI engine over diesel engine. The result shows that at 20% and 40% load condition BTE was reduced and at 60% to 100% it was increased. At 60% load 20.15% BTE was increased for jet 40, while at 100% load 3.37% BTE increased for jet 90.

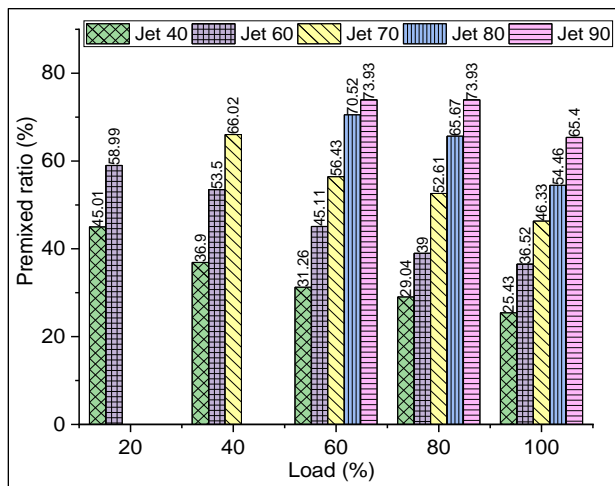


**Figure 5.18** Premixed ratio of propanol under various load conditions for different fuel jets

**Figure 5.18** shows the premixed ratio for five different fuel jets at different load conditions. At 60% and 80% load conditions maximum of 73.93%, premixed ratio of propanol was used for fuel jet 90, while at 100% load conditions minimum of 25.43% premixed ratio of propanol was used for fuel jet 40.

#### 5.3.4.2 Optimization of MFR and the premixed ratio of propanol at different load conditions

Similar sets of weightages and SAW method were used to find out the optimum fuel jets at different load conditions. **Table 5.5** shows the combined score and ranking of different fuel jet numbers under different load conditions.

From table 5.5 it is concluded that all optimum fuel jets are suitable at a particular load by maintaining the highest fuel economy (BTE) and lowest emission compared to diesel engine. P100+D DF-HCCI engine showed superior performance for all load conditions compared to diesel engine.

**Table 5.5** Ranking of different fuel jet for various weightage sets under each load conditions

Load (%)	Type of jet	Y1	Rank	Y2	Rank	Y3	Rank	Y4	Rank
20	CI	0.554	3	0.666	3	0.666	3	0.666	3
	jet 40	0.758	2	0.742	2	0.701	2	0.782	2
	jet 60	0.938	1	0.856	1	0.805	1	0.908	1
40	CI	0.543	4	0.658	4	0.658	4	0.658	4
	jet 40	0.701	3	0.71	3	0.671	3	0.75	3
	jet 60	0.806	2	0.776	2	0.716	2	0.836	2
	jet 70	0.947	1	862	1	0.801	1	0.923	1
60	CI	0.393	6	0.532	6	0.541	3	0.524	6
	jet 40	0.517	5	0.582	5	0.534	5	0.631	5
	jet 60	0.555	4	0.603	3	0.539	4	0.667	3
	jet 70	0.563	3	0.592	4	0.529	6	0.654	4
	jet 80	0.801	2	0.769	2	0.703	2	0.836	2
	jet 90	0.902	1	0.826	1	0.767	1	0.885	1
80	CI	0.426	6	0.545	6	0.561	6	0.528	6
	jet 40	0.571	5	0.64	5	0.601	4	0.678	5
	jet 60	0.605	4	0.645	4	0.598	5	0.693	4
	jet 70	0.657	3	0.682	3	0.632	3	0.731	3
	jet 80	0.764	2	0.758	2	0.701	2	0.816	2
	jet 90	0.971	1	0.905	1	0.851	1	0.959	1
100	CI	0.513	6	0.617	6	0.629	5	0.605	6
	jet 40	0.668	5	0.716	5	0.684	4	0.748	5
	jet 60	0.734	4	0.751	3	0.701	3	0.801	3
	jet 70	0.748	3	0.748	4	0.701	3	0.796	4
	jet 80	0.83	2	0.797	2	0.747	2	0.847	2
	jet 90	0.968	1	0.901	1	0.849	1	0.954	1

From this optimization at each load condition best MFR of propanol is found for lowest emission and highest BTE shown in Table 5.6. Optimum premixed ratio for each load condition is found for MFR and CV of propanol and diesel is shown in **Table 5.6**.

**Table 5.6** Optimum fuel jets, MFR and the premixed ratio of Propanol

Load (%)	Optimize Fuel jet	Propanol MFR (kg/hr)	Optimized premixed ratio (%)
20	Jet 60	0.401	58.98
40	Jet 70	0.542	66.01
60	Jet 90	0.792	73.92
80	Jet 90	0.792	73.92
100	Jet 90	0.792	65.4
Average			67.646

P100+D DF-HCCI engine premixed range is observed in between 58.98% to 73.92%. Means on an average 67.64% diesel fuel can be replaced by propanol with lower emissions and higher BTE compared to diesel engine.

### **5.3.5 Butanol-diesel DF-HCCI engine performance for different load conditions**

In this experiment butanol fuel was supplied through the carburetor with the fresh air at the time of suction stroke and diesel was injected at the end of a compression stroke. In this set of experiments jet 40, jet 60, jet 70, jet 80, and jet 90 were used to change the MFR of butanol at different load conditions. Butanol-diesel (B100+D) DF-HCCI engine performance was compared to the diesel engine.

#### ***5.3.5.1 Influence of varying MFR of butanol on combustion and emission characteristics***

Butanol-diesel (B100+D) DF-HCCI engine showed similar trends like as the E100+D or P100+D DF-HCCI engine. In-cylinder pressure, PRR, HRR for varying MFR has followed the same trend like as E100+D or P100+D DF-HCCI engine with different measured values because of butanol fuel characteristics as shown in **Figure 5.19**.

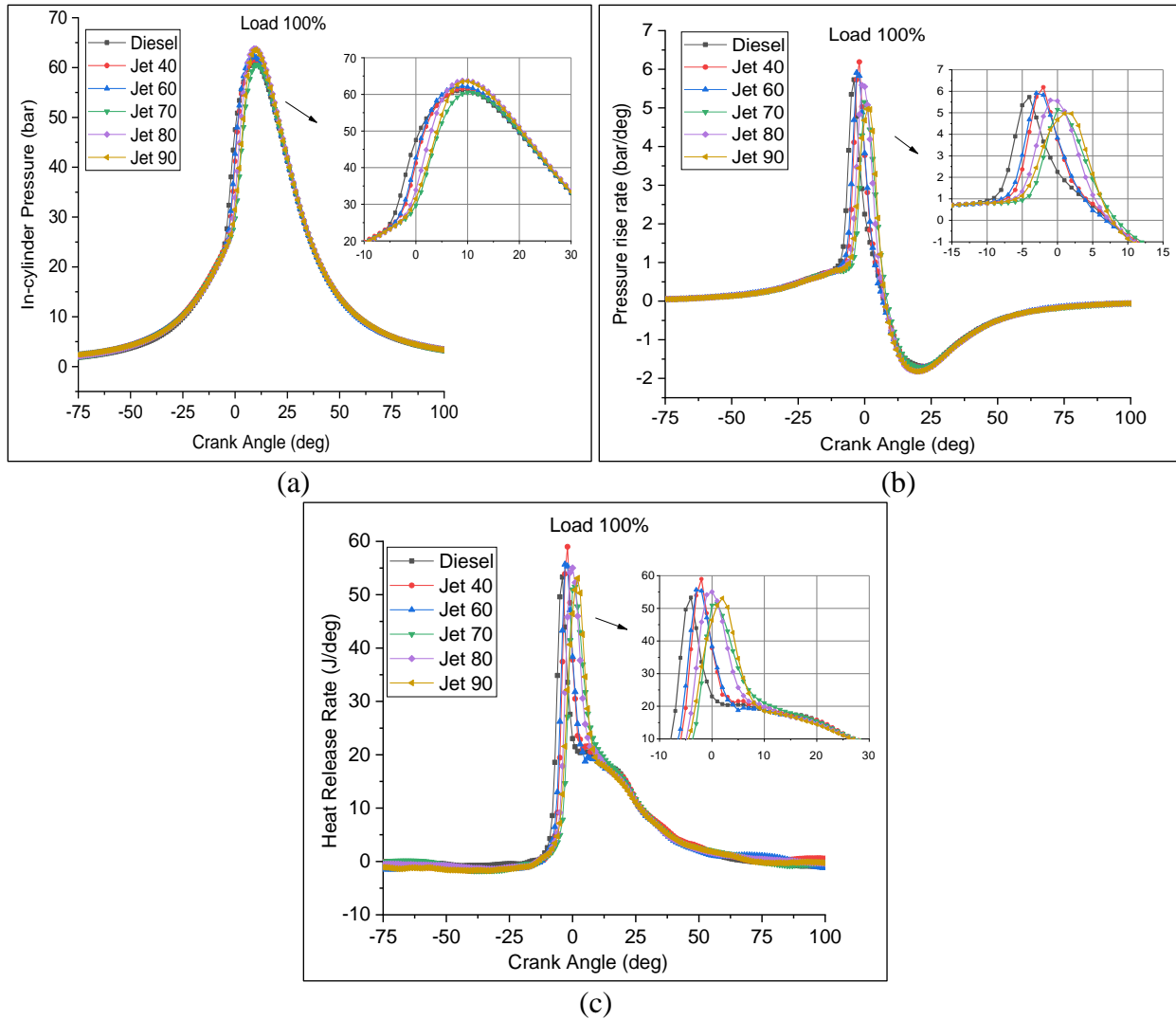


**Figure 5.19** Variation of (a) In-cylinder pressure Vs. CA, (b) PRR Vs. CA, (c) HRR Vs. CA for different MFR of butanol in DF-HCCI engine

Further **Figure 5.20** shows the ID, CD, cooling potential, and exhaust gas temp for different MFR of butanol under various load conditions. These all graphs showed similar kind of trend like as E100+D or P100+D DF-HCCI engine.

**Figure 5.21** shows engine emission and performance graphs for varying MFR of butanol under different load conditions. NO<sub>x</sub> emission and smoke opacity reduced with increasing MFR of butanol while HC and CO emission was increased compared to diesel engine. Further, in B100+D DF-HCCI engine BTE was improved nicely for mid load condition i.e. 60% and 80% load while for low and high conditions it was reduced compared to diesel engine.

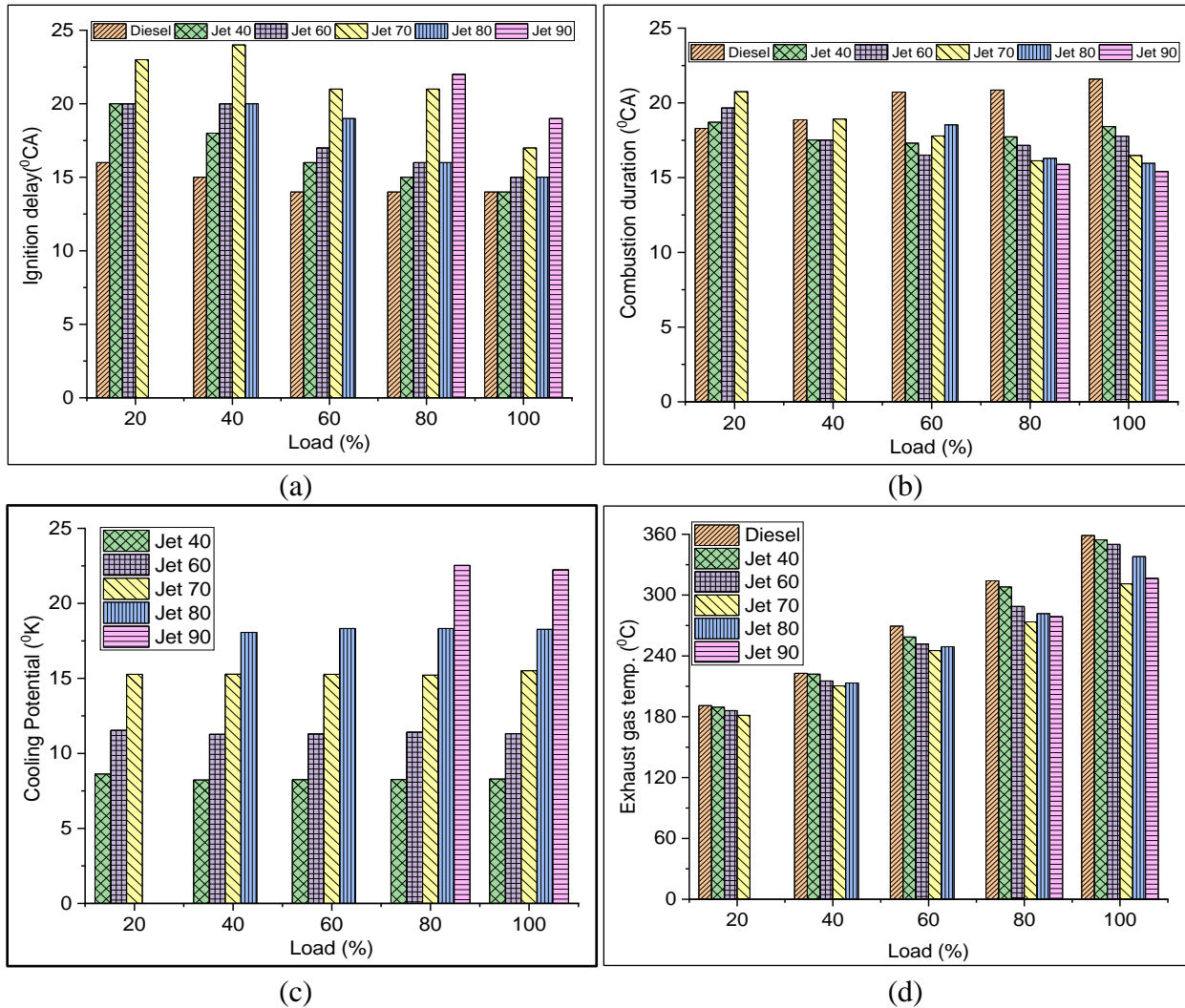


**Figure 5.20:** Variation of (a) ID Vs. engine load, (b) CD Vs. engine load, (c) Cooling potential Vs. engine load (d) Exhaust gas temp Vs. Engine load, for different MFR of Butanol in DF-HCCI engine

**Figure 5.22** shows the performance improvement in B100+D DF-HCCI engine over diesel engine. The positive value on Y-axis denotes the favorable improvement and the negative value on Y-axis denotes non-favorable improvement. **Figure 5.22(a)** shows the reduction of NO<sub>x</sub> emission over diesel engine for various load conditions. Maximum 84.69% NO<sub>x</sub> emission was reduced at 20% load conditions for jet 70, while at 100% load 47.21% NO<sub>x</sub> was reduced for jet 70. At 100% load minimum 18.53% NO<sub>x</sub> was reduced for fuel jet 40.

**Figure 5.22(b)** shows the reduction of smoke opacity of B100+D DF-HCCI engine over diesel engine for different load conditions. At all load conditions, smoke opacity was reduced a lot

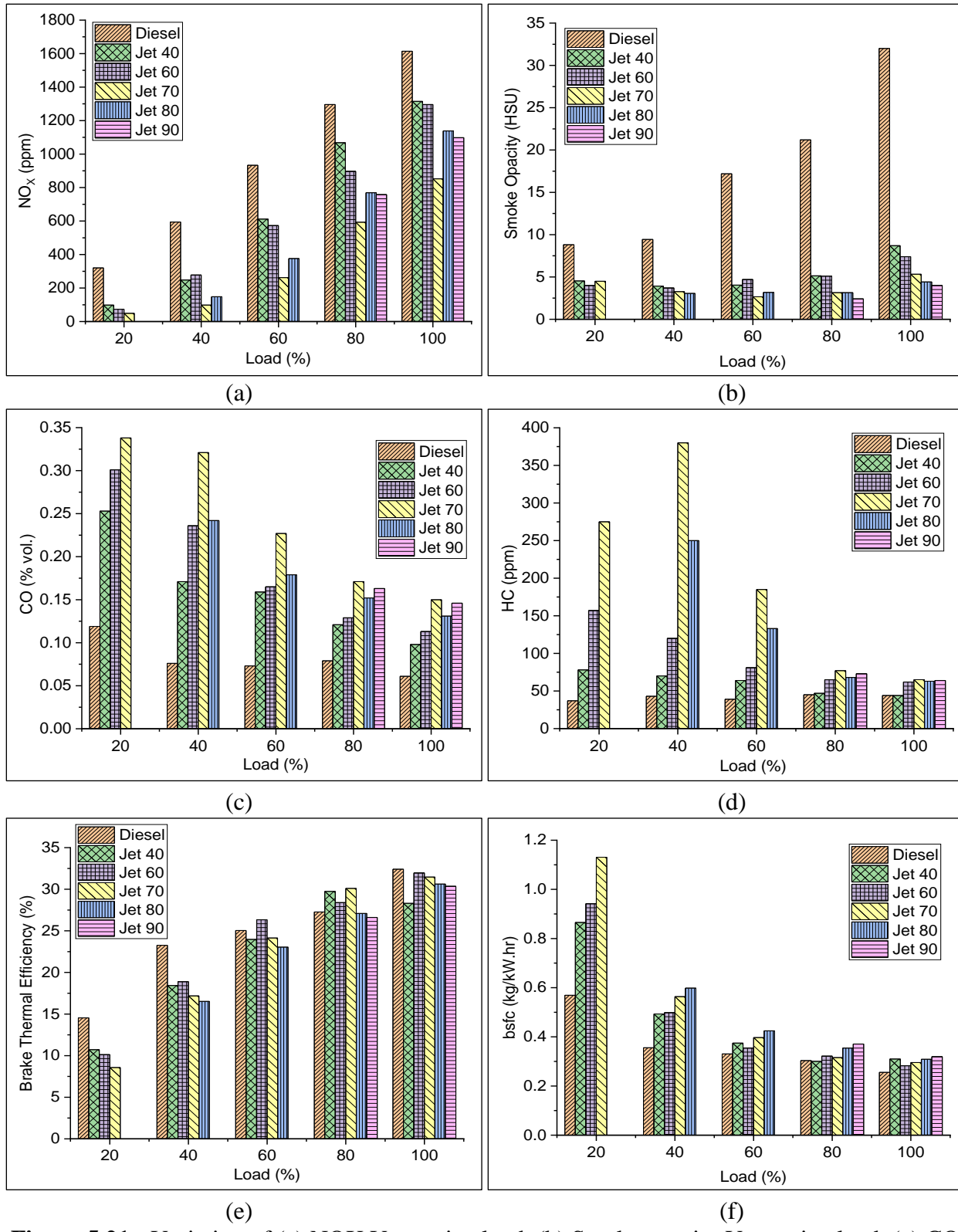


**Figure 5.21:** Variation of (a) NO<sub>x</sub> Vs. engine load, (b) Smoke opacity Vs. engine load, (c) CO emission Vs. engine load (d) HC emission Vs. Engine load (e) Brake thermal efficiency Vs. Engine load, (f) bsfc Vs. Engine load, for different MFR of butanol in DF-HCCI engine

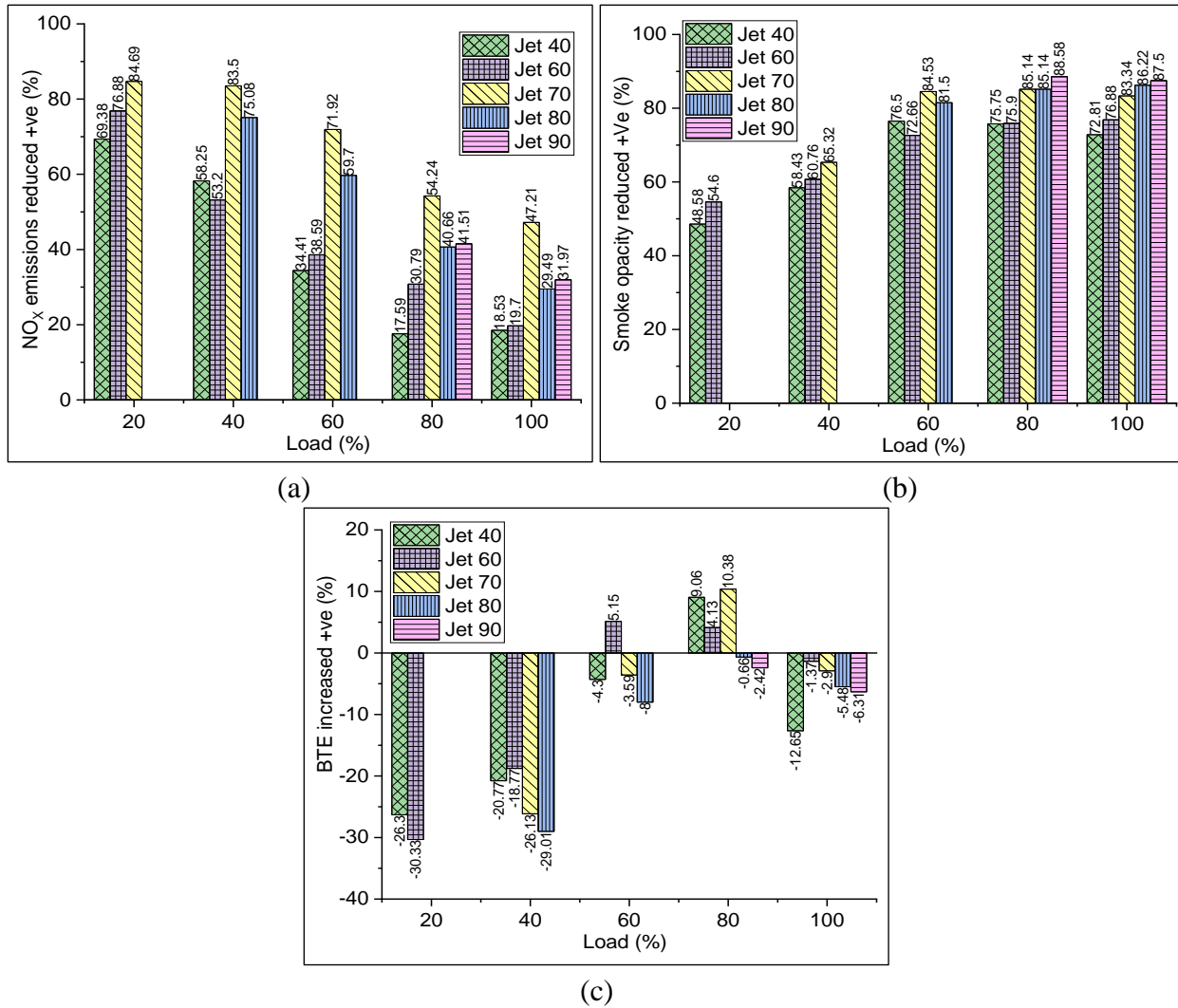


**Figure 5.22:** Improvement of performance over neat diesel engine (a) NO<sub>x</sub> emission reduction Vs. engine load, (b) Smoke opacity reduction Vs. engine load, (c) BTE increased Vs. engine load for different MFR of butanol in DF-HCCI engine

compared to diesel engine. At 80% load maximum 88.58% smoke opacity was reduced for jet 90, while at 20% load minimum 48.58% smoke opacity was reduced for jet 40.

**Figure 5.22(c)** indicates the increment and decrement of BTE in B100+D DF-HCCI engine over a diesel engine. The result shows that at 20%, 40%, and 100% load condition BTE was reduced and at 60% to 80% it was increased. At 80% load maximum 10.33% BTE was increased for jet 70.

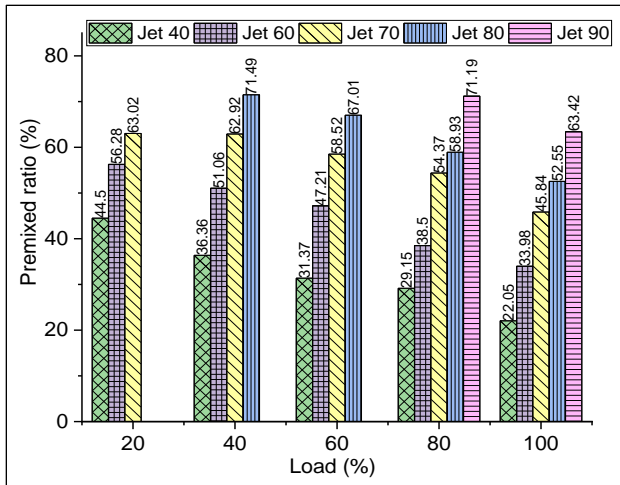


**Figure 5.23** Premixed ratio of Butanol under various load conditions for different fuel jets

**Figure 5.23** shows the premixed ratio for five different fuel jets at different load conditions. At 80% load conditions maximum of 71.19%, premixed ratio of butanol was used for fuel jet 90, while at 100% load condition minimum of 22.05% premixed ratio of butanol was used for fuel jet 40.

#### **5.3.5.2 Optimization of MFR and the premixed ratio of butanol at different load conditions**

Similar four sets of weightages and SAW method were used to find out the optimum fuel jet number at different load conditions. **Table 5.7** shows the combined score and ranking of different fuel jet numbers under different load conditions.

From **Table 5.7** it is concluded that all optimum fuel jets are suitable at a particular load by maintaining the highest fuel economy (BTE) and lowest emission compared to diesel engine. B100+D DF-HCCI engine showed superior performance for all load condition compared to diesel engine.

From this optimization at each load condition best MFR of butanol is found for lowest emission and highest BTE shown in **Table 5.8**. From the MFR and CV of butanol and diesel optimum premixed ratio is calculated for each load condition shown in **Table 5.8**.

**Table 5.7** Ranking of different fuel jets for various weightage sets under each load conditions

<b>Load (%)</b>	<b>Type of jet</b>	<b>Y1</b>	<b>Rank</b>	<b>Y2</b>	<b>Rank</b>	<b>Y3</b>	<b>Rank</b>	<b>Y4</b>	<b>Rank</b>
20	CI	0.535	4	0.651	4	0.651	4	0.651	4
	jet 40	0.705	3	0.687	3	0.661	3	0.714	3
	jet 60	0.785	2	0.725	2	0.687	2	0.763	2
	jet 70	0.825	1	0.732	1	0.698	1	0.767	1
40	CI	0.495	5	0.622	5	0.622	4	0.622	5
	jet 40	0.655	4	0.663	3	0.637	3	0.69	4
	jet 60	0.663	3	0.653	4	0.606	5	0.701	3
	jet 70	0.89	1	0.796	1	0.74	1	0.853	1
	jet 80	0.789	2	0.723	2	0.677	2	0.77	2
60	CI	0.461	5	0.589	5	0.594	5	0.584	5
	jet 40	0.664	4	0.689	4	0.651	3	0.726	4
	jet 60	0.673	3	0.701	3	0.648	4	0.755	3
	jet 70	0.971	1	0.893	1	0.828	1	0.958	1
	jet 80	0.801	2	0.768	2	0.715	2	0.82	2
80	CI	0.492	6	0.605	6	0.614	6	0.595	6
	jet 40	0.67	5	0.732	4	0.713	4	0.75	5
	jet 60	0.691	4	0.726	5	0.697	5	0.755	4
	jet 70	0.921	1	0.894	1	0.846	1	0.942	1
	jet 80	0.812	3	0.803	3	0.772	3	0.834	3
	jet 90	0.887	2	0.854	2	0.82	2	0.887	2
100	CI	0.55	6	0.663	6	0.663	6	0.663	6
	jet 40	0.659	5	0.707	5	0.701	5	0.713	5
	jet 60	0.727	4	0.756	4	0.72	4	0.792	4
	jet 70	0.906	1	0.88	1	0.837	1	0.923	1
	jet 80	0.866	3	0.85	3	0.813	3	0.886	3
	jet 90	0.903	2	0.874	2	0.835	2	0.912	2

B100+D DF-HCCI engine premixed range is observed in between 45.84% to 63.02%. Means on an average 56.93% diesel fuel can be replaced by butanol with lower emissions and higher BTE compared to conventional diesel engine.

**Table 5.8** Optimum fuel jet, MFR and the premixed ratio of Propanol

Load (%)	Optimized Fuel jet	Optimized Butanol MFR (kg/hr)	Optimized premixed ratio (%)
20	70	0.542	63.02
40	70	0.542	62.92
60	70	0.542	58.52
80	70	0.542	54.37
100	70	0.542	45.84
Average			56.93

### 5.3.6 Summary

From this study, for each alcohol-based fuel i.e. ethanol, methanol, propanol, and butanol optimum premixed ratio was found under individual load conditions. This premixed ratio indicates the permissible energy fraction of each alcohol-based fuel at a particular load with low engine emission and high BTE. For each alcohol-based fuel at every individual load optimum premixed ratio is shown in **Table 5.9**.

From this study, it was concluded that E100+D DF-HCCI engine can operate efficiently with low emission and high BTE compared to a conventional diesel engine at 60% load if the energy fraction of ethanol is 69.83%. Similarly, for other load and every alcohol-based fuel (methanol, propanol and butanol) this optimum energy fraction was calculated and is shown in **Table 5.9**.

**Table 5.9** Optimum premixed ratio of each alcohol-based fuel for individual load condition

Load	M100+D	E100+D	P100+D	B100+D
20	43.97	47.55	58.98	63.02
40	40.71	69.9	66.01	62.92
60	37.90	69.83	73.92	58.52
80	33.30	75.94	73.92	54.37
100	31.40	68	65.4	45.84
Average	37.46	66.24	67.64	56.93

- ✓ For M100+D DF-HCCI engine premixed ratio range is 31.4% to 43.97%.
- ✓ For E100+D DF-HCCI engine, premixed ratio range is 47.55% -75.94%.
- ✓ For P100+D DF-HCCI engine premixed ratio range is 58.98 % - 73.92%.
- ✓ For B100+D DF-HCCI engine premixed ratio range is 45.84% - 63.02%.

## 5.4 Objective 3

**Experimentally recognize the suitable fuel among the fuels: Methanol, Ethanol, Propanol, and Butanol supplied through carburetor that yields HCCI like performance.**

In this study, all four alcohol-based fuels were compared with each other and the best alcohol fuel was investigated by analyzing the engine combustion performance and emission. In this experiment, various alcohol-based fuels i.e. methanol, ethanol, propanol, and butanol was supplied through the carburetor by using fuel jet 60, and diesel was injected to start the combustion. The MFR of alcohol-based fuel, is maintained constant for all load conditions (fuel jet 60), and the engine load was controlled by varying the diesel fuel supply. Combustion and emission characteristics for these four different alcohol-based fuels were investigated.

### 5.4.1 Combustion and emission characteristics for different alcohol-based fuels in DF-HCCI engine under different load conditions

**Figure 5.24(a)** presents the in-cylinder pressure with crank angle (CA) for 100% load conditions. Results show that the butanol and propanol fuel pressure curve just after the diesel pressure curve and ethanol and methanol curves are far away from the diesel engine curve. All curves shifted forward (just away from the TDC) compared to diesel engine curve. The increase of carbon number in the alcohol-based fuel means weakens the hydroxyl group which changes the fuel characteristics such as reduction of octane number and ability to resist the autoignition. Methanol fuel has the highest autoignition temperature due to this it resists to start the combustion early. Hence methanol pressure curve moves forward compared to all alcohol-based fuel. There are no considerable changes in the peak in-cylinder pressure and its peak pressure CA.

From the **figure 5.24(a)** the in-cylinder pressure for M100+D DF-HCCI engine is 61.63 bar at  $371^0$  CA, for E100+D DF-HCCI engine it is 62.79 bar at  $371^0$  CA, for P100+D DF-HCCI engine it is 62.6 bar at  $370^0$  CA and for B100+D DF-HCCI engine it is 62.25 bar at  $370^0$  CA. However, for a neat diesel engine, it is 61.16 bar at  $370^0$  CA.

**Figure 5.24(b)** shows PRR with a degree CA for different alcohol-based fuel under 100% load condition. PRR for all alcohol-based DF-HCCI engine is below 6 bar/ $^0$ CA which is nearer to the

value of a neat diesel engine. This indicates the anti-knocking ability of all alcohol-based DF-HCCI engine and shows all these fuels are suitable for DF-HCCI engine combustion.

**Figure 5.24(c)** indicates the HRR with a degree CA for different alcohol-based fuels under 100% load condition. Results show the normal rise of HRR for all alcohol-based fuels compared to diesel engine. There is no sudden rise of heat release means fuel is burning smoothly without misfire. With decreasing the carbon number in the alcohol-based fuel, means delay in heat liberation time, due to this HRR curves shifted forward means late heat-releasing occurs.

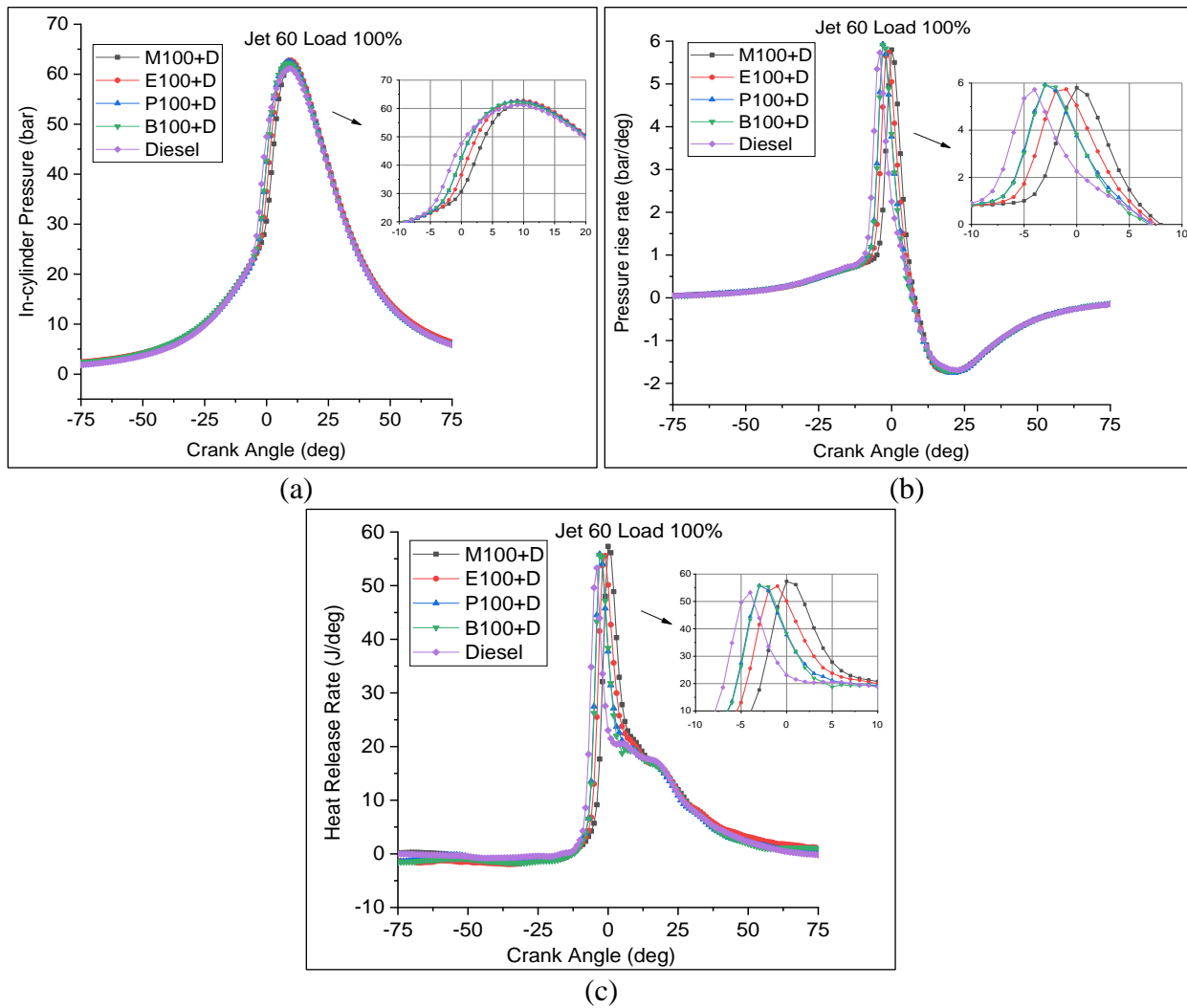


**Figure 5.24** Variation of (a) In-cylinder pressure Vs. Crank angle, (b) PRR Vs. Crank angle, (c) HRR Vs. Crank angle, for different alcohol-based fuel DF-HCCI engine

**Figure 5.25(a)** demonstrated the ID under different load conditions for 4 different alcohol-based fuels. Results show that with increasing the carbon number ID was reduced, which means for less carbon alcohol such as methanol has the highest ID. In ID orders methanol have the highest

ID then ethanol then propanol and then butanol. Butanol fuel has lowest ID compared to rest of the alcohol-based fuel in DF-HCCI engine, however, all alcohol-based fuel has more ID compared to neat diesel fuel. With increasing the carbon number in the alcohol-based fuel, due to polarization, the hydroxyl group weakens and their alkane counterpart decreases. As a result, changes were observed in fuel characteristics such as LHV of fuel decreases with increasing carbon number. Further octane number decreases, cetane number increases, self-ignition temperature decreases with increasing the carbon number. These properties impact the cooling potential of the fuel. Because of high LHV, the cooling potential of methanol is very high which helps to reduce the engine combustion temperature.

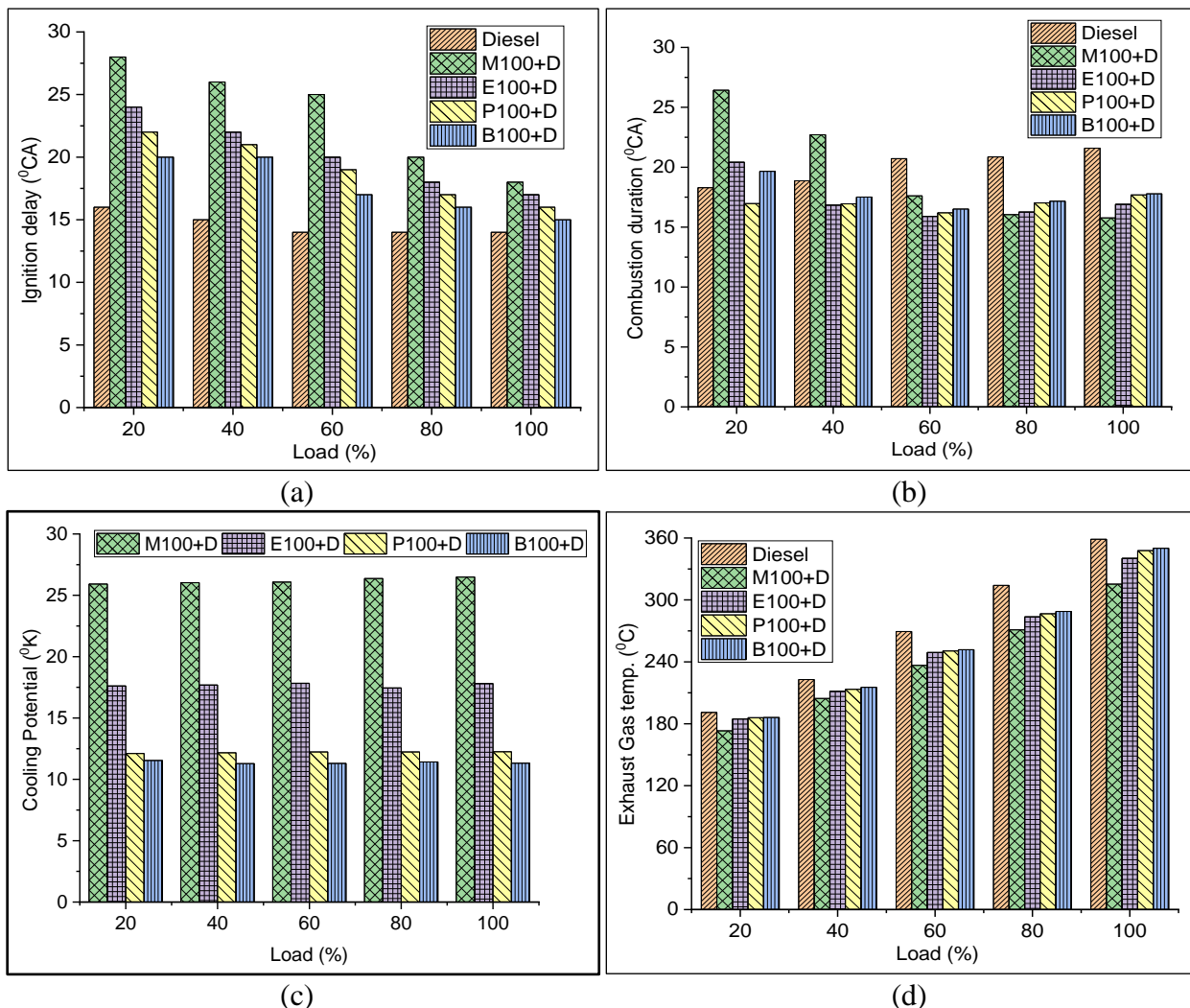


**Figure 5.25** Comparison of (a) ID Vs. Engine load, (b) CD Vs. Engine load, (c) Cooling potential Vs. Engine load, (d) Exhaust gas temperature Vs. Engine load, for different alcohol-based fuel in DF-HCCI engine

**Figure 5.25(b)** demonstrated CD for all different alcohol-based fuels under various load conditions. The result indicates the highest CD for butanol DF-HCCI engine compared to the rest of the alcohol-based fuels. Because butanol fuel has a low ID and low autoignition temperature, it takes time to burn in the premixed combustion phase. Further, less carbon number alcohol-based fuel has a high ID, it got more time to get ready for combustion hence spontaneous and short combustion happens, it leads to reduce CD. However, at low load condition methanol shows high CD because methanol has high cooling potential, which leads to consume more fuel to get required power and engine rpm hence CD was more.

**Figure 5.25(c)** shows the cooling potential for all four different alcohol-based fuel for various load conditions. For all load conditions cooling potential is same for all alcohol-based fuels because in this study alcohol-based fuel MFR is constant and the load was controlled by diesel fuel. The cooling potential depends on the MFR, stoichiometric, and LHV of fuel. Methanol fuel has the highest cooling potential it helps to reduce the engine combustion chamber results in low exhaust gas temperature shown in **figure 5.25(d)**.

**Figure 5.26(a)** presents the  $\text{NO}_x$  emission for 4 different alcohol-based fuels under different load conditions. The results indicate that all alcohol-based DF-HCCI engines the reduction of  $\text{NO}_x$  emission is far better than diesel engine. Methanol fuel reduced the highest  $\text{NO}_x$  emission. Because lower carbon number fuel i.e. methanol has the highest cooling potential it assists to cool the inlet charge leads to reduce combustion chamber.  $\text{NO}_x$  emission depends upon the combustion chamber temperature. Low combustion chamber temperature assists to reduce  $\text{NO}_x$  emission.

**Figure 5.26(b)** show smoke opacity under various load conditions for different alcohol-based DF-HCCI engine. An increase in the carbon number in the fuel reduced smoke opacity. Butanol+D showed the lowest smoke opacity, while M100+D showed the highest smoke opacity. All alcohol-based fuel reduced smoke opacity for all load conditions, except M100+D at low load conditions. Smoke opacity depends upon the fuel-rich region in the combustion chamber. In the DF-HCCI engine premixed homogenous charge prepared outside the engine cylinder; due to which very few chances of fuel-rich region occur.

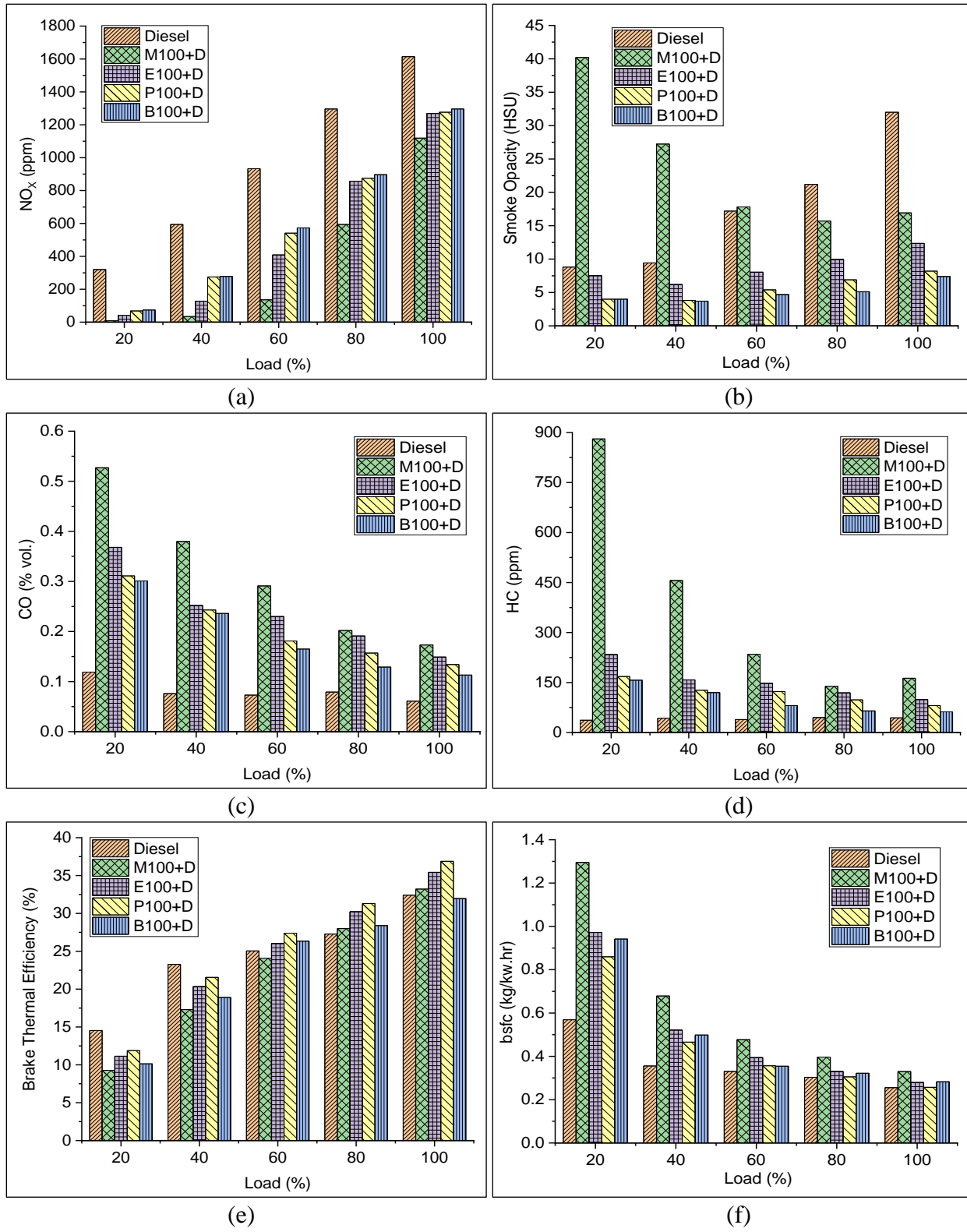


**Figure 5.26** Variation of (a) NO<sub>x</sub> emission Vs. Engine load, (b) Smoke opacity Vs. Engine load, (c) CO emission Vs. Engine load, (d) HC emission Vs. Engine load, (e) BTE Vs. Engine load, (f) bsfc Vs. Engine load, for different alcohol-based fuel under various load conditions

In DF-HCCI engine to ignite the premixed charge diesel is injected which may form a heterogeneous mixture and leads to produce smoke opacity. Further, high CV alcohol-based fuel can contribute more energy ratio means less chance of fuel rich region due to supply of less quantity diesel fuel. While low CV alcohol-based fuel can contribute low energy ratio means high chances of the fuel-rich region. Hence Butanol+D showed the lowest smoke opacity while M100+D showed the highest smoke opacity compared to the rest of the alcohol-based fuel.

**Figure 5.26(c) and figure 5.26(d)** presents the CO and HC emission for various alcohol-based fuels under different load conditions. Results indicate that HC and CO emission increased with reducing carbon number in the fuels. M100+D showed the highest HC and CO emissions while B100+D showed the lowest HC and CO emissions. HC and CO emission was produced due to incomplete fuel consumption. Because of high cooling potential, LTC leads to produce cylinder impingement on liner.

**Figure 5.26(e)** indicates the BTE for four different alcohol-based DF-HCCI engines under various load conditions. At 20% and 40% load conditions all alcohol-based fuel showed lower BTE compared to diesel engine, while at 60%, 80%, and 100% load conditions BTE was increased compared to diesel engine. E100+D and P100+D DF-HCCI engine indicated the highest BTE compared to methanol and butanol DF-HCCI engines. From this comparison, it was observed that propanol fuel is most efficient for DF-HCCI engine compared to other alcohol-based and diesel engine.

**Figure 5.26(f)** shows bsfc for various alcohol-based DF-HCCI engine under different load conditions. In DF-HCCI engine to get the required power and rpm more amount of fuel need to consume due to the low CV of alcohol-based fuel. All alcohol-based DF-HCCI engine showed high bsfc compared to diesel engines. Propanol fuel showed lower bsfc compared to the rest of the alcohol-based fuels.

**Figure 5.27(a)** shows the reduction of NO<sub>x</sub> emission in alcohol-based DF-HCCI engine over a diesel engine. The positive value on Y-axis denotes the favorable improvement and the negative value on Y-axis denotes non-favorable improvement. M100+D reduced the highest NO<sub>x</sub> emission i.e. 97.19% under 20% load conditions. While E100+D reduced 86.88%, P100+D reduced 78.75% and B100+D reduced 76.88% under 20% load conditions. With increase in the

load NO<sub>x</sub> reduction percentage was reduced for all alcohol-based fuel due to the constant MFR of alcohol-based fuel.

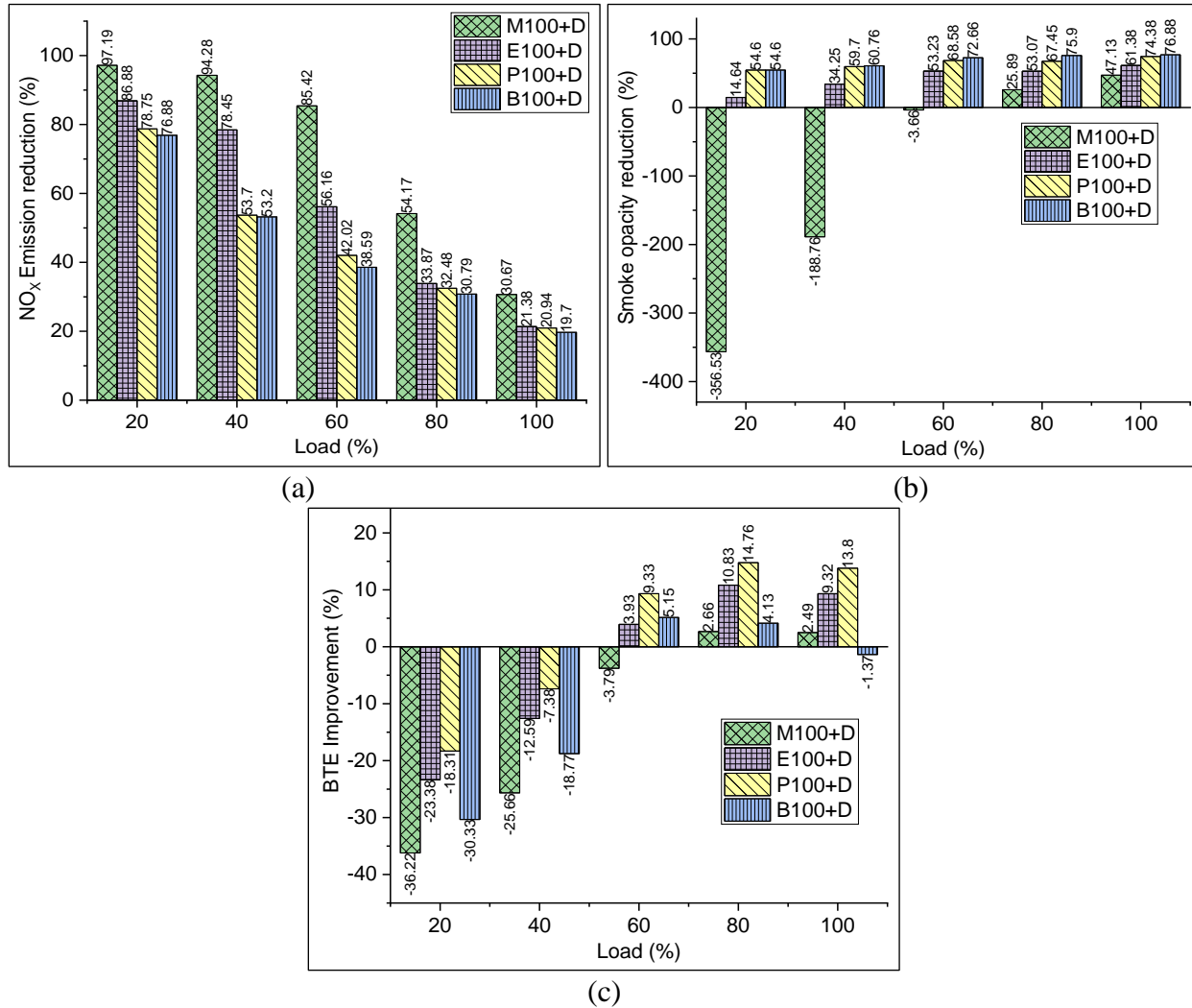


**Figure 5.27** improvement of alcohol-based DF-HCCI engine performance over neat diesel engine (a) NO<sub>x</sub> emission reduction Vs. engine load, (b) Smoke opacity reduction Vs. Engine load, (c) BTE improvement Vs. Engine load

**Figure 5.27(b)** shows the smoke opacity reduction for four different alcohol-based DF-HCCI engines over diesel engine. All alcohol-based DF-HCCI engines reduced smoke opacity for all load conditions except methanol DF-HCCI engine at low load conditions (i.e. 20% and 40%). B100+D DF-HCCI engine reduced the highest smoke opacity for all load conditions compared to the rest of the alcohol-based fuel. B100+D, P100+D, E100+D, and M100+D DF-HCCI engine reduced smoke opacity by 76.88%, 74.38%, 61.38%, and 47.13% respectively under 100% load conditions compared to diesel engine.

**Figure 5.27(c)** presents the influence of alcohol-based fuels on the BTE of DF-HCCI engine over diesel engine. All alcohol-based DF-HCCI engines improved BTE for high load conditions (i.e. at 60%, 80%, and 100% engine load) except butanol at 100% load condition and methanol at 60% load conditions. However, BTE was reduced for all alcohol-based DF-HCCI engine at 20% and 40% load conditions. P100+D DF-HCCI engine showed 14.76% highest increment in BTE at 80% load condition while E100+D improved 10.83%, B100+D improved 4.13% and M100+D improved 2.66% at 80% load condition over diesel engine.

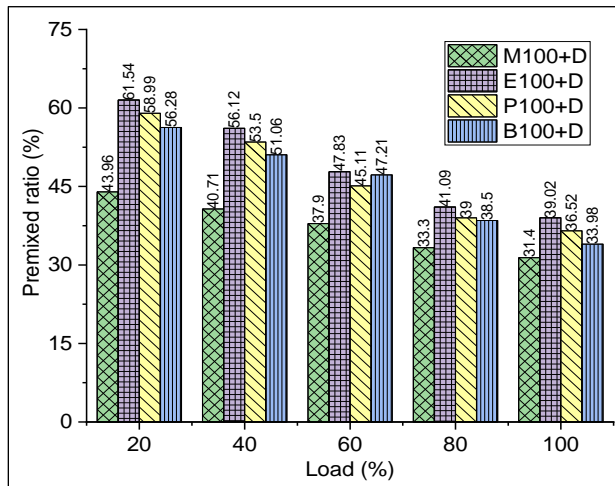


**Figure 5.28** Premixed ratio of all four alcohol-based fuel under various load conditions for DF-HCCI engine

**Figure 5.28** shows the premixed ratio for four different alcohol-based fuels in DF-HCCI engines at different load conditions. Ethanol fuel shows the highest premixed ratio for all load conditions compared to the rest of the alcohol-based fuel. At 20% load condition, premixed ratio of Methanol, Ethanol, Propanol, and Butanol is 43.96%, 61.54%, 58.99%, and 56.28% respectively.

#### 5.4.2 Optimization of alcohol-based fuel in DF-HCCI engine at different load conditions

Four sets of weightages and SAW method were used to find out the optimum alcohol-based fuel in DF-HCCI engine at different load conditions. **Table 5.9** shows the combined score and ranking of different alcohol-based DF-HCCI engine under different load conditions.

From **Table 5.9** it is concluded that alcohol-based fuels are suitable in DF-HCCI engine at a particular load by maintaining the highest fuel economy (BTE) and lowest emission compared to diesel engine. P100+D and B100+D DF-HCCI engine showed superior performance for all load conditions compared to the rest of the alcohol and diesel engine.

From this optimization, the best alcohol-based fuel for suitable operating load range on DF-HCCI mode engine was identified.

**Table 5.9** Ranking of different fuel jet for various weightage sets under each load conditions

Load (%)	Type of alcohol	Y1	Rank	Y2	Rank	Y3	Rank	Y4	Rank
20	CI	0.494	5	0.621	2	0.621	1	0.621	3
	M100+D	0.579	3	0.543	4	0.493	4	0.594	4
	E100+D	0.504	4	0.517	5	0.465	5	0.57	5
	P100+D	0.649	1	0.64	1	0.588	2	0.692	1
	B100+D	0.605	2	0.591	3	0.553	3	0.629	2
40	CI	0.483	5	0.612	3	0.612	2	0.612	5
	M100+D	0.626	3	0.596	4	0.536	4	0.656	3
	E100+D	0.578	4	0.593	5	0.535	5	0.653	4
	P100+D	0.674	1	0.677	1	0.617	1	0.737	1
	B100+D	0.644	2	0.64	2	0.592	3	0.687	2
60	CI	0.444	5	0.571	5	0.579	4	0.562	5
	M100+D	0.714	2	0.689	3	0.622	3	0.756	3
	E100+D	0.622	4	0.639	4	0.573	5	0.705	4
	P100+D	0.707	3	0.716	2	0.652	2	0.78	2
	B100+D	0.732	1	0.74	1	0.69	1	0.79	1
80	CI	0.523	5	0.624	5	0.636	4	0.611	5
	M100+D	0.739	3	0.725	4	0.671	3	0.779	4
	E100+D	0.723	4	0.728	3	0.671	3	0.785	3
	P100+D	0.806	2	0.803	2	0.751	2	0.855	2
	B100+D	0.855	1	0.844	1	0.818	1	0.869	1
100	CI	0.6	5	0.683	5	0.695	4	0.67	5
	M100+D	0.779	4	0.751	4	0.692	5	0.81	4
	E100+D	0.813	3	0.797	3	0.744	3	0.85	3
	P100+D	0.926	1	0.895	1	0.845	2	0.945	1
	B100+D	0.909	2	0.875	2	0.851	1	0.899	2

From the SAW optimization, it was concluded that P100+D DF-HCCI engine gave the best cumulative performance for low load and high load conditions. However, B100+D DF-HCCI engine gave the best performance for mid-load conditions. E100+D gave a moderate performance for all load conditions and M100+D gave the poorest cumulative performance for all load conditions compared to the rest of the alcohol-based DF-HCCI engine.

### **5.4.3 Summary**

In this study, all four alcohol-based fuels (methanol, ethanol, propanol, and butanol) were compared with each other and the best suitable fuel for DF-HCCI engine was examined. It is concluded that the P100+D DF-HCCI engine is best for low and high load conditions and the B100+D DF-HCCI engine is best for mid load conditions.

## 5.5 Objective 4

**To investigate the influence of biodiesel blend (Bio20) in place of diesel in dual fuel HCCI engine on combustion and emission.**

In this experiment in place of diesel, a biodiesel blend was used in the all alcohol-based DF-HCCI engine. Most of the researchers found that 20% blend is most effective to reduce the HC and CO emission, hence in this study, only 20% blend was used. Neem biodiesel blend 20 (Bio20) was used which is the mixture of 80% diesel and 20% neem biodiesel by volume. The influence of Bio20 on DF-HCCI engine was investigated for constant MFR of alcohol-based fuel through the fuel jet 60 carburetor.

### 5.5.1 M100+Bio20 DF-HCCI engine performance over M100+D DF-HCCI engine

In this experiment methanol fuel was carried through the carburetor at the time of suction stroke and to ignite the premixed charge Neem Biodiesel 20 (Bio20) was injected at the end of the compression stroke. Constant MFR of methanol was supplied by using fuel jet 60 in the carburetor and the load was controlled by Bio20. The influence of Bio20 instead of diesel in methanol DF-HCCI engine was investigated.

#### 5.5.1.1 *Influence of Bio20 instead of diesel on combustion and emission characteristics*

**Figure 5.29(a)** presents in-cylinder pressure for M100+D, M100+Bio20, and diesel engines under 100% load conditions. Results show that Bio20 promotes better combustion compared to M100+D DF-HCCI engine. Since methanol has a high octane number, high self-ignition temperature which assists to delay the start of combustion (SOC). Thus combustion is initiated after the end of the compression stroke. Hence most of the combustion part is completed in the expansion stroke, due to which in-cylinder pressure is reduced. But M100 with Bio20 reduces ignition delay (ID) and promotes combustion due to the presence of extra oxygen in the biodiesel blend [144].

**Figure 5.29(b)** and **Figure 5.29(c)** show PRR and HRR curves for M100+D, M100+Bio20, and diesel engines at 100% load condition. It shows that Bio20 helps to start the combustion early because the oxygen inherent Bio20 assists to reduce ID (shown in **Figure 5.30**). Inherent oxygen in the Bio20 increases the cetane number and promotes combustion. Methanol having the same autoignition temperature but due to the change of direct injection fuel in the case of

M100+Bio20 early combustion promoted and ID reduced compare to M100+D DF-HCCI engine. However, both M100+D and M100+Bio20 show more delay in the SOC compared to a conventional diesel engine.

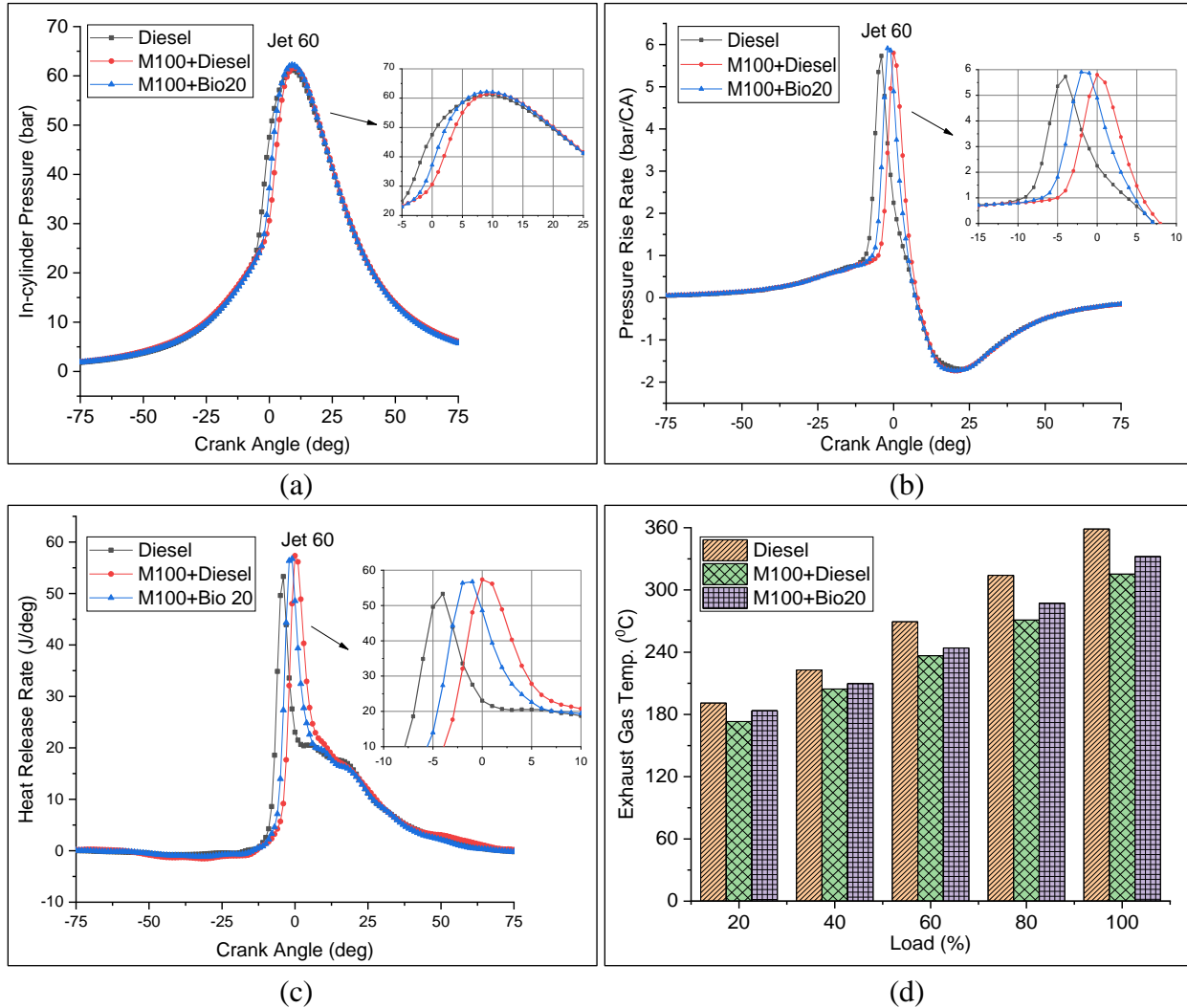


**Figure 5.29** Variation of (a) In-cylinder pressure Vs. Crank angle, (b) PRR Vs. Crank angle, (c) HRR Vs. Crank angle, (d) Exhaust gas temp. Vs. engine load, for methanol DF-HCCI engine

**Figure 5.29(d)** shows the exhaust gas temperature for M100+D, M100+Bio20, and diesel engines under different load conditions. Results show that Bio20 instead of diesel in methanol DF-HCCI engine increased exhaust gas temperature compared to M100+D DF-HCCI engine. Bio20 blend promotes combustion and assists to increase the combustion chamber temperature, which leads to increase in the exhaust gas temperature.

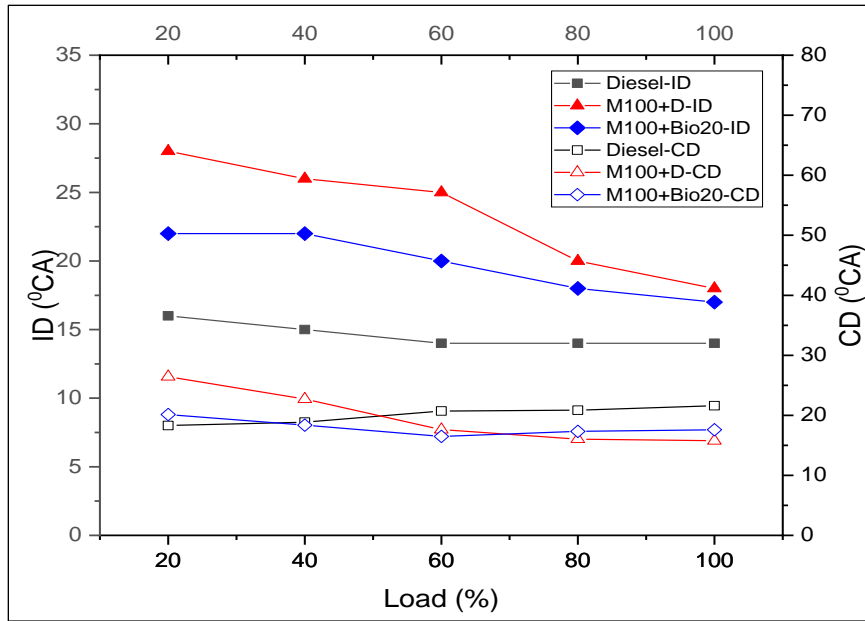


**Figure 5.30** Impact of Bio20 in place of diesel on ID and CD of methanol DF-HCCI engine

**Figure 5.30** shows ID and combustion duration (CD) for M100+D, M100+Bio20, and diesel engine. It is observed that M100+Bio20 reduces ID because extra oxygen present in the Bio20 helps to trigger SOC compared to M100+D DF-HCCI engine. However, CD of M100+Bio20 is more compared to M100+D. Inherent extra oxygen helps to elongate the CD and extend the combustion period. But M100+D and M100+Bio20 both have less CD compared to diesel engine due to sudden combustion of methanol premixed charge.

**Figure 5.31** presents the CO emission and HC emissions for M100+D, M100+Bio20, and conventional diesel engines. In **Figure 5.31** the results revealed that M100+Bio20 reduces more CO emission at low load conditions compared to high load conditions. For all load conditions, more reduction drop occurred in the M100+Bio20 DF-HCCI engine compared to M100+D DF-HCCI engine. Because Bio20 is an oxygenated fuel, it helps to convert CO into  $\text{CO}_2$  emissions leads to a reduction in CO emissions. Also **figure 5.31** shows HC emission for DF-HCCI engine. Results revealed that HC emissions for M100+Bio20 DF-HCCI engine were reduced compared to M100+D. Since oxygen present in Bio20 triggers the combustion, it increases the combustion temperature and reduces HC emissions while the extra oxygen combines with HC and converts it into  $\text{H}_2\text{O}$  and  $\text{CO}_2$  [145].

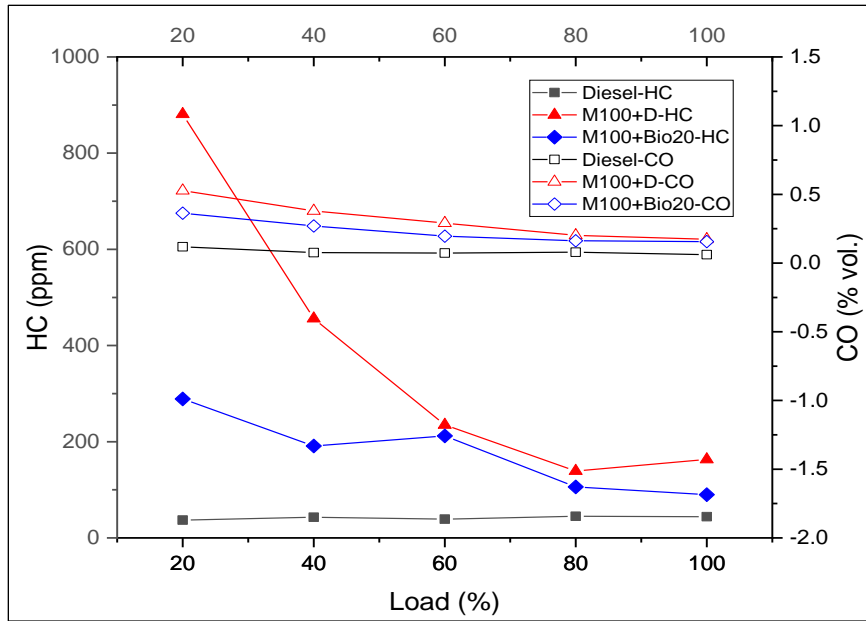


**Figure 5.31** Impact of Bio20 instead of diesel on CO (% vol.) and HC (ppm) emissions of methanol DF-HCCI engine

**Figure 5.32** shows NO<sub>x</sub> emissions and smoke opacity for diesel ignited and Bio20 ignited methanol DF-HCCI engine. NO<sub>x</sub> emissions for M100+Bio20 is increased compared to M100+D DF-HCCI engine for all load conditions. Since extra oxygen in Bio20 combines with NO, it assists in easy conversion into NO<sub>x</sub> emissions. Due to Bio20, SOC got promoted and increased NO<sub>x</sub> emissions. Also as biodiesel cetane number is more, it reduces ID (shown in **Figure 5.30**) due to that premixed combustion reduced, thereby increasing the fraction of diffusion combustion. Hence more fuel is burnt in the diffusion combustion which leads to increasing combustion temperature and forms more NO<sub>x</sub> emissions [22].

With respect to smoke opacity of methanol DF-HCCI engine, results show that the smoke opacity of M100+Bio20 was reduced compared to M100+D DF-HCCI engine. In the M100+D DF-HCCI engine, LHV of methanol is more hence it helps to reduce combustion temperature and more unburned smoke produced. In the Bio20 inherent oxygen promote combustion and achieve the required combustion temperature. Also, homogeneous methanol charge helps to reduce more smoke opacity compared to M100+D engine.

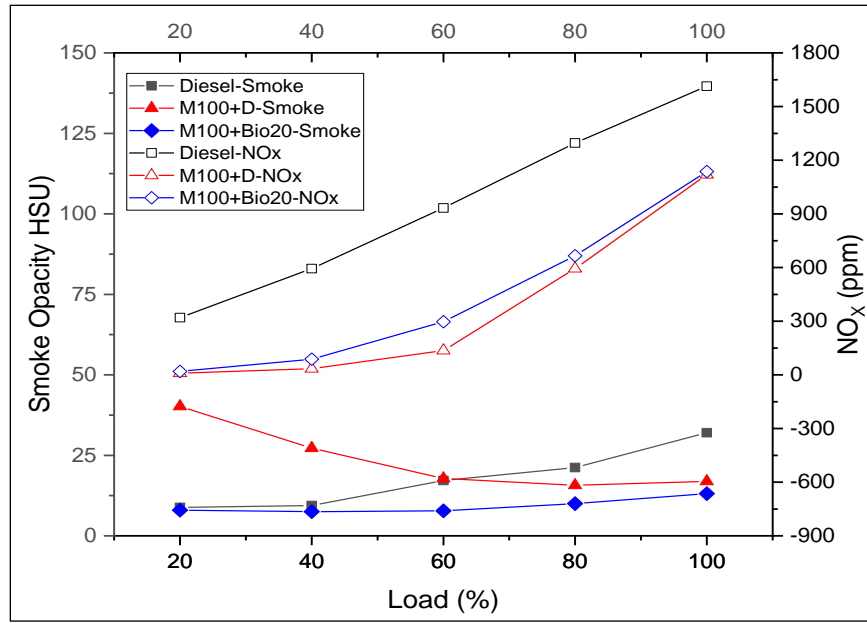


**Figure 5.32** Impact of Bio20 instead of diesel on Smoke opacity and NO<sub>x</sub> emissions of methanol DF-HCCI engine

**Figure 5.33** displays the brake thermal efficiency (BTE) for all load conditions. The results show that high BTE for M100+Bio20 compared to M100+D because HRR for M100+Bio20 is more (shown in **Figure 5.29(c)**). In the case of M100+Bio20, the engine utilized total fuel effectively, and the heat losses were very low hence with low NO<sub>x</sub> emission, and more BTE.

**Figure 5.33(d)** presents the bsfc for M100+D, M100+Bio20 and neat diesel engine under various load conditions. Results show that instead of diesel Bio20 methanol DF-HCCI engine has lower bsfc for all load conditions. The presence of oxygen in the biodiesel helps to increase engine temperature which leads to reduce incomplete combustion. More efficient fuel consumption results in reduction of bsfc for M100+Bio20 compared to M100+D DF-HCCI engine.

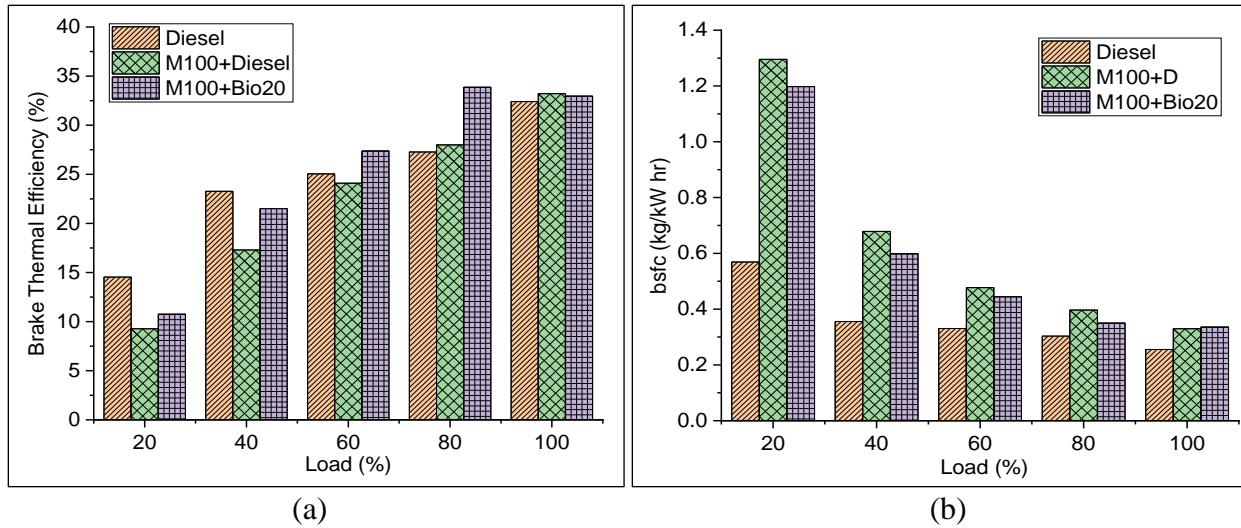


**Figure 5.33** Impact of Bio20 instead of diesel on (a) BTE Vs. Engine load, (b) bsfc Vs. Engine load in methanol DF-HCCI engine

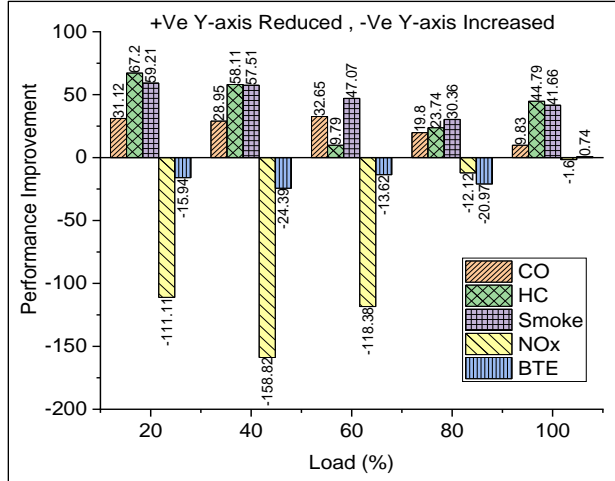


**Figure 5.34** Performance improvement of M100+Bio20 over M100+D DF-HCCI engine

**Figure 5.34** presents the performance improvement by injection of Bio20 instead of diesel in methanol DF-HCCI engine in the term of percentage (%) for CO, HC, NO<sub>x</sub>, smoke opacity, and BTE. A positive value on Y-axis indicates the reduction in percentage and a negative value on Y-axis indicates an increment in percentage. It was observed that M100+Bio20 engine emits low CO, HC, and smoke opacity for all load conditions compared to M100+D DF-HCCI engine. However, NO<sub>x</sub> emissions increased compared to M100+D. Substitute of Bio20 in place of diesel in methanol DF-HCCI engine improved BTE. In the M100+Bio20 DF-HCCI engine at 20% load condition CO, HC, and smoke opacity were reduced by 31.12%, 67.2%, and 59.21% respectively, however, NO<sub>x</sub> was increased by 111.11% compared to M100+D DF-HCCI engine, while BTE was increased by 15.94%. At 100% load conditions CO was reduced by 9.83%, HC

reduced by 44.79%, smoke opacity reduced by 41.66%, and NO<sub>x</sub> increased by 1.6% but BTE was reduced by 0.74% compared to M100+D DF-HCCI engine.

Similarly, Bio20 was injected instead of diesel in ethanol, propanol, and butanol DF-HCCI engine. In-cylinder pressure, PRR, HRR, ID, and CD show a similar kind of trends but values were different, due to individual characteristics of alcohol-based fuel. Biodiesel blend (Bio20) injection instead of diesel reduced the HC and CO emission with good BTE, however, NO<sub>x</sub> and smoke opacity were increased. Performance improvement of all alcohol-based fuel which is ignited by Bio20 instead of diesel discussed below.

### **5.5.2 Impact of Bio20 instead of diesel on reduction of CO emission in alcohol-based DF-HCCI engine**

In this section on Y-axis positive value indicates the reduction of parameter value and the negative value on Y-axis indicates the increment of the parameter value. **Figure 5.35(a)** presents the reduction of CO emission in percentage for M100+Bio20, E100+Bio20, P100+Bio20 and B100+Bio20 over M100+D, E100+D, P100+D and B100+D respectively. All Bio20 ignited instead of diesel alcohol-based DF-HCCI engine performance was compared at different load conditions. The result shows that Bio20 injection assists to reduce the highest CO emission in the methanol DF-HCCI engine at all load conditions except at 100% load conditions compared to the rest of the alcohol-based DF-HCCI engine. At 20% load condition Bio20 injection instead of diesel in alcohol-based DF-HCCI engine reduced the CO emission by 31.12%, 0.27%, 4.7%, and 3.99% in methanol, ethanol, propanol, and butanol respectively. While at 100% load condition P100+Bio20 reduced the highest 19.4% CO emission compared to the rest of the Bio20 ignited alcohol-based DF-HCCI engine.

**Figure 5.35(b)** presents the reduction of HC emission in percentage for M100+Bio20, E100+Bio20, P100+Bio20 and B100+Bio20 over M100+D, E100+D, P100+D and B100+D respectively. Bio20 ignited alcohol-based DF-HCCI engine instead diesel fuel, the performance was compared at different load conditions. The result shows that Bio20 injection helps to reduce the highest HC emission in the methanol DF-HCCI engine at all load conditions compared to the rest of the alcohol-based DF-HCCI engine. At 20% load condition Bio20 injection instead of diesel reduced 67.2% HC emission for methanol DF-HCCI engine, while 2.14%, 4.76%, and 10.19% HC emission were reduced in ethanol, propanol, and butanol DF-HCCI engine.

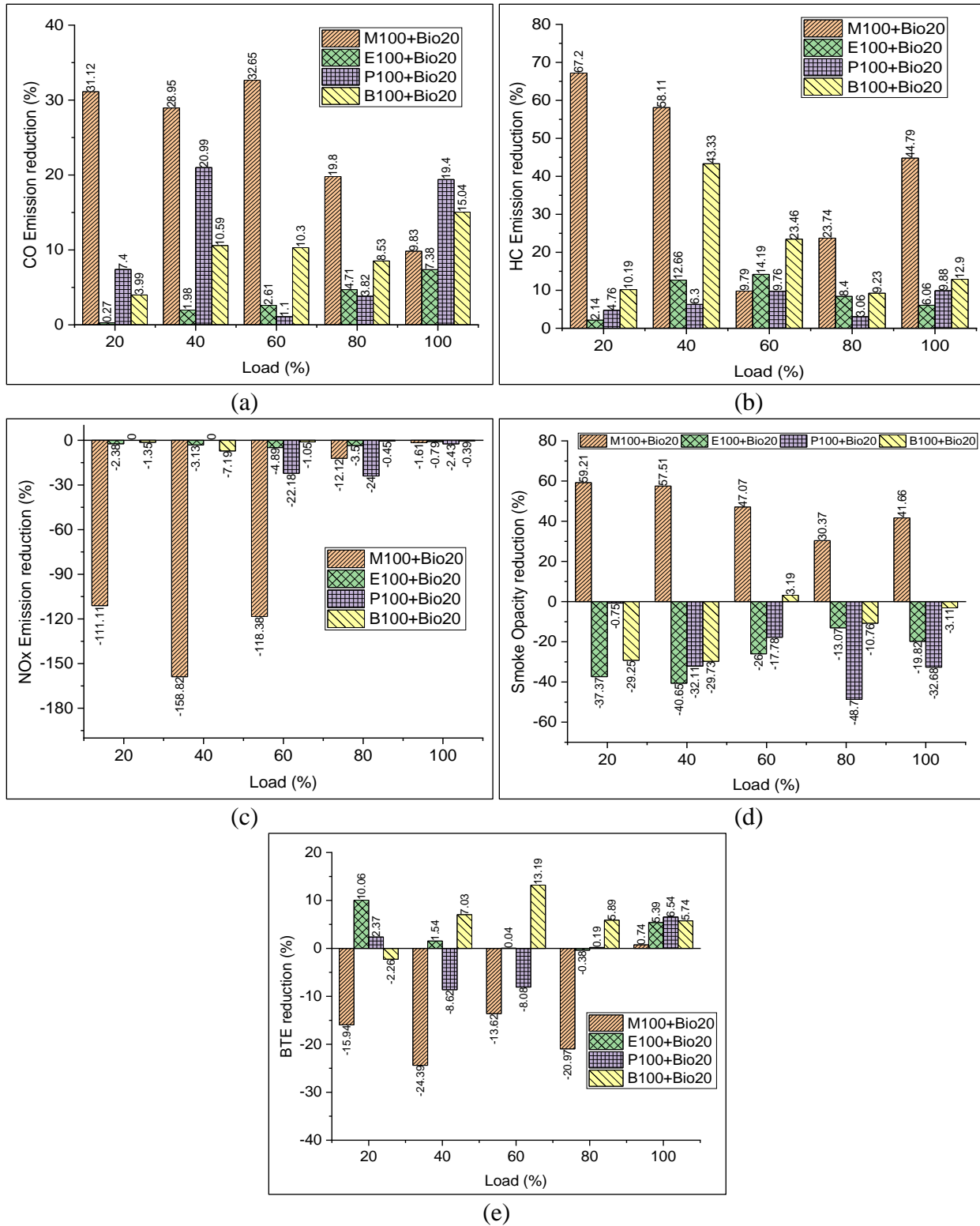


**Figure 5.35** Increment and decrement of (a) CO emission, (b) HC emission, (C) NO<sub>x</sub> emission, (d) smoke opacity, (e) BTE, of Bio20 ignited alcohol-based DF-HCCI engine over diesel ignited alcohol-based DF-HCCI engine

However, at 100% load condition very low reduction was observed in E100+Bio20 DF-HCCI engine.

**Figure 5.35(c)** demonstrated the reduction and increment of NO<sub>x</sub> emission in percentage for M100+Bio20, E100+Bio20, P100+Bio20 and B100+Bio20 over M100+D, E100+D, P100+D and B100+D respectively. Injection of Bio20 instead of diesel increased NO<sub>x</sub> emission at low load condition in methanol DF-HCCI engine compared to rest of the alcohol-based DF-HCCI engine. NO<sub>x</sub> emission is not considerably increased more in ethanol, propanol, and butanol DF-HCCI engine under all load conditions. At 100% load condition very negligible NO<sub>x</sub> emission increment was observed for all alcohol-based DF-HCCI engines compared to the respective diesel ignited alcohol-based DF-HCCI engine (i.e. M100+D, E100+D, P100+D, and B100+D).

**Figure 5.35(d)** revealed the reduction and increment of smoke opacity in percentage for M100+Bio20, E100+Bio20, P100+Bio20, and B100+Bio20 over M100+D, E100+D, P100+D, and B100+D respectively. Injection of Bio20 instead of diesel increased smoke opacity for E100+Bio20, P100+Bio20, and B100+Bio20, however, M100+Bio20 DF-HCCI engine reduced smoke opacity for all load conditions.

**Figure 5.35(e)** presented the reduction and increment of BTE in percentage for M100+Bio20, E100+Bio20, P100+Bio20, and B100+Bio20 over M100+D, E100+D, P100+D, and B100+D respectively. Injection of Bio20 instead of diesel increased BTE for M100+Bio20 at all load conditions except 100% load condition while, and P100+Bio20 at mid load conditions (i.e. 40% and 60%). However, E100+Bio20 and B100+Bio20 reduced the BTE at all load conditions, in a considerable amount.

The overall average performance of Bio20 substitution instead of diesel in all alcohol-based DF-HCCI engine is shown in **Table 5.10**. In this the performance improvement was observed for Bio20 injection instead of diesel in M100+Bio20, E100+Bio20, P100+Bio20, and B100+Bio20 DF-HCCI engine over M100+D, E100+D, P100+D, and B100+D DF-HCCI engine respectively.

**Table 5.10** Overall average performance improvement for Bio20 injection over diesel ignited alcohol-based DF-HCCI engine (+ve value means reduction, -ve value means increment)

Types	M100+Bio20	E100+Bio20	P100+Bio20	B100+Bio20
CO (%)	24.47	3.39	10.54	9.69
HC (%)	40.72	8.69	6.75	19.82
NO <sub>X</sub> (%)	-80.41	-2.94	-9.72	-2.08
Smoke (%)	47.17	-27.38	-26.40	-13.93
BTE (%)	-14.84	3.33	-1.52	5.92

- M100+Bio20 reduced the maximum percentage of CO emissions compared to M100+D, however E100+Bio20 shows very little reduction in CO emissions compared to E100+D.
- M100+Bio20 reduced the maximum percentage of HC emission compared to M100+D, however, P100+Bio20 shows very little reduction in HC emissions compared to P100+D.
- Similarly, M100+Bio20 increased the maximum percentage of NO<sub>X</sub> emission compared to M100+D, however, B100+Bio20 shows very little reduction in NO<sub>X</sub> emissions compared to B100+D.
- M100+Bio20 reduced the maximum percentage of smoke opacity compared to M100+D, however the rest of the alcohol-based fuel increased smoke opacity.
- It was observed that M100+Bio20 and P100+Bio20 increased BTE compared to M100+D and P100+D respectively.

### 5.5.3 Summary

From this study, it was concluded that for methanol DF-HCCI engine Bio20 replacement instead of diesel is better for the reduction of HC, CO, and smoke opacity with increasing BTE. However, for remaining alcohol-based DF-HCCI engine HC and CO emission got reduced by the use of Bio20 instead of diesel with a penalty of high NO<sub>X</sub> emission and smoke opacity with low BTE except P100+Bio20.

## 5.6 Objective 5

**To investigate the technical feasibility of various butanol blends (B10/B20/B30) in the propanol dual fuel HCCI engine.**

In this experiment, propanol was supplied through the carburetor, and to ignite the premixed charge various butanol blend (B10/B20/B30) was injected at the end of compression stroke. Since propanol was observed as a good alcohol-based fuel for DF-HCCI engine compared to rest of the alcohol based fuel. The explanation is given in section 5.4. In this study, MFR of propanol was constant (0.401 kg/hr) and the load was controlled by butanol blend (B10/B20/B30). An experiment was performed for 20% to 100% load condition and improvement by butanol blend injection (B10/B20/B30) over diesel ignited propanol DF-HCCI engine was investigated. Three different butanol blends were used B10 (10% butanol plus 90% diesel), B20 (20% butanol plus 80% diesel) and, B30 (30% butanol plus 70% diesel) on a volume basis.

### 5.6.1 Influence of Butanol blend (B10/B20/B30) on diesel ignited propanol DF-HCCI engine combustion and emissions

**Figure 5.36(a)** presents the influence of butanol blend in place of diesel as a high reactivity fuel on P100+B10/B20/B30 DF-HCCI engine. The results revealed that butanol blend as a direct injection fuel prolongs SOC, and increases ID compared to P100+D DF-HCCI engine. Further, an increase in the blending ratio of butanol, increases ID, which leads to delay in SOC. Since butanol has low cetane number, and high auto-ignition temperature it helps to extend ID, and impact on fuel combustion phase. Most of the fuel burns after the TDC, which leads to a decrease in-cylinder pressure. Peak in-cylinder pressure and its CA for P100+D was 62.6 bar at  $369^0$  CA, for P100+B10 it was 57.42 bar at  $371^0$  CA, for P100+B20 it was 56.78 bar at  $371^0$  CA and for P100+B30 it was 58.04 at  $372^0$  CA.

**Figure 5.36(b)** represents the impact of butanol blend (B10/B20/B30) injection on PRR for 100% load. It was noticed that increase in blend ratio of butanol reduces PRR while peak PRR crank angle was shifted forward compared to P100+D DF-HCCI engine. Further, PRR for all butanol blend ignited propanol DF-HCCI engine is below 6 bar/deg.CA, which indicated anti-knocking combustion.

**Figure 5.36(c)** shows HRR for different butanol blends in place of diesel in propanol DF-HCCI engine. Results show that HRR rate curves for P100+B10/B20/B30 DF-HCCI engine shifted drastically forward compared to P100+D DF-HCCI engine. Since butanol is alcohol-based fuel and has more octane number and low cetane number, it helps to increase total diesel and butanol mixture octane number to extend SOC temperature. However, P100+B20 and P100+B30 increases HRR compared to P100+D because extra oxygen in butanol helps to increase in HRR with increasing butanol blend [146].

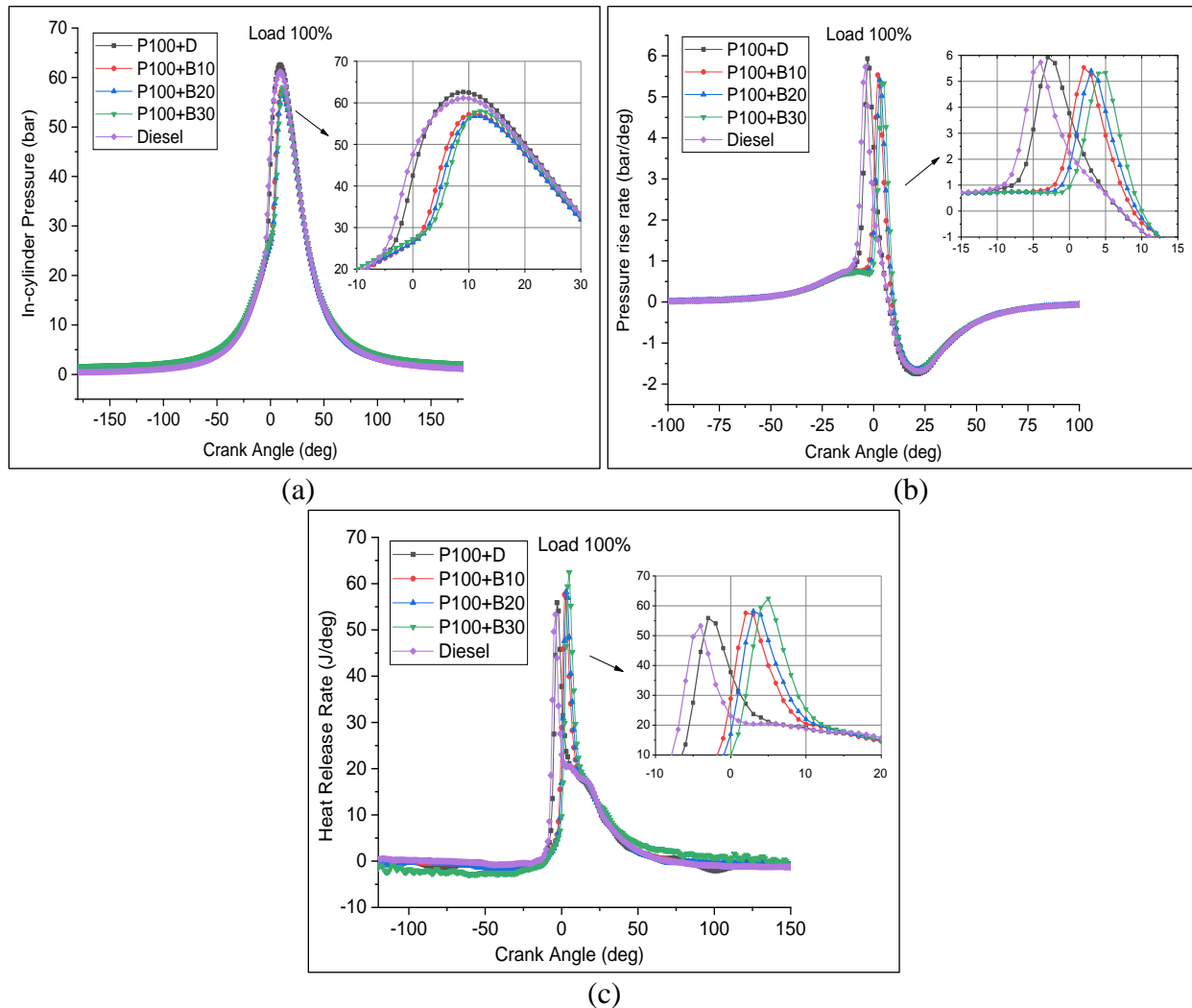


**Figure 5.36** Influence of butanol blend (B10/B20/B30) injection on (a) in-cylinder pressure, (b) PRR, (c) HRR, over diesel ignited propanol DF-HCCI engine under 100% load conditions

**Figure 5.37** indicates the ID and CD for different butanol blends (B10/B20/B30) in propanol DF-HCCI engine. Results show that with increase in fraction of butanol in blends as a high reactivity fuel increased ID and reduced CD compared to P100+D DF-HCCI engine. Because

addition of butanol in blends reduces the cetane number, it increases ignition resistance, and auto-ignition temperature which helps to prolong SOC, and assists in increasing ID. Due to more ID the carburetor supplied fuel and direct-injected fuel mixed properly with air and most of the fuel burns in the premixed phase of combustion leading to a reduction in CD.

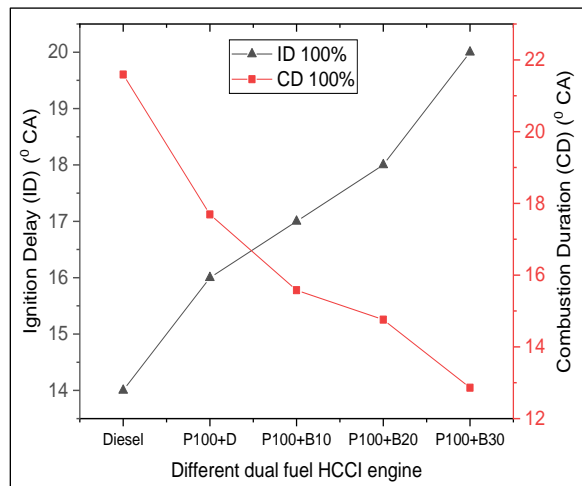


**Figure 5.37** ID and CD for different butanol blends in propanol DF-HCCI engine

**Figure 5.38(a)** shows CO emission for different butanol blend and diesel ignited propanol DF-HCCI engine. It was observed that butanol blends gave better results under higher load conditions for a selected MFR of propanol (0.401 kg/hr). Results revealed that with increase in butanol fraction in blends, CO emissions reduced under higher load conditions. Butanol is oxygenic fuel that helps to reduce CO emission by chemical compositions. Butanol inherent oxygen combines with CO converted into CO<sub>2</sub>; thus CO emissions reduced compared to P100+D DF-HCCI engine. However, at low load conditions, CO emissions increased because butanol blend DF-HCCI engine consumes more fuel at low load conditions to achieve the required power. Propanol, as well as butanol blends, has high LHV compared to diesel which led to lower engine combustion temperature, resulting in incomplete combustion. Further, due to lower calorific value of butanol blend, more air-fuel rich zones produced more CO emissions.

**Figure 5.38(b)** shows HC emissions for different butanol blends and diesel ignited propanol DF-HCCI engine. It was observed P100+B10 and P100+B20 showed a slight difference in HC emissions compared to P100+D DF-HCCI engine under high load conditions. However, P100+B30 considerably reduced HC emissions compared to P100+D DF-HCCI engine. Propanol and butanol blends have high LHV which led to low-temperature combustion due to this increase of HC emissions under low load conditions.

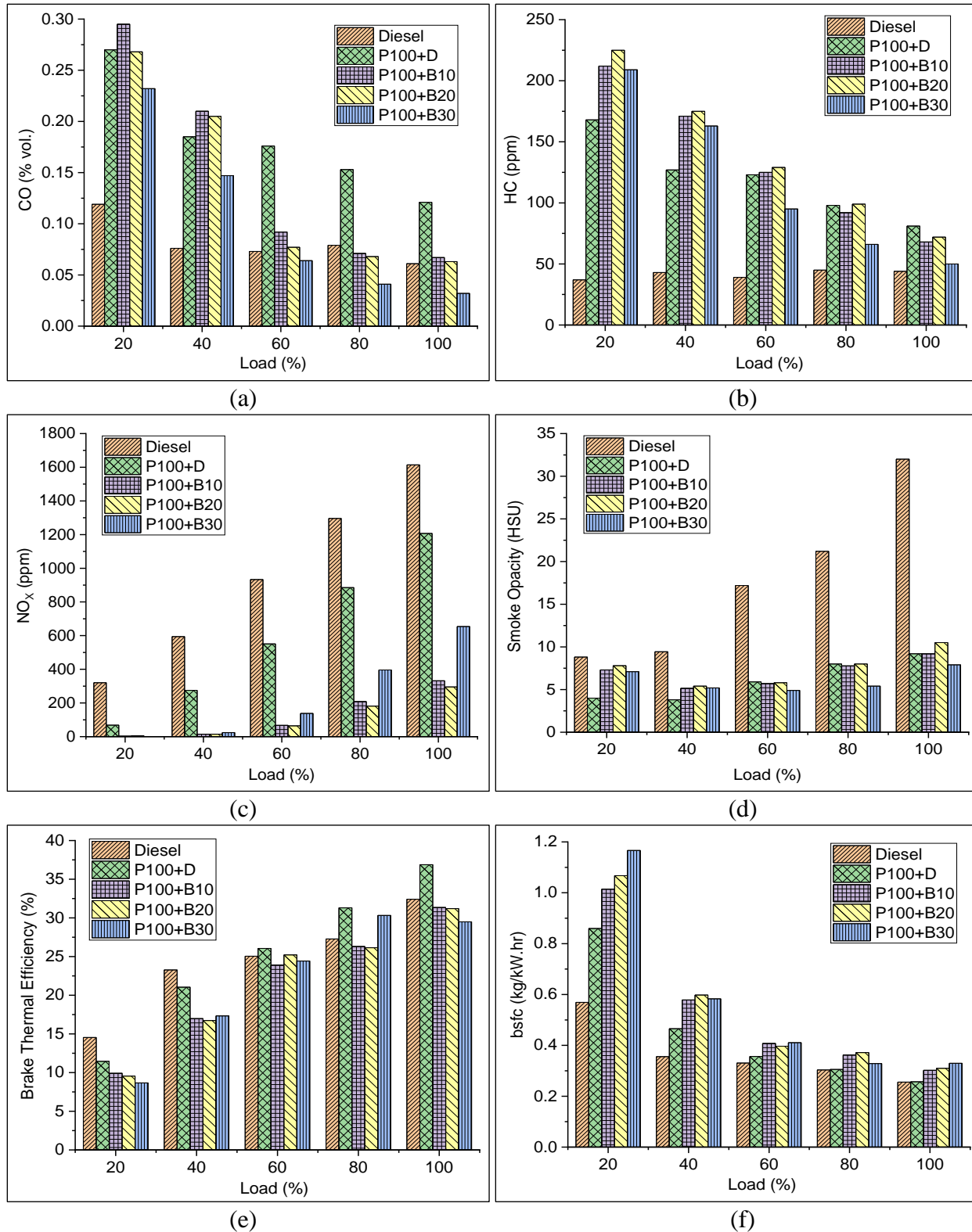


**Figure 5.38** Comparison of different propanol DF-HCCI engine (a) CO emissions (b) HC emissions (c) NO<sub>x</sub> emissions (d) Smoke opacity, (e) BTE, (f) bsfc, under various load conditions

**Figure 5.38(c)** displays NO<sub>x</sub> emissions for different propanol DF-HCCI engine. It was revealed that NO<sub>x</sub> emissions reduced with increasing butanol fraction in blends compared to P100+D DF-HCCI engine. Propanol has low cetane number, high octane number, and high LHV which enabled lowering of temperature in combustion chamber and increasing ID. Similarly, addition of butanol in blends increases its LHV which leads to lowering combustion temperature compared to diesel. Thus both fuels help to reduce the temperature of combustion chamber leading to a reduction in NO<sub>x</sub> emissions compared to P100+D DF-HCCI engine. However, P100+B30 DF-HCCI engine shows adverse effect because excess butanol contribution increases oxygen content, assist to burn fuel-rich regions which liberating more heat energy (shown in **Figure 5.36(c)**) and therefore producing more NO<sub>x</sub> emission.

**Figure 5.38(d)** indicates smoke opacity for different butanol blend and diesel ignited propanol DF-HCCI engine. It was observed that smoke opacity changed only a little for different butanol blends (B10/B20/B30) under higher load conditions, however, at low load conditions, it increased compared to P100+D DF-HCCI engine.

**Figure 5.38(e)** shows BTE for different butanol blend and diesel ignited propanol DF-HCCI engine. It was observed that, P100+D DF-HCCI engine gave better BTE compared to butanol blend ignited propanol DF-HCCI engine (P100+B10, P100+B20, P100+B30). Butanol blend consumes more fuel to get required effective power compared to diesel due to its lower heating value and lower energy content. Further, propanol dual-fuel combustion was done at low temperature and also because of butanol blend ID increased more which helped to extend SOC timing in late expansion stroke. Thus to achieve the required effective power in low temperature, more butanol blend fuels were consumed, which led to reduction in BTE [124].

**Figure 5.38(f)** shows bsfc for different butanol blend and diesel ignited propanol DF-HCCI engine. Butanol ignited DF-HCCI engine shows more bsfc compared to diesel ignited propanol DF-HCCI engine, due to the lower CV of butanol blends compared to neat diesel fuel. To get the requisite power output more butanol blend fuel need to supply.

### 5.6.2 Optimization to find out best high reactivity fuel (D/B10/B20/B30) for propanol DF-HCCI engine.

SAW optimization was applied to diesel engine, P100+D, P100+B10, P100+B20, and P100+B30 as a five alternative for the same five attributes (BTE, smoke opacity, NO<sub>x</sub>, HC, and CO). The same four different weightage sets were considered for examination.

**Table 5.11** Ranking of CI engine and different butanol blend ignited propanol DF-HCCI engine

Load (%)	Type of engine	Y1	Rank	Y2	Rank	Y3	Rank	Y4	Rank
20	CI	0.485	4	0.614	2	0.614	2	0.614	3
	P100+D	0.609	2	0.61	3	0.559	3	0.662	2
	P100+B10	0.532	3	0.534	4	0.49	4	0.578	4
	P100+B20	0.456	5	0.468	5	0.43	5	0.506	5
	P100+B30	0.719	1	0.658	1	0.627	1	0.688	1
40	CI	0.475	5	0.606	5	0.606	4	0.606	5
	P100+D	0.658	4	0.665	3	0.605	5	0.725	3
	P100+B10	0.855	1	0.804	1	0.742	1	0.866	1
	P100+B20	0.806	2	0.741	2	0.698	2	0.785	2
	P100+B30	0.685	3	0.656	4	0.611	3	0.701	4
60	CI	0.422	5	0.548	5	0.55	5	0.545	5
	P100+D	0.674	4	0.689	4	0.623	4	0.756	4
	P100+B10	0.929	1	0.894	1	0.847	2	0.941	1
	P100+B20	0.92	2	0.886	2	0.85	1	0.921	2
	P100+B30	0.784	3	0.793	3	0.774	3	0.811	3
80	CI	0.421	5	0.523	5	0.511	5	0.534	5
	P100+D	0.662	4	0.683	4	0.619	4	0.747	4
	P100+B10	0.81	3	0.791	3	0.758	3	0.825	3
	P100+B20	0.835	2	0.805	2	0.775	2	0.836	2
	P100+B30	0.924	1	0.923	1	0.91	1	0.936	1
100	CI	0.438	5	0.537	4	0.525	5	0.549	5
	P100+D	0.742	4	0.746	3	0.685	4	0.807	4
	P100+B10	0.846	2	0.805	2	0.785	3	0.825	3
	P100+B20	0.874	1	0.839	1	0.81	2	0.868	2
	P100+B30	0.797	3	0.805	2	0.819	1	0.791	1

From the optimization results, it was concluded that butanol blends (B10/B20/B30) ignited propanol DF-HCCI engine showed better cumulative performance under all load conditions compared to diesel ignited propanol DF-HCCI engine. At 20% and 80% load conditions

P100+B30, for 40% and 60% load conditions P100+B10, for 100% load conditions P100+B20 DF-HCCI engine gave an optimized performance.

### **5.6.3 Summary**

From this study, it was observed that butanol blend ignited propanol DF-HCCI engine is always preferable compared to P100+D DF-HCCI engine for the reduction of NO<sub>x</sub> emission HC and CO emissions, however, BTE was reduced. For cumulative performance, butanol blend ignited propanol DF-HCCI engine showed best performance compared to P100+D DF-HCCI engine under all load conditions. P100+B10 and P100+B20 was observed best DF-HCCI engine.

## **Chapter - 6**

### **Conclusions and Future Scope**

---

## 6.1 Conclusion

In this research study, a single-cylinder conventional diesel engine is converted into dual fuel HCCI (DF-HCCI) engine by attaching the carburetor outside the engine manifold. Carburetor selection was done based on MFR capacity of the engine. Two different reactivity fuels were supplied to the DF-HCCI engine. Through the carburetor, alcohol-based fuel was supplied at the time of suction stroke, and to ignite the premixed homogeneous charge diesel or biodiesel blend or butanol blend was injected. The experiments were performed on DF-HCCI engine for various alcohol-based fuels under different load conditions. The DF-HCCI engine combustion performance and emissions over diesel engine were investigated for different load conditions.

From this study following conclusions were drawn:

It was concluded that an alcohol-based DF-HCCI engine can operate throughout the load conditions with varying MFR of alcohol-based fuel and direct injection fuel at particular load conditions.

### Objective 1

- It was observed that alcohol-based fuel (Methanol, Ethanol, Propanol, and Butanol ) are preferable in DF-HCCI engine because of high volatility and high anti-knocking ability, also it can easily mix with the inlet air in the carburetor.
- Hence to investigate the performance of DF-HCCI engine Methanol, Ethanol, Propanol, and Butanol alcohol-based fuel was selected.
- Carburetor location outside the engine was fixed 6-inch, 9-inch, and 12-inch away from the engine cylinder.
- It was observed that little more diesel consumption for 9-inch and 12-inch inlet manifold pipe compared to 6-inch inlet manifold pipe. Which results in a little improvement was observed for 6-inch inlet manifold pipe compared to the rest of the locations (9-inch, 12-inch).
- It was revealed that varying the carburetor location was not showing considerable changes in the engine emission and in-cylinder pressure but to avoid the evaporation losses, friction losses, fuel atomization, fuel molecule sticking to the manifold, a nearer

location of the carburetor was better. Nearer carburetor location will impact the fuel economy of the DF-HCCI engine. Hence to fix the carburetor location in DF-HCCI engine 6-inch length inlet manifold pipe was selected for further studies.

## Objective 2

- Methanol has high LHV so it helps to reduce the inlet air temperature and resist to start of combustion. Hence ID was very high compared to a conventional diesel engine.
- With increasing MFR of methanol NO<sub>x</sub> emission was reduced a lot however, HC, and CO emissions increased more due to low-temperature combustion. It was observed that at load 60%, 80%, and 100% smoke opacity were reduced compared to diesel engine while at 20% and 40% smoke opacity was increased. Maximum 47.13% smoke opacity was reduced at 100% load condition by fuel jet number 60. Further, maximum 97.19% NO<sub>x</sub> emission was reduced at low load conditions by jet 60.
- Methanol+D DF-HCCI engine gave a poor performance in the case of BTE compared to diesel engine. The result shows that at 20% and 40% load condition BTE was reduced lot and at 60% to 100% the BTE is almost equal to diesel engine.
- From the SAW optimization method, it was observed that at 20% and 40% load condition diesel engine showed better performance compared to M100+D DF-HCCI engine, however at 60% to 100% load conditions M100+D DF-HCCI engine was observed better than the diesel engine. Fuel Jet 60 was observed optimum for all load conditions.
- To run the engine on M100+D DF-HCCI engine the optimum premixed ratio of methanol range is found as 31.4% to 43.96%. An average 37.45% diesel fuel can be replaced by methanol with lower emissions and higher BTE compared to diesel engine.
- In the case of E100+D DF-HCCI engine smooth operation was observed for all load conditions. With increase in the MFR of ethanol NO<sub>x</sub> and smoke opacity was reduced, however, HC and CO emission was increased.
- Maximum 96.46% NO<sub>x</sub> reduction was occurred at 40% engine load by jet 70, while jet 40 reduced 19.96% NO<sub>x</sub> emission at 100% load. While maximum 87.84% smoke opacity was reduced by jet 90 under 100% load, and the minimum smoke opacity reduction was 14.1% by jet 40 at 40% load. Further, BTE also improved in E100+D DF-HCCI engine

compared to diesel engine. Jet 40 given the highest 16.5% improvement in BTE for 80% engine load.

- From the SAW optimization method, it is concluded that all optimum fuel jets are suitable at a particular load by maintaining the highest fuel economy (BTE) and lowest emission compared to diesel engine. Jet 40 is suitable for 20% load conditions, jet 70 is suitable for 40% load conditions, jet 80 is suitable for 60% load conditions and jet 90 is suitable for 80% and 100% load conditions.
- From the optimization the optimized premixed ratio of ethanol was calculated, at 20% load conditions it is 47.55%, at 40% load condition it is 69.9%, at 60% load condition it is 69.83%, at 80% load condition it is 75.94% and at 100% load condition it is 68%. The optimum premixed ratio of the ethanol range is between 47.55% to 75.94%. On average premixed ratio of ethanol is 66.24% means 66.24% of diesel fuel can be replaced by ethanol in the E100+D DF-HCCI engine.
- P100+ D gave a similar trend as E100+D DF-HCCI engine. In P100+D DF-HCCI engine maximum NO<sub>X</sub> reduction was 78.75% at 20% load conditions when jet 60 was used, while at 100% load 47.46% NO<sub>X</sub> was reduced by jet 90. Also, smoke opacity was reduced for all load conditions compared to diesel engine, at 80% load maximum 87.5% smoke opacity was reduced by jet 90, while at 20% load minimum 35.63% smoke opacity was reduced by jet 40. In the term of BTE it showed better performance for higher load conditions. At 60% load 20.15% BTE was increased by jet 40, while at 100% load 3.37% BTE increased by jet 90.
- From the SAW optimization method for P100+D DF-HCCI engine, it is concluded that jet 60 is suitable for 20% load conditions, jet 70 is suitable for 40% load conditions, and jet 90 is suitable for 60%, 80% and 100% load conditions. Also, optimum premixed ratio of propanol was calculated, at 20% load conditions it is 58.98%, at 40% load conditions it is 66.01%, at 60%, and 80% load conditions it is 73.92%, and at 100% load condition it is 65.4%. The optimum premixed ratio of the propanol range is between 58.98% to 73.92%. An average premixed ratio of propanol is 67.64% means 67.64% of diesel fuel can be replaced by propanol in the P100+D DF-HCCI engine.
- B100+ D gave a similar trend as E100+D and P100+D DF-HCCI engine. B100+D DF-

HCCI engine showed better performance in terms of NO<sub>x</sub> emission reduction, smoke opacity reduction, and BTE improvement compared to diesel engine. Maximum 84.69% NO<sub>x</sub> emission was reduced at 20% load conditions by jet 70, while at 100% load 47.21% NO<sub>x</sub> was reduced by jet 70. At 100% load minimum 18.53% NO<sub>x</sub> was reduced by fuel jet 40. Also, smoke opacity was reduced maximum 88.58% at 80% load by jet 90, while at 20% load minimum 48.58% smoke opacity was reduced by jet 40. But the BTE result showed a reduction for 20%, 40%, and 100% load conditions while showed increment at 60% and 80% load conditions. At 80% load maximum 10.33% BTE was increased by jet 70.

- From the SAW optimization method for B100+D DF-HCCI engine, it is concluded that jet 70 is suitable for all load conditions. Also, optimum premixed ratio of butanol was calculated, at 20% load conditions it is 63.02%, at 40% load conditions it is 62.92%, at 60% load condition it is 58.52%, at 80% load condition it is 54.37%, and at 100% load conditions it is 45.84%. The optimum premixed ratio of the butanol range is between 45.84% to 63.02%. An average premixed ratio of butanol is 56.93% means 56.93% of diesel fuel can be replaced by butanol in the B100+D DF-HCCI engine.

### Objective 3

- In the comparison of different alcohol-based fuel in diesel ignited DF-HCCI engine, it was observed that:
- ✓ With increasing the carbon number in the alcohol-based fuel, due to weaken hydroxyl group LHV of fuel decreases, these properties impact the cooling potential of the fuel. Methanol showed the highest cooling potential and lowest NO<sub>x</sub> emission compared to the rest of the alcohol-based fuel.
- ✓ It was observed that M100+D reduced the highest NO<sub>x</sub> emission i.e. 97.19% under 20% load conditions. While E100+D reduced 86.88%, P100+D reduced 78.75% and B100+D reduced 76.88% under 20% load conditions.
- ✓ Also, it was revealed that all alcohol-based DF-HCCI engines reduced smoke opacity for all load conditions except methanol DF-HCCI engine at low load conditions (i.e. 20% and 40%). B100+D DF-HCCI engine reduced the highest smoke opacity for all load conditions compared to the rest of the alcohol-based fuel. B100+D, P100+D, E100+D,

and M100+D DF-HCCI engine reduced smoke opacity by 76.88%, 74.38%, 61.38%, and 47.13% respectively under 100% load conditions compared to diesel engine.

- ✓ Further, all alcohol-based DF-HCCI engines improved BTE for high load conditions (i.e. at 60%, 80%, and 100% engine load) except butanol at 100% load condition and methanol at 60% load conditions. However, BTE was reduced for all alcohol-based DF-HCCI engine at 20% and 40% load conditions. P100+D DF-HCCI engine showed 14.76% highest increment in BTE at 80% load condition while E100+D improved 10.83%, B100+D improved 4.13% and M100+D improved 2.66% at 80% load condition over diesel engine.
- ✓ It was concluded that P100+D DF-HCCI engine gave the best cumulative performance for low load and high load conditions. However, B100+D DF-HCCI engine gave the best performance for mid-load conditions. E100+D gave the moderate performance for all load conditions and M100+D gave the poorest cumulative performance for all load conditions compared to the rest of the alcohol-based DF-HCCI engine.

#### **Objective 4**

- It was observed that the substitution of Neem-biodiesel blend 20 (Bio20) instead of diesel in DF-HCCI engine helps to reduce HC and CO emissions due to inherent oxygen in the Bio20.
- It was observed that in the case of M100+Bio20 the emissions like HC, CO, and smoke opacity were reduced however NO<sub>x</sub> emission was increased compared to M100+D. Moreover, a great improvement was observed in BTE.
- It was observed that M100+Bio20 reduced the maximum percentage of CO emissions compared to M100+D, however, E100+Bio20 shows very little reduction in CO emissions compared to E100+D. Also, M100+Bio20 reduced the maximum percentage of HC emission compared to M100+D, however, P100+Bio20 shows very little reduction in HC emissions compared to P100+D.
- Further M100+Bio20 increased the maximum percentage of NO<sub>x</sub> emission compared to M100+D, however, B100+Bio20 shows very little reduction in NO<sub>x</sub> emissions compared to B100+D. While M100+Bio20 reduced the maximum percentage of smoke opacity

compared to M100+D, however, the rest of the alcohol-based fuel increased smoke opacity.

- It was observed that M100+Bio20 and P100+Bio20 increased BTE compared to M100+D and P100+D respectively.
- From this study, it was noticed that for methanol DF-HCCI engine Bio20 replacement instead of diesel is better for the reduction of HC, CO, and smoke opacity with increasing BTE. However, for remaining alcohol-based DF-HCCI engine HC and CO emission got reduced by the use of Bio20 instead of diesel with a penalty of high NO<sub>x</sub> emission and smoke opacity with low BTE except P100+Bio20.

## Objective 5

- Substitution of butanol blend (B10/B20/B30) instead of diesel in propanol DF-HCCI engine improves the cumulative performance of the engine.
- NO<sub>x</sub> emission reduced (avg. 90%) much in the butanol blend ignited propanol DF-HCCI engine, compared to diesel ignited propanol DF-HCCI engine. Also, smoke opacity increased more for low load conditions while at high load conditions less increased.
- It was observed that substitution of butanol blend instead of diesel reduced CO and HC emissions at higher load conditions however, BTE was reduced compared to diesel ignited propanol DF-HCCI engine.
- From the optimization results, it was concluded that butanol blends (B10/B20/B30) ignited propanol DF-HCCI engine showed better cumulative performance under all load conditions compared to diesel ignited propanol DF-HCCI engine. At 20% and 80% load conditions P100+B30, for 40% and 60% load conditions P100+B10, and for 100% load conditions P100+B20 DF-HCCI engine gave an optimized performance.
- It was revealed that butanol blend ignited propanol DF-HCCI engine is always preferable compared to P100+D DF-HCCI engine for the reduction of NO<sub>x</sub> emission HC and CO emissions, however, BTE was reduced.

From this research work, it was observed that propanol with diesel (P100+D) and Ethanol with diesel (E100+D) DF-HCCI engine will be the best alcohol-based DF-HCCI engine to reduce the NO<sub>x</sub> and smoke opacity with considerable improvement in BTE. Around up 66-68% of diesel

fuel would be replaced by alternative fuel i.e. ethanol /propanol with low emission, and without sacrifice in the fuel economy by use of DF-HCCI engine technology. Also it was observed that Methanol with diesel (M100+D) would not be a good DF-HCCI engine, but M100+Bio20 would be a good alternate fuel for DF-HCCI engine with jet number 60 in the carburetor at 100% load condition.

## **6.2 Future scope**

- In the further study, by considering the optimum range of premixed ratio for any alcohol-based fuel, inlet conditions may vary easily like inlet temperature, inlet pressure with direct injection pressure, and injection timing.
- In this work constant CR i.e. 17.5 was used, in further research different CR can be attempted.
- Further, a biodiesel blend would be the best option to reduce HC and CO emissions so in further study different biodiesel can be investigated for ethanol or propanol DF-HCCI engine.
- Butanol blend instead of diesel exposed good performance in the propanol DF-HCCI engine, in further study rest of the alcohol-based DF-HCCI engine can replace butanol blend instead of diesel.
- Attempt can be made to use port injection instead of carburetor for alcohol-based fuels.

## References

- [1] Ganesan V. Internal combustion engine 2007;753.
- [2] US Energy Information Administration (EIA). Country Analysis Executive Summary: India. Eia 2020;1–19.
- [3] DiesDieselnet. EU Emission Standards for Passenger Cars n.d. 2021. <https://doi.org/https://dieselnet.com/standards/eu/ld.php>.
- [4] Duan X, Lai MC, Jansons M, Guo G, Liu J. A review of controlling strategies of the ignition timing and combustion phase in homogeneous charge compression ignition (HCCI) engine. Fuel 2021;285. <https://doi.org/10.1016/j.fuel.2020.119142>.
- [5] Saiteja P, Ashok B. A critical insight review on homogeneous charge compression ignition engine characteristics powered by biofuels. Fuel 2021;285. <https://doi.org/10.1016/j.fuel.2020.119202>.
- [6] Chauvin J, Grondin O, Moulin P. Control oriented model of a variable geometry turbocharger in an engine with two EGR loops. vol. 42. IFAC; 2009. <https://doi.org/10.3182/20091130-3-fr-4008.00009>.
- [7] Warkhade GS, Babu A V. Impact of supercharging and compression ratio on performance characteristics in a single cylinder DICI engine. Int J Heat Technol 2018;36:955–61. <https://doi.org/10.18280/ijht.360323>.
- [8] Ravichandra D, Puli RK, Chandramohan VP. A Review Report on Turbocharged Diesel Engine with Alternative Fuels. J Inst Eng Ser C 2019;100:1043–52. <https://doi.org/10.1007/s40032-019-00510-4>.
- [9] Siva Prasad K, Srinivasa Rao S, Raju VRK. Effect of compression ratio and fuel injection pressure on the characteristics of a CI engine operating with butanol/diesel blends. Alexandria Eng J 2021;60:1183–97. <https://doi.org/10.1016/j.aej.2020.10.042>.
- [10] Alagumalai A. Internal combustion engines: Progress and prospects. Renew Sustain Energy Rev 2014;38:561–71. <https://doi.org/10.1016/j.rser.2014.06.014>.
- [11] Xu L, Bai XS, Li C, Tunestål P, Tunér M, Lu X. Emission characteristics and engine performance of gasoline DICI engine in the transition from HCCI to PPC. Fuel

2019;254:115619. <https://doi.org/10.1016/j.fuel.2019.115619>.

- [12] Xu G, Jia M, Li Y, Chang Y, Liu H, Wang T. Evaluation of variable compression ratio (VCR)and variable valve timing (VVT)strategies in a heavy-duty diesel engine with reactivity controlled compression ignition (RCCI)combustion under a wide load range. *Fuel* 2019;253:114–28. <https://doi.org/10.1016/j.fuel.2019.05.020>.
- [13] Xu L, Bai XS, Li Y, Treacy M, Li C, Tunestål P, et al. Effect of piston bowl geometry and compression ratio on in-cylinder combustion and engine performance in a gasoline direct-injection compression ignition engine under different injection conditions. *Appl Energy* 2020;280:115920. <https://doi.org/10.1016/j.apenergy.2020.115920>.
- [14] Kattela SP, Vysyaraju RKR, Surapaneni SR, Ganji PR. Effect of n-butanol/diesel blends and piston bowl geometry on combustion and emission characteristics of CI engine. *Environ Sci Pollut Res* 2019;26:1661–74. <https://doi.org/10.1007/s11356-018-3704-5>.
- [15] Sindhu R, Amba Prasad Rao G, Madhu Murthy K. Effective reduction of NOx emissions from diesel engine using split injections. *Alexandria Eng J* 2018;57:1379–92. <https://doi.org/10.1016/j.aej.2017.06.009>.
- [16] Datla R, Puli RK, Chandramohan VP, Edwin Geo V. Biodiesel Production Process, Optimization and Characterization of *Azadirachta indica* Biodiesel in a VCR Diesel Engine. *Arab J Sci Eng* 2019;44:10141–54. <https://doi.org/10.1007/s13369-019-04072-6>.
- [17] Vinod Babu VBM, Madhu Murthy MMK, Amba Prasad Rao G. Butanol and pentanol: The promising biofuels for CI engines – A review. *Renew Sustain Energy Rev* 2017;78:1068–88. <https://doi.org/10.1016/j.rser.2017.05.038>.
- [18] Katam GB, Veeresh Babu A, Madhu Murthy K, Warkhade GS. Review on algae for biodiesel fuel production, its characteristics comparison with other and their impact on performance, combustion and emissions of diesel engine. *World J Eng* 2017;14:127–38. <https://doi.org/10.1108/WJE-06-2016-0012>.
- [19] Saxena S, Bedoya ID. Fundamental phenomena affecting low temperature combustion and HCCI engines , high load limits and strategies for extending these limits. *Prog Energy Combust Sci* 2013;39:457–88. <https://doi.org/10.1016/j.pecs.2013.05.002>.
- [20] Reitz RD, Duraisamy G. Review of high efficiency and clean reactivity controlled

compression ignition (RCCI) combustion in internal combustion engines. *Prog Energy Combust Sci* 2015;46:12–71. <https://doi.org/10.1016/j.pecs.2014.05.003>.

[21] Yao M, Zheng Z, Liu H. Progress and recent trends in homogeneous charge compression ignition (HCCI) engines. *Prog Energy Combust Sci* 2009;35:398–437. <https://doi.org/10.1016/j.pecs.2009.05.001>.

[22] Imtenan S, Varman M, Masjuki HH, Kalam MA, Sajjad H, Arbab MI, et al. Impact of low temperature combustion attaining strategies on diesel engine emissions for diesel and biodiesels: A review. *Energy Convers Manag* 2014;80:329–56. <https://doi.org/10.1016/j.enconman.2014.01.020>.

[23] Bendu H, Murugan S. Homogeneous charge compression ignition (HCCI) combustion: Mixture preparation and control strategies in diesel engines. *Renew Sustain Energy Rev* 2014;38:732–46. <https://doi.org/10.1016/j.rser.2014.07.019>.

[24] <https://www.wired.com/2007/08/gms-hcci-engine/> n.d.

[25] Sharma TK, Rao GAP, Murthy KM. Homogeneous charge compression ignition (HCCI) engines: A review. *Arch Comput Methods Eng* 2016;23:623–57. <https://doi.org/10.1007/s11831-015-9153-0>.

[26] Agarwal A, Singh A, RK M. Evolution , challenges and path forward for low temperature combustion engines. *Prog Energy Combust Sci* 2017;61:1–56. <https://doi.org/10.1016/j.pecs.2017.02.001>.

[27] Reitz RD, Duraisamy G. Review of high efficiency and clean reactivity controlled compression ignition (RCCI) combustion in internal combustion engines. *Prog Energy Combust Sci* 2015;46:12–71. <https://doi.org/10.1016/j.pecs.2014.05.003>.

[28] Hasan MM, Rahman MM. Homogeneous charge compression ignition combustion: Advantages over compression ignition combustion, challenges and solutions. *Renew Sustain Energy Rev* 2016;57:282–91. <https://doi.org/10.1016/j.rser.2015.12.157>.

[29] Sharma TK, Rao GAP, Murthy KM. Homogeneous Charge Compression Ignition ( HCCI ) Engines : A Review. *Arch Comput Methods Eng* 2016;23:623–57. <https://doi.org/10.1007/s11831-015-9153-0>.

[30] Onishi S, Jo SH, Shoda K, Jo P Do KS. Active Thermo-Atmosphere Combustion (ATAC)

- A New Combustion Process for Internal Combustion Engines. SAE 790501 1979. <https://doi.org/10.4271/790501>.

[31] Y Noguchi, M Tanaka, Tanaka T TY. A study on gasoline engine combustion by observation of intermediate reactive products during combustion. SAE Tech Pap 1979;790840. <https://doi.org/10.4271/790840>.

[32] Thrlng RH. Homogeneous..Charge Compression.. Ignition (HCCI) Engines. SAE Int 1989;892068. <https://doi.org/10.4271/892068>.

[33] Ishibashi Y, Asai M. Improving the Exhaust Emissions of Two-Stroke Engines by Applying the Activated Radical Combustion. SAE Tech Pap Ser 1996;960742. <https://doi.org/10.4271/960742>.

[34] Aoyama T, Yoshiaki H and, Mizuta J. An Experimental Study on Premixed-Charge Compression Ignition Gasoline Engine. SAE Tech Pap 1996;960081. <https://doi.org/10.4271/960081>.

[35] Karthikeya Sharma T, Amba Prasad Rao G, Madhu Murthy K. Effective reduction of NOx emissions of a HCCI (Homogeneous charge compression ignition) engine by enhanced rate of heat transfer under varying conditions of operation. Energy 2015;93:2102–15. <https://doi.org/10.1016/j.energy.2015.10.083>.

[36] Karthikeya Sharma T, Amba Prasad Rao G, Madhu Murthy K. Effect of swirl on performance and emissions of CI engine in HCCI mode. J Brazilian Soc Mech Sci Eng 2014;37:1405–16. <https://doi.org/10.1007/s40430-014-0247-7>.

[37] Canova M, Garzarella L, Ghisolfi M, Midlam-Mohler S, Guezennec Y, Rizzoni G. A Mean-Value Model of a Turbocharged HCCI Diesel Engine with External Mixture Formation. SAE Tech Pap 2005;ICE2005. <https://doi.org/10.4271/2005-24-034>.

[38] Shi L, Cui Y, Deng K, Peng H, Chen Y. Study of low emission homogeneous charge compression ignition (HCCI) engine using combined internal and external exhaust gas recirculation (EGR). Energy 2006;31:2665–76. <https://doi.org/10.1016/j.energy.2005.12.005>.

[39] Liu M Bin, He BQ, Zhao H. Effect of air dilution and effective compression ratio on the combustion characteristics of a HCCI (homogeneous charge compression ignition) engine

fuelled with n-butanol. Energy 2015;85:296–303. <https://doi.org/10.1016/j.energy.2015.03.082>.

[40] Nakano M, Mandokoro Y, Kubo S, Yamazaki S. Effects of exhaust gas recirculation in homogeneous charge compression ignition engines. *Int J Engine Res* 2000;1:269–79. <https://doi.org/10.1243/1468087001545173>.

[41] Singh AP, Agarwal AK. Combustion characteristics of diesel HCCI engine: An experimental investigation using external mixture formation technique. *Appl Energy* 2012;99:116–25. <https://doi.org/10.1016/j.apenergy.2012.03.060>.

[42] Ganesh D, Nagarajan G, Mohamed Ibrahim M. Study of performance, combustion and emission characteristics of diesel homogeneous charge compression ignition (HCCI) combustion with external mixture formation. *Fuel* 2008;87:3497–503. <https://doi.org/10.1016/j.fuel.2008.06.010>.

[43] Ganesh D, Nagarajan G. Homogeneous charge compression ignition (HCCI) combustion of diesel fuel with external mixture formation. *Energy* 2010;35:148–57. <https://doi.org/10.1016/j.energy.2009.09.005>.

[44] Maurya RK, Agarwal AK. Experimental investigation on the effect of intake air temperature and air-fuel ratio on cycle-to-cycle variations of HCCI combustion and performance parameters. *Appl Energy* 2011;88:1153–63. <https://doi.org/10.1016/j.apenergy.2010.09.027>.

[45] Singh G, Singh AP, Agarwal AK. Experimental investigations of combustion, performance and emission characterization of biodiesel fuelled HCCI engine using external mixture formation technique. *Sustain Energy Technol Assessments* 2014;6:116–28. <https://doi.org/10.1016/j.seta.2014.01.002>.

[46] Cinar C, Uyumaz A, Solmaz H, Topgul T. Effects of valve lift on the combustion and emissions of a HCCI gasoline engine. *Energy Convers Manag* 2015;94:159–68. <https://doi.org/10.1016/j.enconman.2015.01.072>.

[47] Bendu H, Sivalingam M. Experimental investigation on the effect of charge temperature on ethanol fueled HCCI combustion engine. *J Mech Sci Technol* 2016;30:4791–9. <https://doi.org/10.1007/s12206-016-0951-6>.

[48] Bhiogade G, Suryawanshi JG. Investigations on premixed charge compression ignition engine with external mixture formation and exhaust gas recirculation technique. *J Mech Sci Technol* 2016;30:5269–74. <https://doi.org/10.1007/s12206-016-1045-1>.

[49] Karthikeya Sharma T, Amba Prasad Rao G, Madhu Murthy K. Effective reduction of in-cylinder peak pressures in Homogeneous Charge Compression Ignition Engine - A computational study. *Alexandria Eng J* 2015;54:373–82. <https://doi.org/10.1016/j.aej.2015.04.006>.

[50] Takeda Y, Nakagome K, Niimura K. Emission characteristics of premixed lean diesel combustion with extremely early staged fuel injection. *SAE Int* 1996;961163:2887–94. <https://doi.org/10.1299/kikaib.62.2887>.

[51] Nishijima Y, Asaumi Y, Aoyagi Y. Impingement Spray System with Direct Water Injection for Premixed Lean Diesel Combustion Control. *SAE Int* 2002;01–0109. <https://doi.org/10.4271/2002-01-0109>.

[52] Iwabuchi Y, Kawai K, Shoji T, Takeda Y. Trial of New Concept Diesel Combustion System - Premixed Compression-Ignited Combustion -. *SAE Tech Pap Ser* 1999;1. <https://doi.org/10.4271/1999-01-0185>.

[53] Hashizume T, Miyamoto T, Hisashi A, Tsujimura K. Combustion and Emission Characteristics of Multiple Stage Diesel Combustion. *SAE Tech Pap Ser* 1998;980505. <https://doi.org/10.4271/980505>.

[54] Yokota H, Kudo Y, Hiroshi N, Kakegawa T, Suzuki T. A New Concept for Low Emission Diesel Combustion. *SAE Tech Pap Ser* 1997;970891. <https://doi.org/0.4271/970891>.

[55] Hasegawa R, Yanagihara H. HCCI combustion in di diesel engine. *SAE Int* 2003;01–0745. <https://doi.org/10.4271/2003-01-0745>.

[56] Su W, Lin T, Pei Y. A Compound Technology for HCCI Combustion in a DI Diesel Engine Based on the Multi-Pulse Injection and the BUMP Combustion Chamber Reprinted From : Homogeneous Charge Compression Ignition. *SAE Tech Pap Ser* 2003;01–0741. <https://doi.org/10.4271/2003-01-0741>.

[57] Walter B, Gatellier B. Development of the High Power NADI<sup>TM</sup> Concept Using Dual Mode Diesel Combustion to Achieve Zero NOx and Particulate Emissions. *SAE Int* 2002.

<https://doi.org/10.4271/2002-01-1744>.

- [58] Kim MY, Lee CS. Effect of a narrow fuel spray angle and a dual injection configuration on the improvement of exhaust emissions in a HCCI diesel engine. *Fuel* 2007;86:2871–80. <https://doi.org/10.1016/j.fuel.2007.03.016>.
- [59] Reveille B, Kleemann A, Knop V, Habchi C. Potential of narrow angle direct injection diesel engines for clean combustion: 3D CFD analysis. *SAE Tech Pap* 2006;2006. <https://doi.org/10.4271/2006-01-1365>.
- [60] Fang T, Coverdill RE, Lee C fon F, White RA. Effects of injection angles on combustion processes using multiple injection strategies in an HSDI diesel engine. *Fuel* 2008;87:3232–9. <https://doi.org/10.1016/j.fuel.2008.05.012>.
- [61] Das P, Subbarao PM V, Subrahmanyam JP. Control of combustion process in an HCCI-DI combustion engine using dual injection strategy with EGR. *Fuel* 2015;159:580–9. <https://doi.org/10.1016/j.fuel.2015.07.009>.
- [62] Kimura S, Aoki O, Ogawa H, Muranaka S, Enomoto Y. New Combustion Concept for Ultra-Clean and High-Efficiency Small DI Diesel Engines. *SAE Tech Pap Ser* 1999;01–3681. <https://doi.org/10.4271/1999-01-3681>.
- [63] Kimura S, Aoki O, Kitahara Y, Aiyoshizawa E. Ultra-clean combustion technology combining a low-temperature and premixed combustion concept for meeting future emission standards. *SAE Tech Pap* 2001. <https://doi.org/10.4271/2001-01-0200>.
- [64] Gainey B, Yan Z, Lawler B. Autoignition characterization of methanol, ethanol, propanol, and butanol over a wide range of operating conditions in LTC/HCCI. *Fuel* 2021;287:119495. <https://doi.org/10.1016/j.fuel.2020.119495>.
- [65] Ashok B, Denis Ashok S, Ramesh Kumar C. LPG diesel dual fuel engine - A critical review. *Alexandria Eng J* 2015;54:105–26. <https://doi.org/10.1016/j.aej.2015.03.002>.
- [66] Kumaraswamy A, Prasad BD. Performance analysis of a dual fuel engine using LPG and diesel with EGR system. *Procedia Eng* 2012;38:2784–92. <https://doi.org/10.1016/j.proeng.2012.06.326>.
- [67] Tira HS, Herreros JM, Tsolakis A, Wyszynski ML. Characteristics of LPG-diesel dual fuelled engine operated with rapeseed methyl ester and gas-to-liquid diesel fuels. *Energy*

2012;47:620–9. <https://doi.org/10.1016/j.energy.2012.09.046>.

- [68] Brijesh P, Chowdhury A, Sreedhara S. Advanced combustion methods for simultaneous reduction of emissions and fuel consumption of compression ignition engines. *Clean Technol Environ Policy* 2015;17:615–25. <https://doi.org/10.1007/s10098-014-0811-y>.
- [69] Guo H, Neill WS. The effect of hydrogen addition on combustion and emission characteristics of an n-heptane fuelled HCCI engine. *Int J Hydrogen Energy* 2013;38:11429–37. <https://doi.org/10.1016/j.ijhydene.2013.06.084>.
- [70] Maurya RK, Akhil N. Comparative study of the simulation ability of various recent hydrogen combustion mechanisms in HCCI engines using stochastic reactor model. *Int J Hydrogen Energy* 2017;42:11911–25. <https://doi.org/10.1016/j.ijhydene.2017.02.155>.
- [71] Chintala V, Subramanian KA. A comprehensive review on utilization of hydrogen in a compression ignition engine under dual fuel mode 2017;70:472–91.
- [72] Ibrahim MM, Ramesh A. Experimental investigations on a hydrogen diesel homogeneous charge compression ignition engine with exhaust gas recirculation. *Int J Hydrogen Energy* 2013;38:10116–25. <https://doi.org/10.1016/j.ijhydene.2013.05.092>.
- [73] Hegab A, La Rocca A, Shayler P. Towards keeping diesel fuel supply and demand in balance: Dual-fuelling of diesel engines with natural gas. *Renew Sustain Energy Rev* 2017;70:666–97. <https://doi.org/10.1016/j.rser.2016.11.249>.
- [74] Mohamed Ibrahim M, Varuna Narasimhan J, Ramesh A. Comparison of the predominantly premixed charge compression ignition and the dual fuel modes of operation with biogas and diesel as fuels. *Energy* 2015;89:990–1000. <https://doi.org/10.1016/j.energy.2015.06.033>.
- [75] Hairuddin AA, Yusaf T, Wandel AP. A review of hydrogen and natural gas addition in diesel HCCI engines. *Renew Sustain Energy Rev* 2014;32:739–61. <https://doi.org/10.1016/j.rser.2014.01.018>.
- [76] Nieman DE, Dempsey AB, Reitz RD. Heavy-Duty RCCI Operation Using Natural Gas and Diesel. *SAE Int J Engines* 2012;5:270–85. <https://doi.org/10.4271/2012-01-0379>.
- [77] Kakae AH, Rahnama P, Paykani A. Influence of fuel composition on combustion and emissions characteristics of natural gas/diesel RCCI engine. *J Nat Gas Sci Eng*

2015;25:58–65. <https://doi.org/10.1016/j.jngse.2015.04.020>.

- [78] Yousefi A, Birouk M. Investigation of natural gas energy fraction and injection timing on the performance and emissions of a dual-fuel engine with pre-combustion chamber under low engine load. *Appl Energy* 2017;189:492–505. <https://doi.org/10.1016/j.apenergy.2016.12.046>.
- [79] Yang D bo, Wang Z, Wang JX, Shuai S jin. Experimental study of fuel stratification for HCCI high load extension. *Appl Energy* 2011;88:2949–54. <https://doi.org/10.1016/j.apenergy.2011.03.004>.
- [80] Ma X, Zhang F, Xu H, Shuai S. Throttleless and EGR-controlled stoichiometric combustion in a diesel-gasoline dual-fuel compression ignition engine. *Fuel* 2014;115:765–77. <https://doi.org/10.1016/j.fuel.2013.07.052>.
- [81] Tong L, Wang H, Zheng Z, Reitz R, Yao M. Experimental study of RCCI combustion and load extension in a compression ignition engine fueled with gasoline and PODE. *Fuel* 2016;181:878–86. <https://doi.org/10.1016/j.fuel.2016.05.037>.
- [82] Kavuri C, Paz J, Kokjohn SL. A comparison of Reactivity Controlled Compression Ignition ( RCCI ) and Gasoline Compression Ignition ( GCI ) strategies at high load , low speed conditions. *Energy Convers Manag* 2016;127:324–41. <https://doi.org/10.1016/j.enconman.2016.09.026>.
- [83] Tong D, Ren S, Li Y, Wang Z, Zhang H, Wang Z, et al. Performance and emissions of gasoline Homogeneous Charge Induced Ignition ( HCII ) by diesel through whole operating range on a heavy-duty multi-cylinder engine. *Fuel* 2017;197:259–71. <https://doi.org/http://dx.doi.org/10.1016/j.fuel.2017.02.003>.
- [84] Benajes J, García A, Monsalve-Serrano J, Boronat V. Achieving clean and efficient engine operation up to full load by combining optimized RCCI and dual-fuel diesel-gasoline combustion strategies. *Energy Convers Manag* 2017;136:142–51. <https://doi.org/10.1016/j.enconman.2017.01.010>.
- [85] Vipavanich C, Chuepeng S, Skullong S. Heat release analysis and thermal efficiency of a single cylinder diesel dual fuel engine with gasoline port injection. *Case Stud Therm Eng* 2018;12:143–8. <https://doi.org/10.1016/j.csite.2018.04.011>.

[86] Xu Y, Kang H, Gong J, Zhang S, Li X. A study on the combustion strategy of gasoline/diesel dual-fuel engine. *Fuel* 2018;225:426–35. <https://doi.org/10.1016/j.fuel.2018.03.166>.

[87] Wang Y, Yao M, Li T, Zhang W, Zheng Z. A parametric study for enabling reactivity controlled compression ignition (RCCI) operation in diesel engines at various engine loads. *Appl Energy* 2016;175:389–402. <https://doi.org/10.1016/j.apenergy.2016.04.095>.

[88] Lalwani A, Awate S, Chowdhury A, Sreedhara S. Conversion of a single - cylinder internal combustion engine to dual - mode homogeneous charge compression ignition engine. *Clean Technol Environ Policy* 2019;21:23–37. <https://doi.org/10.1007/s10098-018-1613-4>.

[89] Yao C, Pan W, Yao A. Methanol fumigation in compression-ignition engines: A critical review of recent academic and technological developments. *Fuel* 2017;209:713–32. <https://doi.org/10.1016/j.fuel.2017.08.038>.

[90] Maurya RK, Agarwal AK. Experimental investigation of the effect of the intake air temperature and mixture quality on the combustion of a methanol- and gasoline-fuelled homogeneous charge compression ignition engine. *Proc Inst Mech Eng Part D J Automob Eng* 2009;223:1445–58. <https://doi.org/10.1243/09544070JAUTO1238>.

[91] Maurya RK, Agarwal AK. Experimental investigations of performance, combustion and emission characteristics of ethanol and methanol fueled HCCI engine. *Fuel Process Technol* 2014;126:30–48. <https://doi.org/10.1016/j.fuproc.2014.03.031>.

[92] Yao C, Cheung CS, Cheng C, Wang Y, Chan TL, Lee SC. Effect of Diesel/methanol compound combustion on Diesel engine combustion and emissions. *Energy Convers Manag* 2008;49:1696–704. <https://doi.org/10.1016/j.enconman.2007.11.007>.

[93] Geng P, Yao C, Wei L, Liu J, Wang Q, Pan W, et al. Reduction of PM emissions from a heavy-duty diesel engine with diesel/methanol dual fuel. *Fuel* 2014;123:1–11. <https://doi.org/10.1016/j.fuel.2014.01.056>.

[94] Liu J, Yao A, Yao C. Effects of diesel injection pressure on the performance and emissions of a HD common-rail diesel engine fueled with diesel/methanol dual fuel. *Fuel* 2015;140:192–200. <https://doi.org/10.1016/j.fuel.2014.09.109>.

[95] Li G, Zhang C, Li Y. Effects of diesel injection parameters on the rapid combustion and emissions of an HD common-rail diesel engine fueled with diesel-methanol dual-fuel. *Appl Therm Eng* 2016;108:1214–25. <https://doi.org/10.1016/j.applthermaleng.2016.08.029>.

[96] Tutak W, Szwaja S. the Effect of Methanol–Diesel Combustion on Performance and Emissions of a Direct Injection Diesel Engine. *J KONES Powertrain Transp* 2015;22:259–66. <https://doi.org/10.5604/12314005.1165449>.

[97] Pan W, Yao C, Han G, Wei H, Wang Q. The impact of intake air temperature on performance and exhaust emissions of a diesel methanol dual fuel engine. *Fuel* 2015;162:101–10. <https://doi.org/10.1016/j.fuel.2015.08.073>.

[98] Guerry ES, Raihan MS, Srinivasan KK, Krishnan SR, Sohail A. Injection timing effects on partially premixed diesel-methane dual fuel low temperature combustion. *Appl Energy* 2016;162:99–113. <https://doi.org/10.1016/j.apenergy.2015.10.085>.

[99] Jia Z, Denbratt I. Experimental investigation into the combustion characteristics of a methanol-Diesel heavy duty engine operated in RCCI mode. *Fuel* 2018;226:745–53. <https://doi.org/10.1016/j.fuel.2018.03.088>.

[100] Dou Z, Yao C, Wei H, Wang B, Liu M, Chen C, et al. Experimental study of the effect of engine parameters on ultrafine particle in diesel/methanol dual fuel engine. *Fuel* 2017;192:45–52. <https://doi.org/10.1016/j.fuel.2016.12.006>.

[101] Maurya RK, Agarwal AK. Experimental study of combustion and emission characteristics of ethanol fuelled port injected homogeneous charge compression ignition (HCCI) combustion engine. *Appl Energy* 2011;88:1169–80. <https://doi.org/10.1016/j.apenergy.2010.09.015>.

[102] Sarjovaara T, Alantie J, Larmi M. Ethanol dual-fuel combustion concept on heavy duty engine. *Energy* 2013;63:76–85. <https://doi.org/10.1016/j.energy.2013.10.053>.

[103] Kim Y-J, Kim K-B, Lee K-H. A Study on the Combustion and Emission Characteristics of Diesel Fuel Blended with Ethanol in an HCCI Engine. *Fuel* 2015;158:725–32. <https://doi.org/10.4271/2008-32-0026>.

[104] Qian Y, Liu G, Guo J, Zhang Y, Zhu L, Lu X. Engine performance and octane on demand

studies of a dual fuel spark ignition engine with ethanol/gasoline surrogates as fuel. Energy Convers Manag 2019;183:296–306. <https://doi.org/10.1016/j.enconman.2019.01.011>.

- [105] Chu S, Lee J, Kang J, Lee Y, Min K. High load expansion with low emissions and the pressure rise rate by dual-fuel combustion. Appl Therm Eng 2018;144:437–43. <https://doi.org/10.1016/j.aplthermaleng.2018.08.027>.
- [106] Polk AC, Carpenter CD, Srinivasan KK, Krishnan SR. An investigation of diesel-ignited propane dual fuel combustion in a heavy-duty diesel engine. Fuel 2014;132:135–48. <https://doi.org/10.1016/j.fuel.2014.04.069>.
- [107] Krishnan SR, Srinivasan KK, Raihan MS. The effect of injection parameters and boost pressure on diesel-propane dual fuel low temperature combustion in a single-cylinder research engine. Fuel 2016;184:490–502. <https://doi.org/10.1016/j.fuel.2016.07.042>.
- [108] Hodges KA, Aniello A, Krishnan SR, Srinivasan KK. Impact of propane energy fraction on diesel-ignited propane dual fuel low temperature combustion. Fuel 2017;209:769–75. <https://doi.org/10.1016/j.fuel.2017.07.096>.
- [109] Chen Z, Liu J, Wu Z, Lee C. Effects of port fuel injection ( PFI ) of n-butanol and EGR on combustion and emissions of a direct injection diesel engine. Energy Convers Manag J 2013;76:725–31. <https://doi.org/http://dx.doi.org/10.1016/j.enconman.2013.08.030>.
- [110] Yadav J, Ramesh A. Injection strategies for reducing smoke and improving the performance of a butanol-diesel common rail dual fuel engine. Appl Energy 2018;212:1–12. <https://doi.org/10.1016/j.apenergy.2017.12.027>.
- [111] Ganesh D, Ayyappan PR, Murugan R. Experimental investigation of iso-butanol/diesel reactivity controlled compression ignition combustion in a non-road diesel engine. Appl Energy 2019;242:1307–19. <https://doi.org/10.1016/j.apenergy.2019.03.166>.
- [112] Lü X, Hou Y, Zu L, Huang Z. Experimental study on the auto-ignition and combustion characteristics in the homogeneous charge compression ignition (HCCI) combustion operation with ethanol/n-heptane blend fuels by port injection. Fuel 2006;85:2622–31. <https://doi.org/10.1016/j.fuel.2006.05.003>.
- [113] Swami Nathan S, Mallikarjuna JM, Ramesh A. An experimental study of the biogas-diesel

HCCI mode of engine operation. *Energy Convers Manag* 2010;51:1347–53. <https://doi.org/10.1016/j.enconman.2009.09.008>.

- [114] Turkcan A, Ozsezen AN, Canakci M. Effects of second injection timing on combustion characteristics of a two stage direct injection gasoline – alcohol HCCI engine. *Fuel* 2013;111:30–9.
- [115] Polat S. An experimental study on combustion , engine performance and exhaust emissions in a HCCI engine fuelled with diethyl ether – ethanol fuel blends. *Fuel Process Technol* 2016;143:140–50.
- [116] Yousefi A, Birouk M, Lawler B, Gharehghani A. Performance and emissions of a dual-fuel pilot diesel ignition engine operating on various premixed fuels. *Energy Convers Manag* 2015;106:322–36. <https://doi.org/10.1016/j.enconman.2015.09.056>.
- [117] Şahin Z, Durgun O, Aksu ON. Experimental investigation of n-butanol/diesel fuel blends and n-butanol fumigation - Evaluation of engine performance, exhaust emissions, heat release and flammability analysis. *Energy Convers Manag* 2015;103:778–89. <https://doi.org/10.1016/j.enconman.2015.06.089>.
- [118] Zheng M, Li T, Han X. Direct injection of neat n-butanol for enabling clean low temperature combustion in a modern diesel engine. *Fuel* 2015;142:28–37. <https://doi.org/10.1016/j.fuel.2014.10.075>.
- [119] Saxena MR, Maurya RK. Effect of premixing ratio , injection timing and compression ratio on nano particle emissions from dual fuel non-road compression ignition engine fueled with gasoline / methanol ( port injection ) and diesel ( direct injection ). *Fuel* 2017;203:894–914. <https://doi.org/10.1016/j.fuel.2017.05.015>.
- [120] Çelebi Y, Ayd H. An overview on the light alcohol fuels in diesel engines. *Fuel* 2019;236:890–911. <https://doi.org/10.1016/j.fuel.2018.08.138>.
- [121] Benajes J, García A, Monsalve-serrano J, Boronat V. Achieving clean and efficient engine operation up to full load by combining optimized RCCI and dual-fuel diesel-gasoline combustion strategies. *Energy Convers Manag* 2017;136:142–51. <https://doi.org/10.1016/j.enconman.2017.01.010>.
- [122] Masimalai S, Subramaniyan A. A complete assessment on the impact of in-cylinder and

external blending of eucalyptus oil on engine's behavior of a biofuel-based dual fuel engine. *Environ Sci Pollut Res* 2019;26:7938–53. <https://doi.org/10.1007/s11356-019-04285-0>.

- [123] Veza I, Said MFM, Latiff ZA. Progress of acetone-butanol-ethanol (ABE) as biofuel in gasoline and diesel engine: A review. *Fuel Process Technol* 2019;196:106179. <https://doi.org/10.1016/j.fuproc.2019.106179>.
- [124] Nanthagopal K, Kishna RS, Atabani AE, Al-Muhtaseb AH, Kumar G, Ashok B. A compressive review on the effects of alcohols and nanoparticles as an oxygenated enhancer in compression ignition engine. *Energy Convers Manag* 2020;203:112244. <https://doi.org/10.1016/j.enconman.2019.112244>.
- [125] Warkhade GS, Babu AV. Combustion characteristics of linseed (*Linum usitatissimum*) methyl ester fuelled biodiesel blends in variable compression ratio diesel engine. *Aust J Mech Eng* 2019;17:38–51. <https://doi.org/10.1080/14484846.2018.1525170>.
- [126] Agarwal AK, Singh AP, Maurya RK, Chandra Shukla P, Dhar A, Srivastava DK. Combustion characteristics of a common rail direct injection engine using different fuel injection strategies. *Int J Therm Sci* 2018;134:475–84. <https://doi.org/10.1016/j.ijthermalsci.2018.07.001>.
- [127] Uyumaz A. An experimental investigation into combustion and performance characteristics of an HCCI gasoline engine fueled with n-heptane, isopropanol and n-butanol fuel blends at different inlet air temperatures. *Energy Convers Manag* 2015;98:199–207. <https://doi.org/10.1016/j.enconman.2015.03.043>.
- [128] Gawale GR, Naga Srinivasulu G. Numerical and experimental investigations on a dual fuel HCCI engine by using ethanol as primary fuel and diesel as secondary fuel for NOX reduction and better performance. *Int J Ambient Energy* 2020;41:418–27. <https://doi.org/10.1080/01430750.2018.1472645>.
- [129] Gainey B, Lawler B. The role of alcohol biofuels in advanced combustion: An analysis. *Fuel* 2021;283. <https://doi.org/10.1016/j.fuel.2020.118915>.
- [130] Yusri IM, Mamat R, Akasyah MK, Jamlos MF, Yusop AF. Evaluation of engine combustion and exhaust emissions characteristics using diesel/butanol blended fuel. *Appl*

Therm Eng 2019;156:209–19. <https://doi.org/10.1016/j.applthermaleng.2019.02.028>.

- [131] Zhang Z, E J, Chen J, Zhao X, Zhang B, Deng Y, et al. Effects of boiling heat transfer on the performance enhancement of a medium speed diesel engine fueled with diesel and rapeseed methyl ester. *Appl Therm Eng* 2020;169:114984. <https://doi.org/10.1016/j.applthermaleng.2020.114984>.
- [132] Karthickeyan V, Thiagarajan S, Ashok B, Edwin Geo V, Azad AK. Experimental investigation of pomegranate oil methyl ester in ceramic coated engine at different operating condition in direct injection diesel engine with energy and exergy analysis. *Energy Convers Manag* 2020;205:112334. <https://doi.org/10.1016/j.enconman.2019.112334>.
- [133] Bendu H, Deepak BBVL, Murugan S. Multi-objective optimization of ethanol fuelled HCCI engine performance using hybrid GRNN–PSO. *Appl Energy* 2017;187:601–11. <https://doi.org/10.1016/j.apenergy.2016.11.072>.
- [134] R. Venkata Rao. *Decision Making in the Manufacturing Environment*. Gujrat India: Springer India; 2007. <https://doi.org/10.1007/s10895-017-2051-0>.
- [135] Ayodhya AS, Narayanappa KG. An overview of after-treatment systems for diesel engines. *Environ Sci Pollut Res* 2018;25:35034–47. <https://doi.org/10.1007/s11356-018-3487-8>.
- [136] Alkidas AC. The effects of fuel preparation on hydrocarbon emissions of a S.I. engine operating under steady-state conditions. *SAE Tech Pap* 1994. <https://doi.org/10.4271/941959>.
- [137] Meyer R, Heywood JB. Effect of engine and fuel variables on liquid fuel transport into the cylinder in port-injected SI engines. *SAE Tech Pap* 1999. <https://doi.org/10.4271/1999-01-0563>.
- [138] Gold MR, Arcoumanis C, Whitelaw JH, Gaade J, Wallace S. Mixture preparation strategies in an optical four-valve port-injected gasoline engine. *Int J Engine Res* 2000;1:41–56. <https://doi.org/10.1243/1468087001545254>.
- [139] Heywood JB. *INTERNAL COMBUSTION ENGINE FUNDAMENTALS*. McGraw Hill Education; 2011.

[140] Saxena MR, Maurya RK. Effect of premixing ratio, injection timing and compression ratio on nano particle emissions from dual fuel non-road compression ignition engine fueled with gasoline/methanol (port injection) and diesel (direct injection). *Fuel* 2017;203:894–914. <https://doi.org/10.1016/j.fuel.2017.05.015>.

[141] Reed M. Hanson, Sage L. Kokjohn DAS and RDR. An Experimental Investigation of Fuel Reactivity Controlled PCCI Combustion in a Heavy-Duty Engine. *SAE Int* 2010;3:700–16. <https://doi.org/10.4271/2010-01-0864>.

[142] Chen Z, Konno M, Goto S. Study on homogenous premixed charge CI engine fueled with LPG. *JSAE Rev* 2001;22:265–70. [https://doi.org/10.1016/S0389-4304\(01\)00107-2](https://doi.org/10.1016/S0389-4304(01)00107-2).

[143] Aroonsrisopon T, Sohm V, Werner P, Foster DE, Morikawa T, Iida M. An investigation into the effect of fuel composition on HCCI combustion characteristics. *SAE Tech Pap* 2002. <https://doi.org/10.4271/2002-01-2830>.

[144] Gawale GR, Naga Srinivasulu G. Experimental investigation of ethanol/diesel and ethanol/biodiesel on dual fuel mode HCCI engine for different engine load conditions. *Fuel* 2020;263:116725. <https://doi.org/10.1016/j.fuel.2019.116725>.

[145] Damanik N, Ong HC, Tong CW, Mahlia TMI, Silitonga AS. A review on the engine performance and exhaust emission characteristics of diesel engines fueled with biodiesel blends. *Environ Sci Pollut Res* 2018;25:15307–25. <https://doi.org/10.1007/s11356-018-2098-8>.

[146] Sukjit E, Herreros JM, Dearn KD, Tsolakis A, Theinnoi K. Effect of hydrogen on butanol-biodiesel blends in compression ignition engines. *Int J Hydrogen Energy* 2013;38:1624–35. <https://doi.org/10.1016/j.ijhydene.2012.11.061>.

## Publication on this Research

### Journal paper:

1. Ganesh R. Gawale & G. Naga Srinivasulu, (2018) “ Numerical and experimental investigations on a dual fuel HCCI engine by using ethanol as primary fuel and diesel as secondary fuel for NOx reduction and better performance”, *International Journal of Ambient Energy, Taylor and Francis*, (Scopus, ESCI) DOI:10.1080/01430750.2018.1472645.
2. Ganesh R. Gawale & G. Naga Srinivasulu, (2020) “Experimental Investigation of Ethanol/Diesel and Ethanol/Biodiesel on Dual Fuel Mode HCCI Engine for Different Engine Load Conditions”. *Fuel Journal, Elsevier* (Scopus, SCI, Impact factor 5.578), DOI:10.1016/j.fuel.2019.116725.
3. Ganesh R. Gawale & G. Naga Srinivasulu, (2020) “Experimental investigation of propanol dual fuel HCCI engine performance: Optimization of propanol mass flow rate, impact of butanol blends ( B10/B20/B30) as fuel substitute for diesel”. *Fuel Journal, Elsevier* (Scopus, SCI, Impact factor 5.578), Doi:10.1016/j.fuel.2020.118535.
4. Ganesh R. Gawale & G. Naga Srinivasulu, (2021) "Experimental Investigation of Various Ethanol Blends Impact on Combustion and Emissions Characteristics of Diesel Ignited Dual Fuel HCCI Engine" *World Journal of Engineering, Emerald Insight, Scopus, ESCI*, Doi:10.1108/WJE-01-2021-0035.

### International Conference Publication:

1. Ganesh R. Gawale & G. Naga Srinivasulu, “Effect of premixed ratio of gasoline on emissions and performance characteristics of a dual fuel mode HCCI engine”. (*ISHMT Conference 2020 at IIT Roorkee* ).
2. Ganesh R. Gawale & G. Naga Srinivasulu, “Impact of Biodiesel Blend (B20) as a Fuel Substitute for Diesel on Methanol Dual Fuel HCCI Engine Performance”. (*FMFP Conference 2020 at IIT Guwahati* )